Factors influencing the development of a tissue engineered bone to bone ligament

by

Uchena N. G. Wudebwe

A thesis submitted to
The University of Birmingham
for the degree of
Doctor of Philosophy

School of Chemical Engineering
The University of Birmingham
Edgbaston
Birmingham
B15 2TT
United Kingdom

"Observe always that everything is the result of change, and get used to thinking there is nothing Nature loves so well as to change existing forms and make new ones like them."

Marcus Aurelius

UNIVERSITY OF BIRMINGHAM

Abstract

College of Engineering and Physical Sciences
School of Chemical Engineering

Doctor of Philosophy

Factors influencing the development of a tissue engineered bone to bone ligament

by Uchena N. G. Wudebwe

This thesis aimed to quantify the effect of anabolic agents ascorbic acid (AA)/ proline (P) on the rates of contraction of the fibrin hydrogel scaffold as well as develop a process for increasing construct collagen content, tensile strength and widths.

Supplementation with AA/ P, in combination or individually, revealed contrasting effects on the rates of fibrin gel contraction dependent on concentration and culture duration. There appeared to be strong correlations between the extents of contraction and construct collagen content.

Enhancing the stiffness of the fibrin hydrogel augmented widths of the constructs but did not improve construct collagen content or tensile strength. The results further demonstrated that increasing the volume fraction of fibrin fibres present, either by increasing the total volume of reagents or by adjusting the ratio of thrombin to fibrinogen used could be utilised to modify sinew widths.

Constructs prepared using a stiffer fibrin gel formulation, supplemented with AA+P, resulted in enhanced collagen content, sinew tensile strength and improved interface tensile attachment.

The results also demonstrated variation in fibrin gel contraction rates and collagen production due to different cell sources, growth medium employed or the use of metal ion cofactors Zn^{2+}/ Mn^{2+}, thereby suggesting areas that could be investigated further and optimized.

Dedicated to my Mother

And

In loving memory of my Grandmother

Acknowledgements

First and foremost, I would like to thank my supervisor Professor Liam Grover for the opportunity to join his research group and develop academically. I am grateful for his support and guidance throughout my PhD. I would also like to thank Dr Jennifer Paxton, for training me in cell culture methods and her friendship during my PhD. My gratitude to Dr Alan Smith, who trained me in practical rheology techniques and his warm welcome when I visited his group at the University of Huddersfield.

Thank you to Dr James Bowen who offered me much assistance in troubleshooting equipment and agreeing to trial AFM and flow based cell detachment methods with me.

To Mr Paul Stanley and Mrs Theresa Morris from the Centre of Electron of Microscopy, who trained me in SEM techniques, thank you for your patience. Theresa, prepared my samples in Chapter 4 for SEM and TEM, for which I am very grateful.

Further thanks are extended to Dr Dick Shelton and Ms Michelle Holder from the School of Dentistry for allowing me to use their facilities. Michelle designed the primers used in this work and trained me in RT-PCR.

Thank you to Dr Alex Robinson and Dr David Cheneler for their assistance and the work they began on fabricating micropost arrays.

I would also like to thank all my colleagues in my research group, department and throughout the university.

I could not have done this PhD without the support and encouragement of my mother. Thank you mum, for your love and the confidence you have in me. Many thanks also go to my close friends and family who continue to believe me.

Thank you to the funding bodies who helped make this work possible, particularly, the BBSRC.

Contents

List of Figures

List of Tables

Abbreviations

α	**a**lpha
AA	**A**scorbic **A**cid
AA+P	**A**scorbic acid and **P**roline
ACL	**A**nterior **C**ruciate **L**igament
ASC	**A**dipose derived **S**tem **C**ells
β	**b**eta
BMP	**B**one **M**orphogenic **P**rotein
BMSCs	**B**one marrrow **M**esenchymal **S**tem **C**ells
cDNA	**c**complementary DNA
CG	**C**ollagen-**G**lycosaminoglycan
CHO	**C**hines **H**amster **O**vary
CTF	**C**hick **T**endon **F**ibroblasts
DMEM	**D**ulbecco's **M**odified **E**agle's **M**edium
DMOG	**D**i**m**ethyl**o**xalyl**g**lycine
DMSO	**D**i**m**ethyl**s**ulf**o**xide
DNA	**d**eoxyribo**n**ucleic **a**cid
DOE	**D**esign **O**f **E**xperiments
ECM	**E**xtra**C**ellular **M**atrix
EGF	**E**pidermal **G**rowth **F**actor
EMEM	**E**agle's **M**inimal **E**ssential **M**edium
ER	**E**ndoplasmic **R**eticulum / **E**ndoplasmic **R**eticula
ERK	**E**xtracellular signal-**R**egulated **K**inases

ESEM	**E**nvironmental **S**canning **E**lectron **M**icroscope
F	**F**ibre / **F**ibrils / **F**ibrillar
FGF	**F**ibroblast **G**rowth **F**actor
FDA	**F**ood and **D**rug **A**dministration
FT	**F**reeze-**T**haw
GAG	**G**lycos**A**mino**G**lycan
GDF	**G**rowth **D**ifferentiation **F**actor
HA	**H**ydroxy**A**patite
H&E	**H**ematoxylin and **E**osin
hESCs	**h**uman **E**mbryonic **S**tem **C**ells
IGF	**I**nsulin-like **G**rowth **F**actor
iPSCs	**i**nduced **P**luripotent **S**tem **C**ells
L	**L**igament(s)
LCL	**L**ateral **C**ollateral **L**igament
L/T	**L**igaments/**T**endons
LVR	**L**inear **V**iscoelastic **R**egion
M	**M**atrix
MAPK	**M**itogen **A**ctivated **P**rotein **K**inase
MCDB	**M**olecular **C**ellular & **D**evelopmental **B**iology
MCL	**M**edial **C**ollateral **L**igament
MMPs	**M**atrix **M**etalloProteinases
mRNA	**m**essenger RNA
MSCs	**M**esenchymal **S**tem **C**ells
N	**N**ucleus / **N**uclei
NT	**N**o **T**reatment / **N**on-**T**reated
P	**P**roline
PCR	**P**olymerase **C**hain **R**eaction
PEGDA	**P**oly**e**thylene **g**lycol**dia**crylate
PEO	Poly(ethylene oxide)

PFB	**P**rimary **F**ibro**b**last
PGA	**P**oly**g**lycolic-**a**cid)
PLA	**P**oly-(**l**actic **a**cid)
PLGA	**P**oly(**l**actic-co-**g**lycolic **a**cid)
PLLA	**P**oly-**L**-**L**actide
RGD	Arginylglycylaspartic acid
RNA	**r**ibo**n**ucleic **a**cid
ROS	**R**eactive **O**xygen **S**pecies
RPMI	**R**oswell **P**ark **M**emorial **I**nstitute
RT-PCR	**R**everse **T**ranscription–**P**olymerase **C**hain **R**eaction
sDMEM	**s**upplemented DMEM
SEM	**S**canning **E**lectron **M**icroscopy
T	**T**endon(s)
TE	**T**issue **E**ngineering or **T**issue **E**ngineered
TEM	**T**ransmission **E**lectron **M**icroscopy
TGF-β	**T**ransforming **G**rowth **F**actor-**B**eta
TIMP	**T**issue **I**nhibitor of **M**etallo**P**roteinase
UHMWPE	**U**ltra **H**igh **M**olecular **W**eight **P**olyethylene
UV	**U**ltra **V**iolet
V	Transport **V**esicles
VEGF	**V**ascular **E**ndothelial **G**rowth **F**actor

Chapter 1

Introduction

Ligaments and tendons (L/T) are composed of high quantities of collagen, which provide them with their mechanical strength (Rumian et al., 2007). Fibroblasts are involved in wound healing where they remodel fibrin and deposit *de novo* collagen matrix (Wang et al., 2007). They are also the main cell type found in L/T and throughout the body. Consequently, the model used in this thesis was developed from this basis, seeding a fibrin hydrogel scaffold with chick tendon fibroblast cells.

Due to the structural role of collagen and its high quantity in ligaments and tendons, a natural aim of L/T tissue engineering is to enhance construct collagen content and thereby mechanical strength. From a clinical perspective, tissue engineered ligaments and tendons (TE L/T) must be robust enough to handle, be surgically implantable and be able to withstand mechanical loads imposed on them *in vivo* (Hutmacher, 2000). Although synthetic scaffolds offer the flexibility of tailorable mechanical properties, it is advantageous to use a natural scaffold such as fibrin, which could potentially be sourced from the patient thereby reducing the risk of disease transmission or immune rejection (Ahmed et al., 2008).

Supplementation of TE L/T with ascorbic acid (AA), a cofactor for the enzymes that synthesize collagen, and proline (P), an amino acid that stabilizes the collagen molecule resulted in significant increases in collagen compared to those receiving no treatment (Paxton et al., 2012). However, it was observed that AA+P treatment also produced sinews that were much smaller in width than non-treated constructs.

Excessive contraction and rapid depletion of the TE scaffold is generally undesirable (Sung et al., 2004). Most mammalian cells are adherent, which is why a scaffold is employed and if it is rapidly degraded the cells lose their support structure leading to cell apoptosis (Frame and Hu, 1988). Further, the way in which fibroblasts deposit collagen matrix during wound healing, requires the initial presence of fibrin into which collagen is deposited (Young and McNaught, 2011). The fibrin is then gradually remodelled and eventually completely replaced with collagen. Controlling the rates of contraction and remodelling of the fibrin hydrogel are therefore crucial factors in enhancing TE L/T collagen content. In addition, L/T vary in their size, shape and mechanical strength throughout the body (Kannus, 2000). As a result, processes whereby these parameters can be controlled need to be developed. The ability to control or stimulate construct collagen content and contraction of the fibrin hydrogel scaffold could potentially offer a means of predictably producing bespoke tissue.

1.1 Thesis objectives

This thesis has sought to quantify the differences observed between non-treated and AA+P supplemented constructs during culture and elucidate the mechanism behind AA+P action on fibrin gel contraction and construct collagen synthesis. The mechanical properties of the fibrin hydrogel matrix were also altered to determine the effects of scaffold stiffness on contraction rates and construct widths.

Factors that may lead to variability and affect construct development were also investigated such as the effects of cell type, preparation of the fibrin reagents and medium selection, with a focus on general process improvement.

The aims of each of the results chapters in this thesis are briefly described below:

Chapter 4

This chapter aimed to quantify fibrin gel contraction rates due to supplementation. Following prolonged contraction, differences in size observed between constructs were only the widths, therefore construct widths were also quantified. Morphological differences between control and supplemented constructs were also evaluated using various techniques.

Chapter 5

Properties of the fibrin hydrogel were modified to determine their influence on contraction. In addition, it was of interest to characterise the fibrin gels used.

Chapter 6

Based on results from previous chapters, this chapter sought to optimize construct collagen content and widths.

Chapter 7

Quantifiable cell properties and their effects on fibrin gel contraction were evaluated. It was also of interest to determine if TE L/T sinews could be developed using fibroblasts from different sources.

Chapter 2

Background

2.1 Ligament and tendon structure

Ligaments and tendons (L/T) play a crucial role in holding the body together and permitting movement. When damage through injury or pathologies arise it can often be debilitating. L/T impart and guide movement in the vertebral column, in the limbs such as those used in walking and running to L/T found in the jaw involved in talking and chewing.

Whilst ligaments are responsible for connecting bone to bone, tendons connect muscle to bone (Tozer and Duprez, 2005). Although L/T vary in their function, their biological structure and composition are fairly similar (Rumian et al., 2007). Tendons act by transmitting the force from muscles by pulling on the bone to enable movement (Kannus, 2000). In order to function effectively tendons need to be able to withstand high tensile uniaxial forces whilst restricting extension (Rumian et al., 2007). On the other hand, ligaments function to limit excessive or abnormal movement of the joints (Solomonow, 2004) and therefore must cope with high tensile forces. Depending on the joint, forces experienced by ligaments may take on various directions (multi-axial) (Weiss et al., 2002). In addition, L/T are viscoelastic, which allows them to store a certain amount of energy when deformed permitting them to recoil to their original position once the load is removed, depending on the time scale of application (Provenzano et al., 2001). This capability to withstand high tensile forces, store energy and

the functional difference between ligaments and tendons are due to variations in their anatomical location and molecular arrangement in the extracellular matrix (ECM).

The most common cell type found in connective tissues are fibroblasts and they are responsible for synthesizing ECM proteins such as collagen as well as regulatory growth factors involved in maintenance and repair (Calve et al., 2004). Both ligaments and tendons contain up to 90% collagen in dry weight, elastin as well as ground substance made up of glycoproteins, proteoglycans and water (Rumian et al., 2007; Van Eijk et al., 2004). Human tendons contain slightly lower levels of elastin, approximately 2% (dry weight), whereas in ligaments the elastin content can range from 5%, 7.3% to up to 47% elastin (dry weight) as in the human anterior cruciate ligament (ACL), posterior longitudinal ligament (PLL) and ligaments of the spine, respectively (Kuo et al., 2010). Pyridinoline, a crosslinker present in mature collagen is also approximately 34% greater in tendons than in ligaments (Kuo et al., 2010). Collagen fibrils in the tendon are aligned parallel to each other along the axis of the tendon (Figure 2.1) but in ligaments the fibrils are not uniformly aligned to allow function in multiple directions (Rumian et al., 2007).

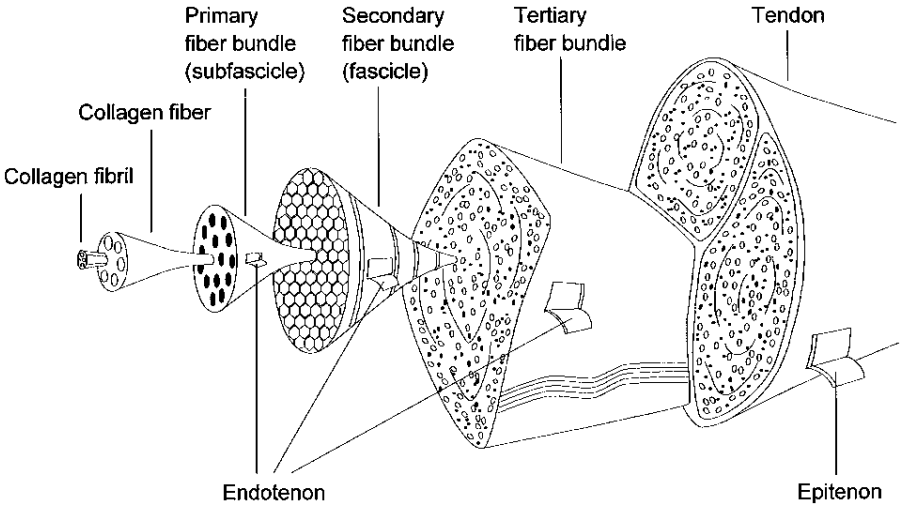

FIGURE 2.1: Tendon Structure. Collagen fibrils are arranged into fibres and consequently larger bundles that form the tendon. Internal bundles of fibres are separated by an endotenon connective tissue and the whole tendon itself is surrounded by a fibrous sheath or epitenon. *From Kannus (2000), with permission.*

Water makes up to 65-75% of tendon wet weight and in combination with proteoglycans (PGs), they are responsible for lubrication and spacing and thereby permit

collagen fibrils to glide past each other (Benjamin and Ralphs, 1997). Ligaments have a higher content of ground substance in comparison to tendons due to greater shearing actions experienced between fibres.

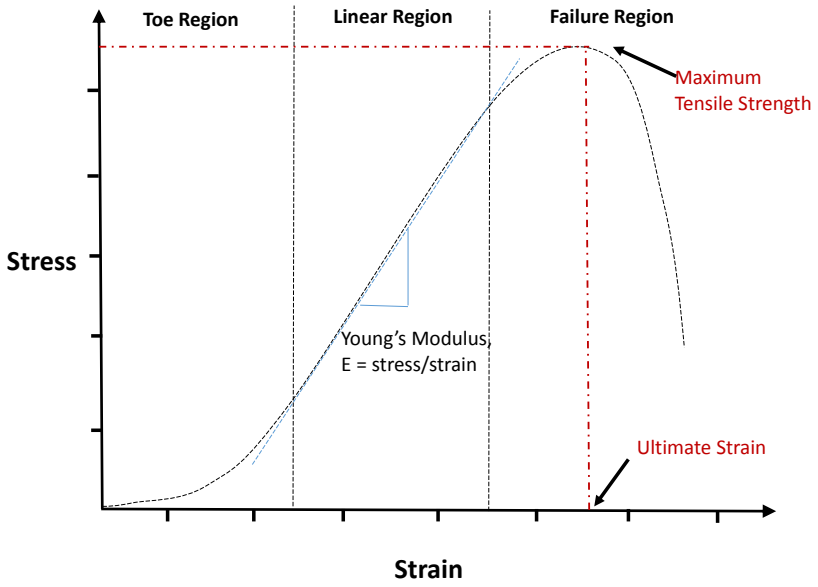

FIGURE 2.2: Ligament stress strain curve. *Adapted from Woo et al. (2000).*

The mechanical attributes of L/T owing to their macromolecular arrangements are best demonstrated by tensile tests. In experimental studies, ligament and tendon mechanical response to strain results in non-linear load-extension or stress-strain curves, which are characterized by three stages (Laurencin and Freeman, 2005). The first is where stress does not change much in relation to strain; this is known as the toe region (Figure 2.2). The toe region corresponds to straightening of crimps that are present in collagen fibres (Laurencin and Freeman, 2005). The crimps are responsible for absorbing the initial loading during extension in both ligaments and tendons and they spring back when tissues return to their original position (Franchi et al., 2010). Following this is the linear region where stress increases with strain in a linear manner. Damage is characterised by a decline in stress when strain is applied, after which failure occurs and consequently this is called the failure region (Laurencin and Freeman, 2005).

The L/T–bone interface or enthesis experiences large stresses and is thus very vulnerable to injury because there is a change in structure from soft to hard tissue (Clark

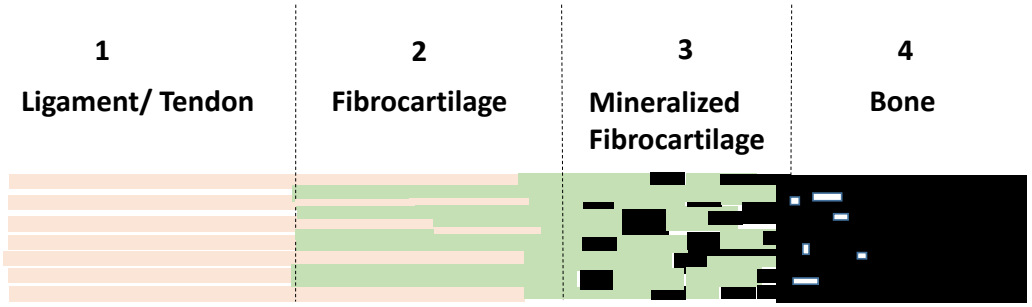

FIGURE 2.3: Zones of the ligament/tendon-bone interface.

and Stechschulte, 1998). However, this change in structure at the interface is graduated, a functional design aimed at minimizing excessive stress concentrations at the region (Benjamin et al., 2006). As a result, injury or failure tends to occur close to the interface – within the ligament itself or at the bone (Hashimoto et al., 2007). The interface gradient is made up of four distinct zones, namely, ligament/tendon, fibrocartilage, mineralized fibrocartilage and bone (Benjamin and McGonagle, 2009; Thomopoulos et al., 2010). At these regions, the cell types differ in relation to the material/ ECM synthesis required. Generally, fibroblasts at the soft tissue and fibrocartilage zones express collagen type I, whilst chondrocytes at the fibrocartilage and mineralized fibrocartilage zones express collagen type II and type X, respectively (Thomopoulos et al., 2010). The bone is formed, maintained and repaired by osteoblastic cells (Mutsuzaki et al., 2004).

At the interface both tensile and compressive loads are experienced and in L/T fibrocartilage is an adaptation to compressive loads that occur during a change in direction (Benjamin and Ralphs, 1998). In addition, the thickness of the mineralized fibrocartilage zone maybe related to the ultimate strength of the L/T (Benjamin et al., 2006).

2.2 Damage to ligaments and tendons and their repair

Injuries to ligament and tendon soft-connective tissue are increasingly common, especially amongst young active people (Adirim and Cheng, 2003). The anterior cruciate

ligament (ACL) is one of the most commonly injured ligaments during sporting activities, occurring at a frequency of 30 ACL injuries out of every 100,000 people in the UK (NHS-Choices, 2012). A human ACL is about 27–32mm in length (Vunjak-Novakovic et al., 2004) and as mentioned earlier, its role is to stabilize the knee joint and it is therefore subject to extreme loads (Rodrigues et al., 2013). Ligaments can withstand maximum loads of up to 1730N and have a stiffness measure of 182N/mm (Vunjak-Novakovic et al., 2004). However, pivoting movements that occur during basketball, soccer, skiing and tennis can lead to ligament injury (Giron et al., 2005).

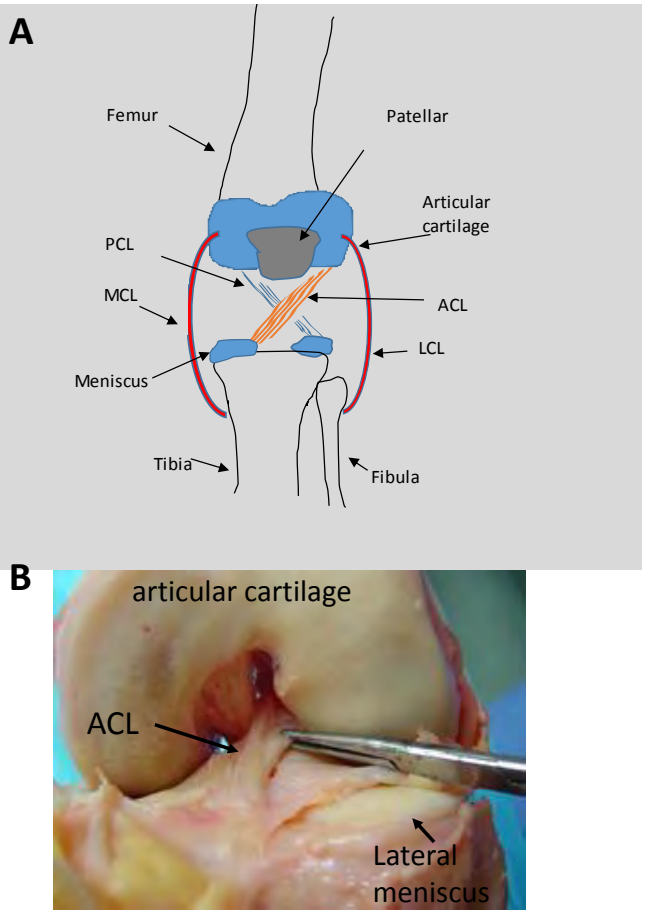

FIGURE 2.4: Anatomy of the left knee. A) Schematic depicting ligaments of the left knee. B) Human ACL of the left knee, adapted from (Zantop et al., 2006), with permission.

Ligament characteristics also vary with anatomic location, age and the presence of disease or injury (Vunjak-Novakovic et al., 2004). The rate of ACL injury is higher in female athletes than in males, resulting even during non-contact activities and that females also sustain their injuries at a younger age (Ireland, 1999; Lohmander et al.,

2004). The cause for the greater occurrence of ligament injuries in females has been attributed to anatomical, hormonal and problems associated with muscles, nerves and proprioception (Hewett et al., 2005). Menstrual hormones such as oestrogen and progesterone are linked to increased risk for ACL damage and have been respectively shown to enhance and decrease the presence of collagenase, a collagen degrading enzyme (Slauterbeck et al., 2002). Anatomical factors due to females having larger 'q' (knee valgus) angles are responsible for putting additional loads on the knee (Ford et al., 2003).

Natural healing of most L/T follows the phases of wound healing, however, this is slow and poor due to low cellularity and limited blood supply (Laurencin and Freeman, 2005). The medial collateral ligament (MCL) is located outside the joint and able to heal without the need for grafting (Leong et al., 2013). However, ruptured or torn ACLs are treated surgically using autografts, allografts and xenografts (Chen et al., 2009). Autografts are taken from the person's own body – such as the middle portion of the patellar tendon along with its bony attachments (Bone-Patellar Tendon-Bone (BPTB) Graft) or two of the four hamstring (gracilis and semitendinosus) tendons (Vunjak-Novakovic et al., 2004). Unfortunately, donor site morbidity is often reported and long healing times are required due to the invasiveness of the procedure (Kartus et al., 2001; Yasuda et al., 1995). Allografts from donor patients are in short supply (Robertson et al., 2006), they usually illicit an immune response as exact tissue matches are difficult to obtain and there is also the potential to transmit disease (Laurencin and Freeman, 2005). Xenografts from synthetic or natural polymers or from animals, such as bovine ligaments, have also been employed (Chen et al., 2009). Rehabilitative exercises are normally recommended immediately after grafting operations in order to return the range of motion, weight bearing ability and to improve general knee stability (Kvist, 2004). Stability of the knee is dependent on several factors such as muscle strength and general proprioceptive ability, consequently, neuromuscular training leads to reduced frequency of ACL injury (Kvist, 2004).

Integration and remodelling of foreign tissue in the body is difficult, especially when xenografts are used, and there is a high occurrence of graft failure (Ventura et al., 2010). In females, ACL graft ruptures occur more frequently, with greater laxity reported after both hamstring and BPTB grafts due to the influence of hormones in

ligament remodelling (Slauterbeck et al., 2002). Not many long-term post-grafting studies have been conducted, however, it is claimed that ACL injury, with or without reconstruction, leads to the development of osteoarthritis, with 50% of patients developing the condition 15 - 20 years after injury (Øiestad et al., 2009).

The achilles tendon is the largest tendon in the body, involved in acceleration and deceleration movements (Trobisch et al., 2010) such as during jumping, running and sprinting and can withstand loads in excess of 12.5 times the body weight (Gajhede-Knudsen et al., 2013). Achilles tendon injuries can make up 90% of reported sporting injuries (Sharma and Maffulli, 2006) and is mostly seen in men aged above 40 years (Hess, 2010). Similarly, quadriceps tendon injury and rupture occur 6 to 8 fold more frequently in men over 60 years of age, normally trying to prevent a fall ((Trobisch et al., 2010) and is often linked to degenerative conditions such as gout, chronic renal failure and others (Ellanti et al., 2012). Due to the strength of tendon, injuries due to over-loading result in ruptures at either the musculotendinous junction or to the osteotendinous junction (Lin et al., 2004). Tendon tears and ruptures are often treated surgically using sutures (Rawson et al., 2013) although allografts from cadavers as well as bovine xenografts have also been used (Magnussen et al., 2011). 70 - 90 % of athletes are reported to return to their sporting activities after achilles tendon surgery, however, 20% require successive operations and around 5% permanently suspend their sporting careers (Kvist, 1994).

As a result of all these factors, methods that will improve ligament and tendon healing are being developed. Tissue engineering of ligament and tendons promises to overcome problems arising due to L/T poor natural healing capacities and the use of grafts.

2.3 Biological aspects of Tissue Engineering

The demand for engineered tissue is rising steadily due to organ donor shortages and the population's increased life expectancy (Atala, 2007). Tissue Engineering (TE), a multi-disciplinary field which is a part of regenerative medicine, aims to provide a means to assist in the regeneration of damaged or diseased tissue and organs (Bonassar and Vacanti, 1998). There are several methods by which this can be achieved,

ideally using autogenic cells from the patient although allogenic and xenogenic sources can also be used (Ikada, 2006). The basic principle involves removing a small amount of tissue, expanding the cells in culture and re-implanting them into the site of injury or disease on a supportive scaffold, leading to eventual integration with native tissue (Fuchs et al., 2001) (Figure 2.5). If the cells are obtained from the patient, this circumvents problems such as immune response rejection and the transmission of infections that can occur with allografts and xenografts.

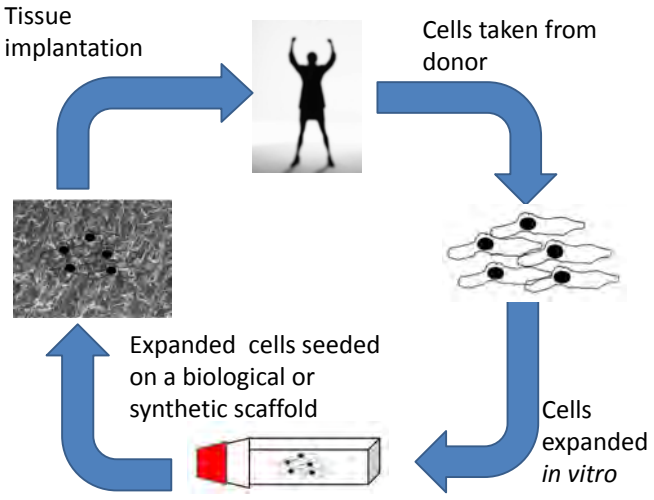

FIGURE 2.5: Tissue Engineering Process

The success of TE depends on understanding the roles of various types of cells, the processes involved in tissue morphogenesis and how cells behave and interact with each other and their environment (Ikada, 2006; Tuan, 2013). The supportive scaffold plays a pivotal role in allowing the migration and proliferation of the cells and guiding the development of the tissue through extracellular matrix deposition and remodelling processes. As a result, scaffold properties and their design have received much attention (O'Brien, 2011). In addition, cells are highly specific and the use of the 'correct' cells, in combination or cells that can be guided down a particular lineage, as with mesenchymal stem cells, is crucial in engineering tissues that resemble native tissue that will lead to functional regeneration (Ge et al., 2005). There should be an emphasis on 'functional' as it is important that the tissues and organs not only appear as found in the body but that the engineered tissues work on a par with or will lead to function that closely matches local tissue (Breidenbach et al., 2013; Butler et al., 2008; Guilak et al., 2001). Due to the complexity and numerous factors

required to engineer functional tissues, which may vary from to tissue to tissue, TE is frequently subdivided into categories relating to the area of application (Saltzman, 2004; Horch, 2006). In recent years, successful applications have been achieved in areas such as bone, cartilage, skin (Horch, 2006) and trachea (Gonfiotti et al., 2014) regeneration.

The following sections will discuss biological aspects relavant to this thesis. Cell functions and their interactions with the matrix are particularly important in understanding the formation of tissues and organs and how to this knowledge can be translated into tissue engineering processes *in vitro*.

2.3.1 Cells and their function

To understand how cells are involved in the development of tissue and organs their behaviors in morphogenesis and wound healing are being studied (Ulloa and Briscoe, 2007). Organs and tissue such as the heart, kidneys, liver, ligaments and tendons, to name a few, all differ in their functions owing to the different properties or specialization of their cells and organization of the extracellular matrix. The cell type used in TE of a specific organ or tissue must therefore match the phenotype and function required or be able to be *induced* to such a type (Ikada, 2006). Primary or differentiated cells are adult and specialized in nature and can be taken from living tissue to be expanded *in vitro*. The use of primary cells is particularly beneficial in autogenic engineering of tissues as they can be sourced from the individual, reducing the risk of rejection and infection (Ikada, 2006). Unfortunately, this is not always productive as some cell types do not proliferate well *ex vivo* and some cells de-differentiate as seen with articular cartilage cells that form fibrocartilage instead of hyaline cartilage (Polak and Bishop, 2006).

Stem cells have gained much attention due to their potential to form any tissue or organ (potency) and their ability to self-replicate (Ulloa and Briscoe, 2007). There are two main types of stem cells, namely, embryonic and adult stem cells. Embryonic stem cells are concerned with embryonic and foetal development, whilst adult stem cells are responsible for growth, maintenance and the regeneration and repair of damaged or diseased tissue (Jukes et al., 2008). The ability for self-renewal could

potentially provide large cell stores of undifferentiated cells for use in tissue engineering (Lanza et al., 2011). Stem cell self-renewal occurs due to the two forms of cell division, symmetric and asymmetric, that can take place. In symmetric division, a stem cell will divide to form two daughter cells that are identical, that will remain either undifferentiated or will both differentiate. Asymmetric division results in one daughter cell remaining as a stem cell and the other differentiating into a progenitor cell, which can only divide a limited number of times and is more specific than a stem cell (Knoblich, 2008). The mechanism for the two forms of division are not yet fully understood but one theory is that the balance between the two modes is determined by developmental and environmental signals (Morrison and Kimble, 2006). The potency of a stem cell is also of importance as it determines the number of cell types it can differentiate into. Current research is largely focused on the use of pluripotent and multipotent stem cells. Embryonic stem cells are pluripotent and can form all three germ layers, ectoderm, mesoderm, and endoderm, which lead to the formation of tissues and organs (Rossi et al., 2010), whereas mesenchymal stem cells (MSCs) are multipotent and can form multiple tissue types such as cartilage, bone and fat (Jukes et al., 2008).

According to Nindl Waite and Waite (2007), differences in cell function are due gene expressions that vary with time and intensity. For example, genome analyses have identified a 99% similarity between the genome of humans and chimpanzees, however it is not the number of genes and their similarity that determine the characteristics of an organism but rather the expression of those genes into mRNAs and proteins and consequently, this provides a similar explanation for differences between cell types in one person or organism (Nindl Waite and Waite, 2007).

Cell communication between individual and neighbouring cells is an important aspect of differentiated cell specialization and in order for cells to function as a unit they need to be able to proliferate, migrate and attach to each other as well as to their supporting extracellular matrix (Friedl and Gilmour, 2009). Almost all mammalian cells are by nature adherent cells that need a surface to attach to and cannot be in suspension, as is the case with blood cells (Cooper and Hausman, 2000). The signals received from cell-cell contacts and cell-matrix adhesion result in the expression of various genes and their translation into mRNA and proteins. This results in regulatory cascades with feed-back and feed-forward loops.

2.3.1.1 Cell proliferation

Cell proliferation has briefly been touched upon in the previous section and will only be shortly expanded on. Most tissues do not contain proliferating cells as fully differentiated cells do not divide, however, cells needed for tissue repair proliferate and normally these are stem cells and progenitor cells (Cooper and Hausman, 2000; Malumbres and Barbacid, 2001). Cell proliferation is an important part of growth; usually, as tissues expand and increase in size, cell number also increases (Saltzman, 2004). However, cell proliferation must be regulated as excess cell growth leads to cancers (Evan and Vousden, 2001) and the balance between cell proliferation and cell death (apoptosis) is achieved by the correct function of the cell cycle (Malumbres and Barbacid, 2009).

Cell division is composed of four stages G1, S, G2 and M, which make up the cell cycle (Figure 2.6).

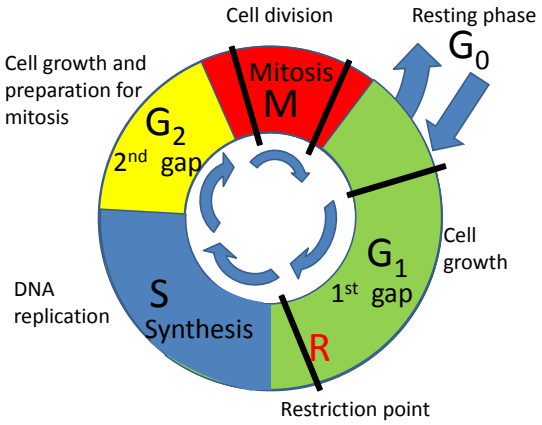

FIGURE 2.6: The typical cell cycle. Stages G1, S and G2 can last 16-24 hours, whilst M may be just an hour or two. There are several checkpoints in the cycle that monitor availability of nutrients and growth factors as well as the accuracy of DNA synthesis and replication before mitosis can go ahead (Cooper and Hausman, 2000; Nussbaum et al., 2007).

S is the synthesis stage where DNA is segregated, M is mitosis where DNA is packaged and chromosomes are split, leading to cell division, G1 is a gap stage between M and S and G2 is is a gap stage between stages S and M (Tyson and Novak, 2001; Cooper and Hausman, 2000). For cell division to occur DNA needs to be replicated and segregation of the sister chromatids needs to occur to result in two genetically identical daughter cells (Tyson and Novak, 2001). Before DNA can be replicated,

activation of the DNA synthesis enzymes, a family of protein kinases called cyclin dependent kinases (Cdk) that produce nucleotides, must happen (Tyson and Novak, 2001; Hyland, 2007). To function or initiate/stop the cell cycle, Cdk forms a complex with a protein (cyclin), which becomes phosphorylated or dephosphorylated thereby turning it on or off (Csikász-Nagy et al., 2006). This process occurs in the late stages of G1. The production of DNA synthesis proteins for cell division depends on the availability of growth factors and nutrients in the extracellular matrix. Quiescent cells in G0/G1 require growth factors to enter the growth phase (Brooks, 1976) and it is only in the G1 stage that cells are sensitive to signals from the ECM (Hyland, 2007). Growth factor signals are needed until the late G1 phase, which is called the restriction point. In order for the cycle to progress from early G1 to late G1, transcription cyclin E must be synthesized and this requires the growth factor E2F. If this step is inhibited by a protein called Rb (retinoblastoma) binding to E2F, proliferation does not occur (Harbour and Dean, 2000). Essentially, Rb works as a arrestor or controller on the proliferation process and proliferation will only resume if Rb is phosphorylated, causing it to release from E2F (Weinberg, 1995). Other proteins can inhibit proliferation by directly binding to Cdk and preventing the enzymatic protein kinase activity. In addition, mitogens or chemical molecules that lead to signal transduction pathways such as cytokines, hormones or growth factors can also be involved in mitosis and act as switches that can turn the cycle from an inactive to active state or vice-versa (Saltzman, 2004). Mitogens activate protein kinases known as Mitogen Activated Protein Kinases (MAPK) to initiate the Ras/Raf/MEK/ERK signaling cascade (Chambard et al., 2007). There are four mammalian MAPK pathways, namely: (i) ERK pathway is activated by cell surface receptors, (ii) p38, (iii) ERK5 and (iv) JNK are activated by growth factors and stress (Roberts and Der, 2007) as well as certain mitogens (Zhang and Liu, 2002). Several studies have shown that ascorbic acid activates the ERK pathway (Park et al., 2005; Mimori et al., 2007; Temu et al., 2010).

A great challenge in tissue engineering is obtaining the required size and shape of TE constructs. Amongst other factors, engineering functional tissue and maintaining their size could be achieved by maintaining a balance between the rate of cell proliferation and apoptosis as well as control of the rates of matrix degradation and remodelling. This necessitates in-depth knowledge of how cells interact with their matrix through cell-matrix adhesion complexes.

2.3.1.2 Cell adhesion

As most mammalian cells are anchorage dependent adhesion to a solid surface or extracellular matrix is crucial for cell survival (Frame and Hu, 1988). The cell membrane consists of a phospholipid bilayer engulfed by a polysaccharide layer called glycocalyx, which is ionizable resulting in a net negative charge on the cell surface (Saltzman, 2004). Tissue culture surfaces such as petri dishes are normally coated with Poly-L-lysine, whose amine groups are positively charged (Mazia et al., 1975; Saltzman, 2004). This allows non-specific adhesion of various types of cells to the solid surface through weakly attractive electrostatic Van der Waals forces (Saltzman, 2004). Cell adhesion plays an important part in tissue engineering and regeneration as the strength of adhesion can affect rates of cell migration, kinetics of cell-cell attachment or result in resistance to diffusion (Saltzman, 2004).

Cells need to function as a unit and respond to their environment in order to migrate, grow, proliferate, differentiate and ultimately form, maintain and repair tissue (Alberts, 2000). In order to do this they have to be able to communicate with each other and gain information about their environment. For cell-cell adhesion to occur and with cells being negatively charged, receptor-ligand interactions are necessary, which can lead to signal transduction pathways such as described in Section 2.3.1.1. Cell-cell adhesion can occur through three modes: (i) a cell membrane receptor attaching to ligands on another cell, (ii) receptor of two cells attached to the same ligand or (iii) cell surface receptors binding to similar receptors on other cells (Alberts, 2000; Saltzman, 2004). Similarly, for cell-matrix adhesion, cells are able to interact with the ECM using cell surface receptors that bind to specific ligands present in the ECM.

In developed tissue, stabilization of cell-cell or cell-matrix contacts are enhanced through the formation of adhesion junctions, namely, tight, anchoring and communicating cell adhesion junctions (Saltzman, 2004). In tight junctions, cells are tightly connected to each other, with little or no space between them (Saltzman, 2004). This allows the cells to act as a protective barrier and gives control over the diffusion of molecules in and out of the cells, for example by only allowing molecules of a specific charge or size to pass through (Hartsock and Nelson, 2008). Anchoring junctions confer mechanical stability and are a result of the associations of intracellular actin filaments, which connect the cytoskeleton to the membrane *i.e.* the cell membrane

and cell surface receptors that form links to ligands on the membrane of a neighbouring cell or the matrix (Saltzman, 2004). Adhesion contacts that consist of several cells are responsible for contractile and folding movements generated during tissue morphogenesis and wound healing (Friedl and Gilmour, 2009). The end points of actin filament bundles present on the cell membrane act as focal adhesion sites that link the cell to the ECM (Wozniak et al., 2004). Focal adhesion points act as mechanical anchors and also transmit signals from the ECM to the cytoskeleton (Ren et al., 2000).

The cell surface receptors involved in cell-cell adhesion are cadherins, whilst those responsible for cell-matrix adhesions are integrins (Weber et al., 2011).

Cadherins

Cadherins are transmembrane proteins responsible for cell-cell adhesion that is Ca^{2+} dependent (Alberts, 2000). These are found in adhesion junctions where they form linkages with actin filaments in the cell cytoskeleton. Vital to the function of cadherins are cytoplasmic proteins called catenins. α, β and γ catenins form complexes with cadherins, which allows the cadherins to function fully as cell adhesives and improves cadherin-cadherin affinity (Kemler, 1993; Saltzman, 2004). α-catenins are responsible for linking cadherins to actin filaments and other transmembrane proteins (Weis and Nelson, 2006).

Integrins

Cell-matrix adhesion requires the participation of cell surface glycoproteins called integrins (Berrier and Yamada, 2007). Integrin molecules contain 1-18 α and 1-8 β subunits arranged in different combinations (van der Flier and Sonnenberg, 2001; Berrier and Yamada, 2007). Many integrins bind to the same ligands on ECM components that contain the amino acid sequence Arg-Gly-Asp commonly known as RGD (Saltzman, 2004). Typical ECM components that have the RGD sequence are vitronectin, fibronectin and tenascin though on collagen and laminin these are more obscure (van der Flier and Sonnenberg, 2001). Fibroblasts do not spread on synthetic polymers that do not contain the RGD sequence (Kourouklis et al., 2014). Integrins also play a role in cell-cell adhesion such as with non-adherent blood cells (Alberts, 2000). Adhesion of cells to the matrix results in the activation of signaling pathways that drive cell growth, proliferation, differentiation and apoptosis (Chen et al., 1994).

Fibroblasts express integrins with subunit arrangement $\alpha_1\beta_1$ and $\alpha_2\beta_1$ that bind to collagen simultaneously, however, $\alpha_2\beta_1$ has been found to have a greater affinity for Collagen type I (Heino, 2000). In three dimensional collagen matrices, cells deficient in $\alpha_1\beta_1$ receptors showed decreased growth whereas presence of $\alpha_2\beta_1$ enhanced the expression of collagen degrading enzymes MMP1- and MMP-13 (Heino, 2000; White et al., 2004). The two integrins appear to have different roles in how they relate to the matrix; during wound healing $\alpha_2\beta_1$ expression is upregulated by fibroblasts whilst that of $\alpha_1\beta_1$ is downregulated (Heino, 2000). Endothelial cells proliferate during wound healing and they possess $\alpha_V\beta_3$ as their most prominent integrin (Hall et al., 2001). In addition, dermal endothelial cells cultured in fibronectin or fibrin gels expressed higher mRNA levels of $\alpha_V\beta_3$ than when cultured in collagen gels. As a result, $\alpha_V\beta_3$ is an integrin implicated in cell-fibrin adhesion. Cell-cell adhesion can also be mediated by fibrinogen though binding of $\alpha_{IIb}\beta_3$ and $\alpha_X\beta_1$ on fibrinogen motifs Lys-Gln-Ala-Gly-Asp-Val (KQAGDV) and Gly-Pro-Arg-Pro (GPRP), respectively (Hynes, 1992).

2.3.1.3 Migration

The movement of cells from one location to another is termed cell migration. This occurs in response to physical or chemical cues in their environment such as during wound healing, angiogenesis, immunogenic response and preferred matrix stiffness (Lo et al., 2000). Migration due to chemical or molecular substances is called chemotaxis (Saltzman, 2004). The term durotaxis is given to the migration of cells in response to the stiffness of the matrix (Lo et al., 2000). Cell-matrix adhesion is an important part of cell migration and different types of cells prefer matrices of differing stiffness (Hadjipanayi et al., 2009) as this can affect their function and ability to mobilize (Reinhart-King et al., 2008). If the matrix is too soft, cells cannot establish adequate adhesion required for motility and if the matrix is too rigid, strong adhesion results and cell migration is impaired. Migrating cells can do so independently or in unison, depending on the cell type, the cytoskeletal arrangement and adhesion to the ECM.

Cells have a definitive front and rear end or cell polarity (Berrier and Yamada, 2007). From the main body of the cell, the front end has protruding lamella and several

lamellipodia extending in the direction of movement (Raftopoulou and Hall, 2004). The rear end of the cell acts as a retractable tail. To propel the cell, the front or leading edge lamellipodia detach and extend forward to establish new adhesive connections, as the new adhesive connections are established, the main body is pulled forward and the rear end detaches, retracts and adheres to the matrix again at a new position (Raftopoulou and Hall, 2004) (Figure 2.7).

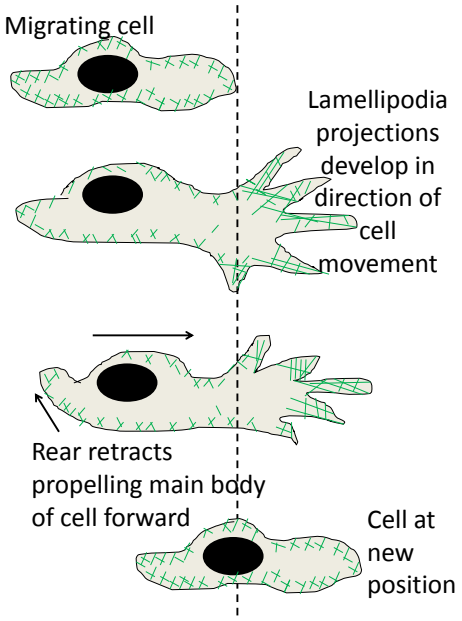

FIGURE 2.7: Cell migration. Migrating cell develops actin cytoskeletal protrusions (lamellopodia), which extend forward, adhering to the matrix. The rear of the cell retracts propelling the main body forward as the cell arrives at its new position. *Note: The green colour represents the actin cytoskeletal filaments.*

These steps require the assembly, disassembly and reorganisation of the actin cytoskeleton as the forward extension of the lamellipodium is due to growth of actin filaments and attachment/detachment involves controlling cell-matrix adhesive contacts (Ballestrem et al., 2000; Raftopoulou and Hall, 2004).

Fibroblasts have highly organized skeletal structures and adhere strongly to the ECM, resulting in slow migration rates. In contrast, immune cells need to act rapidly and consequently have fast amoebic-like migration patterns as they lack highly ordered cytoskeleton and have weak cell-matrix interactions. Some diseases occur due to the migration of cells to the wrong place. Rheumatoid arthritis is the result of inflammatory cells migrating to the joints and degrading the structures leading to disease.

Cancer spreading or metastasizing is the migration of tumor cells to neighboring and distant tissues, which causes secondary tumors.

2.3.1.4 Cell signalling

The development of cell-matrix adhesion contacts is crucial for anchoring the cells and migration but also for creating signal transduction pathways involved in cell growth, proliferation and synthesis or degradation of ECM components. Focal adhesion sites are rich in enzymes such as Focal Adhesion Kinases (FAK), which phosphorylate or dephosphorylate other proteins, thereby acting as on or off switches for various processes. Cell-cell as well as cell-matrix adhesion leads to the activation of Ras and Rho regulated signal transduction pathways. The signalling molecules Ras and Rho belong to the GTPase superfamily. Rho determines, focal adhesion and actin stress fibre formation (Saltzman, 2004), gene transcription, cell cycle regulation and apoptosis (Moon and Zheng, 2003). Ras is also involved in mitogenesis and cyctoskeletal rearrangement as well as vesicle traffic and nuclear transport (Macara et al., 1996).

Myofibroblasts have a specialised contractile function useful in remodelling and contracting granular tissue during wound healing. The expression of alpha-smooth muscle actin, required to generate contractile forces and their expression of Collagen Type I is regulated by TGF-β1, a growth factor cytokine (Tomasek et al., 2002; Wang et al., 2007). Contractile function of myofibrasts can be short-lived or sustained. The short-lived pathway is Ca^{2+} dependent whereas sustained contraction, which appears to be the main pathway, is led by the Rho kinase activity (Tomasek et al., 2002). Tension in the ECM as well as RhoA dependent/mediated cell cytoskeletal tension have been shown to lead to greater expression of the ECM protein Tenascin-C, suggesting that mechanical tension is necessary for ligament and tendon repair (Sarasa-Renedo and Chiquet, 2005; Wang et al., 2007).

2.3.2 Tissue morphogenesis and wound healing

"Morphogenesis is the process by which a population of cells rearranges into the distinctive shape and form of a tissue" (Nelson, 2009). Most tissues such as the heart, liver and kidneys are complex in nature and comprised of more than one

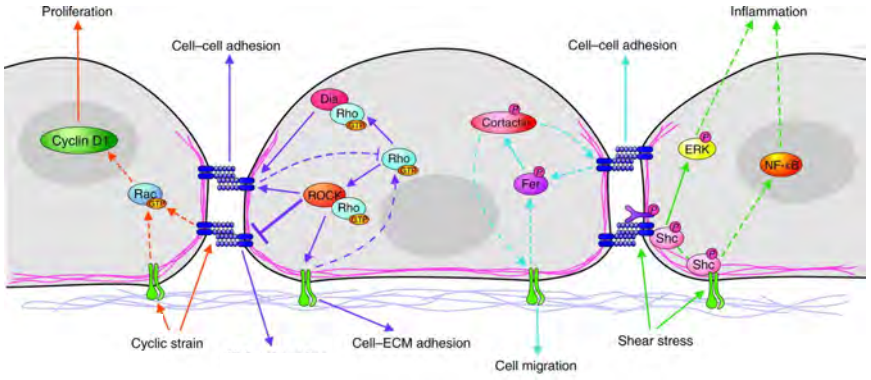

FIGURE 2.8: Cell-cell and cell-matrix adhesion complexes. The interactions initiate signal transduction pathways that result in cell proliferation, migration or stress fibre generation. Image from (Weber et al., 2011), used with permission.

cell type, necessary for tissue development, homeostasis and repair capabilities. For example, the liver tissue is a complex three dimensional arrangement of liver hepatic cells, vascularisation system and bile canaliculi and ducts. One of the challenges in tissue engineering the liver has been that primary hepatocytes do not proliferate well and rapidly deteriorate in function when *in vitro* (Hammond et al., 2006). It has been found that co-culturing hepatocytes with 3T3 fibroblasts leads to increased proliferation and maintained hepatic function (Bhandari et al., 2001; Lu et al., 2005; Seo et al., 2006; Stevens et al., 2013). Since cell-cell communication is vital for determining correct tissue morphology and consequently function, studies including more than one cell type in co-culture are required to understand the formation of complex three dimensional tissue and how to engineer them (Hendriks et al., 2007; Stevens et al., 2013). Aggregate formation is a tool that with further development will allow for better understanding of tissue formation including cell-cell communication (Saltzman, 2004). Some intermingling cell aggregates made up of two or more cell types sort or rearrange themselves into distinct layers or regions. This phenomena is akin to that seen in immiscible liquids, where the liquids separate out into phases due to differences in surface tension (Lecuit and Lenne, 2007). Cell sorting is slightly more complicated than immiscible liquids as rearrangement depends not only on cell surface tension or adhesion molecules but also cell shape (Lecuit and Lenne, 2007; Nelson, 2009). In addition, formation into tissue/organs depends on the (bio)chemical cues or morphogens being present as well as signals from the ECM, particularly the geometry surrounding the cells and mechanical tensile and compressive forces (Nelson, 2009).

When a cut or trauma that causes disruption and exposure of the tissue or organ contents occurs, the wound healing process initiates in order to repair the injured site. Many aspects of wound healing are being studied in order to mimic the processes and use them as models in tissue engineering and regeneration. During the wound healing process, cells migrate to the injured location resulting in cell proliferation, formation of new blood vessels, the deposition of new ECM, formation of scar tissue and its remodelling (Enoch and Leaper, 2008). These processes are regulated by cytokine and growth factor signalling proteins, matrix metalloproteinases (MMPs) and tissue inhibitors of metalloproteinases (TIMPs) and the presence of platelets and inflammation cells (Enoch and Leaper, 2008).

The first stage in wound healing is to minimize loss of blood or haemostasis by constricting blood vessels and arteries and forming a clot to plug the wound. Clot formation is achieved through three possible mechanisms: (i) damage to the endothelial exposes inner tissue cells to blood, leading to a cascade activation of factor X which converts pro-thrombin to thrombin causing fibrinogen to be polymerized to a fibrin clot, (ii) an extrinsic pathway where factor VII is activated eventually resulting in thrombin activation and (iii) activated platelets clump together attaching to collagen to form a clump, which is strengthened by platelet myosin and actin fibres, the von Willebrand factor and the formation of fibrin (Young and McNaught, 2011).

Inflammation is the second stage and its occurrence is usually undesirable as it suggests the presence of an infection. If bacteria or debris are present at the wound, neutrophil and macrophage inflammatory cells migrate to the site in response to signalling chemokines to 'fight' the infection by engulfing the foreign contaminant or releasing toxins to destroy it until the infection is cleared (van Blitterswijk, 2008). Macrophages contain large stores of TGFβ and Epidermal Growth Factor (EGF) required for angiogenesis, which are necessary for nutrient transport to the site of repair. At later stages of inflammation, T-lymphocytes locate to the wound and are responsible for regulating the production of an extracellular matrix scaffold and remodelling of collagen (Young and McNaught, 2011). Platelets express Vascular Endothelial Growth Factor (VEGF) and angiogenesis begins once haemostasis and inflammatory are stabillized (Young and McNaught, 2011). Expression of Platelet Derived Growth Factor (PDGF), Epidermal Growth Factor (EGF), TGF-β and Fibroblast Growth Factor (FGF) results in fibroblasts migrating and proliferating into

the wound to synthesize extracellular proteins such as fibronectin, collagen and proteoglycans (Enoch and Leaper, 2008).

The final stage of wound healing is remodelling. The new ECM is organized and scar tissue is removed.

2.3.2.1 The Extracellular Matrix

As mentioned in previous sections of this thesis, the ECM is the three dimensional space that surrounds cells in a tissue or organ and functions as an adhesive and supportive structure. Thus far, the ECM has been referred to without going into detail regarding its composition. The ECM is made up of proteins, glycosaminoglycans (GAGs) and proteoglycans that provide mechanical strength as well as offering cues required for differentiation, migration, growth, proliferation and gene expression of certain functional proteins (Juliano and Haskill, 1993). As a result, the ECM is constantly undergoing change, responding to environmental stimulus such as mechanical loading and hypoxia (van Blitterswijk, 2008). Fibroblast connective tissue cells and their specialized subfamilies of chondrocyte and osteoblasts are responsible for secreting ECM molecules and proteins in the form of pre-cursors (pro-α-chains) (Ivanova and Krivchenko, 2012). Composition, concentration and spatial arrangement of ECM components varies between tissue and organ types, determining its function (Alberts, 2000). Soft connective tissue are high in structural fibrillar proteins such as collagen types I and II, cartilage obtains its shock absorbing properties from high concentrations of hyaluronan and proteoglycan aggrecans and the rigidity of bone is a function of calcium phosphate present in the fibrillar collagen matrix (Watt and Huck, 2013).

GAGs are linear polysaccharide chains, which are usually highly sulfated and negatively charged (Rudd et al., 2010). Sulfated GAGs include chondroitins, dermatan and keratans whereas heparan, a basement membrane GAG and hyaluronan are unsulfated (Gandhi and Mancera, 2008). GAGs have extensive interaction with proteins such as growth factors, chemokines and cytokines (Taylor and Gallo, 2006) and the GAG long chains shield the proteins from proteolysis (Antonio and Iozzo, 2001). Connective tissues have high quantities of hyaluronan (hyaluronic acid), which aids cell migration and proliferation and maintains tissue hydration (Kogan et al., 2007).

The long chains are not very flexible though highly soluble in water and assume conformations that can trap large volumes of aqueous medium to form hydrated gels, a property that gives cartilage its resistance to compressive stress (Saltzman, 2004). Apart from cartilage, synovial fluid also has a significant hyaluronic acid content to lubricate the joints (Kogan et al., 2007).

Proteoglycans are GAGs that are covalently bonded to a protein and as with GAGs, proteoglycans offer a platform for signal transduction and provide additional structural support to tissues (Linhardt and Toida, 2004). Aggrecan, versican, neurocan and brevican known as lecticans are members of the chondroitin sulfate proteoglycan family that offer resilience to compressive force (Yamaguchi, 2000). Other small-proteoglycans whose proteins have leucine-rich repeat structures (SLRPs), form u-shaped structures suitable for protein-protein interactions (Kresse and Schönherr, 2001). Members of the SLRP family are decorin, biglycan, bromodulin, lumican, and keratoca. Decorin is present in connective tissue and along with other SLRPs, contributes to collagen fibril assembly and its regulation (Kresse and Schönherr, 2001). A study by Matuszewski et al. (2012) with the human supraspinatus tendon, located in the upper back, showed that aggregan and biglycan distribution varied throughout the tendon with highest concentration being in the anterior and posterior regions that experience higher compressive stress and are prone to injury; decorin concentration was high throughout the tendon as expected in areas of high tensile strength. Proteoglycans that contain heparan sulfate play a crucial role in cell growth as growth factors and signalling receptors have a high affinity for heparan sulfate and form complexes with it (Saltzman, 2004).

Fibronectin, a glycoprotein, is the second most prevalent protein found in the ECM next to collagen that has RGD ligands, which are important in integrin mediated cell adhesion. It is found in fibrous connective tissue and basement membranes (Yamada and Kleinman, 1992). The fibronectin molecule is dimeric, consisting of two polypetides joined together by a disulfide bond at the carboxyl termin and folded into several globular domains. These globular domains allow fibronectin to form simultaneous attachments to collagen, other ECM components and cells (Singh et al., 2010; Kadler et al., 2008). Apart from RGD, fibronectin also has a secondary binding region to which neural and lymphocytes can adhere but not fibroblasts (Saltzman, 2004).

Elastin is a nonglycosylated protein that provides elasticity and resilience to tissues, especially those subject to repeated stretching (Mithieux and Weiss, 2005; Saltzman, 2004). Water is paramount for elastin function as elastin is only elastic when hydrated (Debelle and Tamburro, 1999). Elastin content in ligaments is low, except for ligaments found in the cervical column and intervertebrally (Culav et al., 1999). Tenascin is a glycoprotein whose expression increases during embryonic development (Chiquet-Ehrismann et al., 1986) and the initial inflammation stages during wound healing (Midwood and Orend, 2009). Tenascin is also an elastic protein and is seen in tendons as tenascin-C, regarded as a general tendon marker, which is expressed in response to mechanical stress. Fibronectin adhesion properties have been shown to be affected by tenascin, resulting in cell shape changes and consequently detachment from the ECM or inability to attach to the ECM (Chiquet-Ehrismann et al., 1988). Mehr et al. (2000) suggest that tenascin expression in tendons is a cellular adaptation to compression requirements. Thrombospondin is a gylcoprotein released from platelets that interacts with fibronectin and has a role in cell growth. During wound healing, thrombospondin-1 is expressed and Crawford et al. (1998) have shown that thrombospondin-1 leads to activation of TGF-β1 *in vivo*.

Other noteworthy proteins of the ECM are laminin and vitronectin. The ability of basement membranes to hold cells and tissues together is largely attributed to their high content of laminin. In embryonic development, laminin is crucial for vascular development and maintenance (van Blitterswijk, 2008) and allows interaction between plasma membrane cells and the basement membrane (Aumailley, 2013). Vitronectin is found in blood and the ECM where it is usually associated with fibronectin. Many cell types are able to adhere to vitronectin and its name reflects its ability to bind to cells as well as glass beads (Hayman et al., 1983). Vitronectin is very susceptible to protease degradation and enzymes present during wound healing such as thrombin, elastase and plasmin, which have been shown to cleave vitronectin (Schvartz et al., 1999).

2.3.2.2 Fibrin

Fibrin is a major component of blood clots that acts as a plug and matrix to which cells can attach during wound healing (see section 2.3.2 on wound healing). Fibrin is

formed through thrombin mediated cleavage of fibrinogen. Fibrinogen is a glycoprotein composed of two Aα-Bβ-γ chains linked together by disulfide bonds (Mosesson, 2005). A and B are cleaved off the Aα-Bβ-γ chains, located in the middle of the fibrinogen molecule, by the enzyme thrombin. Fibrinopeptides A are cleaved more readily than fibrinopeptides B. Cleavage of A and B fibrinopeptides exposes knobs A and B that fit into complementary holes 'a' and 'b' located on the γ chains (Janmey et al., 2009b). As proposed by Ferry (1952), joining of the protofibrils at A-a is important in creating a half-staggered arrangement whereas B-b interactions promote fibril lateral connections (Janmey et al., 2009b).

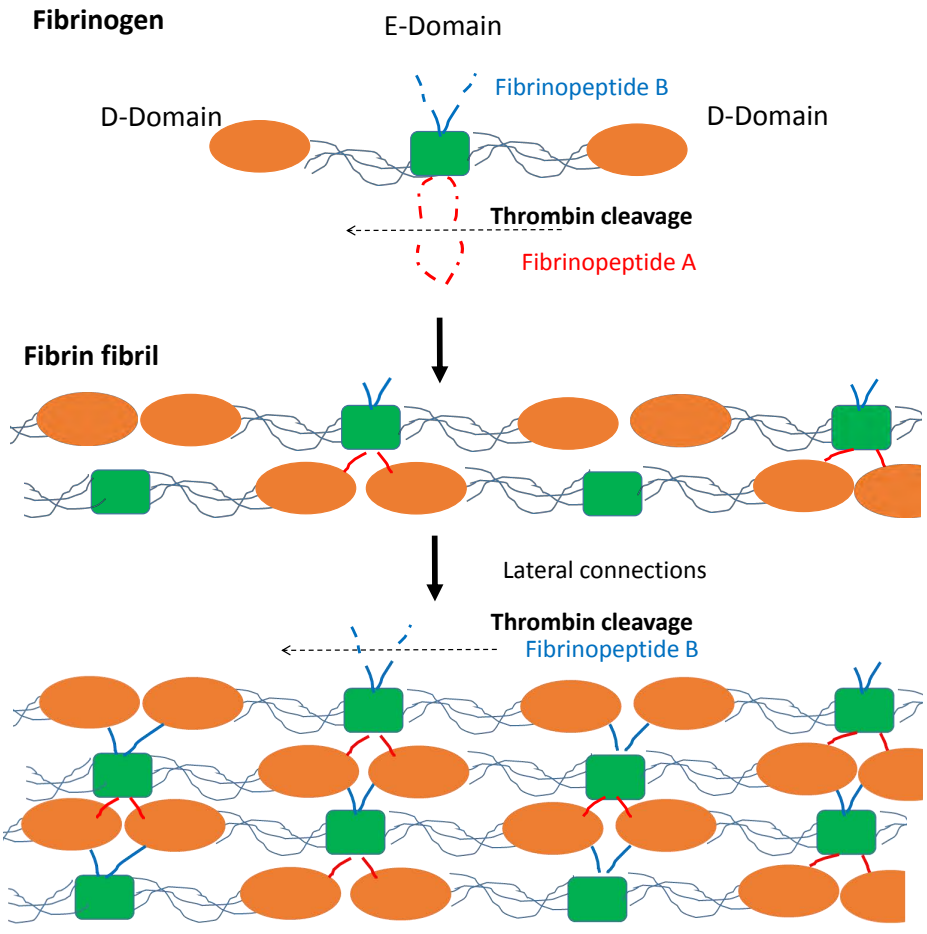

FIGURE 2.9: Fibrin fibril formation. Thrombin cleaves fibrinopeptides A & B to produce staggered fibrils with lateral connections. *Adapted from Janmey et al. (2009a).*

The resulting fibrin monomers lengthen and form double stranded fibrin protofibrils, which aggregate to form fibrin fibrils. Limits to fibrin fibril diameters formed via

lateral connections are due to the increasing amounts of energy required to stretch and link A-a and B-b interactions of the twisted double stranded protofibrils as the diameter increases (Janmey et al., 2009b). When thick fibrils cannot be formed, thinner fibrils ensue with a greater degree of branching. Branching is important for forming a gel network and the extent of branching varies and depends on several factors, three being the concentrations of thrombin, fibrinogen and the pH (Mosesson, 2005). Low levels of thrombin result in thicker fibres with larger pores and high thrombin volumes lead to small diameter fibrin fibres (Standeven et al., 2005; Janmey et al., 2009a).

Fibrin is known to be viscoelastic, possessing both elastic and viscous properties and the mechanical properties of fibrin can also be influenced by the diameters of the fibres, quantity of branching and fibrin concentration (Standeven et al., 2005). *In vivo*, an enzyme, transglutaminase (Factor XIIIa), covalently crosslinks the γ chains to stabilize fibrin and reduce sensitivity to proteolysis (Ahmed et al., 2008). Plasmin inhibitors are cross-linked together with fibrin and simultaneously the generation of fibrin activates the the fibrinolytic system, creating a balance between fibrin formation and degradation, however, only fibrin and not fibrinogen initiates enzymatic digestion, a mechanism that localizes the process (Standeven et al., 2005).

2.3.2.3 Collagen

Collagen is the most abundant protein found in the body. There are over 20 different types, which play different roles - varying in size, function and distribution. Collagen types span several groups, including fibril forming (I, II, XI), fibril associated (IX, XII, XIV), transmembrane (XIII, XVII), network forming (VI, VII, X), anchoring, basement membrane (IV) and unique function collagens although most types fall in the fibril forming category (Gelse et al., 2003).

In connective tissue such as ligaments and tendons, Collagen I is most prevalent, constituting up to 90%, respectively, and will be focused on here. Collagen type I is a structural protein with a triple helical conformation made up of two $\alpha 1$ chains and one $\alpha 2$ chain, that offers load bearing tissue sufficient mechanical strength to withstand unixial and multiaxial loads (Gelse et al., 2003). The folding of the triple helix is due to glycine (Gly) recurring as third residue in the Gly-X-Y amino acid

sequence, where X and Y are most commonly the amino acids proline and hydroxyproline, to give Gly-Pro-Hyp (Ramshaw et al., 1998). It is the close packing of the three stands, hydrogen bonding and the high concentration of amino acids proline and hydroxyproline stabilizes the triple helix (Ramshaw et al., 1998). Gly is hidden in the centre of the structure whereas residues X and Y are highly exposed, giving the amino acid sequence both structural integrity and allowing for intermolecular interactions (Ramshaw et al., 1998). The amino acids proline and 4-hydroxyproline are also referred to as imino acids (Ramshaw et al., 1998; Wu et al., 2011) as they have one hydrogen atom attached to the nitrogen atom and when this is in use, there are no free hydrogen atoms available for hydrogen bonding. As a result, the presence of proline/hydroxyproline in the collagen molecule provides the twists and turns required to form the helical conformation for stability. When X and Y residues are not imino acids, they allow collagen fibril formation through attachment to other collagen molecules, integrins or ECM molecules (Brodsky and Ramshaw, 1997; Ramshaw et al., 1998). It has been determined that hydroxyproline has a greater stabilizing role than proline due to its ability to trap water through a water network with a Gly residue in the same sequence or a Hyp in an adjacent one and this is dependent on Hyp always being present in the Y position (Brodsky and Ramshaw, 1997; Bhattacharjee and Bansal, 2005). Further stabilization of the collagen triple helix is achieved through binding of individual helices (tropocollagens) into collagen fibrils (Bhattacharjee and Bansal, 2005). These fibrils can also join to form bundles and cross-link for enhanced stability (Bhattacharjee and Bansal, 2005).

Synthesis of collagen happens in stages, intracellularly and extracellularly and begins with collagen gene transcription, which depends on the cell types and is instigated by several growth factors and cytokines. In bone, TGFβ and insulin-like-growth factors are responsible but in other tissues FGFs are more important (Gelse et al., 2003).

Once transcription has occurred, the mRNA containing a signal recognition domain, enters the cytoplasm where it is recognised by a signaling molecule on the endoplasmic reticulum and is translated to preprocollagen. After removal of the signal protein, preprocollagen becomes procollagen through further post-translational steps: (i) hydroxylation of the proline and lysine domains happens and is catalysed by enzymes prolyl 3-hydroxylase, prolyl 4-hydroxylase, and lysyl hydroxylase, whose function requires ferrous ions, 2-oxoglutarate (α-ketoglutarate), molecular oxygen and ascorbate

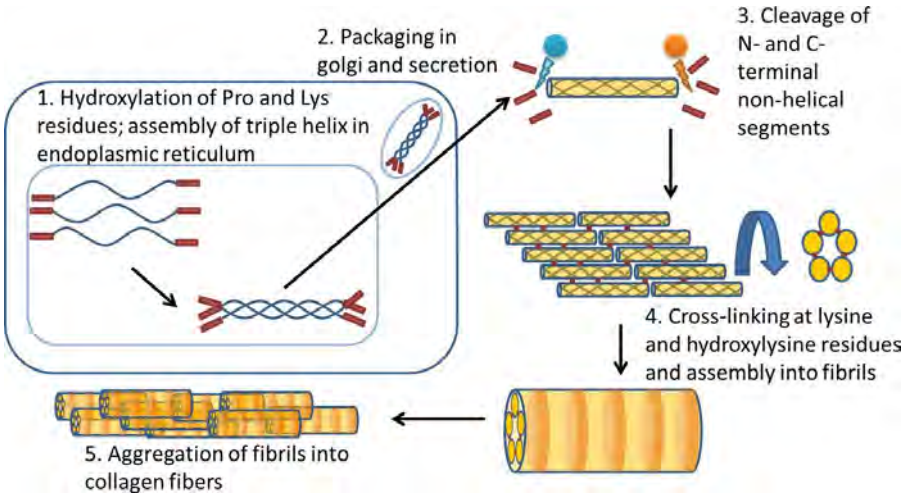

FIGURE 2.10: Collagen synthesis process. Synthesis begins intracellularly and assembly into fibrils and fibres occurs within the ECM. Image from (McKleroy et al., 2013).

as cofactors and (ii) glycosylation through the addition of glucosyl- and galactosyl- to the hydroxylysine (Gelse et al., 2003). Formation and folding of three procollagen molecules occurs through addition of intermolecular disulfide bonds and is mediated by several enzymes, in particular protein disulfide polymerase (PDI) and PPI (peptidyl-prolyl cis-trans-isomerase) (Schönbrunner and Schmid, 1992). The procollagen triplet is then transferred to the golgi apparatus where it is packaged into secretory vesicles. Outside the cell, the terminal C and N peptides on the procollagen are cleaved by Zn^{+2} dependent metalloproteinases, resulting in tropocollagen. Tropocollagens are only weakly stabilized and at this stage tropocollagens can easily be modified by other molecules, temperature and ionic strength leading to the formation of non-cylindrical fibrils (Ottani et al., 2002).

Collagen fibril formation occurs via extracellular self-assembly of tropocollagens. Fibrillar collagens such as Collagen type I have a distinctive staggered arrangement of monomers called a D-period that is about 63-70nm (Gelse et al., 2003), 67nm on average (Saltzman, 2004; Kadler et al., 1996), and fibril diameter can vary widely from 0 to 500nm to more (Ottani et al., 2001). Fibril stabilization due to cross-links form when telopeptide lysine residues are hydroxylized by the catalytic enzyme lysyl oxidase, which is copper dependent. Thereafter, subsequent spontaneous cross-links can occur. The extent of the hydroxylation of these residues varies from tissue to tissue,

complete hydroxylation being seen in cartilage and almost no hydroxylation occuring in skin (Gelse et al., 2003). Orientation of fibrils in the ECM is closely related to function and varies between tissues and organs (Ottani et al., 2001). In ligaments and tendons, fibrils are aligned in parallel and form bundles or fibres. According to Ottani et al. (2001), the parallel arrangement of fibres correlates with the function of the tissue being orientation dependent, as seen in tendons, fibre orientation matches stress direction and loading of tendon fibres at right angles nullifies strength. The arrangement in ligaments is less parallel than in tendons as they need to respond to multi-directional forces (Culav et al., 1999).

2.3.2.4 Matrix metalloproteinases

The role of MMPs has briefly been touched upon in section 2.3.2. MMPs are zinc dependent enzymes involved in maintaining and remodelling the ECM (Matrisian, 1990). Several groups of MMPs have been identified including collagenases, stromelysin, gelatinases and those located on cell membranes (Tang et al., 2009). MMPs are usually secreted in inactive forms into the ECM where they are activated under the correct conditions such as chemical signals or response to cell–cell or cell–matrix interactions. TIMPs are able to deactivate MMPs into their latent form where they can reside in the ECM until required. According to Matrisian (1990) both MMP and TIMP expression can be regulated by growth factors and TGF-β has been shown to block expression of MMPs and thereby prevent degradation of the ECM. Alternatively, growth factors and cytokines bound within the ECM can be released by the action of MMPs when required by the cells (McCawley and Matrisian, 2001). The role of TGF-β has been described in sections 2.3.1.4, 2.3.2 and 2.3.2.1. MMPs implicated in TGF-β release and activation include MMP-2, MMP-3, MMP-9, MMP-13 and MMP-14/ MT1-MMP (Mott and Werb, 2004).

Fibroblasts are the main cell type found in L/T and are responsible for wound healing as well as the development of diseases of the joints (Wang et al., 2007). Clegg et al. (2007) investigated differences between healthy and diseased tendon MMP expression and found that damaged tendons expressed lower levels of MMP-3 than normal tendons. In addition, ruptured tendons had elevated levels of MMP-1 and MMP-9 expression and decreased expression of MMP-3 and MMP-7.

TABLE 2.1: Examples of MMPs and some of their substrates. *Adapted from (McCawley and Matrisian, 2001).*

	MMP Group				
	Collagenase	**Gelatinase**	**Stromelysin**	**Minimal Domain**	**Membrane Type**
MMP name	MMP-1, MMP-8 MMP-13	MMP-2, MMP-9	MMP-3, MMP-10, MMP-11	MMP-7, MMP-26	MMP-14, -15, -16, -17 MMP-24, -25, MMP-12, MMP-19
Substrates	Collagen I, II, III, VII, X, Tenascin	Collagen I, IV, V, VII, X, XI, gelatin, fibronectin elastin, laminin	Fibrin, Fibrinogen, Tenascin, Collagen III, IV, V, IX, X, XI, Fibronectin, Proteoglycans	Fibrin, Fibrinogen, Tenascin	Fibrin, Fibrinogen, Collagen, Gelatin

Tang et al. (2009) found differences in the MMP expression of damaged human ACL and MCLs sourced from amputees. They found that higher levels of MMPs were expressed in the damaged ACLs than in MCLs and that type of MMPs and TIMPs expressed varied with time. Interestingly, MMP-1 expression increased by 276%, MMP-2 by 429%, MMP-7 by 746% and MMP-14 by 667% in ACLs and were significantly greater than expressed by MCL cells.

Degradation of fibrin gels due to MMP activity can be prevented by the use of galardin (GM6001) or aprotinin as was shown by (Ahmed et al., 2007) where chondrogenic cells expressed MMP-2 and MMP-3 to breakdown fibrin hydrogels. Research on MMPs is advancing due to their involvement in adhesion, migration and proliferation of cells, which when not regulated properly result in disease and cancers. Ehrbar et al. (2011) showed that cell migration is dependent on the stiffness of the scaffold matrix and MMP activity, as cell migration was prevented by treatment with an MMP inhibitor (Galardin/ GM6001) on stiff gels.

The use of synthetic MMP inhibitors and TIMPs have been investigated as potential treatments for disease and cancers. As a result, these inhibitors can also be used during tissue engineering *in vitro* in combination with other methods such as tailoring the mechanical properties of their scaffold in order to control its degradation rates and guide the formation of tissue.

2.3.2.5 Hydrogels

Tissue and organ ECM generally contains less than 1% solid matter and is a gel composed of interconnected fibrils and fibres that provide resistance to tensile stress and a hydrated network of GAGs supplying resistance to compressive stress (Lutolf and Hubbell, 2005). The low quantity of solid matter and high water content make it a hydrogel. According to Peppas et al. (2000), hydrogels are hydrophillic, polymeric networks capable of trapping large volumes of water or biological fluids and may have covalent bonds or physical cross-links such as entanglements or crystallites. Hydrogels can further be classified according to the charges on their building blocks or based on their physical structure (amorphous, supramolecular or hydrocolloidal) (Van Vlierberghe et al., 2011). Physiologically active hydrogels have polymer complexes can be broken down or exhibit swelling, depending on environmental factors such as temperature, pH, ionic strength and electromagnetic radiation (Peppas et al., 2000). Hydrogel scaffold mechanical properties can be tailored by controlling elasticity, viscoelastic properties, tensile and compressive strength and failure strain (Drury and Mooney, 2003). Additional crosslinking can further stabilize hydrogel scaffolds and retard degradation, which can occur through proteolysis, dissolution or hydrolysis (Drury and Mooney, 2003).

Hydrogels can be either synthetic or naturally derived materials. Synthetic hydrogels include poyl(ethylene oxide) (PEO), poly(acrylic acid) (PAA)(Drury and Mooney, 2003) as well as composites with PLGs. However, PLGs are hydrophobic and gelling them with encapsulated cells is difficult and the process tends to be cytotoxic due the use of UV irradiation during their processing. To overcome this encapsulation problem, it is possible to first gel the PLA polymer and then seed the cells on top. This leads to a 2D layer, which does not resemble *in vivo* conditions. The advantage of hydrogels is that cells can be encapsulated within the gel to form 3D constructs (Tibbitt and Anseth, 2009), whose size and shape is mainly limited by nutrient and waste diffusion requirements. Synthetic hydrogels lack cell adhesive properties and peptides containing RGD sequence need to be incorporated.

Naturally derived polypeptides can form hydrogels and are employed as TE scaffolds and vehicles for cell delivery (Hunt and Grover, 2010). Examples of such naturally

derived hydrogels are agarose, gelatin, alginate used in TE of bone, neural, cartilage, adipose and dermal tissue (Kemençe and Bölgen, 2013; Tseng et al., 2013; Kim et al., 2012); chitosan for its wound healing attributes and preferential adhesion of osteoblasts over fibroblasts (Croisier and Jérôme, 2013; Douglas et al., 2013); collagen for various tissues due to its ubiquitous presence, elastin for blood vessels and ligament TE (Daamen et al., 2007) and fibrin as a scaffold for adipose tissue, bone, cardiac tissue, cartilage, liver, nervous tissue, ocular tissue, skin, tendons, and ligaments (Ahmed et al., 2008; Paxton et al., 2012). Hydrogels comprised of ECM biopolymers such as collagen and fibrin can regulate cell adhesion, migration, proliferation and differentiation better than synthetic polymers (Balakrishnan and Banerjee, 2011). Major drawbacks of natural biopolymer hydrogels are their low mechanical strength, poor reproducibility due to donor variability and rapid degradation.

2.4 Current ligament and tendon tissue engineering strategies

The structure of L/T have been described in above sections as were cell processes and their role in synthesizing the ECM and forming tissue. In recent years, a number of studies on L/T tissue engineering research have focused on scaffold development, the use of MSCs and the L/T attachment sites (entheses). Composite or hybrid scaffolds that aim to improve scaffold mechanical properties, promote growth factor release and/or enhance cell adhesion and proliferation have been employed by several researchers (Vaquette et al., 2010; Kuo et al., 2010; Tamayol et al., 2013). The use of composite materials allows the balancing of scaffold mechanical properties with biological requirements for cell processes and ultimately tissue formation (van Blitterswijk, 2008). Electrospun fibres are attractive as spinnable fibres tend to be fairly robust and alignment of the fibres can be achieved, which can direct tissue growth (Teh et al., 2013). As collagen is the greatest component of ligaments and tendons, its use provides cells with a L/T matrix-like environment (Kew et al., 2011). Embryonic stem cells (ESCs) are highly attractive due to their potential to form any of the three germ layers and the less mature differentiated cells may offer greater efficacy for TE applications (Cohen et al., 2010; van Blitterswijk, 2008). Often these approaches have been used in combination to maximise the potential of optimising

the engineered L/T. In the following sections, several selections of the individual strategies used in TE L/T will be outlined.

2.4.1 Growth factors

Several growth factors including but not limited to BMP-12, BMP-13 (Haddad-Weber et al., 2010; Heisterbach et al., 2012), GDF5 (James et al., 2011; Park et al., 2010), IGF, FGF, PDGF (Cummings et al., 2012) and TGF-β1 have been used in L/T TE (Hsu et al., 2010; Steinert et al., 2011; Wang et al., 2012; Leong et al., 2013; Gross and Hoffmann, 2013).

Sahoo et al. (2010), were the first to show growth factor enhanced mechanical strength of *in vitro* TE ligament/tendon constructs. They developed a silk/PLGA electrospun scaffold capable of sustained release of the growth factor bFGF for L/T TE, using BMSCs, which resulted in the enhanced proliferation of cells and expression of tenogenic proteins collagen I, collagen III, biglycan and fibronectin. In addition, the mechanical properties of the constructs with bFGF were also greater than the cell and/or growth factor negative groups. Their design was based on several advantages and challenges: that MSCs proliferate faster and produce more collagen than ligament fibroblasts; silk degrades slowly and has suitable mechanical properties; PLGA provides a temporary scaffold, which in combination with silk provided better cell attachment, proliferation and ECM deposition; and for a stem cell based L/T TE approach, the scaffold had to provide signalling molecules.

Recombinant human platelet-derived growth factor-BB (rhPDGF-BB) has been shown to increase ligament and tendon healing through enhanced cell recruitment and proliferation to the injured site as well as greater ECM synthesis (Hee et al., 2012).

Hagerty et al. (2012) investigated the effect of growth factors TGFβ, IGF-1, GDF-7 at varying concentrations and combinations over 7 -10 days. Using fibroblasts isolated from a human ACL in a fibrin hydrogel matrix, collagen synthesis was enhanced 5.2 fold and the maximum tensile load 5.7 fold when supplemented with TGFβ, IGF-1, GDF-7 and 200μM ascorbic acid. In contrast, EGF resulted in constructs with decreased collagen content and consequently lower mechanical load capacity. These

studies emphasise how growth factor expression and requirements differ depending on cell type and other environmental factors.

A recent demonstration of how gene expression varies depending on cell type or anatomical origin and cell age is that by Brown et al. (2014). They showed that supplementation with growth factors to stimulate gene expression could have little or no effect or even adverse effects unless the cells were at the correct development stage or originated from a particular location. For example, using mouse embryonic cells at different stages of growth and taken from either the limbs or trunk, Brown et al. (2014) observed that expression of scleraxis, collagen type I, tenomodulin and elastin varied. Attempting to stimulate gene expression with growth factor FGF-4 significantly upregulated collagen type I in limb cells but not cells sourced from the trunk of the body. In addition, gene regulation by FGF-4 appeared to depend on cell development stage as not all limb cells upregulated collagen. Conversely, TGF-β2 upregulated scleraxis at all developmental stages regardless of cell anatomical location (Brown et al., 2014). Their findings were interesting as both FGF-4 (Edom-Vovard et al., 2002) and TGF-β2 growth factors (Edom-Vovard and Duprez, 2004) have been implicated in scleraxis expression, the marker for tendons (Schweitzer et al., 2001).

2.4.2 Cell source

Due to the limited potential of adult derived MSCs, Chen et al. (2010) investigated the use of MSCs derived from hESCs (hESC-MSCs) both *in* and *ex vivo* for tendon tissue engineering. hESC-MSCs seeded on a knitted silk-collagen scaffold differentiated into a tenogenic lineage upon dynamic mechanical loading and expressed tendon related gene markers for collagen type I, collagen type III and scleraxis as well as cell adhesion markers for integrins α1, α2 and β1 and myosin stress fibres.

Adipose derived stem cells (ASCs) have been explored as an alternative to MSCs or bone-marrow stem cells, for L/T TE by several researchers due to their multipotency and proliferative efficiency (Eagan et al., 2012; Little et al., 2010; James et al., 2011; Park et al., 2010; Uysal et al., 2012). The study by Uysal et al. (2012) treating a severed rabbit achilles tendon using ASCs and platelet-rich-plasma (PRP) revealed a doubling in tensile strength and 70% increase in collagen quantity of the treated group in comparison to the ASC cell negative control group. They evaluated the presence

of TGFβ-1,-2,-3, VEGF and FGF growth factors and found high levels of FGF and VEGF and collagen type I in the ASC treatment group, however, TGFβ-1,-2,-3 were significantly lower than with the control.

2.4.3 Interface

The L/T–bone interface is the location of high stress concentration and although the transitional zones allow the gradual transmission of loads from L/T to bone, the site is frequently injured during sporting activities or is afflicted by disease (Ho et al., 2010). The current challenge in tissue engineering the L/T–bone interface is reproducing the gradation, which does not regenerate following graft therapy and is the site prone to failure post-surgery (Thomopoulos et al., 2010).

MSCs with high viral-mediated expression of smad8ca and BMP-2 were investigated for their potential to spontaneously form interfaces in subcutaneous and intramuscular sites of mouse (Shahab-Osterloh et al., 2010). The researchers found that intramuscular murine MSC implantation resulted in the formation of bony tissue with tenogenic-like and cartilage-like insertions; human MSCs however, formed bony structures but not the interface and from their observations TGF-β and FGF showed greater efficacy in hMSCs chondrogenic expression than BMP-2 (Shahab-Osterloh et al., 2010). Other researchers have investigated the co-culture of osteoblast and fibroblast cells or tri-culture with MSCs, for the formation of the enthesis and some studies have included mechanical loading and/or growth factor treatments such as BMP-2 or TGF-β (He et al., 2012; Sahoo, 2011).

2.4.3.1 Use of bone mimetics

Up to 65% of bone tissue is composed of carbonated hydroxyapatite the rest being mainly collagen and water (Vallet-Regi and González-Calbet, 2004). Osteoblasts and osteoclasts are the main cell type present, responsible for synthesis and remodelling of bone, respectively. Hydroxyapatite (HA) cements show good biocompatibility and are frequently used in bone tissue engineering (Paxton et al., 2008). However, the resorption of the scaffold and integration with native tissue are also important factors

for bone mimetics (Hutmacher, 2000). Brushite is synthesised at a lower pH than HA and is more readily resorbed by the body at a pH of 7.4 (Klammert et al., 2010).

Tissue engineered bone–L/T–bone constructs show great promise in forming soft tissues with an intact interface. Ma et al. (2011) developed a three-dimensional bone–ligament–bone construct consisting of tissue engineered bone and ligament-like tissue produced by BMSCs. When these constructs were placed side by side, they fused together to form constructs that were broader in dimension, which were then implanted into a sheep as an ACL graft. After 6 months *in vivo*, the ligament-like structure had a defined interface, resembled the native ACL in morphology and with closely matching tensile strength (Ma et al., 2011).

Using a similar bone-ligament-bone model to Ma et al. (2011), Paxton et al. (2008) developed bone mimetic anchors from RGD functionalised Poly(ethylene glycol) (PEG) hydrogels containing HA and found that the PEG HA and PEG HA RGD gels significantly promoted PFB cell proliferation and the anchors remained attached for longer than anchors that did not contain HA and that attachment duration was dependent on HA concentration. Following this work, (Paxton et al., 2010a) went on further to develop brushite cement anchors where they found that brushite cement composition and anchor shape were factors that determined duration of interface attachment and strength.

2.4.4 Mechanical loading

Mechanical loading has been shown to increase fibroblast cell alignment and stimulate collagen production by cells (Riehl et al., 2012; Xu et al., 2014). Aligned silk fibroin hybrid scaffolds coupled with dynamic loading increased rabbit BMSC cell proliferation, collagen synthesis and resulted in greater expression of ligament/tendon related proteins such as collagen type I and tenascin-C in comparison to statically cultured construct with aligned and random fibres or dynamic cultured random fibre constructs (Teh et al., 2013). Similarly Subramony et al. (2013) investigated the effects of a poly(lactide-co-glycolide) scaffold fibre alignment with or without mechanical loading on human MSC differentiation into fibroblasts and determined that loading did not increase collagen type I expression although other matrix proteins such as collagen type III, tenascin-C and fibronectin were upregulated; cell proliferation

and expression of adhesion integrins was also upregulated in both aligned/ unaligned constructs by loading.

Collagen synthesis due to mechanical loading has been attributed to the activation of MAPK pathways (ERK and p38) (Lee et al., 2000), due to increased TGF-β, which has been shown to increase after exercise (Klein-Nulend et al., 1995; Hayashida et al., 1999). Paxton et al. (2011) used ERK1/2 expression to optimise cyclic loading duration and as expected enhanced ERK 1/2 correlated positively with increased construct collagen type I content. The MAPK signal transduction pathways are also linked to many other cells processes such as growth, proliferation, gene expression, cell metabolism and apoptosis (Cowan and Storey, 2003). In the recent study by Brown et al. (2014) discussed in section 2.4.1, mechanical loading affected tendon progenitor cells differently depending on their site of origin in the body and development stage as following mechanical loading, TFG-β2 was down-regulated in both limb and trunk tendon lineage cells and scleraxis was upregulated in limbs and not axial skeletal cells.

2.4.5 Scaffolds and scaffold design

The scaffold plays a pivotal role in tissue engineering as most mammalian cells are adherent and will not survive long in floatation. As a result, cells are combined with a suitable scaffold or matrix to form a construct that facilitates cell adhesion, migration, growth and differentiation (van Blitterswijk, 2008). Numerous complex factors need to be considered when selecting a suitable scaffold that depend on the cell type(s) and function of the engineered tissue. Among these considerations are scaffold biocompatibility, bioresorptability and its mechanical properties. Biocompatible scaffolds allow the adhesion, proliferation and migration of cells and do not illicit an immune response once implanted in the body; bioresorbable scaffolds will degrade and allow cell remodelling, ideally at a controlled rate; mechanical properties of the scaffold should closely match those of native tissue and be robust enough to withstand implantation and any forces it is subjected to *in vivo* (Hutmacher, 2000). One of the main challenges in TE scaffold design is ensuring adequate mechanical stiffness of the scaffold and that the scaffold will breakdown or is resorbed at a rate that matches cell *de novo* ECM synthesis.

A significant amount of research has been conducted using two dimensional (2D) scaffolds *in vitro*. However, it is now apparent that these 2D scaffolds do not accurately represent the natural cell environment. Researchers are now focusing on three dimensional *in vitro* studies, which pose challenges in ensuring that the scaffolds possess the correct porosity and mechanical attributes to allow cell processes to occur as well as facilitate nutrient mass transport. Mass transfer and tissue development needs mean that scaffolds have low volume fractions. Increasing the porosity must be in balance with the overall mechanical strength of solid scaffolds, which is dependent on the density of the material that constitutes the pore walls or edges (van Blitterswijk, 2008). Several methods can be utilized to prepare 3D porous scaffolds such as gas foaming, phase separation, freeze-drying and porogen leaching (Chen et al., 2002). Cell invasive fibre scaffolds have the advantage of having high surface areas, they can be aligned in a specific direction to guide cell growth and generally allow permeability between fibres. The fibres can by fabricated using non-woven extrusion methods for micron diameter fibres or electro-spinning for submicron to micron diameter fibres (van Blitterswijk, 2008). Individual fibres can be bundled into larger scaffolds with greater pore interconnectivity, through braiding and weaving. Other methods developed or being used to fabricate TE scaffolds and are solid free-form fabrication, laser and UV based fabrication techniques and 3D printing.

Both synthetic and biological polymers are being investigated for their use as tissue engineering scaffolds. Common materials include ceramics, polyhydroxyesters and collagen. In ligament and tendon tissue engineering, the most often used natural polymers are collagen and silk fibroin.

2.4.5.1 Synthetic

The surface adhesiveness of synthetic polymers determines cell spreading, average cell height and rate of cell growth (Saltzman, 2004). Most synthetic polymers do not contain the biological motifs required for cell adhesion and are often functionalised by coating with RGD peptide containing proteins such as fibronectin, vitronectin or laminin (Shin et al., 2003). Alternative methods that modify the surface to be positively charged to allow weak cell adhesion may also be used. Synthetic polymers can be non-degradable or biodegradable. Biodegradable polymers are generally more

desirable as they can partake in the healing or regeneration process by permitting cell infiltration and scaffold remodelling. Common biodegradable synthetic polymers that are US Food and Drug Administration (FDA) approved are polyesters such as poly(glycolic acid) (PGA), poly(lactic acid) (PLA) and their copolymer poly[lactic-co-(glycolic acid)] (PLGA) (Chen et al., 2002). Biodegradable synthetic polymers are attractive due to the tailorability of their mechanical properties, their reproducibility porosity, tendency to be functionalised and biodegradability, however, biodegradation does not suggest complete elimination from the body but rather that the polymer can be biologically attacked and break into fragments that may or may not persist (Hutmacher, 2000).

Several synthetic materials have been used to replace ruptured ligaments. Among these are FDA approved non-degradable synthetic ligaments or ligament augmenters such as Leeds-Keio Ligament (polyethylene terephthalate), Kennedy Ligament Augmentation Device (polypropylene) and Gore-Tex (Vunjak-Novakovic et al., 2004; Laurencin et al., 1999; Ge et al., 2006). Carbon fibres and silastic sheets have also been used for the repair of functional tendons (Calve et al., 2004). Advantages of these are their high strength as they adequately provide the support lacking due to the injured ligament. However, these synthetic replacements fail over time as they cannot replicate the mechanical complexity of the native tissue. Extension gradually results in permanent deformation of the prostheses, wear on sharp bone edges at the point of fixation cause debris that lead to inflammation and poor tissue ingrowth has also been noted (Vunjak-Novakovic et al., 2004; Laurencin et al., 1999; Ge et al., 2006).

A PLLA twist-braid scaffold with similar stress-strain behaviour to natural ligament was developed by Freeman et al. (2007) and a composite of the PLLA twist-braided scaffold with a polyethylene glycol diacrylate (PEGDA) hydrogel, increased scaffold viscoelastic properties as well as maintaining fibroblast cell proliferation over 4 weeks. Twisting of fibres is frequently used in the yarn industry to improve fibre tensile strength and braiding supplies reinforcement for axial loads. Recent work by Bach et al. (2013) studied the use of acellular twist-braided PVA for use as a prosthetic device for ACL replacement and determined its viscoelastic nature and ultimate tensile strength of 2000N to be similar to native ACL. Combining PVA with ultrahigh molecular weight polyethylene (UHMWPE) further enhanced mechanical strength. Due to the synthetic nature, this material will not favour natural remodelling and

interface integration; the authors state that further *in vitro* and *in vivo* work will need to be conducted.

2.4.5.2 Natural

Mammalian tissue from humans, bovine, porcine and equine has been employed as biological tissue engineering scaffolds (Longo et al., 2012). The tissue is first cleaned and treated to remove non-collagen cellular components such as DNA and lipids as these would illicit an immune response leaving a scaffold comprised mainly of collagen type I. However, the decellularization process can be harsh and lead to damage of the required ECM (Gilbert et al., 2006; Crapo et al., 2011). Collagen structure can be compromised by decellularization leading to an ECM with significantly lower mechanical strength (Badylak et al., 2009). Tischer et al. (2007) demonstrated the use of decellularized rabbit tendon in maintaining tissue strength and permitting successful seeding of cells. A review of decellularization methods for orthopeadic tissue engineering purposes was recently conducted by Cheng et al. (2014) detailing physical, chemical and enzymatic methods.

An alternative method of using biological polymers is to use enzymes or chemicals to synthesize the biopolymers *in vitro*. This method is currently preferred as potentially, the enzymes/ primary reagents can be isolated from the patient thus eliminating exogenic transplantation. Cells can then be seeded onto these polymers and secrete their own ECM components to form tissue that closely resembles that found in the body. Advantages of using natural ECM polymers include presence of receptors necessary for cell attachment and that cells are able to remodel and proteolytically degrade the scaffold (Lutolf and Hubbell, 2005). Challenges of this method are that the mechanical and biochemical properties of the scaffold must be ideal to provide the required signals to induce such action within the cells. Biochemical stimulants are frequently required in combination with tailoring scaffold properties.

Porous collagen-glycosaminoglycan (CG) scaffolds were developed by Caliari et al. (2011) as an alternative to fibrous electrospun scaffolds for tendon tissue engineering. The CG scaffolds have a low density, anisotropic core surrounded by a CG membrane shell with tunable shell elasticity and thickness. Cross-linking and aligning the pore structure improved tensile mechanical properties and the shell did not limit nutrient

transport and cell viability was not adversely affected. The rationale behind their design was that TE scaffolds often require porosities >90%, which result in scaffolds being too soft for tendon tissue engineering and although mechanical loading can be used to enhance mechanical properties, they often do not reach those of native tendon. They stated that composite core-shell designs are found in nature, such as plant stems that have an osmotic core and shell with suitable tensile, bending stiffness (Caliari et al., 2011). Further work has shown that increasing anisotropic density improves cell attachment, expression of tenascin-c and scleraxis, including decreased cell-mediated contraction of the scaffolds and decreased MMP-1 / -13 expression (Caliari and Harley, 2011). Use of multiple growth factors and their use in sequestration rather than as soluble factors maintained tenocyte phenotype and cell proliferation and other bioactivity, crucial for tissue regeneration (Caliari and Harley, 2013).

2.4.5.3 Use of MMP inhibitors or TIMPs

The use of growth factors for L/T TE has been detailed in section 2.4.1. However, growth factor use although generally successful has been shown to have limitations particularly due to variations in inherent cell programming. A current review by Lo et al. (2014) suggests that since growth factors have the potential to illicit immune response and the high costs associated with their commercial production, the focus of tissue engineering for musculoskeletal purposes should be on *small bioactive molecules* such as MMP inhibitors or TIMPs, in the case of ligament tissue engineering. The studies by Lui et al. (2013a,b) as cited by Lo et al. (2014) using alendronate showed great efficacy in promoting ligament healing by reducing MMP-1 and MMP-3 expression.

As mentioned in section 2.3.2.4, Galardin and Aprotinin are two MMP inhibitors that successfully attenuated fibrin matrix degradation, however, thorough understanding of which MMPs are up- or downregulated and when, are necessary in order to design successful MMP inhibition paradigms. MMP expression in natural tissue undergoing healing showed that MMPs 9 and 13 were upregulated between the first and second week, whereas MMPs 2, 3 and 14 (MT1-MMP) were upregulated throughout a 4 week investigative period and as result, the findings suggested that MMP-9 and MMP-13

were responsible for collagen degradation and MMP-2 -3 and -14 degraded as well as remodelled the matrix (Yang et al., 2013).

2.5 Opening Remarks

This chapter has highlighted the importance of ligaments and tendons and has reported tissue engineering methods relevant to their regeneration. This thesis has aimed to build upon current ligament and tendon tissue engineering strategies based on the function of the supportive fibrin scaffold and the roles of ascorbic acid and proline in cell collagen synthesis.

Chapter 3

General Methods and Materials

3.1 Cell Culture

3.1.1 Supplemented medium

500mL of DMEM (D6546, Sigma-Aldrich, UK) was supplemented to contain 10% v/v FBS (A15-105, PAA UK), 2.4% v/v L-Glutamine (G7513, Sigma-Aldrich UK), 2.4% v/v Hepes Buffer (H0887, Sigma-Aldrich UK) and 1% v/v Penicillin/Streptomycin (P4333, Sigma-Aldrich UK). This supplemented DMEM is referred to as sDMEM throughout this thesis and was the standard medium for Chick Tendon Fibroblasts (CTFs) cells unless stated otherwise. Where DMEM (D5796, Sigma-Aldrich UK) was used, no L-Glutamine was added.

3.1.2 Supplemented F12 Ham

F12 Ham medium (N4888, Sigma-Aldrich UK) for Rat Tendon Primary Fibroblasts (PFBs) was supplemented with 20% v/v FBS, 1% v/v Antiobiotic/Antimycotic (ABAM) (A45955, Sigma-Aldrich UK) and 0.5% v/v 1mM L-Glutamine. This was used for PFB cell culture unless otherwise stated.

3.1.3 Cell thawing

A 1mL vial of CTFs or PFB cells stored in Liquid Nitrogen at -196°C was quickly thawed in a waterbath (JB Aqua 12, Grant Instruments) at 37°C. The 1mL cell suspension was transferred to a 50mL tube, to which 9mL of sDMEM was added. The 10mL cell suspension was pipetted up and down several times before centrifuging (MSE Mistral 2000) for 3 minutes at 1000rpm. The supernatant was aspirated off and the cells were resuspended in fresh 10mL of sDMEM. The cell suspension was then transferred into a T-75cm^2 flask for expansion in a humidity controlled incubator (InCusaFe MCO-15AC, Sanyo) at 5% CO_2 and 37°C.

3.1.4 Cell culture

Cells in T-75cm^2 flasks were cultured until ≈70% confluency and then passaged into T-175cm^2 flasks. The growth medium (sDMEM) was changed every 2 to 3 days. Cells between passages 2-5 were used for TE L/T or were split before reaching confluency.

3.2 Tissue engineering ligament/tendon

3.2.1 Preparation of stock solutions

3.2.1.1 3.5M Ortho-phosphoric acid with 50mM Citric Acid

Orthophosphoric acid (H_3PO_4) (Fisher, UK) was supplied as 85% v/v in water, a concentration of 15.2M. To prepare 100mL of 3.5M acid, 77mL of distilled water was added to 23.03mL orthophosphoric acid. 96mg of Citric Acid, molecular weight 192g/mol, was added to the acid, to obtain 50mM Citric Acid in 3.5M orthophosphoric acid.

3.2.1.2 Thrombin

1% w/v BSA in F12K was prepared by adding 1mg BSA powder (A9418, Sigma-Aldrich UK) per mL of Ham's F12K (Kaighn's) medium (21127022, Invitrogen UK). 5mL of the BSA/F12K medium was added to each 1000 Units Thrombin (UT) vial (605157-1KU, Calbiochem UK or BT 1002 a, Enzyme Research Laboratories, Swansea UK) resulting in a stock of 200UT/mL. Solutions of 200UT/mL were transferred into Bijou tubes and frozen at -20°C.

3.2.1.3 Fibrinogen

Fibrinogen solutions were prepared by dissolving 20mg of fibrinogen (F8630 Sigma-Aldrich UK) per mL of Ham's F12K (Kaighn's) medium (21127022, Invitrogen UK) in a waterbath at 37°C for a period of 4 hours. The 20mg/mL fibrinogen solution was gently swirled every hour to ensure dissolution of the fibrinogen powder. Thereafter, the fibrinogen was sterile filtered using 0.22μm syringe filters. Alternatively, fibrinogen was sterilised by leaving under UV light in the laminar flow hoods (BSB, Gelaire Inc Biomedicals) overnight.

3.2.1.4 Phosphate Buffered Saline solution

Two PBS tablets (P4417, Sigma-Aldrich UK) were dissolved in 400mL of distilled water to yield 0.01M phosphate buffer, 0.0027M potassium chloride and 0.137M sodium chloride. Alternatively, 4 PBS-Dulbecco A tablets (BR0014G, OXOID UK) were dissolved in 400mL of distilled water. The PBS solutions were sterilised by autoclaving at 115°C for 15 minutes.

3.2.1.5 Ascorbic Acid and Proline solutions

L-ascorbic acid 2-phophate sesquimagnesium salt hydrate (A8960, Sigma-Aldrich UK) was dissolved in phosphate buffer saline (PBS) by dissolving 0.869g in 12mL of PBS. The final solution had a concentration of 250mM and was syringe filtered to sterilise.

50mM L-Proline solutions were prepared by dissolving 69mg of L-Proline (P5607, Sigma-Aldrich UK) in 12mL of PBS. The solutions were sterilised by syringe filtering.

3.2.2 Sylgarded petri-dishes/ well plates

Sylgard polymer solution was prepared by mixing the base to catalyst at a ratio of 10:1 (Sylgard 184 Silicone Elastomer Kit, Dow). Approximately 1.5mL of the polymer solution was added to 35mm diameter petri-dishes or well plates. Where smaller or large diameter dishes were used, the polymer volume was adjusted accordingly. The polymer filled dishes/ plates were left to polymerise at room temperature for 3 – 4 days.

3.2.3 Brushite cement anchors

Brushite cement anchors were prepared from a reaction between β-TCP and ortho-phosphoric acid (Equation 3.1). The paste was prepared using 3.5g β-TCP per 1mL of ortho-phosphoric acid (Figure 3.1-1). The paste was rapidly mixed on a vibrating platform and then spread onto anchor molds. Stainless steel minutien pins, 0.20mm in diameter (Austerlitz) were inserted through the cement paste prior to hardening. The cement filled molds were left in an incubator (LEEC, UK) at 37°C to harden overnight.

$$Ca_3(PO_4)_2(s) + H_3PO_4(l) + 6H_2O(l) \longrightarrow 3CaHPO_4 \cdot 2H_2O(s) \tag{3.1}$$

3.2.4 Fibrin hydrogel preparation

200mM 6-Aminohexanoic Acid (AH) (A7260, Sigma Aldrich) and 10mg/mL Aprotinin (10981532001, Roche UK) were each added to sDMEM at a volume of 2μL per mL of sDMEM (Figure 3.1-2). 50μL of 200UT/mL Thrombin were also added per mL of sDMEM. 500μL of sDMEM containing thrombin, AH and AP was added to each 35mm petri-dish or well and spread to evenly cover the surface. 200μL of a

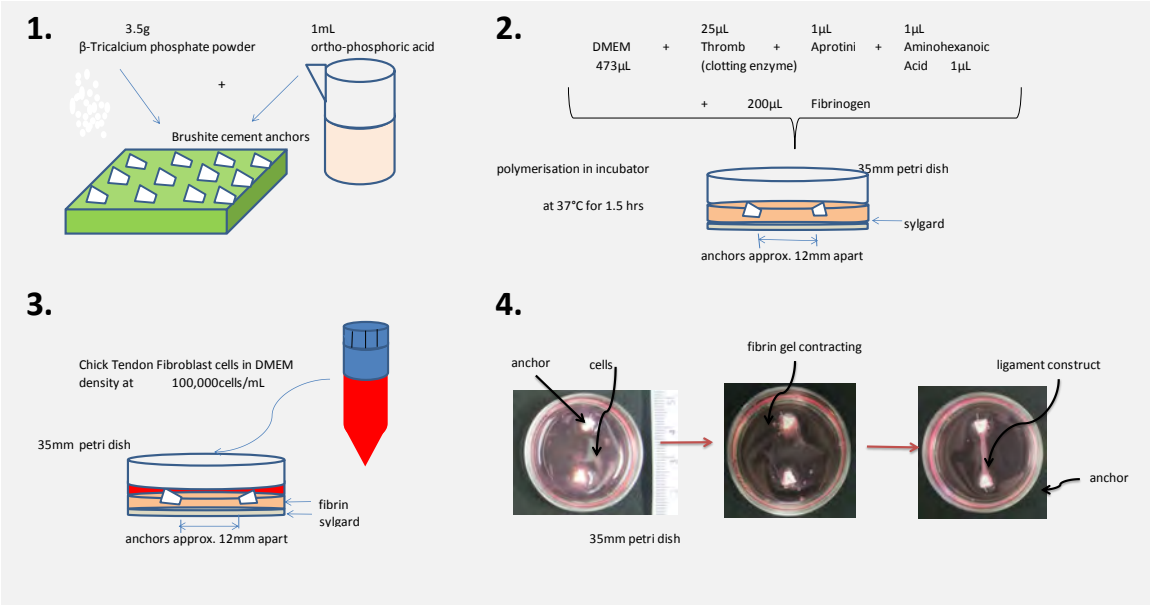

FIGURE 3.1: General method for TE L/T construct formation. 1) Brushite cement anchor formation. 2) Thrombin, AH and AP are added to sDMEM, of which 500μL is then evenly spread onto petri-dishes, followed by 200μL fibrinogen. 3) Seeding at 100,000cells/mL and 4) Cells contract the gel about the anchors and remodel the matrix.

20mg/mL Fibrinogen solution was then evenly distributed onto each dish/ well and gently mixed by rotating. The dishes/plates were placed in an incubator at 37°C and left to polymerise for 1 hour.

3.2.5 Cell dissociation from flasks

Spent medium was aspirated off and the cells were washed in PBS. Once PBS was removed, 1mL of TrypLE Select 1X solution (12563-029, Invitrogen UK) was added to a T-75cm^2 flask and incubated for 1-3 minutes at 37°C. To aid cell detachment from the flask, the flasks were tapped gently to assist the dissociation process. TrypLE was deactivated by adding 9mL of sDMEM. Where T-175cm^2 flasks were used, 2mL of TrypLE was added, which was deactivated using 8mL of sDMEM.

3.2.6 Cell counting

12μL of a cell suspension was loaded onto a haemocytometer and cells in the 5 squares were counted. The total cell count in the 5 squares was multiplied by 2000 to give the cell count in 1mL of sDMEM. This was then multiplied by the total volume of cell suspension present. At least two counts were taken and the average count was taken.

3.2.6.1 Using Trypan Blue

Trypan Blue stains dead cells a dark blue colour thereby allowing an estimate of live/dead cells in the suspension (Strober, 2001). 500μL of Trypan Blue was added to 500μL cell suspension in an eppendorf tube and gently pipetted using a 1mL pipette. 12μL of the cell suspension was loaded on a haemocytometer and the number of live and dead cells was determined as above. (Note: the haemocytometer counts using the trypan blue method represented the cell density in 500μL of the suspension. Therefore to obtain the density in 1mL, the count was multiplied by 2 and then by 2000).

3.2.7 Construct formation - cell seeding

Cell suspensions for seeding fibrin gels were prepared at a density of 100,000 cells per mL of sDMEM (Figure 3.1-3). The cell seeding density of 100,000cells/mL was obtained by resuspending the total cell count, acquired using the method in section 3.2.6, in an appropriate volume of medium (Equation 3.2). Where the volume of medium required for resuspension was too great, the cell suspension was concentrated by a factor, for example by X10 or X100. The cell seeding density was then obtained by dividing the concentrated suspension by its concentration factor and adding that volume of cell suspension to acellular sDMEM (Equations 3.3 and 3.4).

$$\text{Cell seeding density (100,000cells/mL)} = \frac{\text{Total cell count}}{\text{Appropriate volume of medium (mL)}} \tag{3.2}$$

$$\text{Conc. cell suspension for seeding} = \frac{\text{Total volume of cell suspension required for seeding}}{\text{Concentration factor}}$$
$$\text{Cell seeding suspension} = \text{Volume of medium required} + \text{Conc. cell suspension for seeding} \tag{3.3}$$

For example, to prepare a total volume of 25mL cell suspension for seeding, using a X10 concentrated cell suspension:

$$\text{Conc. cell suspension for seeding} = \frac{25mL}{10} = \text{2.5mL}$$
$$\text{Cell seeding suspension} = \text{22.5mL of medium} + \text{2.5mL conc. cell suspension for seeding} \tag{3.4}$$

1mL of the cell seeding suspension was then evenly distributed on top of the polymerised fibrin hydrogels and left to incubate at 37°C for 3 days before changing the medium. Where constructs were supplemented with AA+P, the supplements were added directly to the cell suspension at 1μL supplement per mL of sDMEM before seeding.

3.2.8 Changing growth medium

After the initial 3 day incubation, medium was changed every 2 to 3 days. Generally, 6 constructs were set up per group and cultured for a period 5 weeks unless shown otherwise.

3.3 Contraction Imaging and Quantification

Generally, images of constructs were taken every day for the first 14 days using a compact digital camera (Canon PowerShot A3100 IS00), under a laminar flow hood. A black cloth was used as dark backing and the digital camera was mounted on a metal stand. The cloth, camera and stand were all sprayed with 70% v/v ethanol prior to placement in a sterilised hood to prevent contamination. Images were taken

with open petri-dish/ well plate lids and a ruler was placed next to the samples during imaging for calibration. No flash was used.

ImageJ software (NIH) was used to determine the percentage fibrin gel areas as well as construct maximum and minimum widths (Figure 3.2).

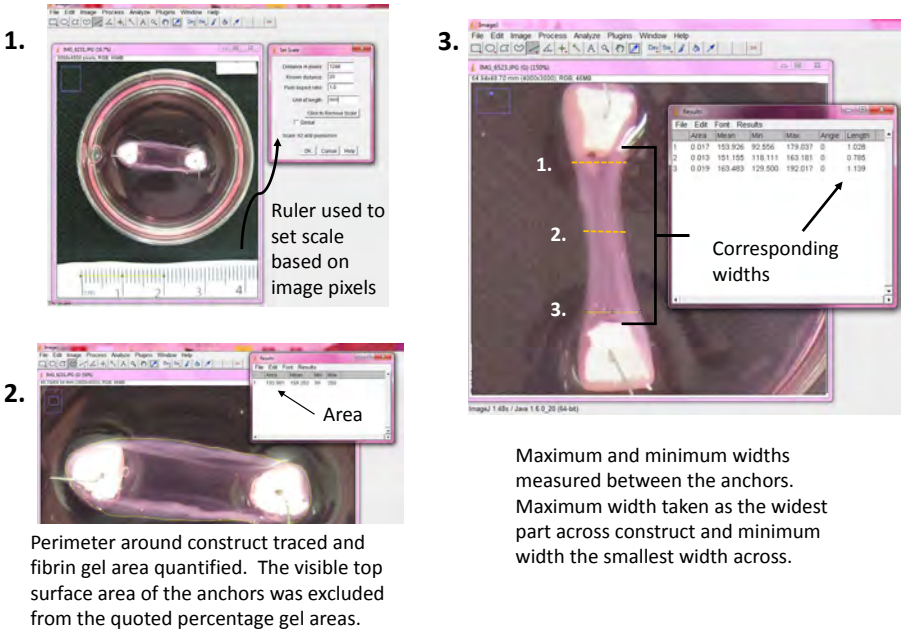

FIGURE 3.2: Quantification of fibrin percentage gel area and max/min widths using ImageJ.

The imaged ruler was used to set the scale in mm. To measure area, the perimeter around the construct was traced and the software computed the corresponding area based on the set scale. Anchor surface areas at measured plane were quantified on Day 0 for each construct and subtracted from the computed area so that the measurements reflected only the area of the fibrin hydrogel. The maximum and minimum widths were taken as the broadest and narrowest dimension, respectively, perpendicular to the construct lengths and in-between the anchors.

3.4 Collagen quantification

Generally, the amount of collagen in the constructs was determined using an hydroxyproline assay (Acid Hydrolysis Method) modified from Neuman (1950), by Paxton

et al. (2010b, 2012). As the hydroxyproline assay is destructive, quantification was generally performed after 5 weeks of TE L/T development.

3.4.1 Preparation of Reagents

3.4.1.1 Aldehyde-perchloric acid reagent

10mL of the reagent was made by dissolving 1.5g of para-dimethylaminobenzaldehyde in 6mL of iso-propanol, followed by 2.6mL of perchloric acid (70%) and topped up to the required volume using distilled water.

3.4.1.2 Chloramine-T Solution

141mg of Chloramine-T was dissolved in 10mL distilled water before use and kept away from bright light.

3.4.1.3 Hydroxyproline Buffer

500mL of the buffer at pH 6.0 – 6.5 were made from a mixture of 4mL acetic acid, 16.6g citric acid, 40g sodium acetate and 11.4g sodium hydroxide in distilled water. A small amount of toluene (0.25mL) was added as a preservative and the solution was stored in the dark.

3.4.2 Method

Dry L/T samples were weighed in eppendorfs tubes before being hydrolysed in 200μL of 6N hydrochloric acid for 3 hours at 130°C under closed lids in a fume cupboard. Thereafter the eppendorf lids were opened and liquid was allowed to evaporate off for 30–45 minutes. The resulting dark residue of the samples was then resuspended in 200μL of hydroxyproline buffer. Standards with known quantities were prepared by dissolving hydroxyproline powder (Sigma Aldrich UK) in hydroxyproline buffer. Each of the samples was then diluted in hydroxyproline buffer at a ratio of 1:3. 150μL of

Chloramine-T was added to the diluted samples and the standards. After vortexing, the samples and standards were left at room temperature for 20 minutes. 150μL of the aldehyde-perchloric acid reagent was then added to each of the samples and standards. They were then vortexed and incubated at 60°C with the eppendorf lids closed for 15 minutes. The samples and standards were then transferred into clear 96-well plates and the absorbance at 550nm measured using a micro plate reader (Glomax Multidetection System, Promega). The standards of known hydroxyproline concentration were used to plot a calibration curve.

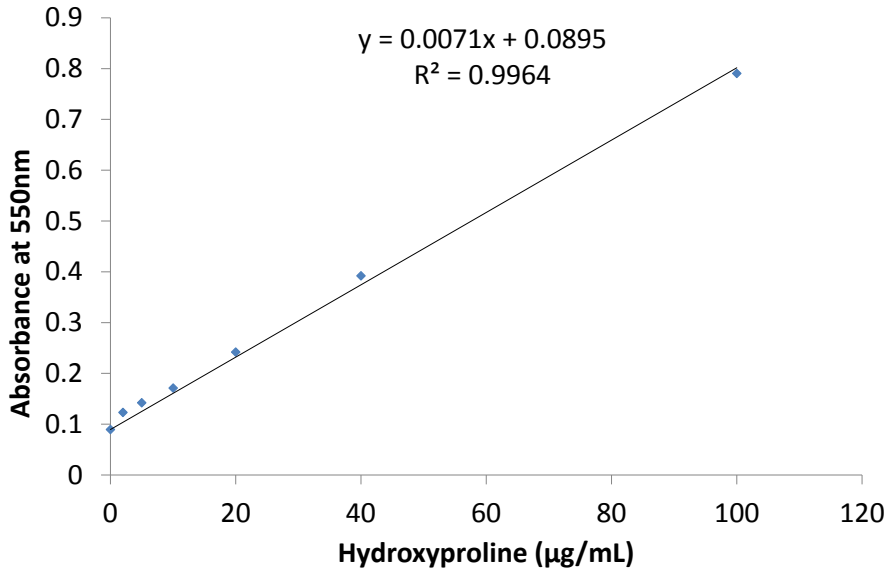

FIGURE 3.3: Hydroxyproline caliberation curve. This is one of the curves obtained during collagen quantification experiments in this thesis. A standard curve was obtained for each experiment conducted.

From Neuman and Logan, hydroxyproline is estimated to constitute 13.4% of the total collagen present in the tissue. Using this basis, the quantity of collagen present in the samples as a percentage of the construct dry weight was calculated using the following equation:

$$\frac{\mu\text{g hydroxyproline in lysate}}{0.134} \times \frac{1}{\mu\text{g dry construct}} \times 100 \tag{3.5}$$

An example calculation is shown in Appendix A.

3.5 Mechanical Testing

3.5.1 Rheology

Oscillatory dynamic shear tests were conducted on pre-formed gels, which were prepared as described in section 3.2.4. Viscoelastic materials exhibit both viscous (liquid-like) and elastic (solid-like) behavior described by the equation:

$$G^* = G' + jG'' \tag{3.6}$$

G′ is the storage modulus, which describes the elastic part of the equation and is a measure of the energy stored during deformation and G″ is the loss modulus, which represents the viscous part, the energy lost as heat when the material is deformed (Gunasekaran and Ak, 2000). Materials that behave more like a solid have a G′ greater than G″ and conversely, the more liquid-like the material, G″ exceeds G′ (Yan and Pochan, 2010). The stress response of the elastic and viscous parts of a viscoelastic material respond differently to an applied strain and are out-of-phase with each other. For an oscillatory sinusoidal strain, the strain is time dependent and related to angular frequency:

$$\gamma(\mathrm{t}) = \gamma_0 \sin(\omega \mathrm{t}) \tag{3.7}$$

and the corresponging sinusoidal stress response is:

$$\sigma = \gamma_0 (G'(\omega) \sin \omega \mathrm{t} + G''(\omega) \cos(\omega \mathrm{t})) \tag{3.8}$$

and both G' and G" are functions of angular frequency (Weitz et al., 2007).

3.5.1.1 Strain and Frequency Sweeps

Where the stiffness of pre-formed fibrin gels was measured, the gels were placed between two 40mm stainless steel sandblasted parallel plates (993244 and AC20-3

Cover Plate, TA Instruments). The fibrin gels were prepared such that the diameter of the gels matched the diameter of the geometry (Figure 3.4). Sandblasted bottom and top plates were used to prevent the gels from slipping. To determine the Linear Viscoelastic Region (LVR) of the gels, where stress is independent of strain, the frequency was kept constant at 1 rad/s, at a temperature of 37°C. The strain range was set at either 0.1 – 100% or 0.1 – 150%. The robustness of the gels within the LVR, was measured by adjusting the frequency from 0.1 – 50rad/s, at a set strain of either 0.5% or 1% strain and constant temperature of 37°C.

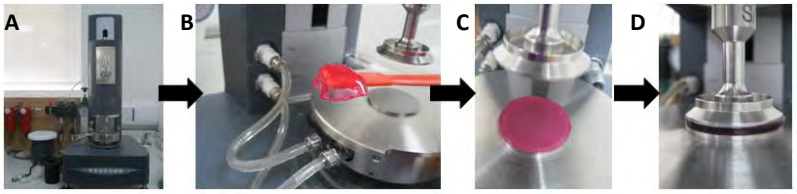

FIGURE 3.4: Equipment and sample loading for rheological experiments. A) Rheological properties were characterised using an ARG2 Rheometer (TA Instruments). B) Samples were robust enough to handle. C) Sample diameter matched that of geometry. D) Sample between parallel plates, top plate was lowered enough so that normal force was maintained positive and close to zero.

3.5.1.2 Time Sweeps

Time sweeps investigated the change in stiffness with time during gelation. Thrombin, AP and AH were added to sDMEM as previously described and 500μL of this was added to an eppendorf tube, followed by 200μL of Fibrinogen. The mixture was gently pipetted one or twice, using a 1000μL hand pipette, and loaded onto the centre of the rheometer bottom plate. A 40mm stainless steel cone geometry (992493, TA, Instruments) was used, which was quickly lowered before starting the test. The test was set to run for 1 hour, as cells are normally seeded on top of the gels following 1 hour gelation in the incubator.

3.5.2 Tensile Testing

3.5.2.1 Equipment set-up

The mechanical testing apparatus was set up as shown in Figure 3.5-1). First, the 10N load cell was fitted onto the machine (Instron 5800 series) before assembling the water bath. Once the water bath was fully connected, it was filled with 1.2L PBS solution and the pump was started to heat and recirculate the PBS to 37°C. The load cell was then calibrated using the Bluehill software program before connecting the custom made upper grip. The test was set at an extension rate of 0.4mm/s.

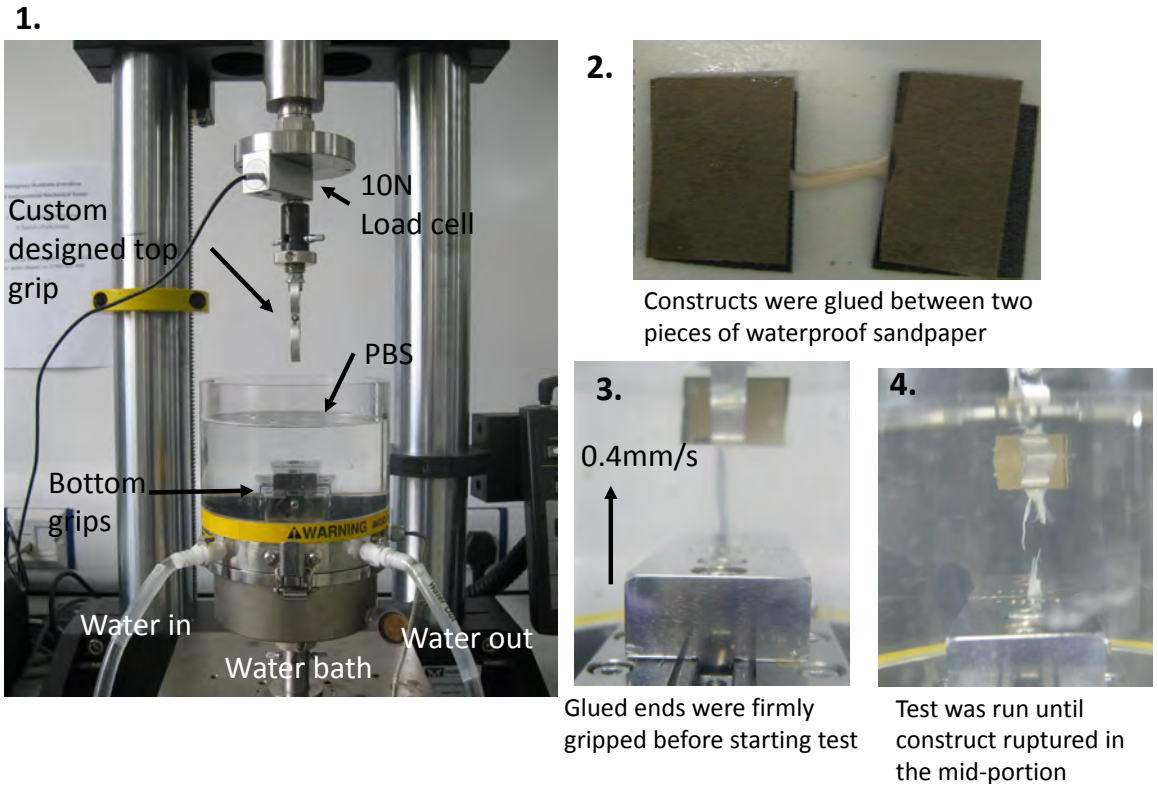

FIGURE 3.5: Equipment and sample loading for construct tensile testing. 1) Set-up of Environmental Microtester (Instron 5800) with 10N load cell, water bath and sample grips. 2) Construct gripped between two pieces of sandpaper. 3) Sample loaded on to machine before starting test. 4) Test stopped on rupture of construct in the mid-section.

3.5.2.2 Sample preparation

To test the soft TE L/T, the anchors were gently pealed away from the constructs. Both ends of the constructs were then glued between two pieces of sandpaper, they were imaged using a compact digital camera and the gauge length between the two pieces of sandpaper was measured using callipers. One end of the constructs was then connected to the top grip, ensuring that the edge of the sandpaper, towards the tissue, was aligned with the edge of the grip, to ensure accuracy of the measure gauge length. The gripped construct was then lowered to the bottom grip inside the water bath, and gripped in a similar manner as the top grip, so that only the tissue was visible between the grips. The pump was stopped during the running of each test to prevent water currents influencing the results. The test was started manually and stopped manually on complete rupture of the tissue. The pump was immediately restarted after each test to maintain the water bath temperature.

3.6 Construct cell quantification

To determine whether AA+P supplementation affect cell proliferation, cells were detached from constructs to allow quantification. Constructs were scaled down and grown in 12-well plates, to improve the efficiency of cell dissociation from the matrix.

3.6.1 Reagents

3.6.1.1 TESCA Buffer

TESCA buffer was prepared as a solvent for Collagenase I (C0130, Sigma-Aldrich). The buffer was composed of 50 mM TES (T5691, Sigma-Aldrich) and 0.36 mM Calcium chloride (C3881, Sigma-Aldrich) in distilled water. The buffer solution was sterile filtered using a bottle top system (10211321 , Fisher UK).

3.6.1.2 Collagenase I Solution

Collagenase is activated by Ca^{2+} and therefore it is recommended that the powder be reconstituted in TESCA buffer (Sigma). Stock solutions were prepared at a concentration of 10mg/mL and the aliquotes were frozen at -20°C. When used during construct matrix digestion, the collagenase stock was diluted to 1mg/mL.

3.6.1.3 Calcein-AM Solution Preparation

50μg vials of Calcein-AM (C3100MP, Invitrogen) was dissolved in 950μL DMSO (dimethlyl sulfoxide).

3.6.2 Cell dissociation from constructs

A series of enzymatic digestion stages were used to digest the fibrin and collagen matrices in order to release the cells. First, under a sterile laminar flow hood, spent sDMEM was removed from the constructs and constructs were then washed in PBS. Once the PBS was removed, constructs were cut into smaller pieces using an ethanol sterilised scalpel. 500μL of TrypLE was added to each well and incubated at 5% CO_2 and 37°C for 15 minutes. Then 1mg/mL collagenase I in tesca buffer was added to each well at a volume of 500μL and the constructs were transferred to a shaker incubator (Innova 4000, New Brunswick Scientific) at 37°C and 100rpm for 1.5 hour. The constructs were taken out of the shaker incubator and pipetted up and down before returning for another 1.5 hour. Thereafter, 500μL of 0.25% EDTA Trypsin was added and construct were returned to the shaker incubator for 5-10 minutes. 500μL of DMEM was then added to the constructs and they were pipetted up and down again ensuring any small fragments were disrupted.

3.6.3 Quantification using calcein-AM

The cell suspension was then transferred into 1mL eppendorfs and centrifuged for 3 minutes at 1000 rpm. The supernatant was removed and replaced with 1mL PBS per tube. 10μL of Calcein-AM was added to each tube and incubated for 40 minutes.

The cell suspensions were then loaded on to 96-well black bottom plates and the fluorescence was read at 490nm using a Spectrophotometer (Glomax Multi Detection System, Promega). Standard curves were use to quantify construct cell number. The standard curves were obtained by seeding known quantities of Calcein-AM treated cells on a 96-well black bottom plate and correlating the fluorescence to the seeded cell number. Figure 3.6 shows two such standard curves.

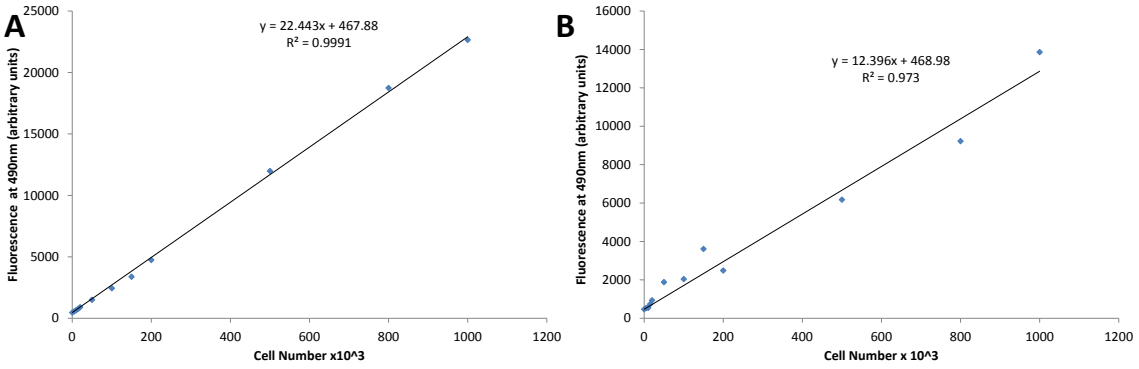

FIGURE 3.6: Standard curves used to quantify construct cell proliferation using calcein-AM. A) CTF standard curve. B) PFB standard curve.

3.6.4 Cell viability in reagents

Viability of cells in reagents used for dissociation was determined. A calibration curve using known quantities of CTF cells was prepared as above. A cell suspension of CTF cells at a density of 5,000cells/mL was prepared and seeded on 96-well black bottom plates. Cells were left to attach for 4 hours in a 5% CO_2 incubator at 37°C. The media was then replaced with either TrypLE, Collagenase I, Trypsin or left in DMEM (control) and returned to the incubator.

Every hour over a period of 3 hours, individual plates were stained with Calcien-AM and the calibration curve was used to quantify cell number and consequently viability. The results showed that cells survived well in TrypLE, Collagenase I and DMEM. However, leaving cells in Trypsin for a prolonged period was detrimental to cell viability.

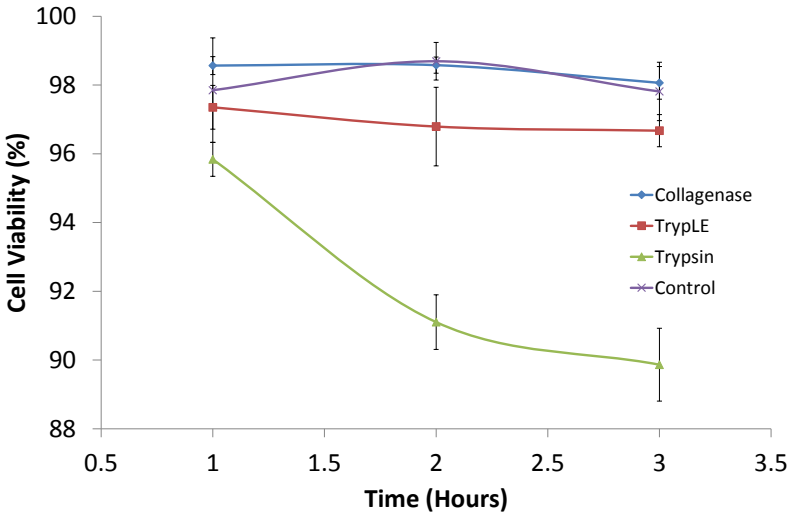

FIGURE 3.7: Viability of CTF cells in reagents used for dissociation.

3.7 Fluorescence Microscopy

3.7.1 DAPI staining

Constructs were washed in PBS before adding 300μL of 300nM DAPI stain and incubating for 20–30 minutes. No fixation or permeabilization was done for DAPI only staining. The DAPI stain was brought to 300nM by adding 3μL of the 10.9mM stock solution to 50mL of PBS solution. Constructs were imaged in a dark room using a confocal microscope (DM 2500, Leica).

3.7.2 Calcein-AM stained contraction impeded gels

Thin rings of filter paper were cut and pinned onto sylgard coated 35mm petri-dishes (Figure 3.8). The dishes with filter paper were sterilised with 70% ethanol under a laminar flow hood before gelling fibrin on top of the paper. The volume of fibrin was doubled due to the absorption of liquid reagents by the filter paper prior to gelation.

Due to the strong adhesion of the gel to the paper, over 7 days the cells were unable to laterally contract the gel. Constructs were either supplemented or unsupplemented or the stiffness of the gel was adjusted. They were fed every 2 to 3 days as standard.

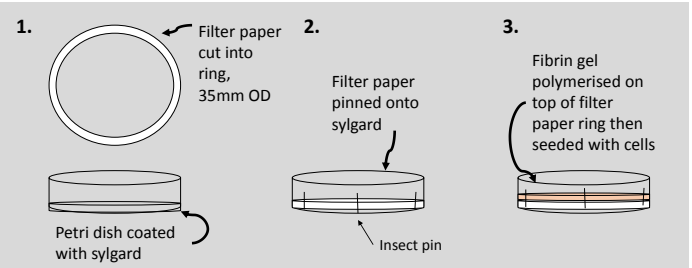

FIGURE 3.8: Preparation of contraction impeded constructs.

Constructs were stained with Calcein-AM and Propidium Iodide to observe cell viability and proliferation. Constructs were visualized and imaged using a fluorescence microscope.

3.8 Electron Microscopy

3.8.1 Scanning Electron Microscopy

3.8.1.1 Karnovsky's Fixative

A 0.2M sodium cacodylate buffer solution was prepared by dissolving 8.56g sodium cabodylate trihydrate (C0250, Sigma-Aldrich UK), 33g of dihydrous calcium chloride (C3881, Sigma-Aldrich), 2.5mL 0.2N hydrochloric acid (Fisher) in 200mL distilled water. 100mL stock of Karnovsky's fixative contained 8% v/v Formaldehyde, 50% Glutaraldehyde and 40mL sodium cacodylate buffer. The fixative was stored in 15mL tubes at -20°C until use.

Constructs or fibrin gels were fixed in Karnovsky's fixative for 3 hours or 1 hour, respectively, before dehydrating in ethanol (fixative was not was not diluted).

3.8.1.2 Sample dehydration

Samples were dehydrated in a series of ascending ethanol grades for 15 minutes in each. The ethanol solutions used were 15%, 20%, 30%, 50%, 70%, 80%, 90%, 95%, 100% and 100%.

3.8.1.3 Critical point CO_2 drying

Care was taken to ensure that the samples did not air dry by keeping them immersed in 100% ethanol. Samples were placed in individual metallic baskets in a sample boat, they were flooded with ethanol and then placed in the critical CO_2 chamber (Figure 3.9A). The chamber was filled with liquid CO_2 at a pressure of 800lb/in^2 and then the ethanol was completely flushed out.

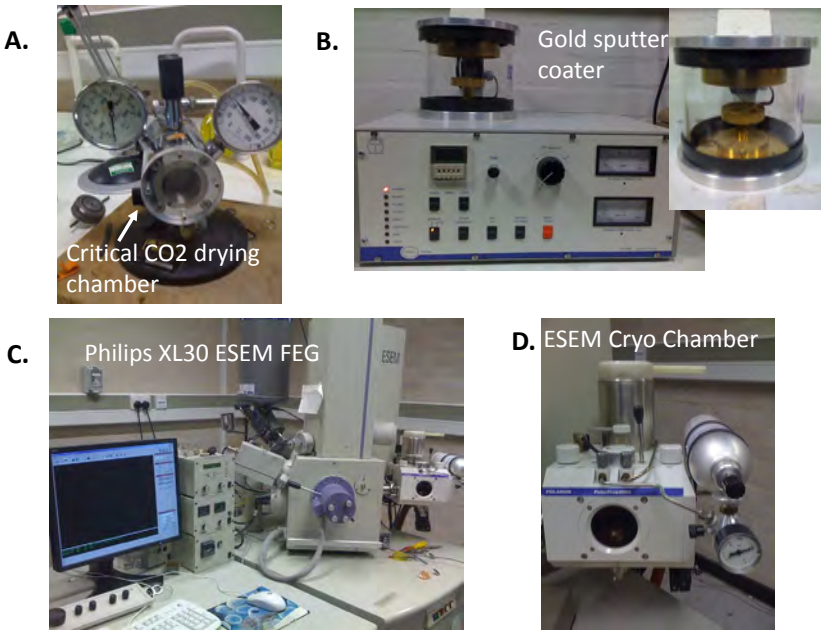

FIGURE 3.9: Equipment used for scanning electron microscopy.

Once all the ethanol was flushed, all the valves were closed at the samples left in liquid CO_2 for 10 - 20 minutes. The liquid CO_2 was then drained to a level just above the sample and vaporised by turning on the hot water tap. When a pressure of 1600 lb/in^2 and temperature of 38°C was reached, the hot water tap was closed and the CO_2 chamber pressure was let down/ vented. Dried samples were removed from the chamber and stored or sputter coated in gold (Figure 3.9B) and imaged using ESEM (XL30 ESEM FEG, Philips) (Figure 3.9C).

3.8.2 Cryo-Scanning Electron Microscopy

Samples were rapidly frozen in liquid nitrogen before being transferred into the ESEM machine's prep-chamber (Figure 3.9D). The samples were etched for 20 minutes at

-90°C. Once etched the temperature was reduced to -176°C and samples were sputter coated in gold. The samples were then moved into the imaging chamber.

3.9 Histology

3.9.1 Construct preparation

Constructs were fixed in 4% formaldehyde (Sigma) in PBS overnight. The constructs were then dehydrated in an ascending series of ethanol washes, 30%, 50%, 70%, 80%, 90%, 95% and twice in 100%, for 15–20 minutes in each solution. Dehydrated samples were cleared in Histoclear (HS-200, National Diagnostics) for 20–30minutes. Samples were placed in embedding cassettes and embedded in wax for 30 minutes to 1 hour, depending on the size and robustness of the sample, at 60°C (Wax Embedder, Leica EG 1160). The wax infiltrated samples were left to harden on the cold plate for 1 hour. 5-8μm sections were cut using a microtome (Leica RM 2035). Sections were collected in a water bath set at 45°C (Klinipath Good(s) in Pathology, WB28040). Sections were transferred onto slides (J2800AMNZ, Thermo Scientific), which were left to dry on a hot plate at 65°C. After drying, the slides were cleared in Histoclear for 15 minutes and rinsed in 100% then 70% ethanol, followed by a rinse in distilled water.

3.9.2 Hematoxylin and Eosin staining

The protocol supplied by Sigma-Aldrich with the reagents was used as a guide for staining. Slides were stained in hematoxylin (HHS16, Sigma-Aldrich UK) for 2.5 minutes, rinsed in running tap water followed by 10s in the differentiating solution. Slides were then blued in Scotts Tap Water for 2 minutes and in 95% ethanol for 2 minutes before staining in Eosin (HT-110116, Sigma-Aldrich) for 1 minute. Stained slides were dehydrated in 70% - 100% ethanol and cleared in Histoclear for 10mins. Slides were then mounted (Histomount, HS-103, National Diagnostics) and imaged using a light microscope (CETI) with an in-built camera (CETI, Si-3000).

3.9.3 Masson's Trichrome Staining

Constructs were prepared for masson's staining (HT15, Sigma Aldrich) as above and the slides were complexed with Bouins solution at 55°C under a fume hood for 20 minutes. Moderately remaining Bouin's was washed off the slides under running tap water until clear (prior washes were disposed off using special measures due to the fixative's harmful effects). The slides were then stained in Weigert's Working Hematoxylin solution for 10 minutes and rinsed in distilled water. This was followed by Biebrich scarlet acid fuchsin solution for 5 minutes, a rinse in distilled water and then Phosphomolybdic phosphotungstic acid solution for 15 minutes. The sections were then placed in Aniline Blue for 10 minutes, rinsed in distilled water followed by a rinse in 1% acetic acid. Sections were then dehydrated in 70%, 80%, 90%, 95% and 100% ethanol and mounted. Samples were imaged using a light microscope.

3.10 Reverse Transcription Polymerase Chain Reaction

Constructs at weeks 2, 3 and 4 were used. Cells were dissociated from the fibrin matrix using enzyme digestion as described in section 3.6.2. The cell suspensions were centrifuged at 1000 rpm for 3 minutes, washed in PBS and centrifuged again into pellets. Thereafter, the protocols supplied with the RNeasy Mini Kit (74104, Qiagen) were followed from Appendix D (pages 69–70) and the Handbook (pages 25 –30). The cell pellets were disrupted to extract DNA by adding 350μL of Buffer RW1 and centrifuging at 10,000 rpm for 30s followed by the addition of 80μL of the DNase I incubation mix (72954, Qiagen). The samples were then left to stand at room temperature for 15 minutes. Because RNA is more sensitive to degradation than DNA, RNA was extracted once all samples were collected. The DNA samples were stored at -20°C until required.

To extract RNA, 500μL of buffer RPE was added to each sample. They were then centrifuged at 10,000 rpm for 15 seconds and the flow through discarded. Buffer RPE was added again at 500μL per sample and centrifuged at 10,000 rpm for 2 minutes. 30–50μL of RNase free water was then added to each sample before centrifuging for

1 minute at 10,000 rpm. Samples were stored in a freezer at -80°C prior to reverse transcription and PCR.

Total RNA in each of the samples was determined using the Eppendorf Biophotometer Plus. The Tetro cDNA Synthesis Kit (BIO-65042, Bioline) protocol was then followed. Solutions of forward and reverse primers in Biomix Red (BIO-25005, Bioline) were prepared for GAPDH as well as for 9 target mRNAs (primers are shown below in Table 3.1). mRNAs regulate genes that encode for proteins, which control cell function. The mRNAs investigated are referred to according to the genes they regulate and/or the proteins encoded for by those genes.

GAPDH was normalised first before PCR for the targets was conducted. Generally for each sample, 2μL of sample was added to 23μL of the primer mix to prepare cDNA and amplified by thermocycling for 23 – 35 cycles (RT-PCR). 1.5% agarose gels with 3μL Ethidium Bromide were prepared and loaded with the samples and ladder (11300, Norgen). The gels were run at 120 volts for 20 minutes. The gels were then placed in a PCR cabinet (Geneflow) and results were quantified relative to GAPDH using GeneSnap (Geneflow).

TABLE 3.1: Chick primers used for PCR.

Primer	Full Name	Species	Sequence	Annealing temp	Size bps
GAPDH	GAPDH	Chicken	F- TGACCACTGTCCATGCCATC R - AGAACTGAGCGGTGGTGAAG	60	565
MMP1	MMP1	Chicken	F - TTCGCAGTGTAGCTGAAGCA R - TGCACATCTCCACCAAGACC	60	624
MMP2	MMP2	Chicken	F - CGATGCTGTCTACGAGTCCC R - ACAGTTCAGCAACCCAACCA	60	429
MMP9	MMP9	Chicken	F- CCAAGAGCATGGTGATGGGT R - AGAAGCCCCACTTCTTGTCG	60	644
COL1A1	collagen - type I alpha 1	Chicken	F - AGTTTGAGTACGGCGGTGAG R - GGTGACCCCATAGGTGAAGC	60	230
MMP3	MMP3	Chicken	F - ACTGGGATAGGAGGGGATGC R - AGCATCAAAGCCAGCTACCA	60	519
RhoA	RhoA	Chicken	F - AAGCGTGGCTTCAGTGCTAT R - GAGTGTGAGCAGGCTGTCTT	60	466
TenC	Tenascin C	Chicken	F - GCGAGTGTCACAGACAGACA R - CGTCCCTGCGTCTAATCCTC	60	442
ACTA2	alpha smooth muscle actin	Chicken	F- ACTCTGCTGACTGAAGCACC R- CTGTCTGCAATGCCTGGGTA	60	629
SCX	scleraxis	Chicken	F - TCAAAGCCGGCAAGAGGAG R - TCCTGTCGCGGTCTTTACTC	60	402

3.11 Statistical Analysis

Results are quoted as mean ± standard deviation. Statistical variance was determined using ANOVA (SPSS v 21, IBM). Significance was set a $p \leq 0.05$ and generally pair-wise comparison between group means was evaluated using Tukey's post hoc. However, where groups sample sizes varied, Games-Howell post hoc was used instead.

Chapter 4

Contraction of ascorbic acid and proline supplemented constructs

4.1 Introduction

Improving the mechanical strength of tissue engineered ligaments and tendons (L/T) and ensuring they exhibit the histological morphology of native tissue is the focus of many studies (Marturano et al., 2013; Teh et al., 2013; Herchenhan et al., 2013; Leong et al., 2013). Due to the structural supportive role of L/T, mechanical properties of tissue engineered analogues must closely match those of native tissue in order to withstand imposed forces once *in vivo* and to facilitate the regeneration process.

The synthesis of collagen, which is a structural protein and the predominant component of L/T tissues, has long been known to require ascorbic acid (AA) as a cofactor for the synthesizing enzymes (Peterkofsky, 1972; Murad et al., 1981). Consequently, AA is frequently employed as a supplement during cell culture (Osiecki et al., 2010). This is also likely due to its anti-oxidative properties (Arrigoni and De Tullio, 2002), which have implications on fertility (Luck et al., 1995), MSC differentiation (Otsuka et al., 1999; Franceschi, 1992) and cancer treatment (Padayatty et al., 2006).

The amino acid proline (P) is responsible for the helical conformation and stability of the collagen molecule (Vitagliano et al., 2001) and is involved in several metabolic pathways (Phang et al., 2008; Wu et al., 2011). *In vivo*, proline is hydroxylated after

synthesis of the collagen precursor peptide into hydroxyproline, however, soluble hydroxyproline is poorly incorporated into collagen whereas proline shows better efficacy (Prockop and Juva, 1965). Nevertheless, the effects these supplements have on the depletion of the tissue engineering scaffold and construct final dimensions have not been widely reported.

Using the methodology employed in this thesis, supplementation of constructs with 50μM AA and 50μM P from the 7th day in culture, over a period of 5 weeks, resulted in TE sinews with a higher collagen quantity of 8.34 $\pm$ 0.37% when compared to the unsupplemented control group 1.34 $\pm$ 0.2% (Paxton et al., 2010a). In addition, the anchor-TE ligament interface strength and sinew modulus increased 3-fold and 18-fold, respectively, over the control group. Part of the published work featured in this thesis reports further enhanced sinew collagen content to 15.45 $\pm$ 0.49% after 5 weeks in culture when supplementation concentration was increased to 250μM AA in combination with 50μM P (Paxton et al. (2012), Appendix D). Yet, constructs treated with these concentrations of AA+P were visibly thinner than non-treated constructs. OCT imaging further revealed that cross-sectional areas of AA+P sinews were significantly smaller than control sinew cross-sections (Paxton et al., 2012).

Excessive contraction of the supportive TE scaffold is generally undesirable as it does not allow sufficient time for tissue formation with adequate mechanical integrity. As most mammalian cells are adherent, rapid depletion of the scaffold also leads to cell apoptosis (Chiarugi and Giannoni, 2008). Consequently, the ideal scaffold has a degradation rate that resembles the rate of new matrix deposition by the cells (Sung et al., 2004).

Studies were set-up to determine the effect of AA+P supplementation on cell mediated contraction of the fibrin hydrogel scaffold and to quantify the rates of contraction. The aim of the studies was to supply data, which would be useful in producing alternative supplementary regimes or other methods to further optimise collagen content whilst controlling the extent of contraction.

Biological characterisation of the TE L/T was conducted utilising microscopy and histological techniques to compare non-treated control constructs with those where AA+P was administered during culture.

4.2 Materials and Methods

4.2.1 Construct preparation

Constructs were prepared as described in Chapter 3 section 3.2.

4.2.2 Supplementation

4.2.2.1 Ascorbic acid and proline

On seeding day, groups were fed with either sDMEM only for the controls or sDMEM supplemented with AA, P or AA+P. Thereafter, constructs were fed every two to three days.

4.2.2.2 Varying concentration of either ascorbic acid or proline

Where AA or P concentrations were varied, during combined AA+P supplementation, either AA was kept constant at a concentration of 250μM or P was maintained at 50μM. When varied, concentrations of the varied group were 50μM, 250μM and 500μM.

4.2.2.3 Collagen inhibition with DMOG

To inhibit collagen formation, constructs were fed with sDMEM supplemented with either 25μM or 100μM DMOG (D3659, Sigma-Aldrich UK).

4.2.3 Collagen quantification

Collagen was quantified as described in Chapter 3 section 3.4.

4.2.4 Microscopy

4.2.4.1 Scanning Electron Microscopy

Samples were fixed in 2.5% Glutaraldehyde in 0.1M Phosphate buffer for 1 hour. This was followed by a series of dehydration washes at 50%, 70%, 90% and 100% ethanol, twice for 15 minutes in each. The ethanol in the samples was replaced with liquid CO_2, followed by critical point drying. Samples were then mounted and sputter coated in gold. Images were taken using the XL30 ESEM FEG (Philips).

4.2.4.2 Transmission Electron Microscopy

Primary fixation and dehydration were conducted in a similar manner as for SEM. TEM included a secondary fixation step in 1% Osmium Tetroxide for 1 hour prior to dehydration. After dehydration, samples were infiltrated with a 1:1 mixture of Propylene Oxide and Resin for 45 minutes, followed by 1 hour in 100% Resin. The samples were embedded beneath the surface of the resin in embedding moulds and left under vacuum for 30 minutes before returning samples to atmospheric pressure. The resin was left to polymerize at 60°C for $\geq$ 16 hours. The samples were cut into semi-thin sections of about 1μm, which were mounted on slides and stained with toluidine blue. Ultra-thin sectioned were prepared from the semi-thin sections. The sections were collected on Formvar/carbon coat TEM grids and stained with uranyl acetate and lead citrate. Samples were imaged on the JEOL 1200EX TEM.

4.2.5 Histology

Samples were prepared for histology as decribed in Chapter 3 section 3.9.

4.2.6 Reverse transcription polymerase chain reaction

RT-PCR was conducted as described in Chapter 3 section 3.10.

4.2.7 Statistical Analysis

Results are quoted as means ± standard deviation. Measurements of constructs treated with AA, P or receiving no treatment, were statistically compared to the AA+P group using independent t-tests on a day by day basis, based on the priori that AA+P supplemented groups would differ from other groups. For overall comparisons over the course of the study, all measurements were compared using one-way analysis of variance (ANOVA) and Tukey's test of significance. All other experiments were compared using one-way analysis of variance (ANOVA) and Tukey's post-hoc on a day by day basis. $p<0.05$ was considered significant. (IBM SPSS Statistics v. 21)

4.3 Results

4.3.1 Effect of ascorbic acid and proline on fibrin gel contraction

Constructs in this section were either non-treated (NT) controls or were supplemented with ascorbic acid only (AA), proline only (P) or both ascorbic acid and proline (AA+P).

All constructs, supplemented and non-treated, contracted to less than half the original fibrin gel surface area by day 3 and continued to contract significantly over the duration of the 52 day study (Figure 4.1). Differences in construct dimensions were not visibly apparent in the first week, however, by day 22 constructs treated with AA+P appeared thinner in width in relation to constructs of the other groups.

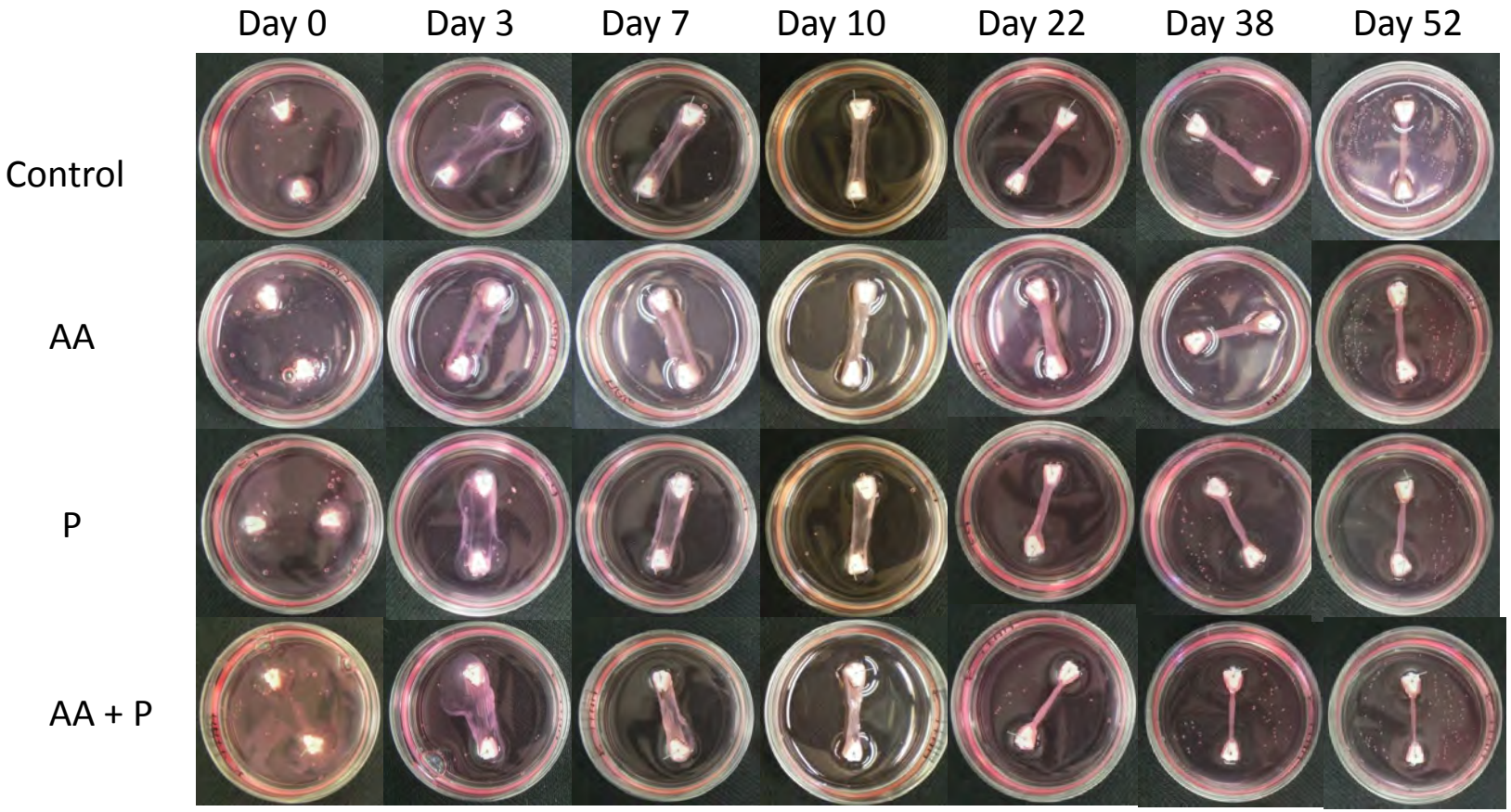

FIGURE 4.1: Images showing contraction of AA/ P/ AA+P supplemented constructs. No obvious differences observed in the first 3 days. AA and AA+P treated constructs appear denser than those treated with P only and control (NT) constructs on day 10. By day 22, AA+P supplemented noticeably thinner in width than other constructs, becoming even more apparent on day 52. n=7

4.3.1.1 Fibrin percentage gel areas

Fibrin gel percentage areas were measured daily in the first two weeks and then periodically over the 52 day study. This was conducted to determine if a particular trend due to treatment with AA, P or AA+P could be established.

Quantification of fibrin gel surface area changes supported visual representations. The greatest decline in gel area was observed on day 1, where all group areas decreased by over 50% (Figure 4.2). Supplementation with AA only on seeding day resulted in the greatest reduction in fibrin gel area to 38.69 ± 9.86% by day 1, which differed significantly ($p<0.05$) from P (46.40 ± 12.80%) and AA+P (45.52 ± 12.99%) supplemented groups. The difference between AA and the control group gel area of 40.83 ± 11.03% was not significant ($p=0.823$).

The general trend from day 4 to day 13 was that AA only treated constructs contracted the most, P only gels the least and the control and AA+P fibrin gel areas fell in between the two.

However, no statistically significant differences in fibrin gel area were observed until day 36 where AA+P showed the greatest decrease in fibrin gel area to 3.41 ± 1.24% in comparison to AA at 4.0 ± 0.68% ($p=0.010$), P at 4.27 ± 1.68% ($p=0.011$) and the control (NT) group, which was at 3.97 ± 1.13% ($p=0.008$).

By day 52 of the study, AA+P group had the lowest fibrin percentage gel area remaining of 2.73 ± 0.28%, which differed significantly from AA percentage gel area of 2.85 ± 1.96% ($p=0.036$) and P percentage gel area 3.81 ± 0.91% ($p=0.018$) but not from non-treated control group 3.41 ± 1.24% ($p=0.179$).

Comparisons of the overall rates of contraction over the 52 day period indicated that there were significant differences between the groups although AA only supplementation did not differ from the rate of contraction of the control group ($p=0.324$) and AA+P showed no significant difference when compared to the P group ($p=0.906$).

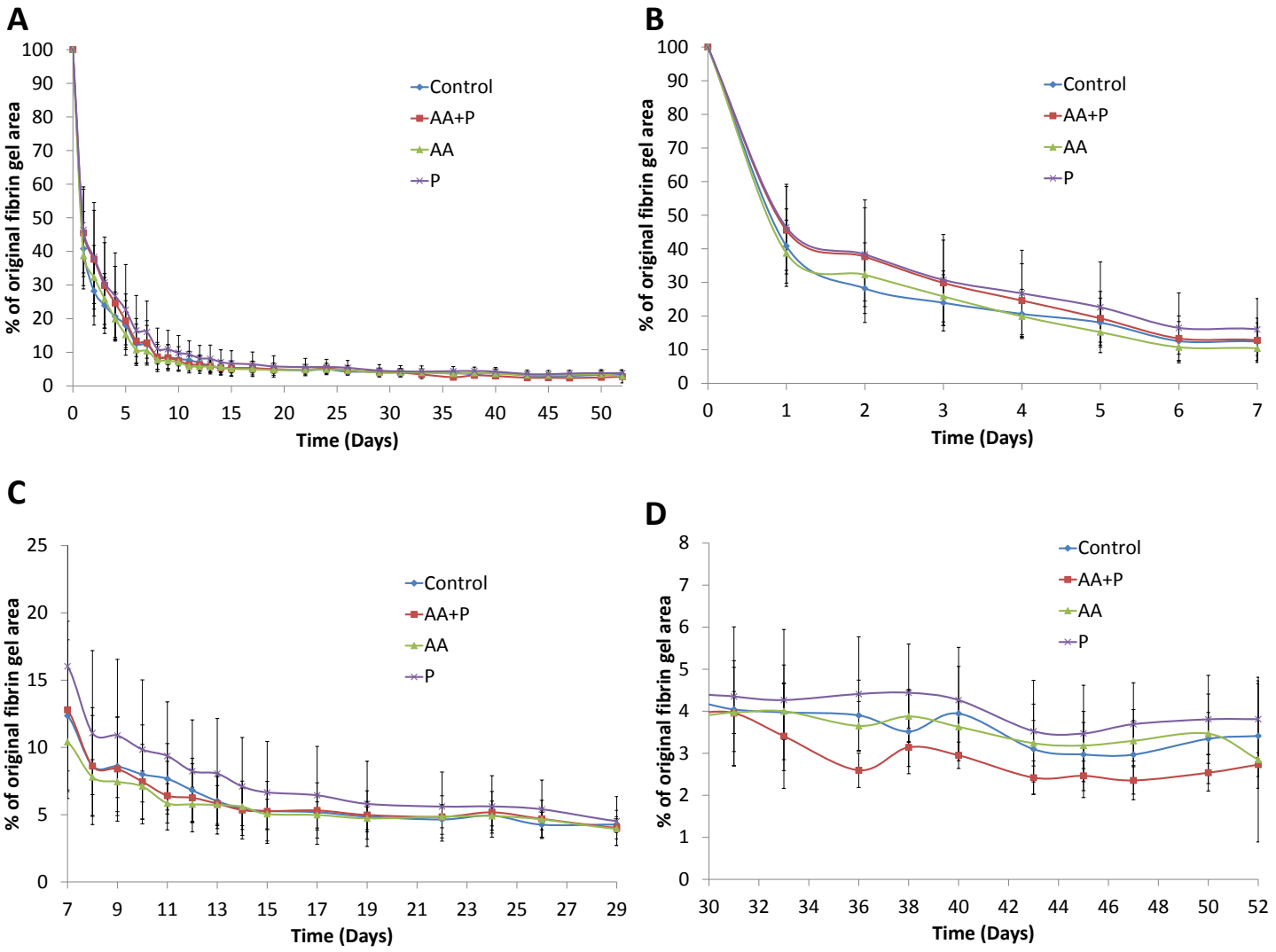

FIGURE 4.2: Quantification of fibrin gel areas of constructs treated with AA/P or AA+P. (A) is an overview of the overall rates of fibrin contraction. (B) Contraction over the first 7 days; the control and AA groups exhibited the fastest rate of contraction and P the slowest. (C) Control, AA and AA+P rates fairly similar, though extent of contraction of P less. (D) Statistically significant differences in percentage gel areas observed between AA+P and other treatment groups.

4.3.1.2 Maximum and minimum widths

Both maximum and minimum widths were measured because it was observed that constructs did not form uniformly. Although the average width could be quoted, this would not adequately represent limits on contraction. For example, it was considered that the maximum width could be dependent on the anchors, whilst the minimum width reflected continued contraction due to the supplements. However, irregular remodelling within the constructs due to the supplements, nature of the fibrin gel or other factors could not be discounted. As a result, both maximum and minimum widths are quoted throughout this thesis.

For all groups, no statistically significant differences were observed between the maximum and minimum widths during the first four weeks (Figure 4.3).

However, by the fifth week of culture, the maximum widths of AA+P group were thinner than the control and proline treated groups. On day 33, AA+P had a maximum width of 2.12 ± 1.05mm, which differed significantly from the control (NT) group 3.46 ± 0.59mm ($p=0.016$). AA+P minimum widths were also smaller in comparison to control constructs, with final dimensions of 1.48 ± 0.15mm and 2.41 ± 0.48mm, respectively ($p=0.016$). After the 5^{th} week, minimum widths of AA+P treated constructs were relatively constant at about 0.91mm, shown in Figure 4.3. Minimum widths of AA+P treated constructs differed significantly from control and proline treated groups from day 45 ($p<0.05$).

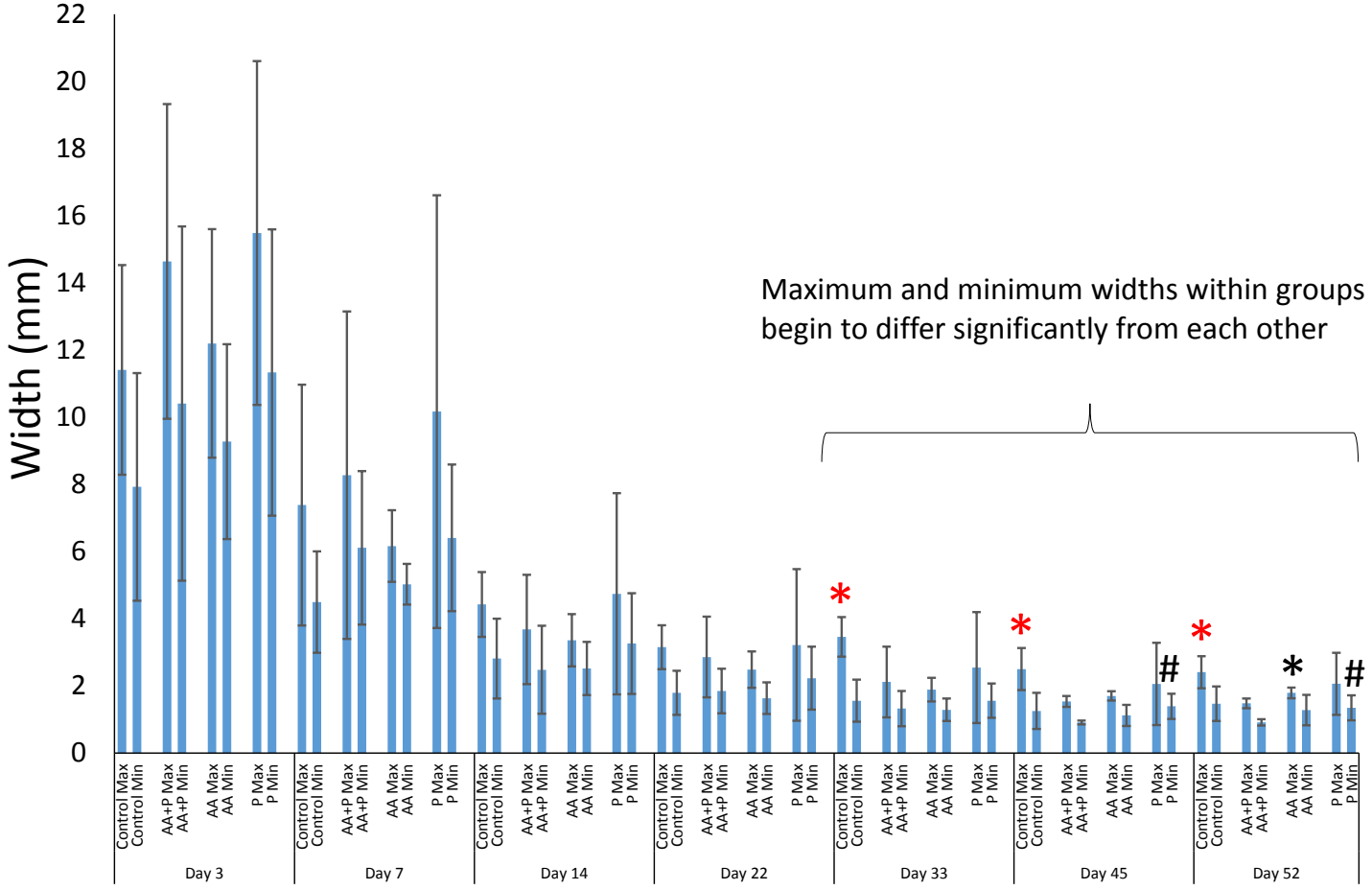

FIGURE 4.3: Construct maximum and minimum widths. There were variations in construct maximum and minimum widths, significant differences between AA+P and other groups becoming apparent after 5 weeks in culture. *Significant difference from AA+P max width denoted by * and significant difference from minimum width by #.*

4.3.2 Scanning electron microscopy

4.3.2.1 Control and ascorbic acid + proline construct longitudinal sections

Scanning electron microscopy was used to examine the longitudinal and cross-sectional morphology of control and AA+P treated constructs (Figures 4.4, 4.5 and 4.6). The outer surface of the control sinews had a high concentration of cells, which appeared to have raised cell bodies (Figure 4.4A and B). The cells also appeared to be aligned along very thin fibres ($\approx 0.2\mu$m) shown in Figure 4.4C. In contrast, AA+P treated sinews had a flat sheath-like cover, composed of flat cells (Figure 4.4D and E). Under the external sheath-like layer, a densely populated cell layer, similar to those of the control group were seen, however, these also appeared slightly flatter than those of the control group Figure 4.4 G and H. AA+P treated sinews also exhibited cell alignment parallel to the construct length (Figure 4.4F) surrounded by the thin similarly aligned fibres. The fibres were harder to identify than in the control constructs as AA+P sinews were more densely compacted.

4.3.2.2 Control construct cross-sections

Cross-section images of control constructs showed multiple folds within that resembled folded sheets (Figures 4.5A and B). The fibres that make up the constructs were distinguishable, particularly on the outer layers of the construct (Figure 4.5D). Apart from the sheet-like arrangement across the constructs (Figure 4.5E), the "sheets" also appeared to have perpendicularly aligned fibres connecting them together (Figures 4.5F and G).

4.3.2.3 Ascorbic acid + proline construct cross-sections

In AA+P treated constructs, distinct folds were visible along with the sheet-like arrangement across the sinews (Figures 4.6A and D). AA+P treatment appeared to result in greater compaction of the tissue (Figures 4.6B and C). In addition to the enhanced compaction, the "sheets" were connected by thin and densely matted fibres

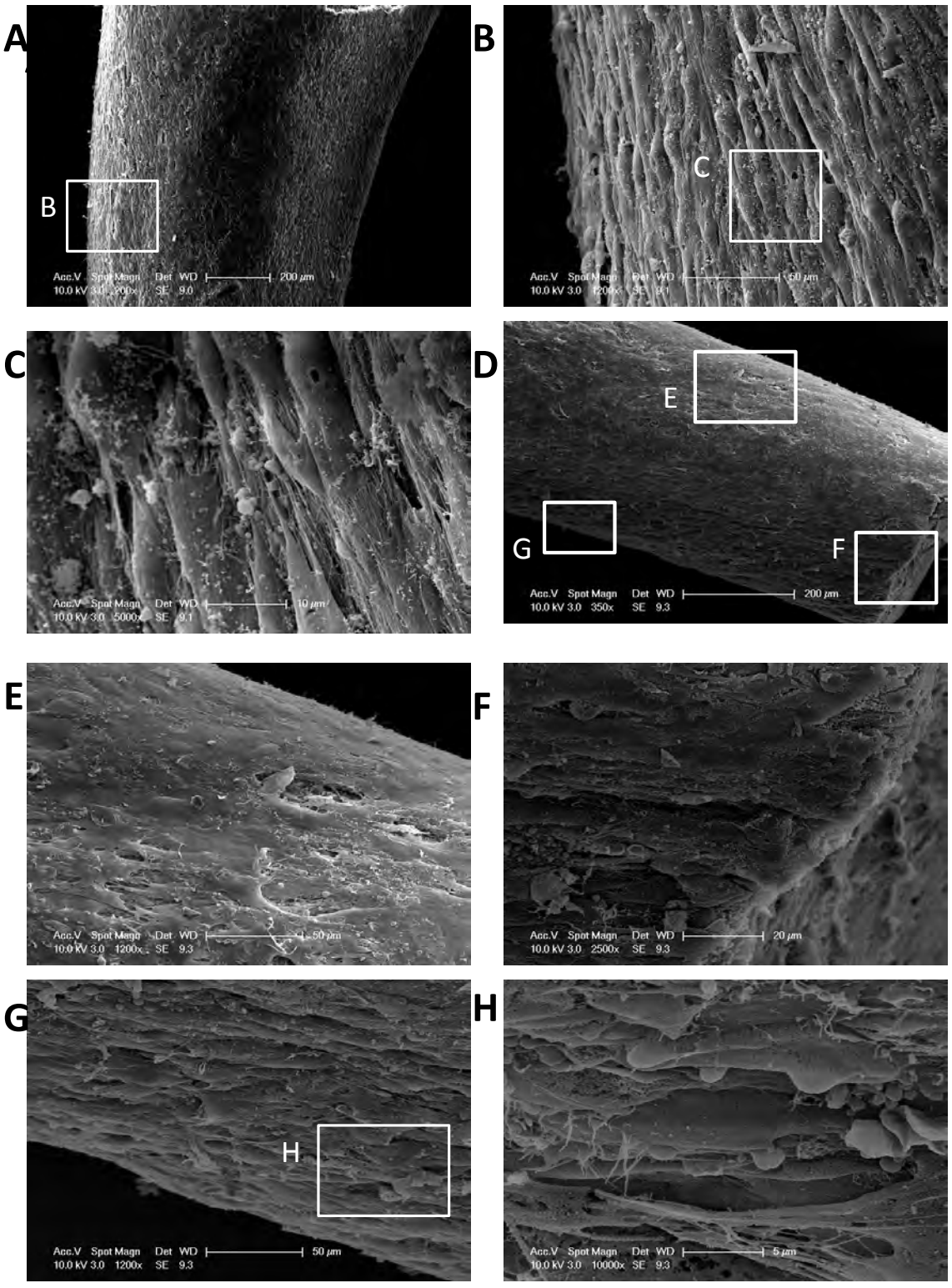

FIGURE 4.4: Longitudinal SEM images of control (NT) and AA+P treated sinews. Cells on the outer layer of control contructs were aligned in the direction of tension and appeared to have raised cell bodies (A–C). On the surface of AA+P treated cells appeared much broader and flatter in comparison to the controls (E–H).

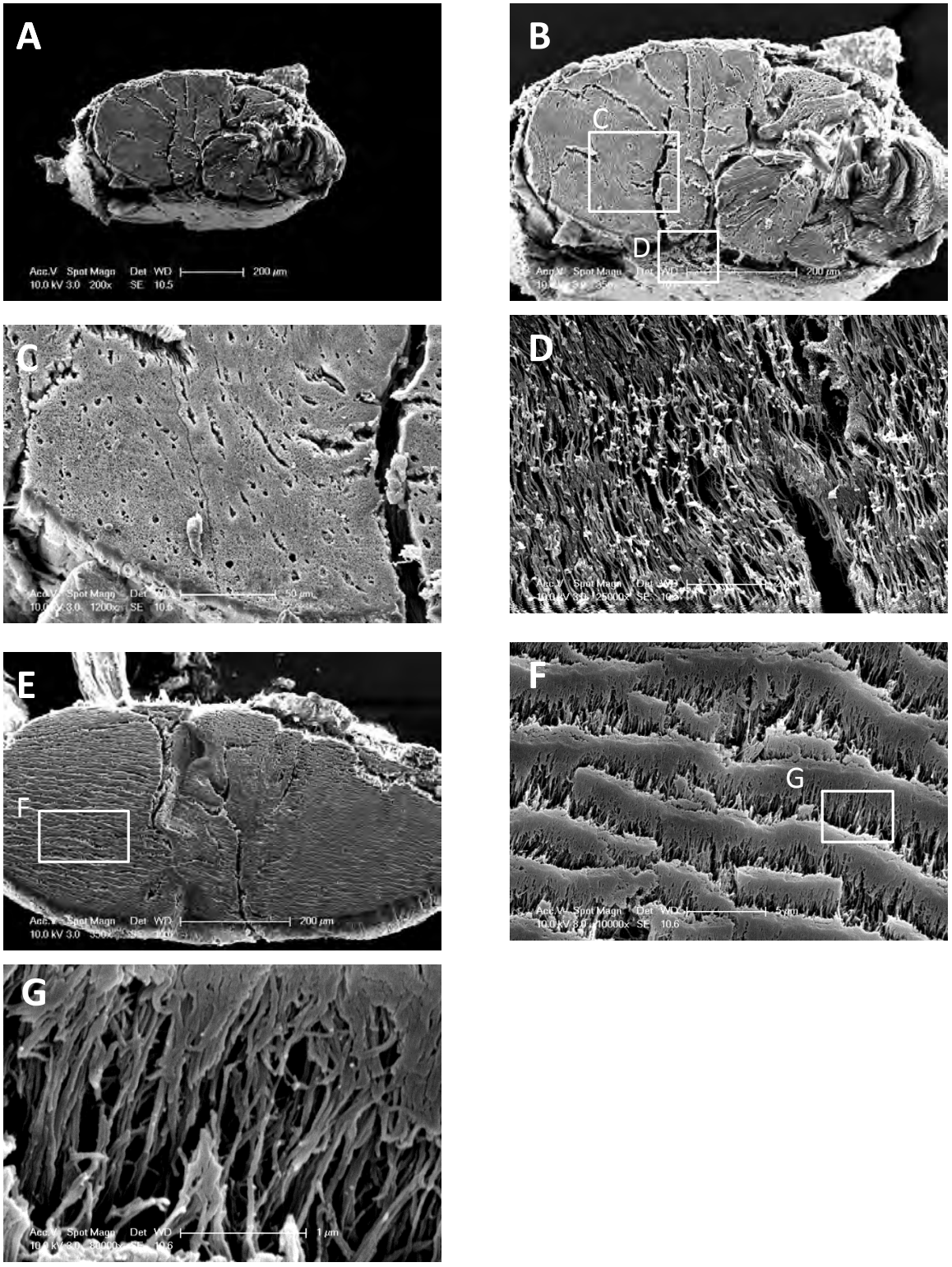

FIGURE 4.5: Cross-sectional electron microscopy images of control (NT) sinews. Contraction folds were visible within the sinew (A–C). Individual fibres were aligned in a parallel direction to each other (D). Thicker sheets were layered across the cross-section (E & F) and joined by fibres running perpendicular to them (G).

(Figure 4.6F and G), which differed in appearance from those of the control group (Figure 4.5F and G).

4.3.3 Histology

4.3.3.1 Hematoxylin and Eosin

H&E staining of longitudinal control constructs showed cell alignment in the mid portion of the constructs, with higher cell densities present on the periphery of the sinew (Figure 4.7a). AA+P supplemented constructs exhibited a similar morphology though the mid-portion appeared to be composed of a thicker fibrillar arrangement and generally, the cell densities throughout the AA+P sinews were lower than for the controls (Figure 4.7d). In native tissue, cells appear uniformly aligned along collagen fibres as in the rat tail tendon shown in Figure 4.7g.

Cross-sectional staining of the control constructs showed multiple folds within the constructs with one larger central fold (Figure 4.7b and c). In contrast, AA+P cross-sections, indicated a rolling formation of the sinews from the outside-in (Figure 4.7e and f). On the periphery of control and AA+P constructs, a fibrillar arrangement running across the sinew cross-sections was observed (Figures 4.7c and f), similar to the "sheet" arrangement seen with SEM (Figures 4.5 and 4.6).

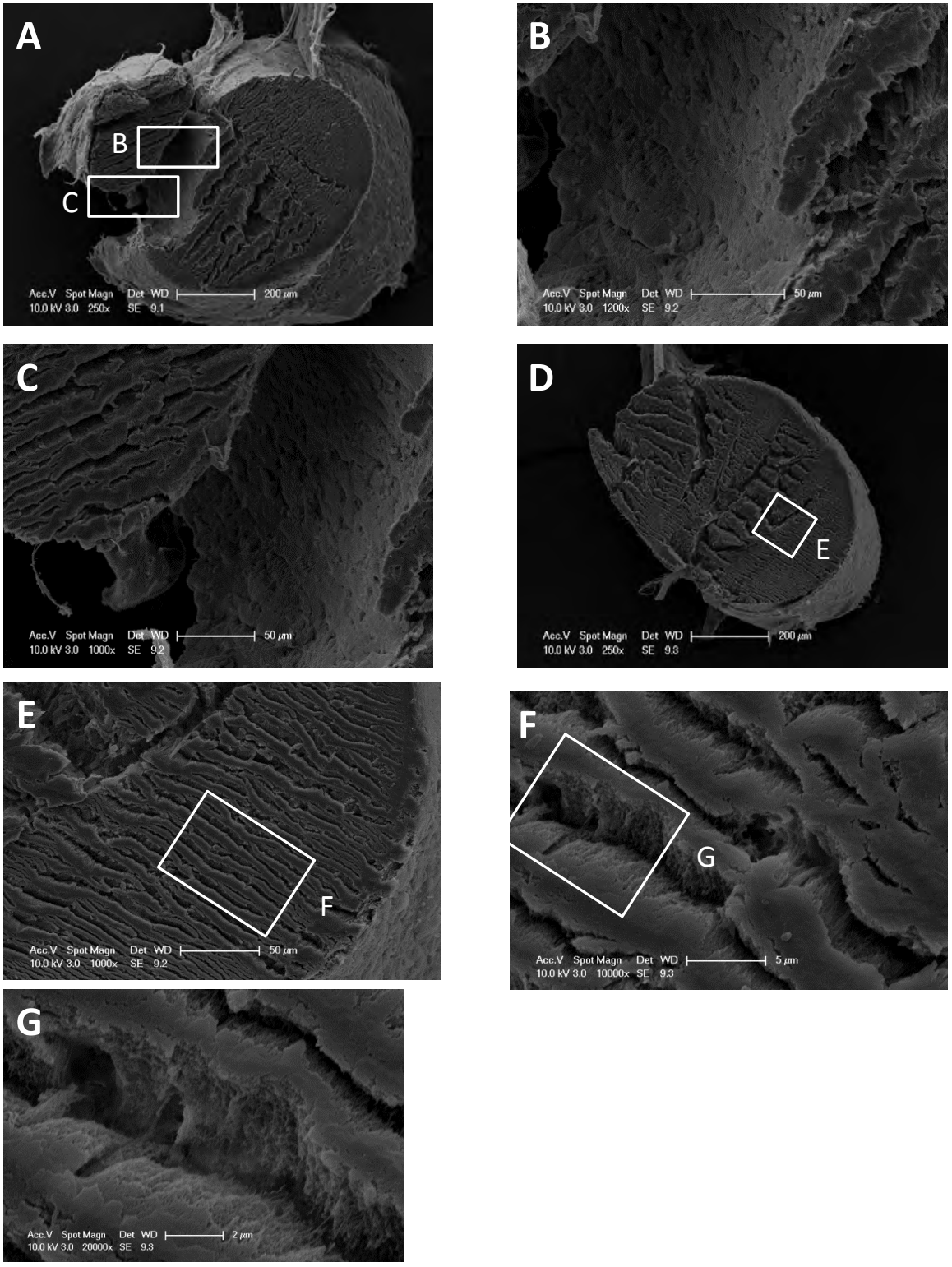

FIGURE 4.6: Cross-sectional electron microscopy images of AA+P treated sinews. AA+P constructs appeared denser although the folds (A–C) and sheets across (D–G) were also visible. The sheets were joined by largely matted fibres (F & G), indicating a greater extent of remodeling.

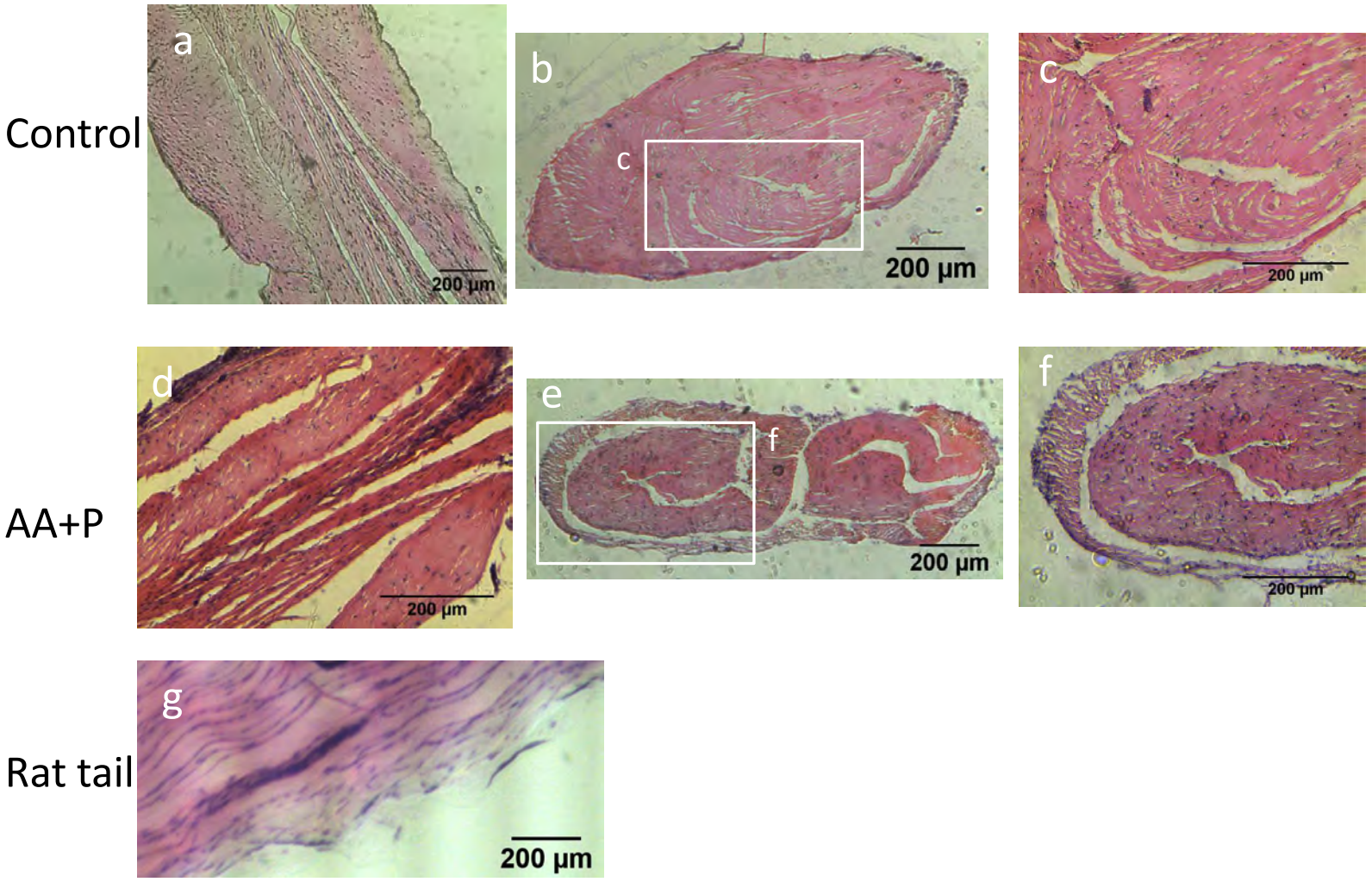

FIGURE 4.7: H&E stained sections of control and AA+P treated constructs. Longitudinal sections showed cells were aligned along the direction of tension in the mid-portion of a) control constructs and d) AA+P constructs. g) rat tail tendon indicating the morphology of native tissue. Cells were present throughout the cross-sections (b, c, e & f) of the constructs. e) & f) AA+P rolling formation was apparent.

4.3.3.2 Masson's Trichrome

Masson's Trichrome was used due to its ability to stain collagen blue/green and fibrin pink/red (Isenberg et al., 2006; Lanza et al., 2011). Control cross-sections revealed a darker red staining of fibrin around the outer portion of the constructs and within the folds whereas toward the centre of the construct fibrin stained a lighter pink (Figure 4.8a). At higher magnification the control constructs appeared to be flooded with blue specs (Figure 4.8b), which were distinguishably smaller than cell nuclei (Figure 4.8c).

The periphery of AA+P treated constructs stained blue for collagen to a greater extent than control constructs and the fibrin tissue also predominantly stained a darker red colour (Figure 4.8d and f). Patches of blue were found throughout the central portion of AA+P constructs (Figure 4.8e).

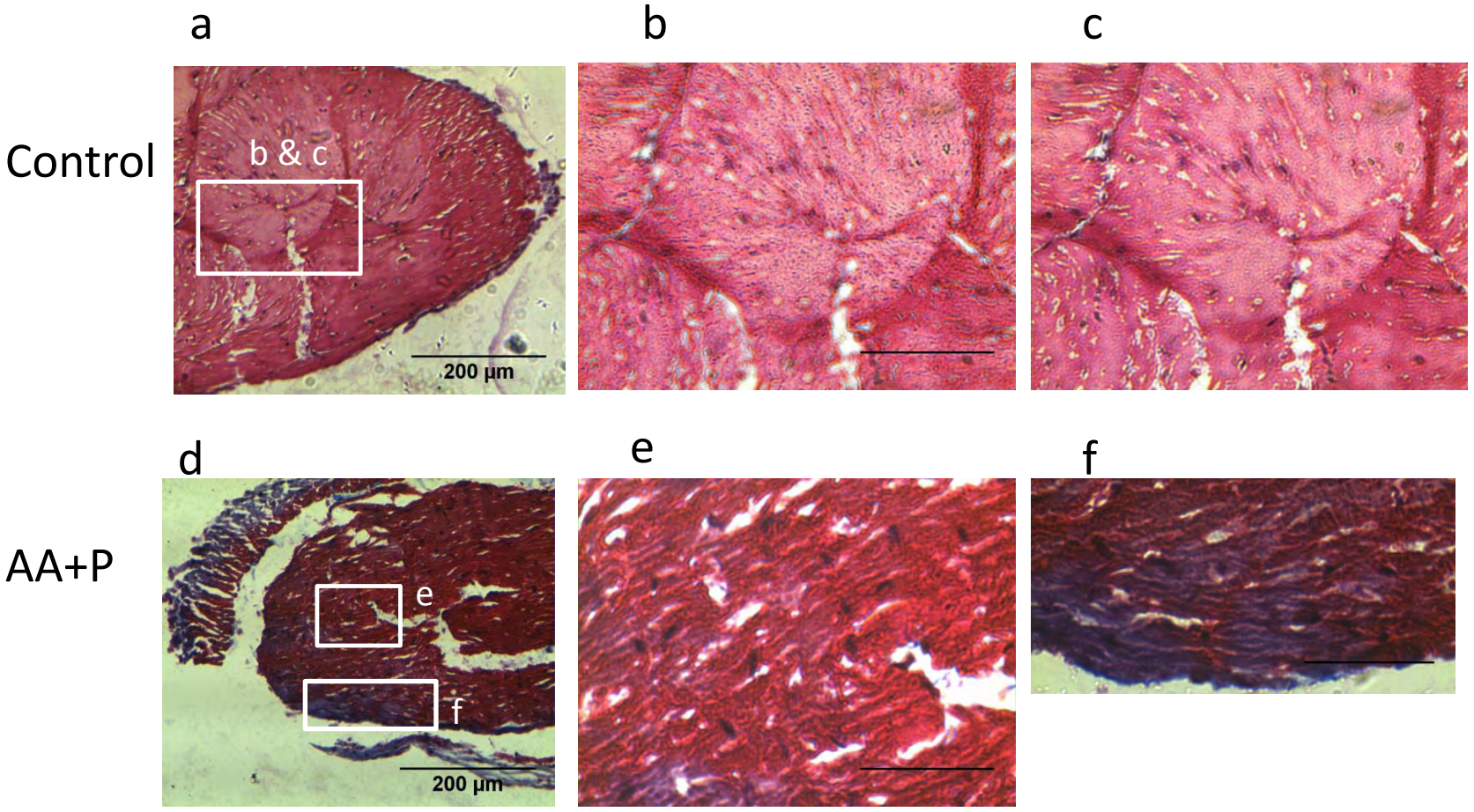

FIGURE 4.8: Control and AA+P sections stained for collagen using Massons Trichrome. a) cross-section of control construct. b) Blue specks were darted throughout the control cross-sections, which were identified as collagen and were significantly smaller than cell nuclei (c). AA+P cross-sections (d) stained darker and collagen was mostly situated on the periphery of the constructs (e) although collagen was also present within the construct (f). *Scale bar is 200µm for all images.*

4.3.4 Transmission electron microscopy

4.3.4.1 Control construct longitudinal sections

The constructs were characterized further at the submicroscopic level using TEM. Within the control constructs elongated cells as well as dark patches (P) were aligned along the length of the constructs (Figures 4.9a and b). Throughout the constructs needle- and speck-like structures were present. On the outer edge of the construct cells were densely packed, as shown with SEM, followed by an organised fibrillar arrangement (F), after which the needle-like and speck-like morphology appeared towards the middle (Figure 4.9c and d). Towards, the middle of the control constructs, there were areas free of the needle-like morphology along which only cells were aligned (Figure 4.9e). In addition, collagen (C) was identified and appeared to be aligned in both transverse and longitudinal directions. At higher magnification (Figure 4.9h), the banding pattern present in collagen was clearly apparent. Collagen fibres were also present within some of the dark patches and branched structures (S) (Figures 4.9f and g). The cells also contained large and numerous transport vesicles (V) (Figure 4.9f and g).

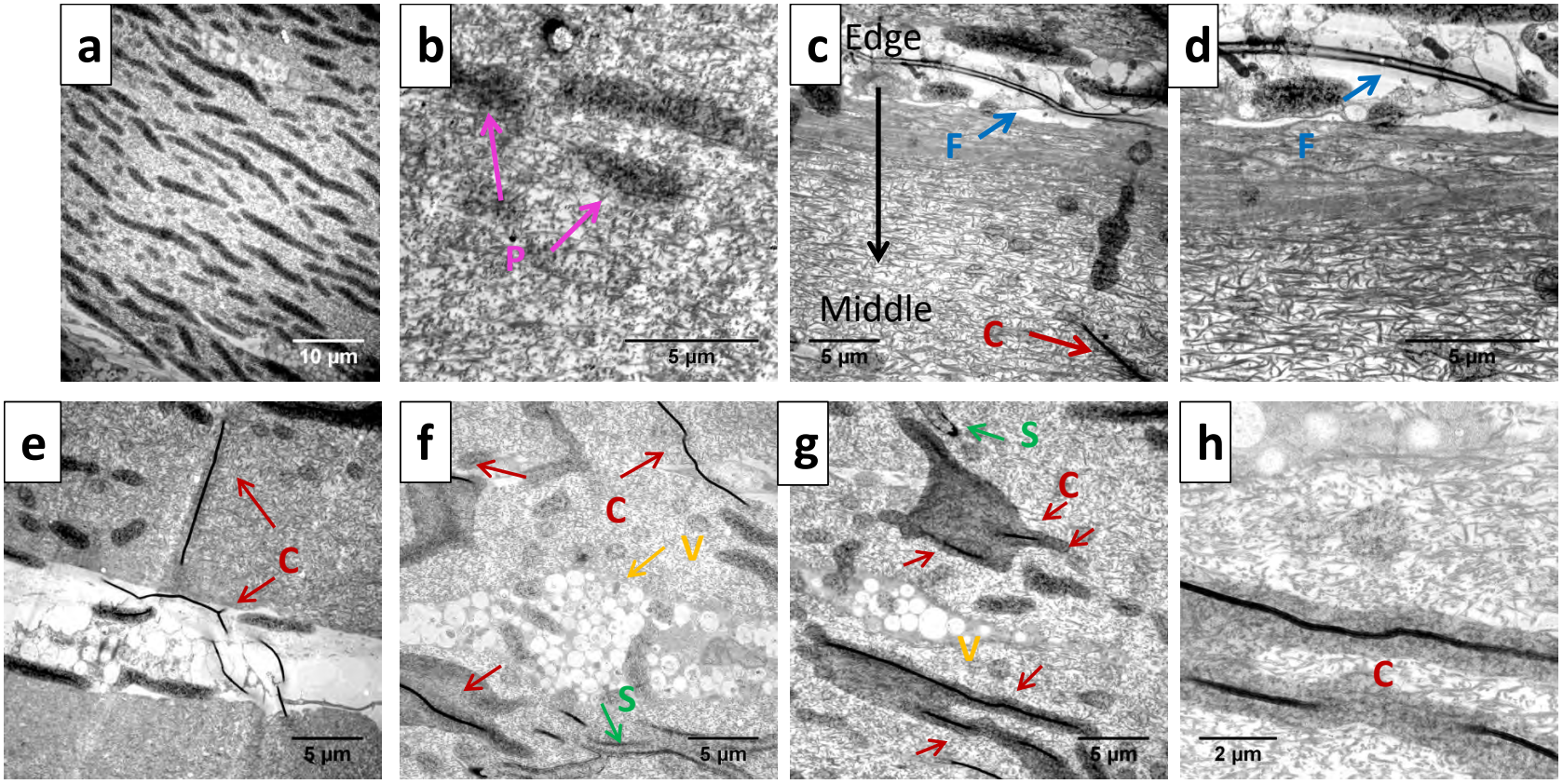

FIGURE 4.9: Longitudinal transmission electron micrographs (TEM) of control constructs. a) Dark patches (P) were aligned along the direction of tension along with cells. b) The patches were surrounded by needle-like structures. c) & d) Greater fibril (F) arrangement and general organisation was observed from the outside in. e)– h) The cells had large transport vesicles (V) and collagen (C) fibrils were arranged haphazardly within the construct.

4.3.4.2 Ascorbic acid + proline construct longitudinal sections

On the outer edges of AA+P constructs, cells were highly populated and aligned along fibres (F) whereas towards the middle of the constructs, dense matrix (M) was present with fewer cells (Figures 4.10a, b and c). Cells on the edge of AA+P treated constructs had prominent endoplasmic reticula (ER), as shown in Figure 4.10a. Strands of collagen (C) were present in dark patches within the constructs and in close proximity to the cells (Figure 4.10d and e). Within the dense matrix there were areas of aligned cells (Figure 4.10f) and the cells appeared thinner and more elongated than control cells in Figure 4.9. A large number of transport vesicles (V) were also present within the cells (Figure 4.10g and h). Some cells were very small, circular or irregular with tiny nuclei (Figure 4.10h).

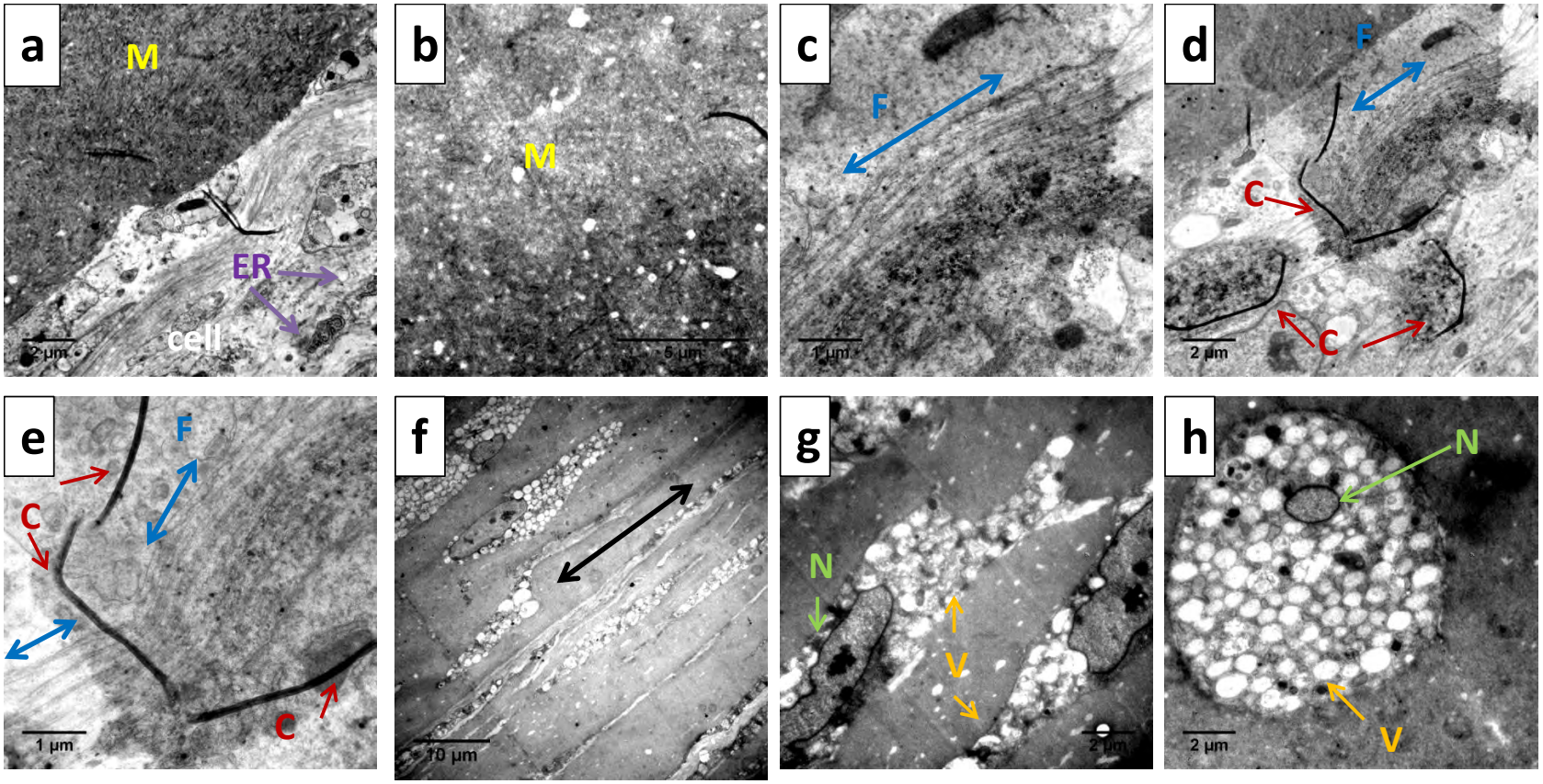

FIGURE 4.10: Longitudinal transmission electron micrographs (TEM) of AA+P constructs. a) Construct edge had numerous cells with visible endoplasmic reticula (ER) and b) the matrix (M) was extremely dense. c) Some form of fibril (F) arrangement was visible and d) collagen (C) was present. e) Cells were aligned along the construct, varied in nuclei (N) size and f) contained numerous transport vesicles (V).

4.3.4.3 Control construct cross-sections

Cross sectional images also showed a larger number of cells on the periphery of the constructs (Figure 4.11a). Collagen fibrils and the needle-like morphology were present throughout the central portion of the constructs (Figure 4.11b). The dark patches observed in the longitudinal sections (Figure 4.9) were also visible in the cross-sections and were bounded by strands of collagen fibrils that appeared to be in the process of joining to form rings (Figure 4.11c). The collagen fibrils also appeared in close proximity to the cells (Figure 4.11d and e). Collagen was identified by the banding visible in Figure 4.11f.

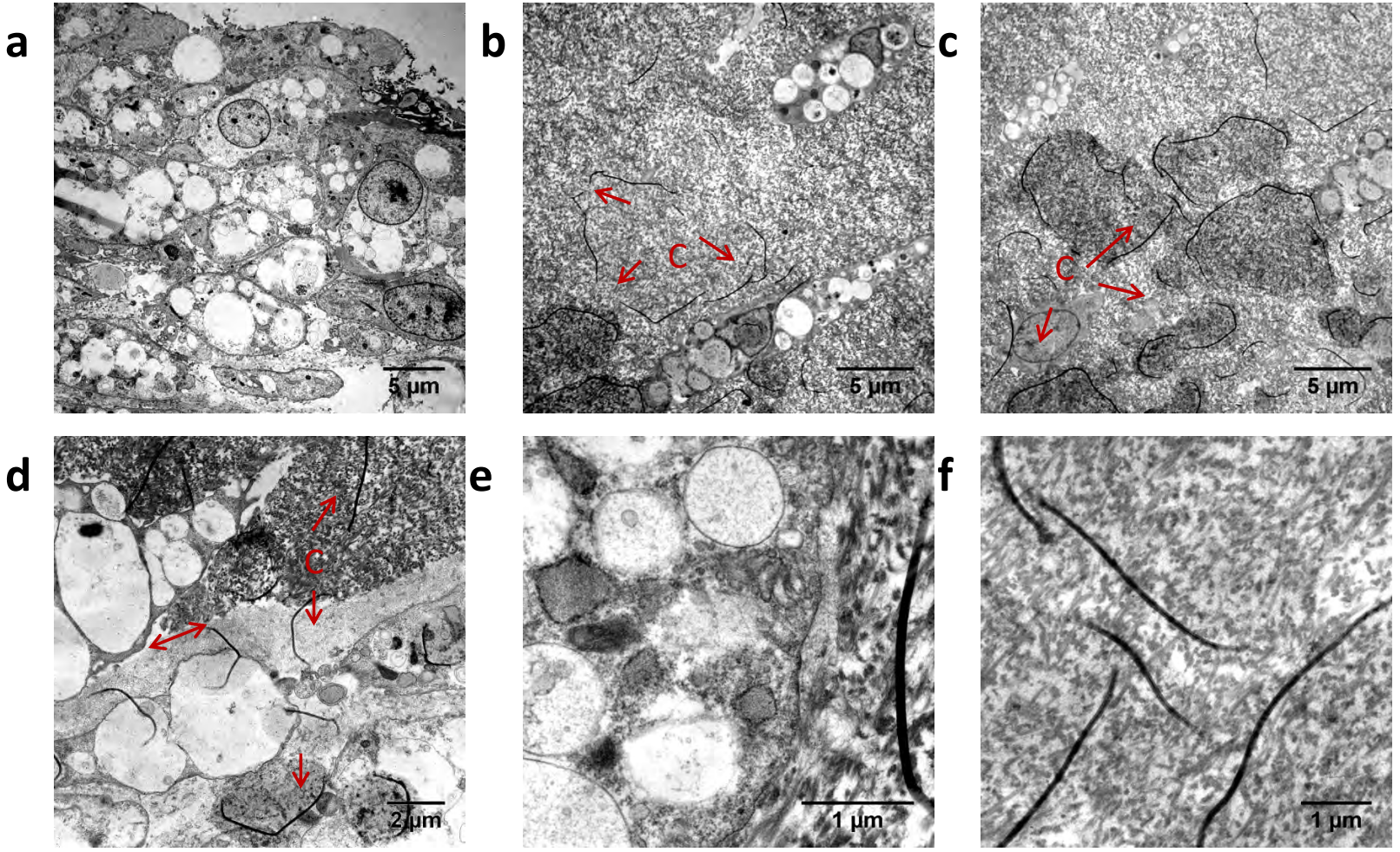

FIGURE 4.11: Cross-section TEM images of control (NT) constructs. a) A large number of cells were found on the edge of the constructs. b)–c) Collagen fibres surrounded the dark patches and were local to the cells d) & e). The collagen fibres were identified by the banding patten (f).

4.3.4.4 Ascorbic acid + proline construct cross-sections

The cross-sectional edge of AA+P constructs had a high cell number, as was prevalent in all other sections, however, a greater amount of collagen strands were observed on the periphery of the AA+P cross-sections (Figure 4.12a). The cells on the periphery also exhibited prominent endoplasmic reticula (Figure 4.12b). Some of the collagen fibrils formed rings, in the centre of which were numerous cross-sections of collagen fibrils (Figures 4.12c and d). Towards the center of the constructs, the matrix (M) was dense and fewer cells were visible (Figure 4.12c and e). Dark patches within the matrix (M), were identified as bundles of collagen fibrils were present throughout the tissue though at higher concentrations in proximity of cells (Figure 4.12f and g).

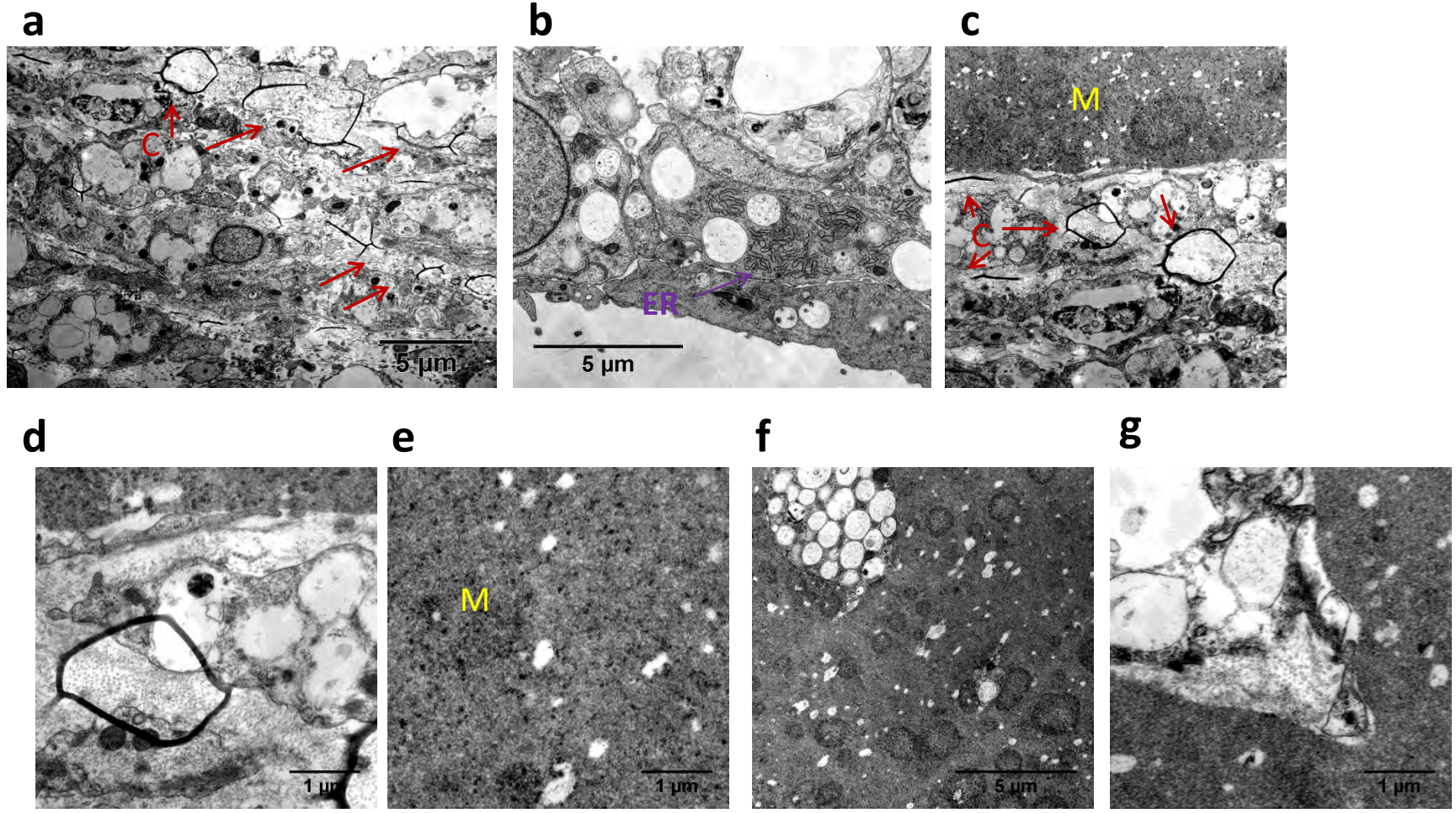

FIGURE 4.12: Cross-section TEM images of AA+P constructs. a) The construct edge had a higher cell density. b) Endoplasmic reticula (ER) were visible. c)–f) collagen fibres and arranged bundles were visible. g) Secretion of collagen was also local to cells.

4.3.5 Effect of varying ascorbic acid and proline concentrations on fibrin contraction

The effects of varying AA or P concentrations whilst maintaining one of the two supplements constant during AA+P supplementation were assessed. This was done to establish if increasing or reducing either AA or P would attenuate the extensive contraction seen at the combined 250μM AA + 50μM P concentrations. Varying the concentration of either AA or P would also shed some light as to which of the supplements was responsible for enhancing extent of contraction.

Constructs supplemented with differing concentrations of AA along with the control constructs displayed no noticeable contraction in the first two days. However, by day 3 constructs in all groups had contracted, although those in the proline varied groups appeared more translucent than those in the AA treatment varied groups (Figure 4.13 and 4.14A).

4.3.5.1 Fibrin percentage gel areas and max/min widths

Day 3 results showed that the control group had contracted to 21.4 ± 7.85% (Figure 4.14A). Increasing AA concentrations resulted in increased extents of the fibrin gel contraction to 34.34 ± 13.70%, 28.03 ± 12.34% and 20.47 ± 6.05%, for 50AA, 250AA and 500AA, respectively. Conversely, increasing concentrations of P showed a decreased rate of fibrin gel contraction with 50P contracting to 30.09 ± 6.25%, 250P to 38.81 ± 7.21% and 500P to 36.40 ± 9.73%. Generally, when compared to the control group, supplementation reduced initial rates of contraction.

The case was different when supplemented groups were compared to each other. Percentage gel areas of the 250AA group were significantly lower than 50AA, 250P and 500P, whilst 500AA had significantly less fibrin percentage gel area than 250P and 500P on day 3 ($p<0.05$). This indicated that AA and P had opposing effects on contraction. The lowest maximum and minimum widths were observed in the control group at 11.97 ± 2.71mm and 8.29 ± 2.23mm (Figure 4.14D). Maximum and minimum widths of AA treatment varied constructs were higher with decreasing concentrations of AA. However, there was no clear trend for P supplement varied constructs, although maximum widths of the control and AA treatment varied groups

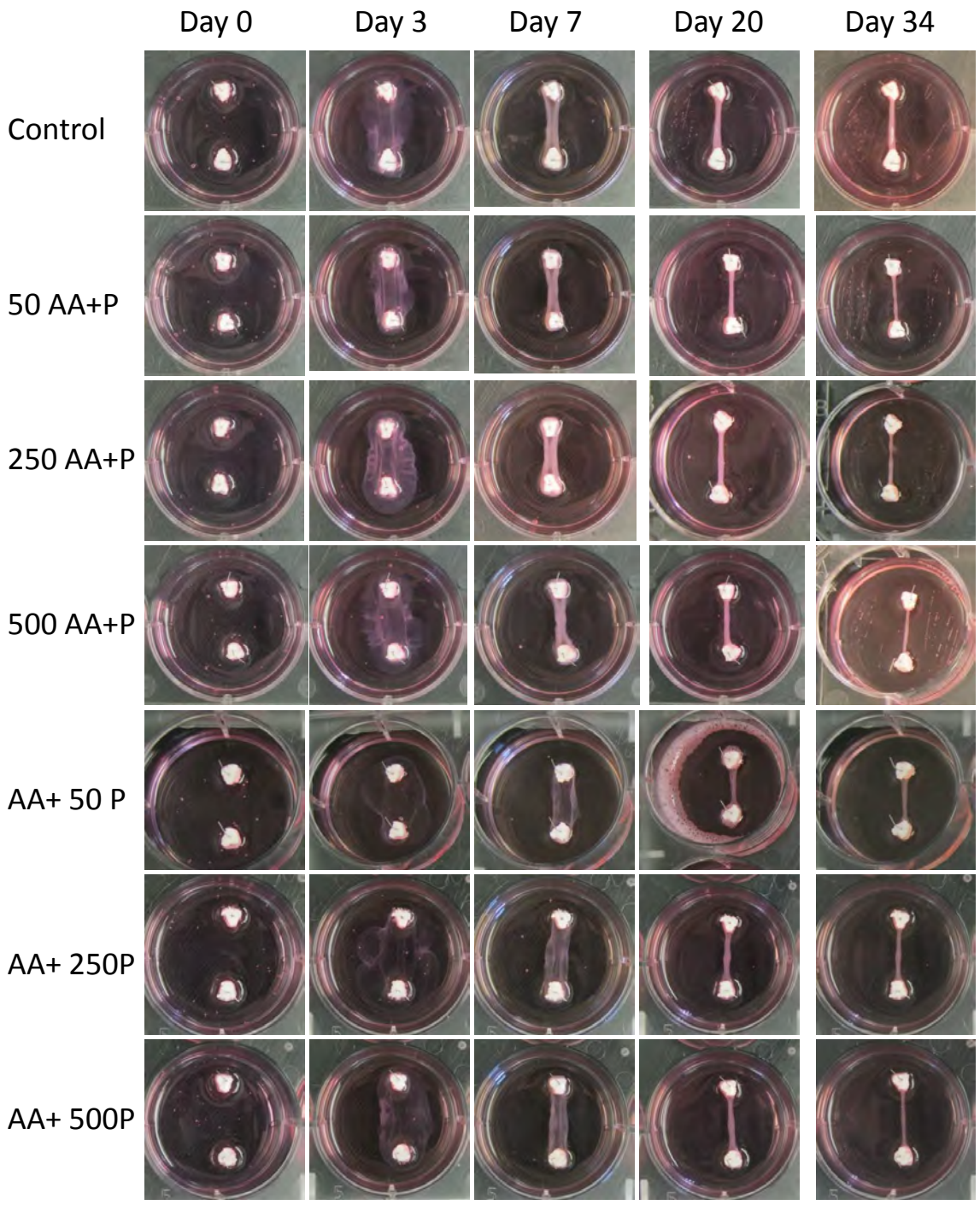

FIGURE 4.13: Contraction images showing effect of varying AA concentration or P concentration. In the first three days constructs treated with varying concentrations of P appear more translucent in comparison to those were AA is varied. By day 7, P treated constructs appear greater in width, though by the end of the study this difference is visually less apparent.

differed significantly from 250P, which expressed the greatest maximum width of all groups at 20.97 ± 2.67mm ($p<0.05$).

A similar trend was observed for day 7 percentage gel areas and maximum/ minimum widths (Figure 4.14B and D). Again, increasing concentrations of AA appeared to increase the rate of fibrin gel contraction 7.39 ± 1.53% (50AA), 6.39 ± 1.69% (250AA) and 4.68 ± 1.13% (500AA). Increasing concentrations of P showed no discernible trend as the lowest concentration 50P (7.82 ± 0.85%) was not dissimilar from the highest concentration of 500P (7.95 ± 0.84%), however, the median concentration had a higher fibrin percentage gel area (8.75 ± 0.73%). Statistically significant differences were largely between the 500AA group and all the P treatment varied groups ($p<0.05$). Day 7 500AA maximum widths also differed significantly from all P varied groups and 50AA, whereas the minimum widths of AA supplement varied constructs differed significantly from P treatment varied constructs. Essentially, during the first two weeks, increasing AA had a greater effect on contraction than increasing P.

From day 12 to day 33/34, construct percentage gel areas did not differ significantly from each other, however, there were statistically significant differences between the maximum and minimum widths from day 20. By day 34, control maximum widths were the largest of all groups at 1.20 ± 0.17mm. Varying AA supplement concentration resulted in constructs widths being lowest with increasing AA concentration, 1.38 ± 0.43mm (50AA), 1.19 ± 0.09mm (250AA) and 1.13 ± 0.16mm (500AA). Minimum widths of AA treatment varied groups exhibited a comparable trend although smaller in effect with 50AA= 0.98 ± 0.28mm, 250AA =0.88 ± 0.15 and 500AA=0.83 ± 0.26mm. The control group max width differed significantly from 250AA and 500AA ($p=0.017$ and $p=0.002$, respectively), with no statistically significant differences between individual AA groups.

Interestingly, at this point the trend for P supplement varied groups also resembled AA treatment groups in that increasing P concentrations reduced maximum and minimum widths. For 50P, 250P and 500P max widths were 1.61 ± 0.18mm, 1.32 ± 0.15mm and 1.14 ± 0.08mm, whilst the minimum widths were 1.09 ± 0.16mm, 1.02 ± 0.13mm and 0.95 ± 0.07mm, in the order of supplementation. Only the maximum widths of the 50P group displayed statistically significant differences from 250AA ($p=0.012$) and 500AA ($p=0.002$). Whilst only the minimum widths of 250P differed from 500AA only ($p=0.024$).

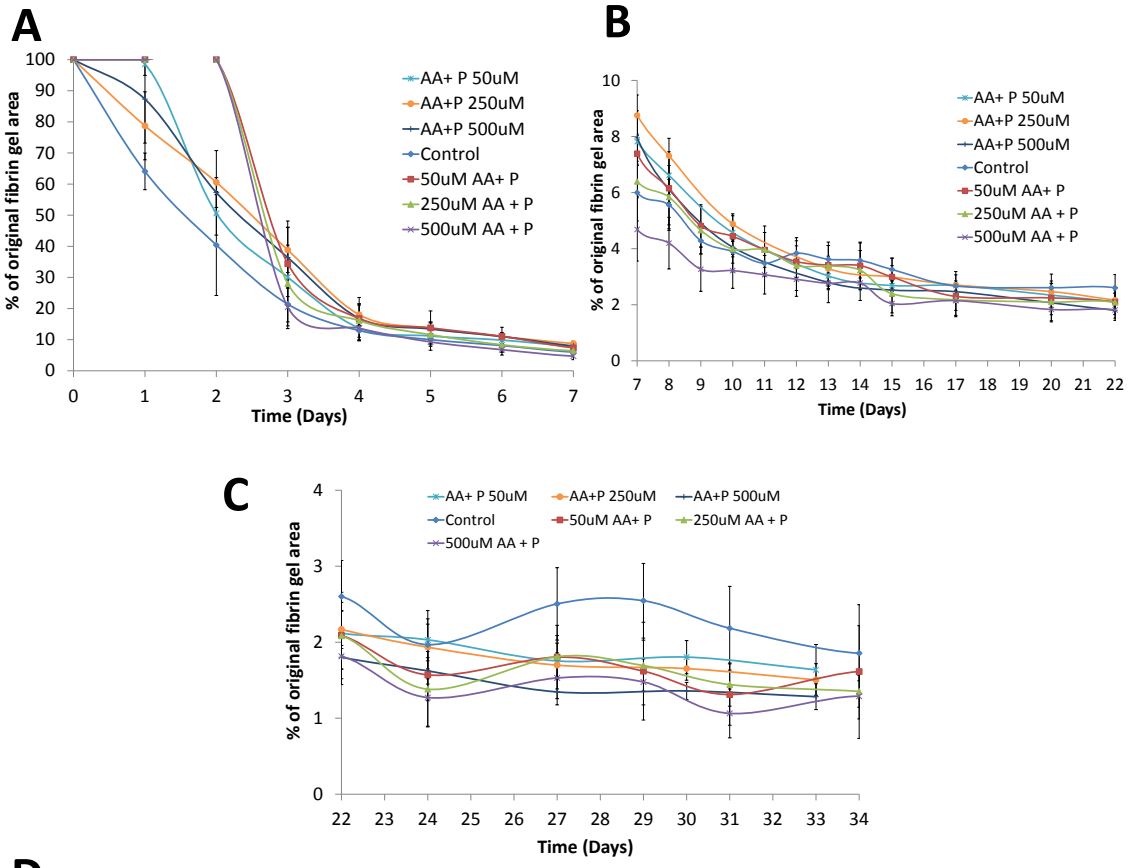

D

	Maximum Width (mm)						
Day	Control	50uM AA+P	250uM AA+P	500uM AA +P	AA+P 50uM	AA+P 2 50uM	AA+P 500 uM
0	35.00	35.00	35.00	35.00	35.00	35.00	35.00
3	11.97 ± 2.71	14.43 ± 5.43	13.42 ± 3.71	12.02 ± 2.71	16.18 ± 3.10	20.97 ± 2.67 *	16.71 ± 3.04
7	4.22 ± 0.62	5.10 ± 1.05 *	4.75 ± 0.73 *	3.70 ± 0.54 *	5.36 ± 0.70	5.95 ± 0.35	5.16 ± 0.46
20	1.85 ± 0.25	1.57 ± 0.43	1.48 ± 0.10 *	1.45 ± 0.30 *	2.01 ± 0.23	2.03 ± 0.29	1.66 ± 0.18
22	1.87 ± 0.32	1.44 ± 0.34	1.38 ± 0.17 *	1.31 ± 0.28 *	1.96 ± 0.23	1.91 ± 0.27	1.87 ± 0.20
33 /34	1.61 ± 0.22 *	1.38 ± 0.43	1.19 ± 0.09	1.13 ± 0.16	1.61 ± 0.18 *	1.32 ± 0.15	1.14 ± 0.08

	Minimum Width (mm)						
Day	Control	50uM AA+P	250uM AA+P	500uM AA +P	AA+P 50uM	AA+P 2 50uM	AA+P 500 uM
0 /34	33.00	33.00	33.00	33.00	33.00	33.00	33.00
3	8.29 ± 2.23	12.12 ± 5.64	10.08 ± 3.03	8.60 ± 1.49	13.76 ± 3.65	15.50 ± 4.38	14.69 ± 2.53
7	3.15 ± 0.55	3.43 ± 0.55	3.24 ± 0.45	2.13 ± 0.41 *	4.73 ± 0.80 *	4.60 ± 0.62 *	4.39 ± 0.48 *
20	1.39 ± 0.10	1.20 ± 0.20	1.18 ± 0.17	1.15 ± 0.15 *	1.34 ± 0.20	1.52 ± 0.14 *	1.33 ± 0.10
22	1.34 ± 0.17	1.18 ± 0.21	1.15 ± 0.17	1.05 ± 0.25 *	1.39 ± 0.22	1.43 ± 0.14 *	1.26 ± 0.22
33 /34	1.20 ± 0.17	0.98 ± 0.28	0.88 ± 0.15	0.83 ± 0.26 *	1.09 ± 0.16	1.02 ± 0.13 *	0.95 ± 0.07

FIGURE 4.14: Rate of contraction and widths due to varying AA/P concentrations. A) Delayed contraction seen in AA treated constructs in the first two days. B) From day 7, statistically significant differences seen between fibrin percentage gel areas of control and 250P, 50AA and 500AA, 250AA and 250P, 500AA and 50AA/all P treated constructs. C) No significant differences observed except on day 22, between the control and 500AA & 500P. D) Significant differences in maximum and minimum widths, variations largely being between AA supplemented constructs and the P treated group or control. ** denotes statistically significant differences referred to in the text.*

4.3.6 Collagen content of supplemented constructs

The effect of varying AA+P concentrations on resultant sinew collagen content was evaluated. Control sinews had an average collagen content of 6.92 ± 4.01%, which was significantly less than 50AA with 39.18 ± 15.05% (p=0.018) and 500AA, 43.10 ± 32.07% (p=0.000). Apart from the control, the 500AA group's collagen content was also significantly higher than all P treated groups where 50P contained 10.91 ± 1.14% (p=0.000), 250P had 14.53 ± 1.26% (p=0.000) and 500P had 16.18 ± 2.30% (p=0.001) collagen.

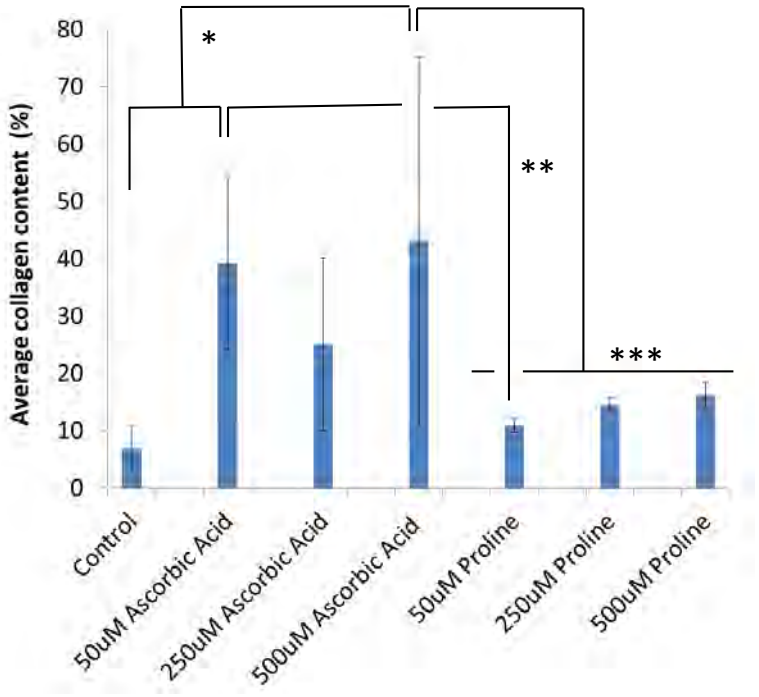

FIGURE 4.15: Effect of varying AA/P concentration on collagen content. Supplementation enhanced sinew collagen content, increases in AA concentration having a greater effect on collagen content than increases in P. ($p<0.05$ for 500AA compared to all P groups & control and 50AA compared to control & 50P.)

4.3.7 Effect of collagen synthesis inhibition on contraction

To determine the effect of collagen synthesis on fibrin gel contraction rates and sinew widths, constructs were supplemented with either 25μM DMOG or 100μM DMOG to inhibit collagen synthesis.

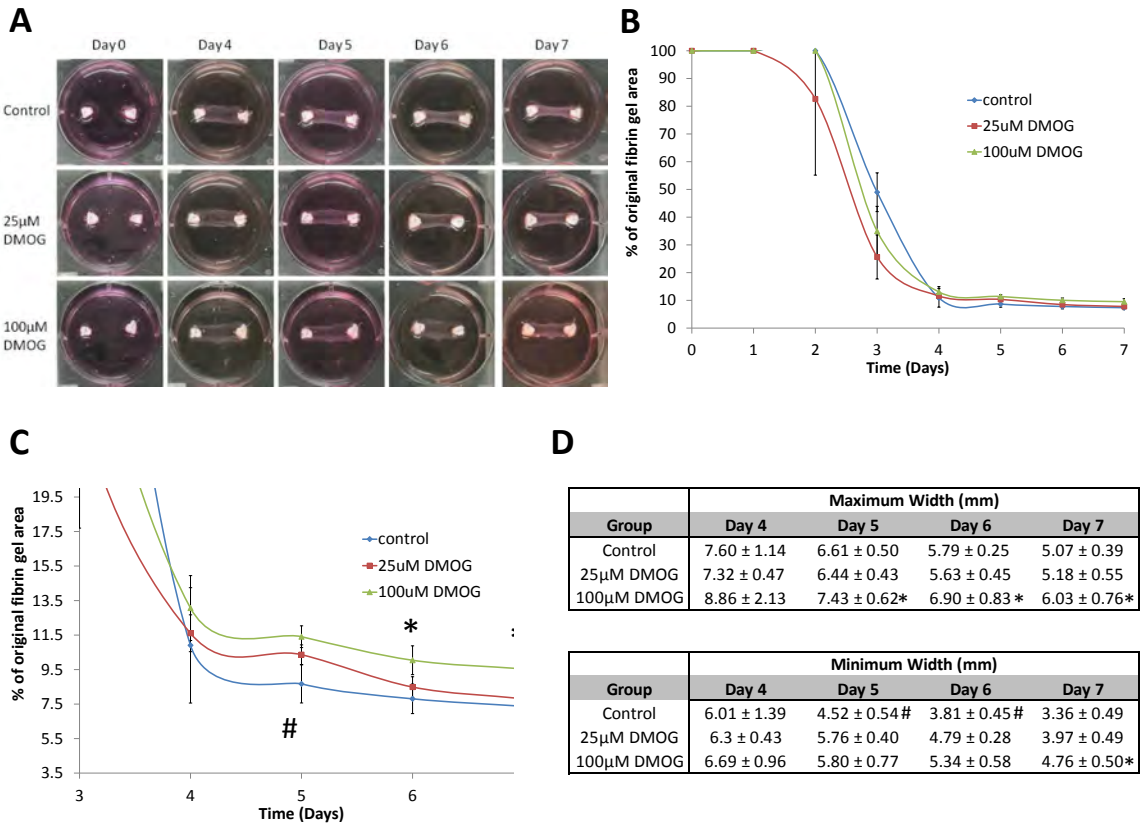

D

Group	Maximum Width (mm) Day 4	Day 5	Day 6	Day 7
Control	7.60 ± 1.14	6.61 ± 0.50	5.79 ± 0.25	5.07 ± 0.39
25μM DMOG	7.32 ± 0.47	6.44 ± 0.43	5.63 ± 0.45	5.18 ± 0.55
100μM DMOG	8.86 ± 2.13	7.43 ± 0.62*	6.90 ± 0.83 *	6.03 ± 0.76*

Group	Minimum Width (mm) Day 4	Day 5	Day 6	Day 7
Control	6.01 ± 1.39	4.52 ± 0.54#	3.81 ± 0.45#	3.36 ± 0.49
25μM DMOG	6.3 ± 0.43	5.76 ± 0.40	4.79 ± 0.28	3.97 ± 0.49
100μM DMOG	6.69 ± 0.96	5.80 ± 0.77	5.34 ± 0.58	4.76 ± 0.50*

FIGURE 4.16: Effect of collagen synthesis inhibitor on construct contraction. Increasing concentrations of DMOG had a significant effect in slowing down the rate of fibrin gel contraction.

No statistically significant differences in the rate of fibrin gel contraction were observed in the first three days although the presence of DMOG supplements appeared to slightly enhance initial contraction (Figure 4.16B).

However, there was a sudden decrease in contraction from day 4. On day 5, fibrin gel areas of treated constructs were 10.36 ± 0.57% for the 25μM group and 11.41 ± 0.63% for 100μM. These differed significantly from control group ($p<0.05$), which had a gel area of 8.67 ± 1.10% (Figure 4.16).

The maximum width of 100μM supplemented constructs were also broader and differed significantly from both the control and 25μM groups. The minimum widths of both the 25μM and 100μM groups of 5.76 ± 0.40mm and 5.80 ± 0.77mm, differed significantly from the control group of 4.52 ± 0.54mm, suggesting the continued contraction of the control constructs.

Control fibrin gel areas continued to be the lowest and by day 7 had reduced to 7.37 ± 0.75% compared to 25μM at 7.81 ± 0.93% and 100μM at 9.54 ± 1.06%. The gel area of the 100μM group differed significantly from control and 25μM groups. The maximum (6.03 ± 0.76mm) and minimum widths (4.76 ± 0.50mm) of the 100μM group were broadest compared to the other groups and showed statistical significance ($p<0.05$).

4.3.8 RT-PCR detection of transcripted mRNAs

Reverse-transcription polymerase chain reaction (RT-PCR) was used to evaluate differences in the expression of specific messenger ribonucleic acids (mRNAs). Collagen type I expression was investigated to determine whether it varied between control and AA+P constructs or if differences were due to collagen downstream processing events. Although results in sections 4.3.1 and 4.3.5 indicated AA+P constructs to be highly contractile, this needed to be confirmed and separated from fibrin and possibly collagen matrix degradation. Consequently, the expression of MMP-1, -2, -3 and -9 were also evaluated due to their implication in collagen and fibrin degradation (see Chapter 2 sections 2.3.2.4 and 2.4.5.3 on MMPs).

At weeks 2 and 3 none of the targeted mRNAs were detected and these results are for constructs at week 4. The expression of the targeted mRNAs in control and AA+P treated constructs were compared, relative to GAPDH. In control constructs RhoA and MMP-2 expression were upregulated by 42% and 25%, respectively. There was an increase in the number of targeted mRNAs upregulated as result of AA+P supplementation.

RhoA was 144% greater in AA+P constructs than in the control group. COL1A1, MMP-2 and ACTA-2 were also upregulated by 69%, 65% and 436%, compared to the control group. In addition, the expression of Ten-C in AA+P treated constructs was over 5-fold greater than for control constructs. The expression of MMP-1 was greater for control constructs than for AA+P treated constructs. No significant differences were observed in MMP-3 and MMP-9 expression between the control and AA+P groups.

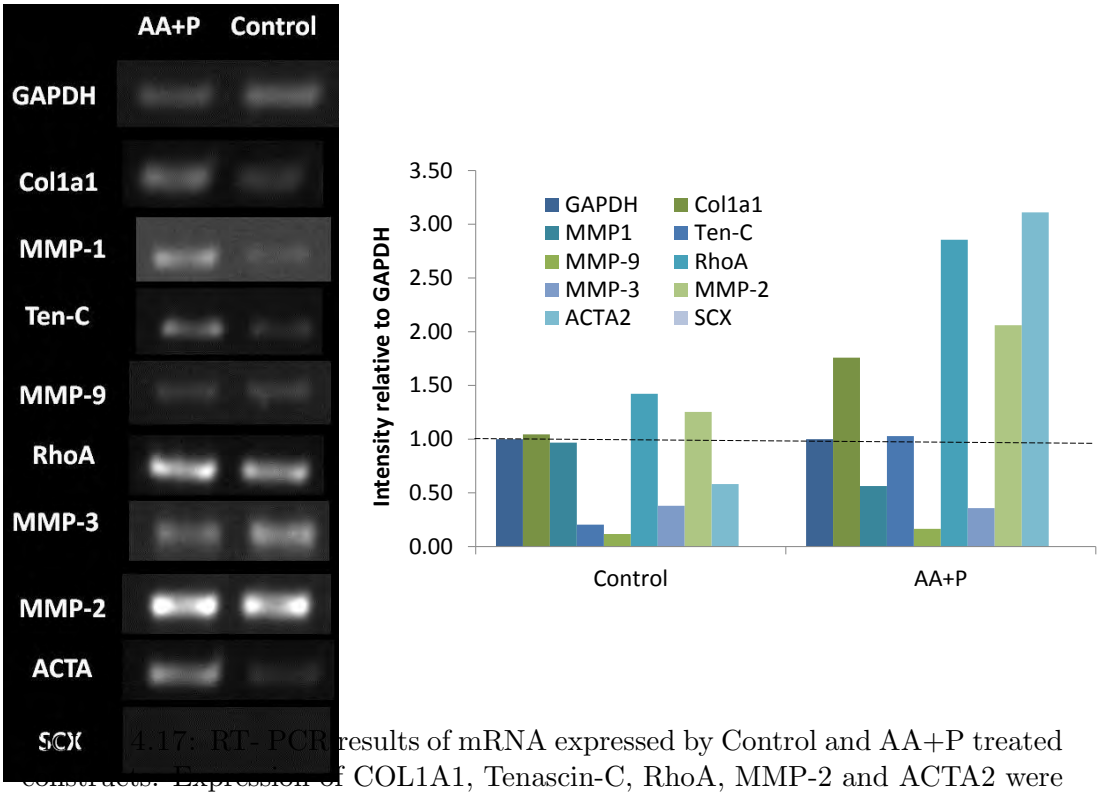

4.17: RT- PCR results of mRNA expressed by Control and AA+P treated constructs. Expression of COL1A1, Tenascin-C, RhoA, MMP-2 and ACTA2 were upregulated in AA+P treated constructs compared to the controls. However, expression of MMP-1 was downregulated.

4.4 Discussion

Proline reduced rates of fibrin contraction

As expected, supplementation with AA, P or AA+P resulted in subtle yet significant variations in the rates of contraction of the fibrin hydrogel scaffold and statistically significant differences in the rate of fibrin gel contraction due to AA+P were observed around Week 5 of the study (Figure 4.2). Comparisons of the overall reduction in fibrin gel areas between treated and non-treated groups, indicated that the contraction profile for AA+P constructs closely correlated with that of the proline treated group whereas response to AA treatment was related to the control group. This is likely because the presence of proline attenuated initial rates of contraction in both AA+P and P only groups. As a result, these correlations suggested that treatment with AA had the general effect similar to no treatment and therefore AA had no direct effect on the gross rate of fibrin gel contraction. Since the overall effects of proline contraction were not statistically different from AA+P treatment, this appeared to suggest

that proline supplementation was the governing factor in fibrin gel contraction rates but not necessarily the extent of contraction.

Nonetheless, these contraction measurements did not explain the difference in widths observed as AA+P constructs were visibly thinner in width in comparison to the other groups, especially when compared to proline only supplementation. An explanation for this may be due to contraction and depletion of the fibrin gel being two separate phenomena, which are implemented during remodelling of the TE sinew. Consequently, the maximum and minimum widths of the constructs were quantified to determine how the TE sinews developed in between the anchor points.

AA+P supplementation significantly reduces construct widths

Similar to fibrin percentage area results, differences in maximum and minimum widths of the AA+P treated groups were only significant after 5 weeks in culture (Figure 4.3). By day 52, maximum widths of AA+P were significantly larger than AA group, although the minimum widths were not. However, there were significant differences between the minimum widths of AA+P constructs, which were significantly smaller than P treated constructs and the control group. This indicated that AA+P treatment resulted in constructs with overall widths amid those supplemented with AA only or P only, suggesting a combined effect due to AA and P supplementation. This further suggested that altering the concentrations of either AA or P, during combined supplementation, would increase or decrease the maximum or minimum widths achieved as well as maintain enhanced collagen production.

Supplementation of constructs with AA+P affects morphology of cells, construct internal structure and collagen formation

Figures 4.4B and E showed that the outer surface of the constructs had a high cell density, however, SEM also indicated differences in the morphology of AA+P supplemented constructs when compared to the controls that received no treatment. AA+P cells appeared much flatter, possibly due to a higher concentration of contractile actin stress fibres, as spread cells have been shown to contain greater actin (Dalby et al., 2004).

Cross-sectional images indicated a greater extent of fibrin remodelling in AA+P constructs than the controls as individual fibres (possibly fibrin) were still distinguishable in the controls (Figure 4.5) but in AA+P constructs, they appeared more interconnected and matted (Figure 4.6). Collagen staining using Masson's Trichrome confirmed the enhanced presence of collagen in AA+P sinews compared to control constructs (Figure 4.8). What was interesting was that control sinews were flooded with "specks" that were smaller in dimension than cell nuclei; blue staining by Masson's Trichrome suggested they were collagen (Figure 4.8b). TEM images also showed the presence of needle- and speck-like structures throughout the longitudinal and cross-sections of control constructs (Figures 4.9 and 4.11). Comparison of these images with those shown by Christiansen et al. (2000), confirmed that these "needles" and "specks" were indeed collagen subunits. In particular, Figure 4.11f closely resembled observations by Christiansen et al. (2000) shown in Figure 4.18 of collagen fibril formation.

In contrast, these collagen subunits were harder to identify in the longitudinal sections of AA+P treated constructs as the matrix was significantly denser, although areas of dark patches were observed (Figure 4.10). Cross-sections of AA+P did however, show the "specks" or cross-sections of collagen subunits to be present throughout the matrix (Figure 4.12e) and bundles of these collagen units (Figure 4.12f). In AA+P treated constructs, collagen fibrils appeared to form rings in proximity to cross-sections of collagen fibril bundles (Figure 4.12b and c). Fusion of collagen at the tips has been shown by Graham et al. (2000), where collagen fibrils in suspension fused at their tips to form rings following 16 hours of swirling (Figure 4.19). It was not clear however, whether swirling or shear stress could be the only cause of collagen fibril fusion. If so, contractile forces may have contributed to ring formation.

AA+P construct cells at the periphery also exhibited more prominent ER, however, numerous and large transport vesicles were seen in both control and non-treated constructs. The cell organelles and collagen were identified using various studies such as those by Canty and Kadler (2002); Silver et al. (2003); Calve et al. (2004); Bayer et al. (2010).

Increasing either AA or P concentrations, increased rates of fibrin gel contraction

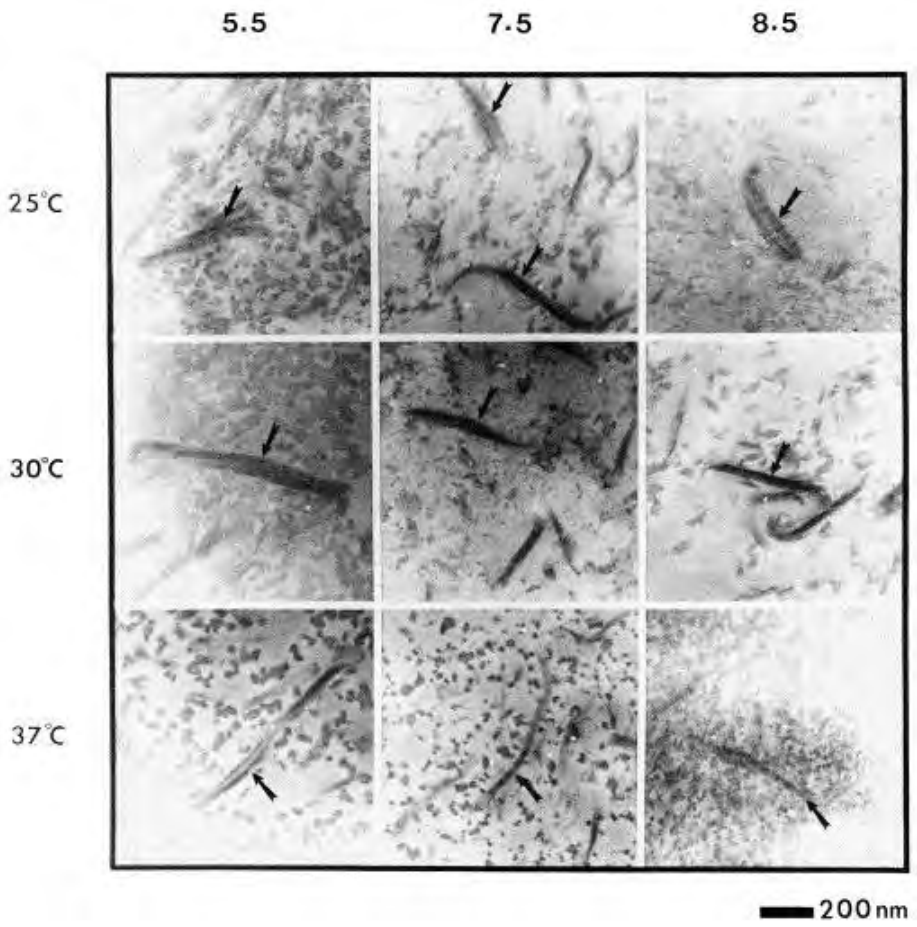

FIGURE 4.18: Formation of collagen fibrils as shown by Christiansen et al. (2000). The TEM images show formation of collagen fibrils at different temperatures and pH. Used with permission (Elsevier).

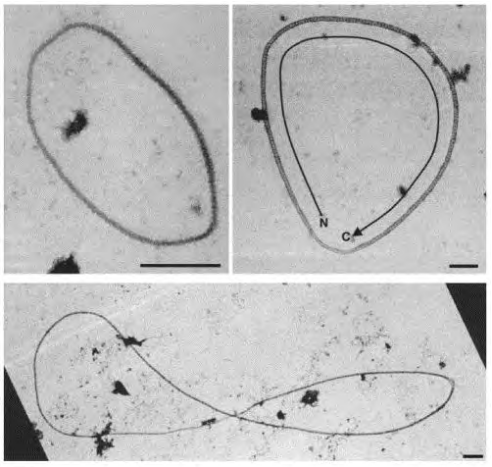

FIGURE 4.19: Fusion of the tips of collagen fibril to form rings as shown by Graham et al. (2000). The TEM images show full length fibrils, that fused at the tips following swirling. Used with permission (Elsevier).

Varying AA+P concentrations by altering the concentration of one component whilst maintaining the other one constant was evaluated to determine its effects on the rate of fibrin gel contraction and construct widths (Section 4.3.5). Previously, the control and constructs treated with AA/ P or AA+P all contracted the fibrin gel by day 1 (Figure 4.2B). In these experiments no contraction was observed in the control and those treated with varying concentrations of AA in the first two days (Figure 4.14). Constructs treated with varying concentrations of P also appeared more translucent in the first few days in comparison to those where AA was varied (Figure 4.13). Reasons for this could be due differences in cell metabolism of AA / P or other factors such as minor variances in cell seeding density or the fibrin hydrogel properties. After day 3, the effect of supplementation behaved as expected in that increasing AA concentration increased the extent of fibrin gel contraction whereas increasing P concentration decreased the extent of contraction. Statistical assessment, supported this analysis as construct gel percentages of the 250AA group differed significantly from the lowest AA treatment group (50AA) and the higher P treatment groups, 250P and 500P. The 500AA treatment group also differed from the 250P and 500P, further indicating the polar effects of the treatments. As expected the percentage gel areas of the 250AA and 50P groups were not statistically different, as they were in fact the same group.

There was a correlation between the maximum and minimum widths and fibrin percentage gel areas of constructs supplemented with varying concentrations of AA. However, widths were similar for the lowest 50P and the highest 500P group and 250P resulted in constructs with the lowest widths, showing no clear trend due to P treatment. Possible causes for this may be due to the fact that proline requires ascorbic acid for its hydroxylation and there may be an optimum AA:P ratio required by the enzymes.

Towards the end of the study, AA supplemented constructs were generally smaller in width than non-treated constructs, with 250AA and 500AA groups showing significant differences from the control widths. Proline max/min widths were not significantly smaller than the control group, falling somewhere in between the effects of the higher 250AA and 500AA treatments and no supplementation. Why construct dimensions with increasing P treatment fell towards the 5 week period was not clear but could be due to increasing collagen production and its effect on the remodelling

of the fibrin gel scaffold. As high concentrations of P reduced construct maximum widths, this supplementation regime was deemed unsuitable for the purpose of enhancing construct widths.

There is a correlation between construct collagen content and extent of contraction

Collagen content of the TE sinews was quantified in an attempt to identify its relationship with the concentrations of AA+P supplements, the rate of contraction of the fibrin gel and sinew maximum and minimum widths. Non-treated constructs expressed the least amount of collagen of only 6.92 ± 4.01%. This was lower and differed significantly from the supplemented groups, except for the 250AA group, though this lack of statistical significance could be attributed to experimental error. Increasing concentrations of both AA and P appeared to increase collagen content, with the effect being greater as a result of AA treatment.

Collagen synthesis inhibition did not impede contraction but gradually reduced rates of fibrin gel contraction

To further investigate the correlation between collagen synthesis, gel contraction and sinew width, constructs were treated with DMOG (dimethyloxalylglycine), an inhibitor of collagen synthesis (Thoms and Murphy, 2010). Iron, ascorbic acid and α-ketoglutaric acid are cofactors required for proline hydroxylation by prolyl-4-hydroxylase enzymes (Trackman, 2005). DMOG is an α-ketoglutaric acid analogue (Thoms and Murphy, 2010) and acts by competing for the active site on the hydroxylase enzyme preventing collagen triple helix formation (GCinzler and Weidmann, 1997).

It was unexpected that supplementation with DMOG would actually increase the initial rates of contraction, which occurred in the first 3 days. Interestingly, by day 5, the presence of DMOG significantly slowed down fibrin contraction, with the 100μM group having a greater effect than 25μM. The maximum and minimum widths of the 100μM group also differed significantly from both the control and the 25μM treated group. This behaviour continued and was similarly observed on day 7 of the study, supporting the hypothesis that collagen synthesis affects the rate of the fibrin

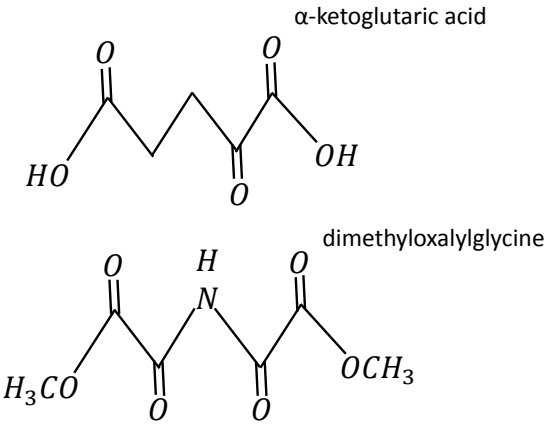

FIGURE 4.20: Structures of α-ketoglutaric acid and its analogue DMOG.

gel contraction and consequently the maximum and minimum widths of the sinews, possibly due to remodelling phenomena.

AA+P treatment upregulates COL1A1, RhoA, ACTA2 expression, MMP-2 and Tenascin-C

The preliminary RT-PCR results showed that COL1A1 expression was significantly greater in AA+P supplemented constructs than in the controls (Figure 4.17), thereby supporting collagen content results shown in section 4.3.6. In addition, AA+P increased cell mediated contraction as indicated by upregulated RhoA and ACTA2 expression. RhoA has been implicated in the control of α-sma contractility in non-muscle cells (Yee Jr et al., 2001; Wheeler and Ridley, 2004). Alpha-smooth muscle actin has been shown to drive contraction and generation of tensile forces in myofibroblasts, (Hinz et al., 2001; Hinz and Gabbiani, 2003a). The roles of RhoA and α-sma have been discussed in Chapter 2 section 2.3.1.4. The results in this chapter indicating upregulation of COL1A1, RhoA and ACTA2 help explain the increased collagen content, extensive contraction of the fibrin matrix and smaller widths observed in AA+P treated constructs in comparison to the non-treated controls.

RT-PCR results also indicated an upregulation of MMP-2 due to AA+P treatment. MMP-2 is secreted extracellularly as pro-MMP2, which is activated by MT1-MMP (Kinoh et al., 1996; Haas et al., 1998) and MT1-MMP (MMP-14) has been implicated in the enzymatic degradation of both Collagen Type I and fibrin (Hotary et al., 2002; Werb, 1997). These results suggested that AA+P increased the rate of fibrin

remodelling through MMP action and although collagen synthesis was upregulated, the upregulation of MMP-2 may also have resulted in remodelling and perhaps degradation of newly formed collagen type I. Ahmed et al. (2007) showed the expression of MMP-2, MMP-3 and MMP-9 in fibrin matrices and that fibrin gel degradation was reduced by the use of Aprotinin, a serine proteinase inhibitor. Similarly, Collen et al. (2003) identified the presence of MMP1, MMP2 and MT1-MMP (MMP-14) expression in cells cultured in collagen-fibrin matrices and Clark (2001) suggested that MMPs 1, 2 and 3 expressed by fibroblasts were capable of degrading fibrin clots during wound healing.

Constructs did not form uniformly, though small variations in anchor distance or size were not responsible for observed differences in supplemented groups

The above results indicated differences in fibrin gel contraction and maximum and minimum widths. To fully attribute the difference in contraction to the supplements, potential sources of error had to be eliminated.

The ratio of maximum to minimum width was determined to better illustrate non-uniformity of the constructs and to determine if construct irregularity varied significantly in certain experimental groups and how this difference in construct width differed with culture duration. Surprisingly, supplementation with AA, P or AA+P appeared to result in constructs with a ratio closer to 1, when compared to the control constructs (Appendix B). This was possibly an indication of remodelling or matrix arrangement process that occurred within. Additionally, anchor positioning is necessary to provide tension required for the formation of TE sinew, as without them, the extensive contraction and depletion of the fibrin gel occurs resulting in the formation of small spherical ball (Figure 4.21).

However, anchor distance was not the only factor that could have affected construct fibrin gel area and maximum/minimum width measurements. Fibrin percentage gel area measurements were conducted such that the area of the anchors at the measurement plane were subtracted from the total area, to give only the area of the fibrin gel. As a result, differences in anchor areas could have potentially been the cause of observed differences between supplemented groups rather than the supplements themselves (Appendix B).

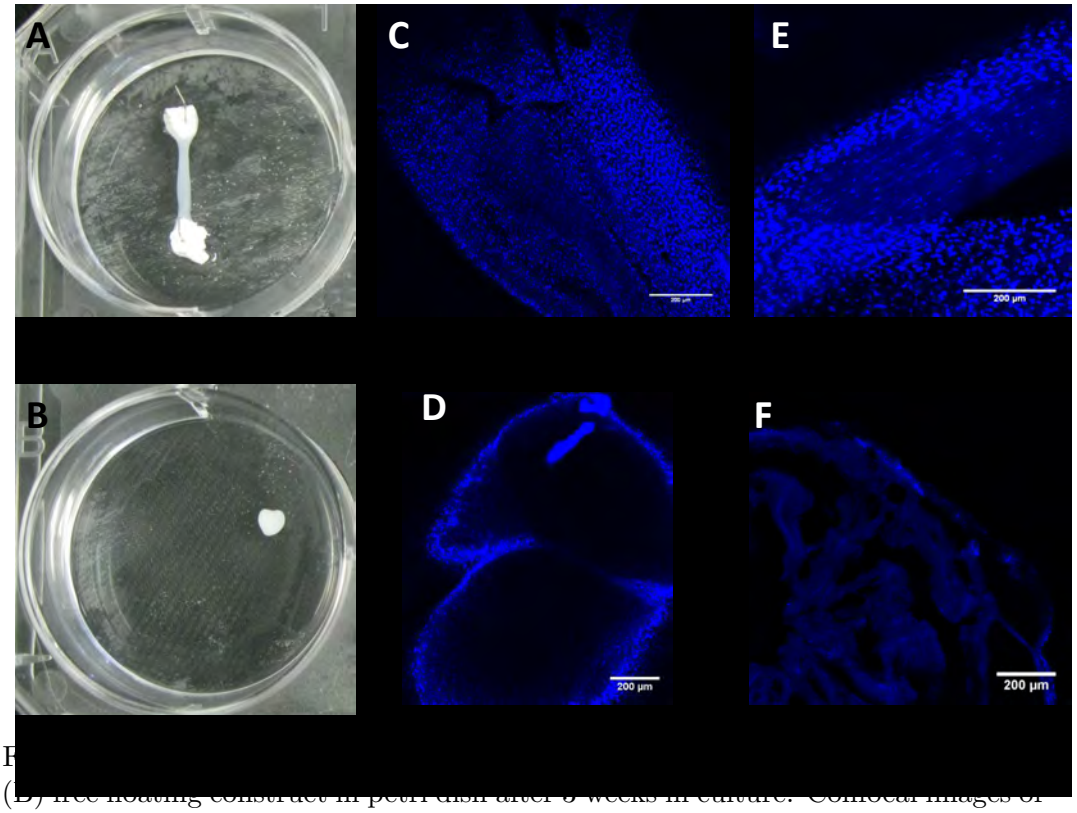

(B) free floating construct in petri dish after 3 weeks in culture. Confocal images of a DAPI stained tensioned construct (C) and a free floating construct (D), showing high proliferation of cells. (E) Cell alignment seen towards anchor edge of tensioned construct. (F) Almost no cells visible inside the free floating construct. Greatest cell proliferation is on periphery of tensioned and free floating constructs (E & F).

No significant differences were observed between anchor distances or aspect ratios. Within individual experiments, no statistical differences were observed between the visible anchor total surface areas and as a result these were not contributing factors for the observed differences in the rate of fibrin gel contraction.

4.5 Conclusion

The above results suggested that AA and P had significant effects on the rate of contraction of the fibrin hydrogel. There were distinct differences between the morphology of control and AA+P supplemented TE sinews. SEM and TEM images revealed that AA+P supplementation affected construct formation in terms of collagen morphology and the expressed quantity. RT-PCR also confirmed the upregulation of Collagen type I in AA+P supplemented constructs as well as RhoA, Actin stress

fibres and MMPs involved in matrix degradation. What was unclear from the results was whether AA+P also directly impacted fibrin matrix compliance. If AA+P softened or stiffened the matrix, then it was possible that altering fibrin gel mechanical properties could replicate the results obtained without supplementation.

Chapter 5

Influence of fibrin gel formulation on contraction

5.1 Introduction

Chapter 4 showed that AA+P supplementation resulted in overall greater extents of contraction of the fibrin hydrogel and that this was likely due to upregulated expression of contraction mediating proteins and proteolytic enzymes. However, it was unclear what effect supplementation had on fibrin gel compliance.

Scaffold properties are crucial to tissue engineering as cells have been shown to respond to their extracellular environment (Discher et al., 2005; Shapira-Schweitzer and Seliktar, 2007; Hadjipanayi et al., 2009; Dado and Levenberg, 2009). Optimum conditions of the scaffold can vary from tissue to tissue and for the cell type utilized (Dado and Levenberg, 2009). Strategies to improve the mechanical properties of TE scaffolds include altering the composition of the reagents and cross-linking (Dado and Levenberg, 2009; Shen et al., 1974; Wolberg and Campbell, 2008). Tissue morphogenesis depends not only on intra- and extracellular chemical signals but also on the spatial arrangement of the matrix (Vogel and Sheetz, 2006) and its stiffness (Discher et al., 2005), which are sensed through forces generated by cell-matrix adhesion complexes described in Chapter 2 section 2.3.1.2. Researchers have proposed that cell response to scaffold stiffness is independent from the response to scaffold thickness

at certain length scales and that further work is required in this area to elucidate the mechanisms (Buxboim et al., 2010; Lin et al., 2010).

Challenges of producing engineered tissue of the correct size and shape affect several branches of tissue engineering. For example, cartilage is said to vary in thickness from 500μm – 7.1mm and tissue engineered constructs should be able to fill defects of varying shapes and thickness, whilst maintaining cell viability (Bryant and Anseth, 2001; Chen et al., 2003). Ligament and tendon sizes and shape also vary depending on their location and how they are attached to the bone, which may be wide and flat, cylindrical, fan or ribbon shaped (Kannus, 2000).

The following experiments were conducted to further help elucidate the mechanism behind AA+P treatment on construct development by investigating if the mode of AA+P action was on fibrin gel stiffness. Furthermore, experiments were conducted to determine if properties of the fibrin hydrogel such as volume and stiffness affected the rate of contraction of the fibrin gel and the extent to which the gel would contract, in terms of sinew maximum and minimum widths. If AA+P acted by softening or stiffening the gel then evaluating contraction without AA+P supplementation at fibrin gel stiffnesses below or above the standard (control) gel stiffness would result in constructs with similar geometries and collagen content. Additionally, because ligaments and tendons vary in size and shape throughout the human body, if fibrin gel properties affected construct geometry and mechanical strength, then gel stiffness or thickness could be used to control the rates of contraction and sinew widths whilst modulating TE sinew collagen content/ tensile strength.

5.2 Materials and Methods

5.2.1 Supplementation of acellular gels with AA+P

Fibrin gels were prepared as previously described (Chapter 3 section 3.2.4). Groups were divided such that gels were either supplemented with 250μM AA and 50μM P or non-treated. The gels were left in an incubator at 37°C for a period of 5 or 7 days.

5.2.2 Fibrin gel rheology

Gels were prepared for rheology as described in Chapter 3 section 3.5.1.1. Gels of varying UT/mgF (method described in 5.2.3.3) were either cell seeded or acellular.

Briefly, dynamic oscillatory shear stress (G'/G") was determined from frequency sweeps conducted at 1% strain, over 0.1–50 rad/s and at 37°C. A 40mm SS sand blasted parallel plate geometry was used on the ARG2 Rheometer (TA Instruments). For time sweeps, a 40mm truncated geometry was used, set to observe change in G' during gelation over 1 hour (3600s). Following gelation, in situ strain and frequency sweeps were conducted.

5.2.3 Construct preparation

5.2.3.1 Altering fibrinogen volume

500μL of sDMEM containing 25μL of thrombin was added to each petri-dish and spread evenly. Groups were divided such that they contained differing volumes of fibrinogen: 100μL, 200μL, 500μL and 800μL, which were then left to polymerize for $\approx$1 hour in an incubator at 37°C and 5% CO_2. Thereafter, cells were seeded at a density of 100,000cells/mL as described in Chapter 3 section 3.2.

Increasing or lowering the volume of fibrinogen altered the total volume present in the petri-dish and consequently the thickness of the fibrin gel (Table 5.1). The standard protocol utilizes a total volume of 700μL of reagents (made up of 500μL sDMEM with thrombin plus 200μL fibrinogen) to produce fibrin gels of approximately 0.73mm in thickness. The thrombin in sDMEM volume was kept constant at 500μL. Lowering the volume of fibrinogen added to 100μL decreased the thickness of the gels to 0.62mm. Additions of 500μL and 800μL fibrinogen resulted in gels of 1.04mm and 1.35mm thick, respectively. An example calculation is shown in Appendix A.

5.2.3.2 Altering total fibrin volume

The sDMEM with thrombin to fibrinogen ratio was kept constant as per standard formulation (see Chapter 3 section 3.2.4) at 5:2 (from 500μL sDMEM (with thrombin)

TABLE 5.1: Approximate fibrin gel thickness at increasing total volume of reagents in 35mm petri-dish.

Total volume (µL)	700	600	1000	1300
Fibrin gel thickness (mm)	0.73	0.62	1.04	1.35

to 200μL fibrinogen). Group total volumes were set at 500μL, 700μL, 1000μL and 1500μL total volume. For example, the 500μL total volume group was made up of 357μL thrombin + 143μL fibrinogen - a ratio of 2.5:1 or 5:2. Gels were left to polymerize for 1 hour and CTF cells were seeded on top at a density of 100,000 cells/mL, as per standard protocol (Chapter 3 section 3.2.7).

5.2.3.3 Altering fibrin gel stiffness

Relationships of thrombin to fibrinogen used in method 5.2.3.1 were converted to UT/mgF, which allowed the volumes to be kept constant (Table 5.2).

TABLE 5.2: Determining UT/mgF from fibrinogen and thrombin volumes.

Fibrinogen stock = 20mg/mL
Thrombin stock = 200UT/mL, added as 50µL per mL of DMEM = 200*0.050 = 10UT/mL sDMEM

Group (µL fibrinogen)	**100µL**	**200µL**	**500µL**	**800µL**
Milligrams Fibrinogen (mgF) in well	2	4	10	16
Units thrombin (UT) in 500µL Thombin in sDMEM in well	5	5	5	5
Equivalent groups (UT/mgF)	**2.50**	**1.25**	**0.50**	**0.313**

An example calculation demonstrating how the ratios were determined is available in Appendix A.

5.2.4 Calcein-AM staining

Gels were stained with calcein-AM and imaged as detailed in Chapter 3 section 3.7.2.

5.2.5 Cell proliferation

Cells were dissociated from fibrin gels and quantified as described in Chapter 3 section 3.6.

5.2.6 Fibrin fibre diameter and pore sizes

Fibrin fibre diameters were measured from +75 points on SEM images for each group. Pore sizes of fibrin gels of varying thrombin to fibrinogen ratio, were determined from cryo-SEM images. 60-65 pore areas were measured per image/ group.

SEM methods were detailed in Chapter 3 section 3.8.1. ImageJ was calibrated using the scale-bar on the images.

5.3 Results

5.3.1 Supplementation of acellular gels with ascorbic acid + proline

To determine if AA+P directly affected the stiffness of the fibrin hydrogel, the stiffness of acellular gels, with or without AA+P supplementation on days 0, 5 and 7 were compared to determine if AA+P resulted in softening or stiffening of the fibrin gel through a direct action on the gel.

Figure 5.1 showed that the gels were robust and linear up to 50rad/s. The experiment was initially conducted employing a 5 day incubation period. Day 0 gels had an initial G' of 51.45 ± 1.65Pa and on day 5, G' for both the control and AA+P treated gels had reduced to 40.22 ± 9.45Pa and 45.76 ± 3.08Pa, respectively, at a frequency of 1 rad/s. At the range of frequencies investigated, the groups showed no statistically significant differences in stiffness from each other.

To determine if longer incubation was required, AA+P treated and non-treated acellular gels were incubated for 7 days. Day 0 control gels had a G' of 14.54 ± 4.74Pa.

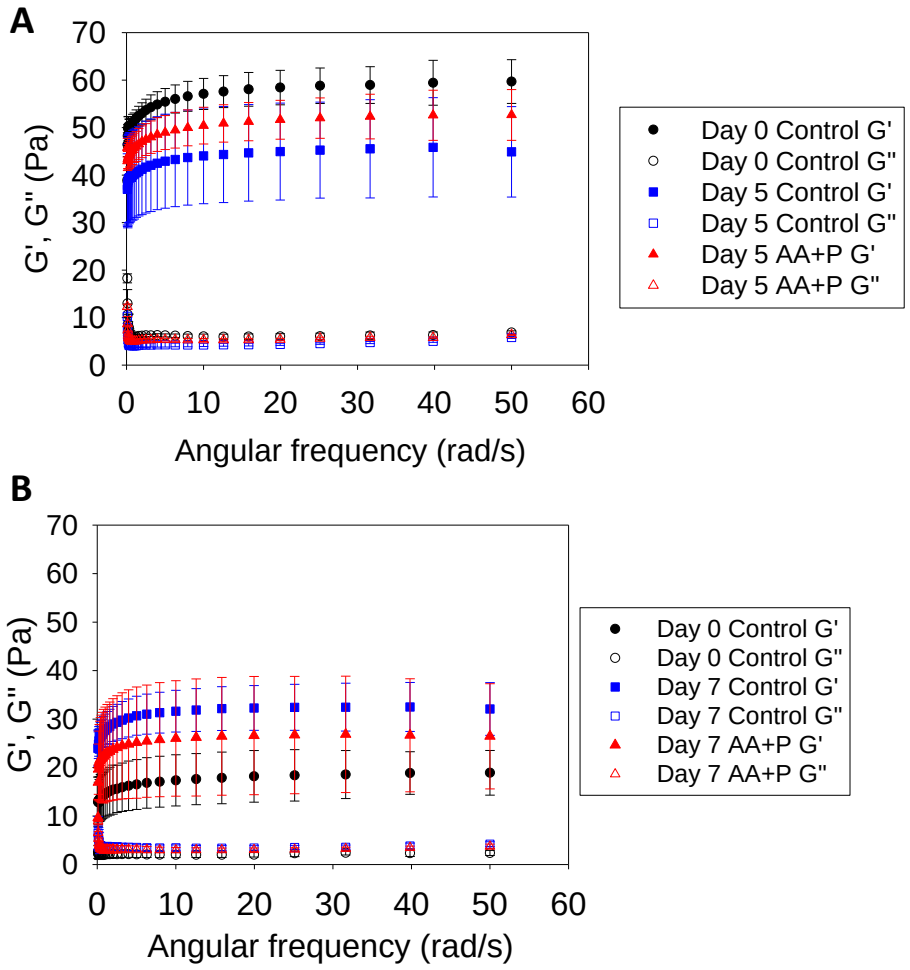

FIGURE 5.1: Frequency sweeps of acellular fibrin gels. The dynamic shear modulus of the fibrin gels was measured on day 0 and A) on day 5 and in an independent experiment on B) day 7 following supplementation with AA+P. Day 5 and 7 control and AA+P gels did not differ significantly from each other.

By day 7, G' of the control group had risen to 27.70 ± 3.33Pa, whilst G' of AA+P acellular gels had increased to 22.70 ± 9.80Pa. The increase may have been due to slowed gelation on day 0.

5.3.2 Altering fibrinogen volume

Here, constructs were set up using fibrin gels where the stiffness was adjusted by increasing or decreasing the volume of fibrinogen used, whilst maintaining the volume of thrombin in sDMEM constant.

Fibrin gels prepared using the lowest volume of fibrinogen (100μL) contracted to the greatest extent by day 3 and those of the highest fibrinogen volume (800μL) contracted the least (Figure 5.2), indicating that increase in fibrinogen volume and consequently stiffness reduced extent of fibrin gel contraction.

5.3.2.1 Fibrin percentage gel areas

Measuring fibrin percentage gel areas revealed differences in contraction between the two lower and two higher fibrinogen volume groups.

On day 3, there were no significant differences in the percentage fibrin gel areas between the 100μL (10.89 $\pm$ 2.50%) and 200μL (13.31 $\pm$ 2.56%) groups (p=0.968) (Figure 5.3A). However, both these groups differed significantly from the 500μL (61.66 $\pm$ 18.30%) and 800μL (90.19 $\pm$ 6.41%) groups, which also differed significantly from each other (p=0.000 for all instances).

By day 7, the 100μL group had contracted to 2.86 $\pm$ 0.22% of the original fibrin gel area and the 200μL group had reduced to 4.25 $\pm$ 0.78% (Figure 5.3B). For the higher volumes, the percentage gel area for the 500μL group was 21.55 $\pm$ 15.80% and 21.23 $\pm$ 5.47% for the 800μL group. Differences between the extent of contraction of the 100μL gel and the 800μL gel were close to 7.5 fold. The trend seen on day 7 continued to the end of the study on day 34, with the two lower fibrinogen volumes not differing significantly from each other and similarly the two higher volume groups showing no signifcant differences (Figure 5.3C).

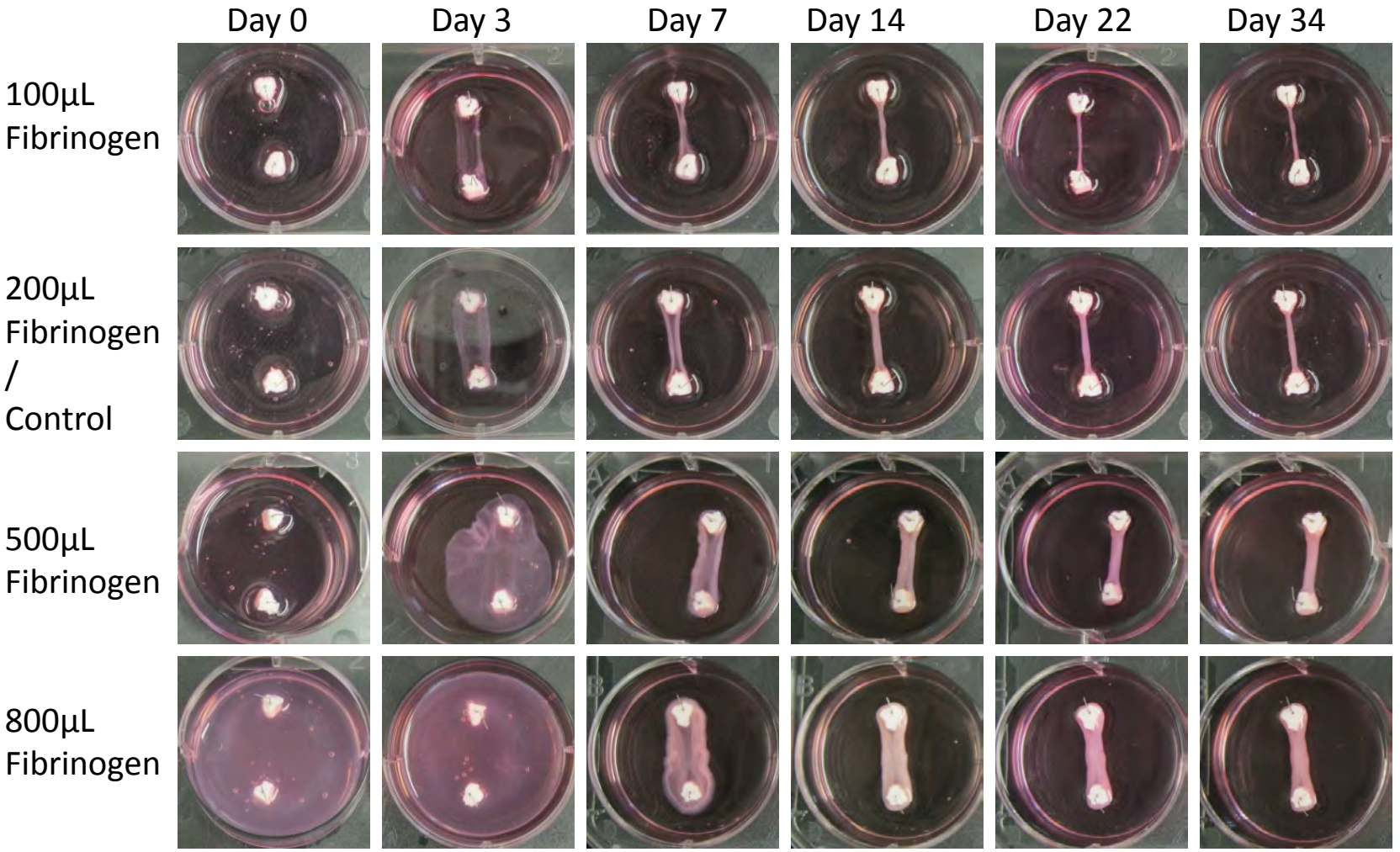

FIGURE 5.2: Images of constructs prepared with varying volumes of fibrinogen. Increasing volume of fibrinogen and consequently stiffness of fibrin delayed contraction of the fibrin gel.

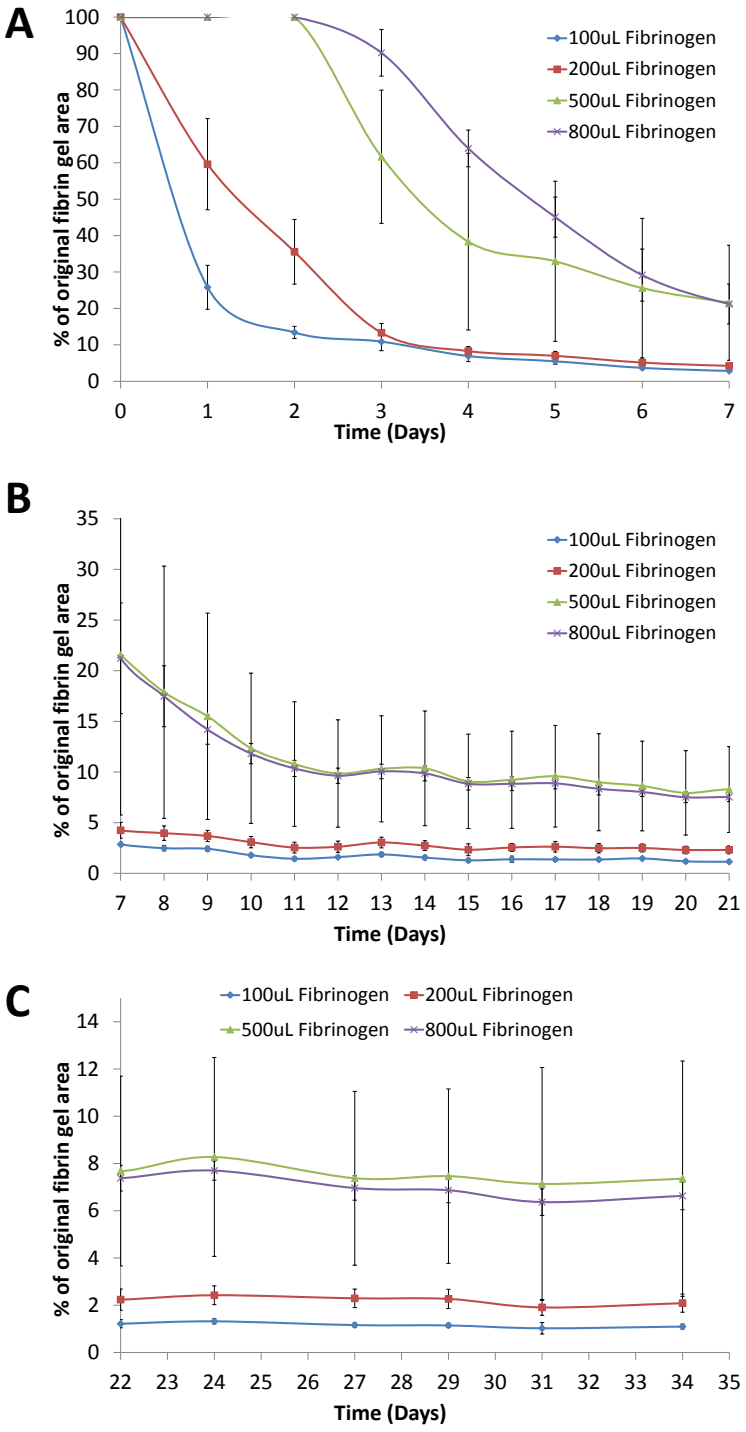

FIGURE 5.3: Effect of changing fibrinogen volume. Fibrin percentage gel areas between: A) days 0–7, B) days 7–21 and C) days 22–34. Lower fibrinogen volumes of 100μL and 200μL resulted in the fastest rates of fibrin gel contraction in comparison to higher volumes of 500μL and 800μL.

5.3.2.2 Construct widths

Throughout the study, it was visibly apparent that increasing the volume of fibrinogen resulted in increased construct sinew widths (Figure 5.2). Day 3 maximum and minimum widths of constructs in the 500μL group were 26.15 $\pm$ 5.84mm and 20.78 $\pm$ 9.42mm respectively, differed significantly from those of the 800μL group 33.73 $\pm$ 2.07mm and 31.55 $\pm$ 2.30mm (Figure 5.4). 100μL and 200μL groups respectively had maximum widths of 8.14 $\pm$ 2.53mm and 8.20 $\pm$ 1.40mm and minimum widths of 6.00 $\pm$ 1.27mm and 6.98 $\pm$ 1.05mm, respectively ($p > 0.05$). Although the maximum and minimum widths of the 100μL and 200μL groups did not differ significantly from each other, differences were statistically significant when compared to 500μL and 800μL groups ($p=0.000$, when 100μL or 200μL was compared to either 500μL or 800μL).

By day 7, maximum and minimum widths of the 500μL and 800μL groups continued to be significantly greater than those of the lower fibrinogen groups (100μL and 200μL) although they no longer exhibited major differences between each other at 11.03 $\pm$ 6.23mm and 12.78 $\pm$ 2.76mm for the maximum and 7.45 $\pm$ 3.92mm and 9.01 $\pm$ 3.31mm for the minimum, respectively. The maximum widths of the 500μL and 800μL groups were between 3.4 to 4.5 fold greater than those of group 100μL at 2.81 $\pm$ 0.45mm and group 200μL at 3.23 $\pm$ 0.68mm. Minimum widths of the 100LμL group were 1.60 $\pm$ 0.35mm and 2.67 $\pm$ 0.50mm for the 200μL group, which were 4.66 to 8.5 times lower than those of groups 500μL and 800μL. This trend continued for the remainder of the study.

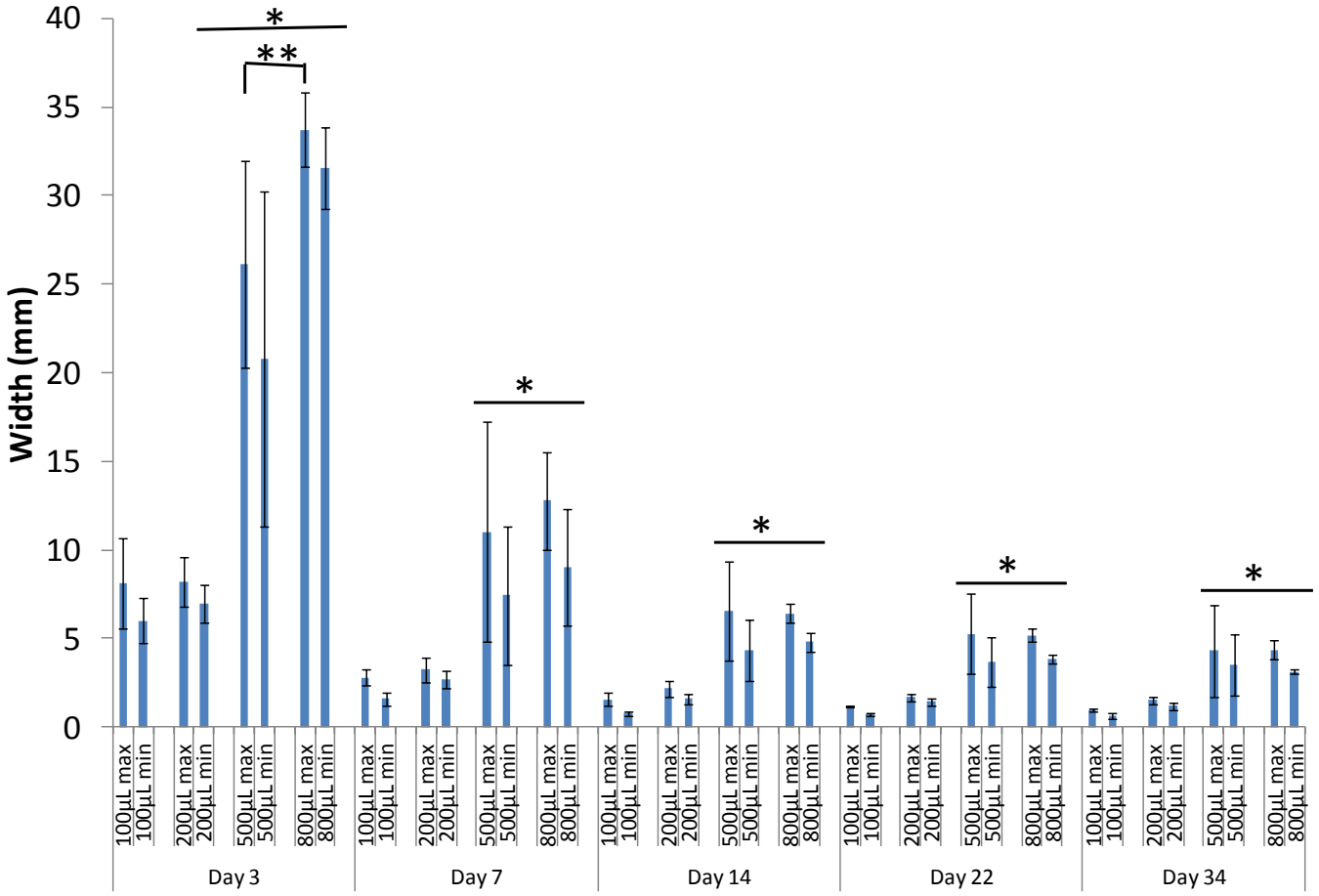

FIGURE 5.4: Effect of fibrinogen volume on construct maximum and minimum widths. On day 3, widths of 500μL and 800μL fibrinogen constructs differed significantly from each other. Throughout the study, both 500μL and 800μL constructs had significantly greater widths than constructs containing lower volumes of fibrinogen. ** denotes $p < 0.05$ compared to other groups, ** $p < 0.05$ compared to each other.*

5.3.3 Altering total fibrin volume at a constant thrombin to fibrinogen ratio

The method used in Section 5.3.2 varied both the volume and the stiffness of the fibrin gel. Consequently it was difficult to come to any firm conclusions about which property, stiffness or volume was responsible for the observations. The effects of fibrin volume and fibrin stiffness needed to be decoupled. Keeping the ratio of reagents constant, only the total volume used to prepare the fibrin gels was altered.

Naturally, increasing the total volume of reagents using a petri-dish of constant diameter, increased the thickness of the fibrin hydrogels (Table 5.3).

TABLE 5.3: Approximate thickness of fibrin gels based on total volume of reagents in petri-dish.

Volume (mL)	0.7 (1X)	4.2 (6X)	7.0 (10X)	10.5 (15X)
Thickness (mm)	0.73	1.49	2.48	3.71
Petri dish diameter (mm)	35	60	60	60

5.3.3.1 Fibrin percentage gel areas

At the lowest volume of 500μL, constructs showed a visibly higher extent of contraction (Figure 5.5A), at 18.01 $\pm$ 4.49% on day 3 (Figure 5.5B). The percentage gel area of the 500μL group was half the value of the 700μL of 37 $\pm$ 5.06%, 3.35 times lower than the 1000μL group of 60.32 $\pm$ 6.60% and 4.31 times less than the 1500μL group of 77.58 $\pm$ 8.44%. As such, fibrin gel contraction was appeared to proportional to fibrin volume.

Comparison of day 3 fibrin gel percentage areas, indicated that all groups had statistically significant differences from each other ($p<0.05$). This was the general trend over the course of the 22 day study although on days 4, 7 and 12 no statistically significant differences were observed between the 500μL and 700μL groups ($p=0.529$, $p=0.074$ and $p=0.121$, respectively).

On day 12, the 1000μL (10.53 $\pm$ 1.39%) group only differed significantly from the 500μL (3.87 $\pm$ 0.52%) and the 1500μL (14.47 $\pm$ 2.37%) groups whereas the 1500μL

differed from all groups (Figure 5.5C). Throughout the study, fibrin gel percentages were higher with increasing volumes of fibrin. By day 22 fibrin gel percentage areas had reduced to 2.78% ± 0.25% for 500μL, 3.42 ± 0.13% for 700μ, 4.41 ± 0.29% for 1000μL and 6.10 ± 0.42% for 1500μL ($p<0.05$ for all group comparisons).

5.3.3.2 Construct widths

Day 7 maximum widths of 500μL constructs (3.84 ± 0.54mm) did not differ significantly from those of the 700μL group (4.79 ± 0.42mm) whereas constructs made of higher initial fibrin gel volumes of 1000μL and 1500μL were much broader and differed significantly from each other as well as all other groups at 6.12 ± 0.68mm and 9.14 ± 0.72mm, respectively (Figure 5.5D). Minimum widths of all groups differed significantly from each other at 2.63 ± 0.42mm, 3.92 ± 0.67mm, 5.06 ± 0.47mm and 5.50 ± 0.47mm for 500μL, 700μL, 1000μL and 1500μL, respectively. This trend was similar on day 12, however on day 22, maximum widths of groups 500μL, 700μL and 1000μL showed no significant differences from each other at 1.82 ± 0.27mm, 2.24 ± 0.25mm and 2.71 ± 0.16mm. Only the maximum widths of the 1500μL group of 4.22 ± 0.48mm differed significantly from all other groups. Minimum widths on day 22 were 1.35 ± 0.28mm, 1.74 ± 0.03mm, 2.26 ± 0.23mm and 3.37 ± 0.39mm for groups 500μL, 700μL, 1000μL and 1500μL, in that order ($p<0.05$, for 1500μL min width compared to all other groups).

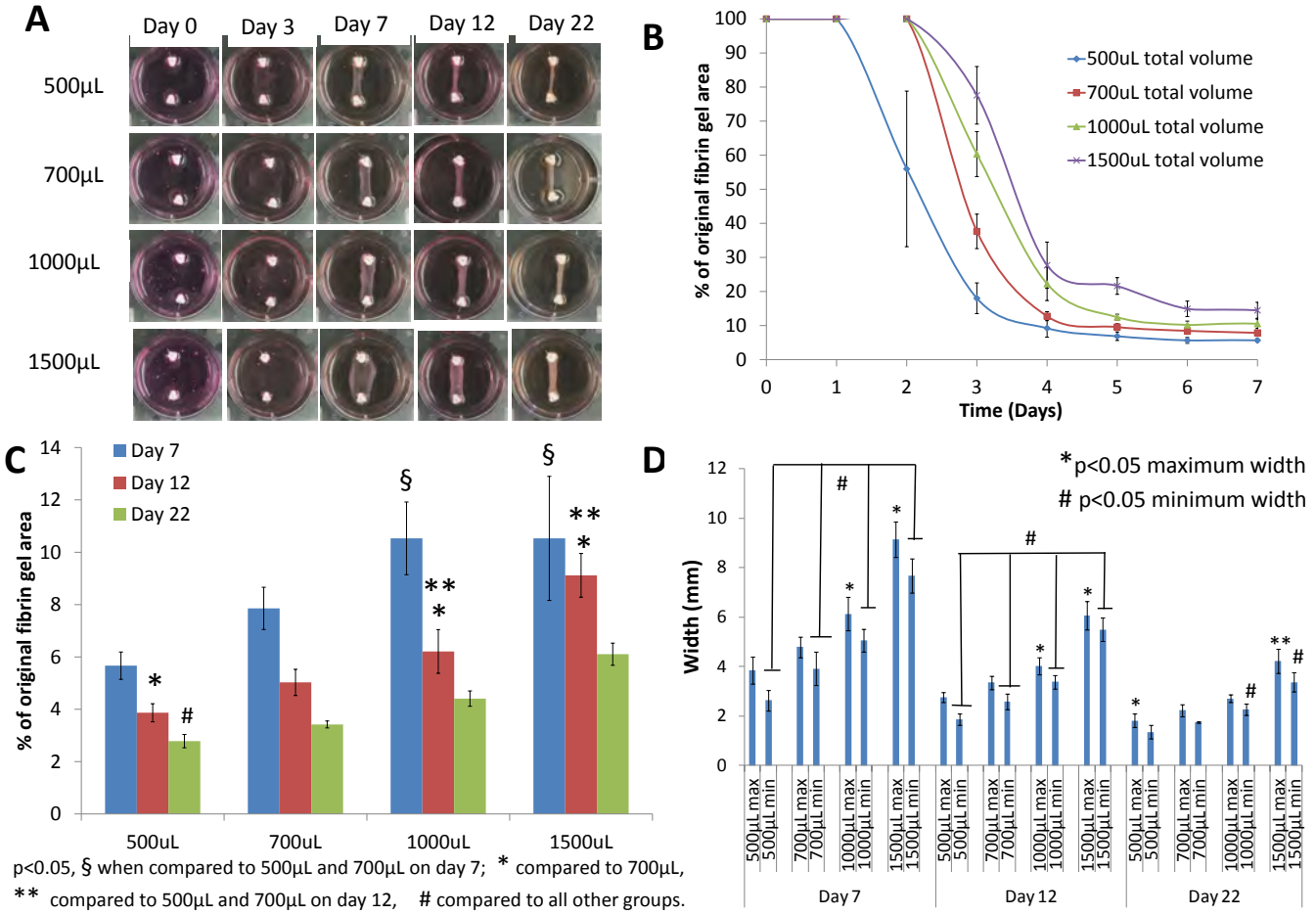

FIGURE 5.5: Effect of varying fibrin volume at a constant thrombin to fibrinogen ratio (1.25UT/mgF). A) Images of constructs prepared using varying volumes of fibrin gel. B) Fibrin percentage gel areas in the first week showing significant differences on contraction rates between all groups on day 3. C) After the first week, percentage gel areas of the two lowest volume groups differed significantly from the two highest groups. D) Maximum and minimum widths of the constructs also differed.

5.3.3.3 Strain sweeps of gels of varying volume/ thickness

Strain sweeps were conducted to determine the linear viscoelastic region (LVR) of the gels.

Figure 5.6A shows strain sweeps of gels of varying volumes. At low strains (<5%) 6X and 10X gels exhibited a linear G' of approximately 7.5 Pa and 10.5 Pa respectively, whereas 15X gels were linear over a very short period between 0.1% - 0.3% strain (Figure 5.6B).

The linear viscoelastic region was therefore taken to be below 5% strain as thereafter the G' of gels began to decline steadily and the exact critical strain was difficult to pinpoint. Total disruption of gel structure was taken to be where G" exceeded G' and these were at strain of >121.7% for 6X, at 79.84% for 10X and 31.83% for 15X, with corresponding G'/G" of 0.75Pa/0.60Pa, 0.65Pa/0.74Pa and 1.01Pa/1.02Pa (Figures 5.6 C, D & E).

TABLE 5.4: G' of gels of various volumes at different strain percentages.

	Average G' ± SD (Pa)			
Volume	**1% strain**	**3% strain**	**10% strain**	**65% strain**
6X	7.49 ± 1.57 #	7.25 ±1.56	6.59 ± 1.60	3.28 ± 0.89 *
10X	10.61 ± 6.96	10.22 ± 6.92	9.22 ± 6.65	1.01 ± 0.75
15X	16.36 ± 4.48	13.77 ± 4.65	6.35 ± 4.07	0.29 ± 0.37

and * denote significant difference compared to 15X and 10X /15X, respectively.

Within the LVR region at 1% strain, the stiffness of 6X gels was significantly lower than 15X gels at 7.4 ± 1.57% (Table 5.4). The strain of the 15X group of 16.36 ± 4.48% was double the value of the 6X gels.

Conversely, at higher strains, it can be seen that 6X remained more robust, with G' higher than both 10X (1.01 ± 0.75Pa) and 15X (0.29 ± 0.37Pa) gels at 3.28 ± 0.89Pa (Table 5.4). No significant differences were observed between the 10X and 15X gels over the range of strains investigated.

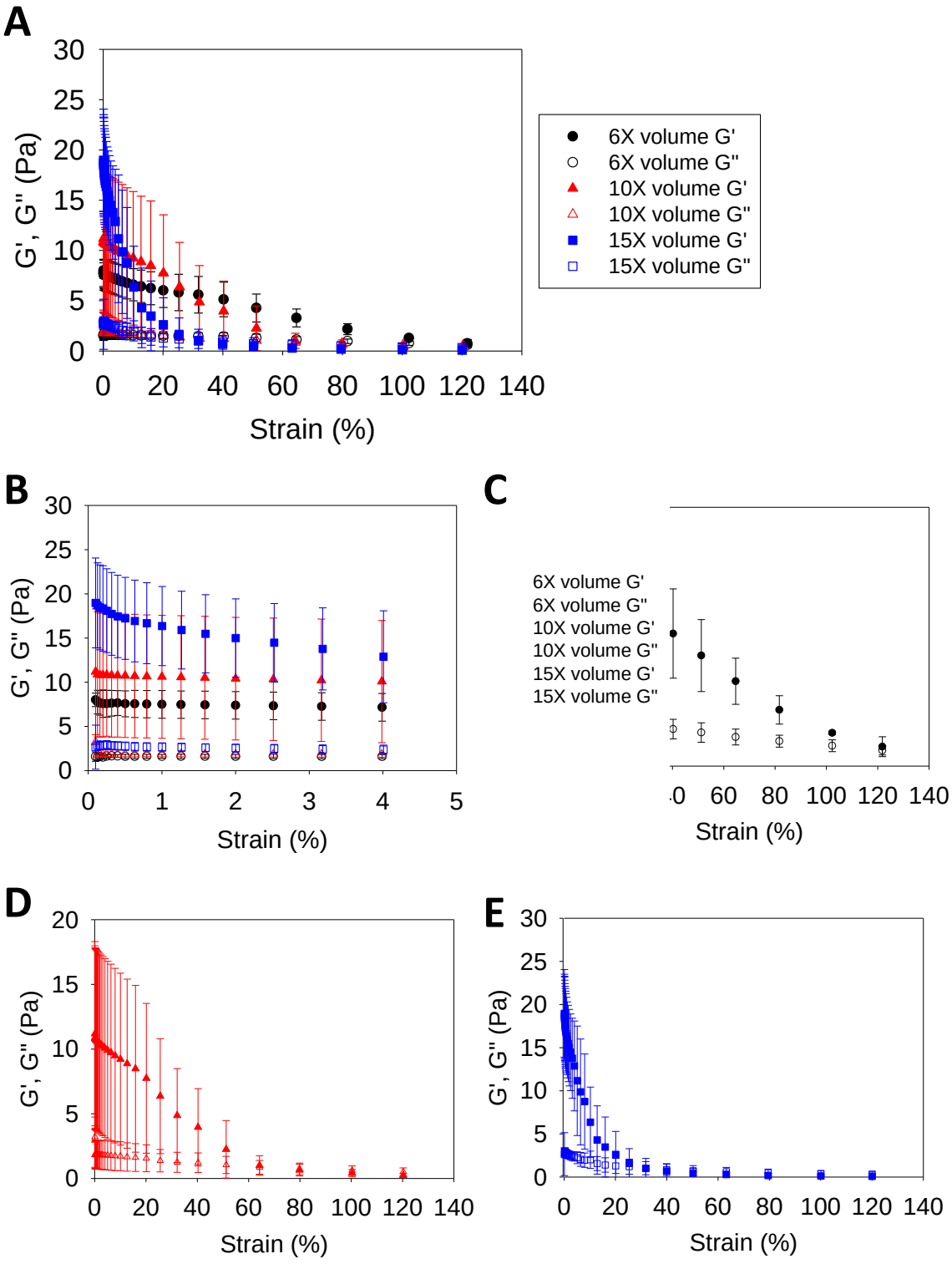

FIGURE 5.6: Strain sweeps of gels of differing total fibrin volume. A) Strain profiles over the investigated range, 0.1 –120% at 1 rad/s, B) At low strains, gel response was linear and C) – E) show individual strain curves for gels of volumes 6X, 10X and 15X. (n=3)

5.3.3.4 Frequency sweeps of gels of varying volume/ thickness

At constant strains of 1% (within the LVR), gels appeared to stiffen at low angular frequencies <10rad/s until a plateau was reached, which remained fairly stable over 10rad/s - 50rad/s (Figure 5.7A and B).

TABLE 5.5: G' of gels of various volumes at different frequencies.

	Average G' ± SD (Pa)			
Volume	0.5 rad/s	1.0 rad/s	10 rad/s	50 rad/s
6X	7.20 ± 1.25#	7.85 ± 1.32 #	10.36 ± 1.53#	9.18 ± 1.05*
10X	11.49 ± 4.29	12.39 ± 4.72	15.64 ± 6.08	17.17 ± 4.96
15X	17.52 ± 2.69	17.95 ± 2.17	21.19 ± 1.79	23.65 ± 1.85

significant difference compared to 15X
* represents significant difference from both 10X & 15X.

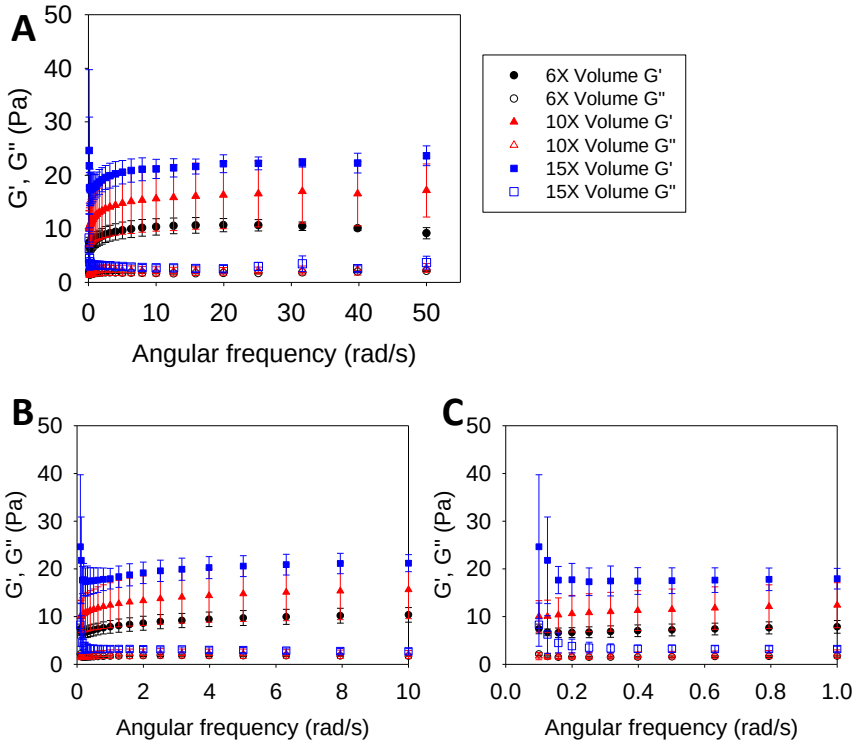

FIGURE 5.7: Frequency sweeps of gels of differing total fibrin volume. A) Gel response over the range 0.1 –50rad/s. B) Profiles suggested a slight frequency dependency at <10rad/s although this was not significant C). Overall, the G' of the low volume gel 6X was significantly lower than the highest volume gel 15X. (n=3)

G' of 6X differed significantly from the 15X group at angular frequencies <10rad/s (Table 5.5), indicating that increasing volume increased stiffness of the gels as they resisted small deformations. However, in Figure 5.7C, it can be seen that for each curve, G' of successive points at <1rad/s do not differ significantly from each other in magnitude. As a result, the gels were taken to be frequency independent.

5.3.4 Altering fibrin gel stiffness (thrombin to fibrinogen ratio) whilst maintaining a constant volume

To determine the effect of fibrin gel stiffness on contraction the ratios of thrombin to fibrinogen were altered whilst maintaining a constant fibrin volume of 700μL. It was observed that with decreasing thrombin to fibrinogen ratios, the extent of contraction of the fibrin gel decreased. By day 7 and throughout the rest of the study, 2.5UT/mgF were visibly smaller in width than 0.313UT/mgF constructs (Figure 5.8).

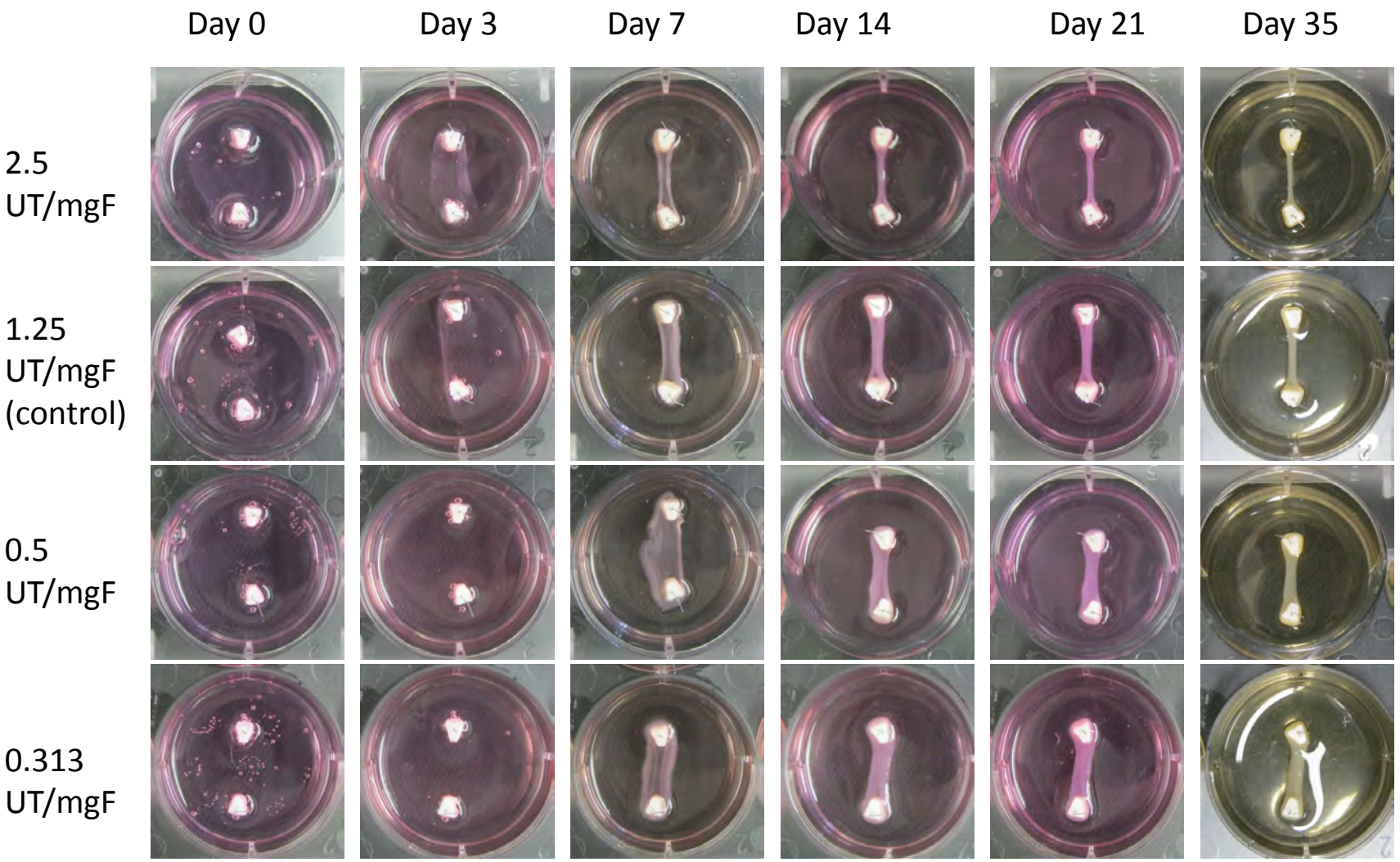

FIGURE 5.8: Effect of varying fibrin gel stiffness whilst maintaining a constant fibrin volume. Gel formulations were such that the higher the thrombin:fibrinogen ratio was then the softer the gel. By day 35 constructs of the softest gel had contracted the gel the most and were thinnest whereas constructs of the stiffest gel were broadest.

5.3.4.1 Fibrin percentage gel areas

On day 3, the percentage fibrin gel area of 2.5UT/mgF was lowest (25.21 ± 8.70%) and differed significantly from 0.5UT/mgF (58.96 ± 9.11%) and 0.313UT/mgF (77.68 ± 20.09%) but not from 1.25UT/mgF controls (40.65 ± 6.28%) (Figure 5.9A). The 1.25UT/mgF (control) group only differed significantly from the 0.313UT/mgF group.

By day 7, percentage gel areas of all groups had decreased to approximately 20% of day 3 percentage gel areas and were greater with increasing stiffness/ decreasing UT/mgF. Percentage gel areas were 5.18 ± 0.64%, 8.59 ± 0.96%, 14.64 ± 2.19% and 17.50 ± 4.63% for 2.5UT/mgF, 1.25UT/mgF, 0.5UT/mgF and 0.313UT/mgF, respectively (Figures 5.9A & B). Groups 0.5UT/mgF and 0.313UT/mgF differed significantly from 1.25UT/mgF and 2.5UT/mgF, though not from each other.

Changes between days 14 and 21 were very small although the stiffer the fibrin gels were the greater the change in fibrin percentage gel area was. For groups 2.5UT/mgF, 1.25UT/mgF, 0.5UT/mgF and 0.313UT/mgF the reduction in fibrin percentage gel areas from day 14 to 21 were 0.46 ± 0.11%, 0.41 ± 0.08%, 0.9 ± 0.42% and 1.32 ± 0.22%, respectively ($p<0.05$ between all groups) (Figure 5.9B & C). Percentage of original fibrin gel areas on day 21 were 2.76 ± 0.20%, 3.83 ± 0.46%, 5.45 ± 0.30% and 6.16 ± 0.25% (group ratios descending; all groups differed significantly from each other ($p<0.05$)).

Day 35 percentage gel areas had further reduced to 1.68 ± 0.30%, 2.13 ± 0.36%, 3.07 ± 0.42% and 3.52 ± 0.41% ($p<0.05$ between groups 2.5UT/mgF, 1.25UT/mgF and 0.5UT/mgF, 0.313UT/mgF). Decrease in percentage gel areas between days 21 and 35 were 0.61, 0.56, 0.56 and 0.57 fold for 2.5UT/mgF, 1.25UT/mgF, 0.5UT/mgF and 0.313UT/mgF, respectively.

5.3.4.2 Construct widths

The trend shown by the maximum and minimum widths on day 3 differed slightly from percentage gel areas shown above in that significant differences in width were

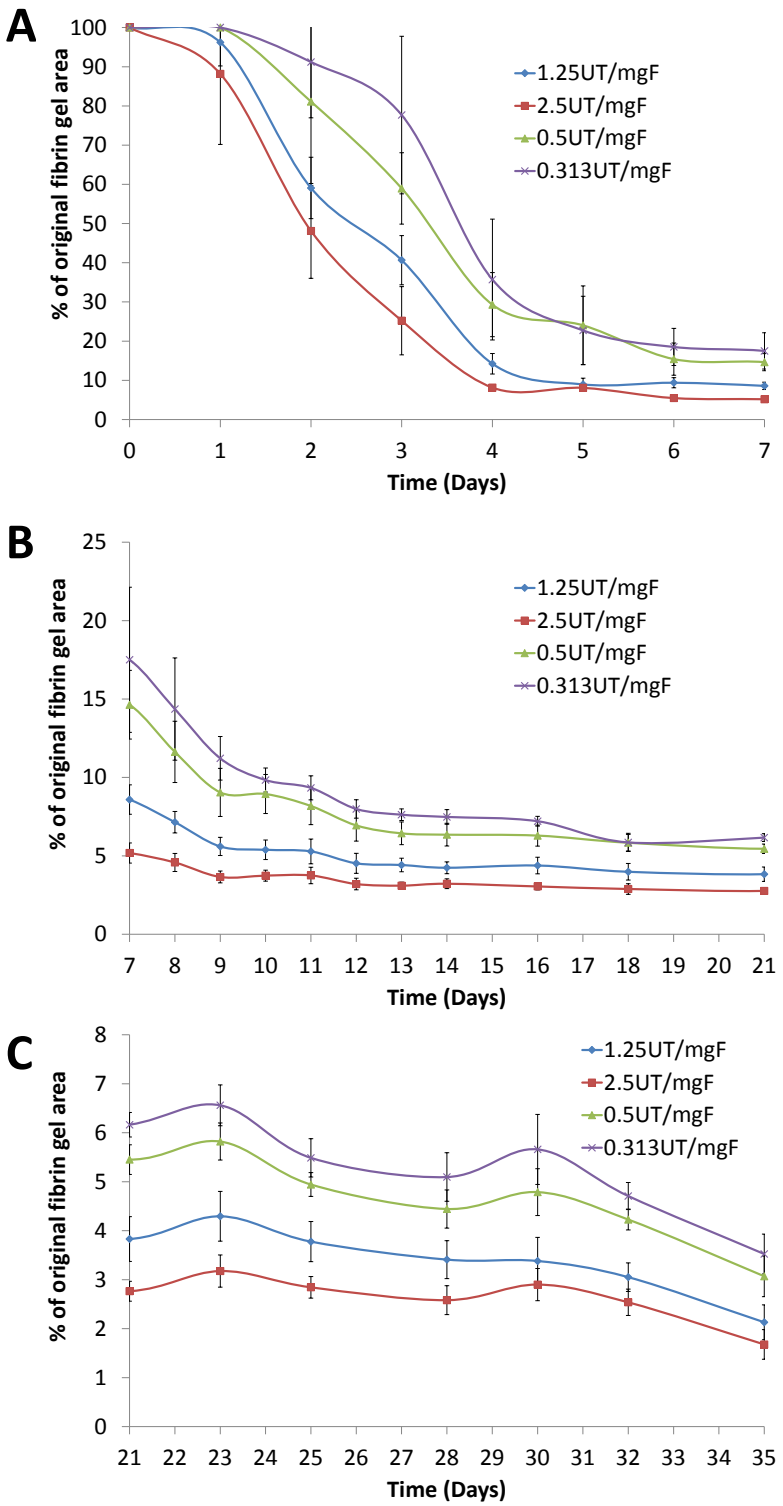

FIGURE 5.9: Fibrin gel percentage areas of constructs of prepared from fibrin gels of varying stiffness. A) shows fibrin percentage gel areas between days 0–7, B) between days 7–21 and C) days 21–35. Decreased thrombin to fibrinogen ratios (UT/mgF) reduced the rates and extent of contraction.

observed between constructs of the softest (2.5UT/mgF) and stiffest (0.313UT/mgF) gel formulations, which also differed from the other two groups (Figure 5.10A).

Increased rates of contraction in the 1.25UT/mgF (control) and 0.313UT/mgF groups led to comparable max/min widths between the 2.5UT/mgF and 1.25UT/mgF and between 0.5UT/mgF and 0.313UT/mgF on day 7 (Figure 5.10B).

All maximum widths differed significantly from each other on day 14. However, the minimum widths of both the 2.5UT/mgF and 1.25UT/mgF constructs differed significantly from groups 0.5UT/mgF and 0.313UT/mgF but not from each other.

Interestingly, on day 21 all minimum widths differed from each other. The maximum widths differed of groups 2.5UT/mgF and 1.25UT/mgF differed from each other as well as from both 0.5UT/mgF and 0.313UT/mgF. This was perhaps indicative of limits on maximum widths posed by the anchors, not present in minimum widths thereby allowing them to contract further.

After 5 weeks in culture, maximum widths of 0.313UT/mgF constructs were significantly broader than of both 1.25UT/mgF and 2.5UT/mgF (day 35). This was likely due to contraction still occurring in 0.313UT/mgF maximum widths but due the higher stiffness of the fibrin matrix, constructs were still wider than constructs of softer fibrin gel formulations. Again, all minimum widths differed significantly from each other, perhaps as no restrictions were posed on minimum widths by the anchors.

5.3.4.3 Fibrin fibre diameters and pore sizes

SEM images were used to quantify fibrin fibre diameters (Figure 5.11b, c and d). Measurements of average fibre diameter showed large variations in the 2.5UT/mgF group of $0.13 \pm 0.078\mu$m (Figure 5.11). Average fibre diameters of the 1.25UT/mgF, 0.5UT/mgF and 0.313UT/mgF groups were $0.092 \pm 0.015\mu$m, $0.090 \pm 0.038\mu$m and $0.074 \pm 0.016\mu$m, respectively, ($p>0.05$). This was surprising, as stiffer fibrin gels produced from lower thrombin volumes are said to result in thicker fibrin fibres.

Images showing the cryo-fractured structure of the gels suggested porosity decreased with decreasing UT/mgF ratios, with a greater extent of pore variation occurring in the 0.313UT/mgF group (Figure 5.12). Pore size analysis indicated statistically

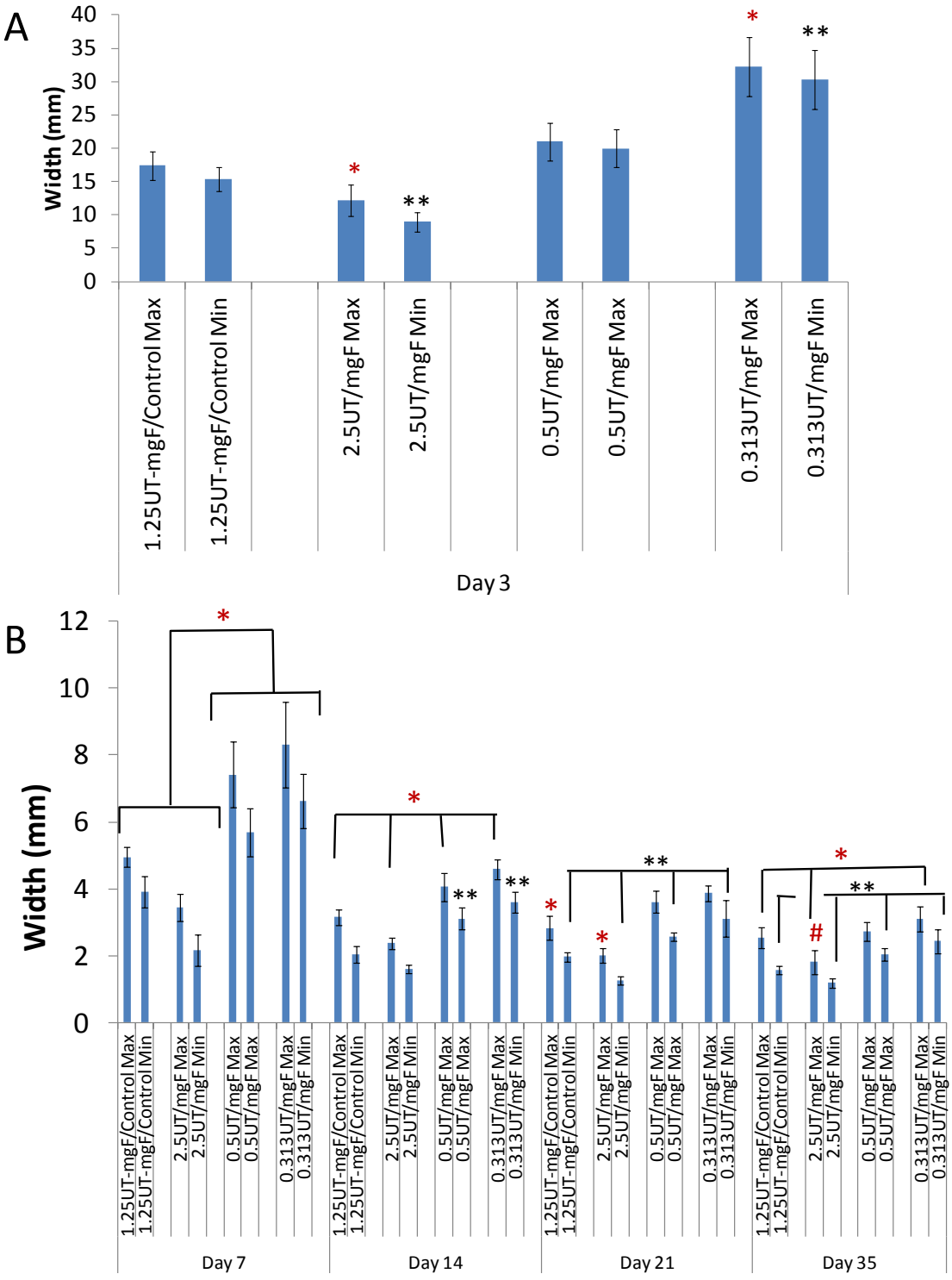

FIGURE 5.10: Effect of fibrin gel stiffness on sinew maximum and minimum widths. On day 3 maximum and minimum widths of the 2.5UT/mgF group differed significantly from all other groups, as did the 0.313UT/mgF. Over the 5 week study, widths continued to vary although differences mainly occurred between either just the maximum or the minimum widths. *$p<0.05$ for * max width, ** min width and # compared to all group max widths.*

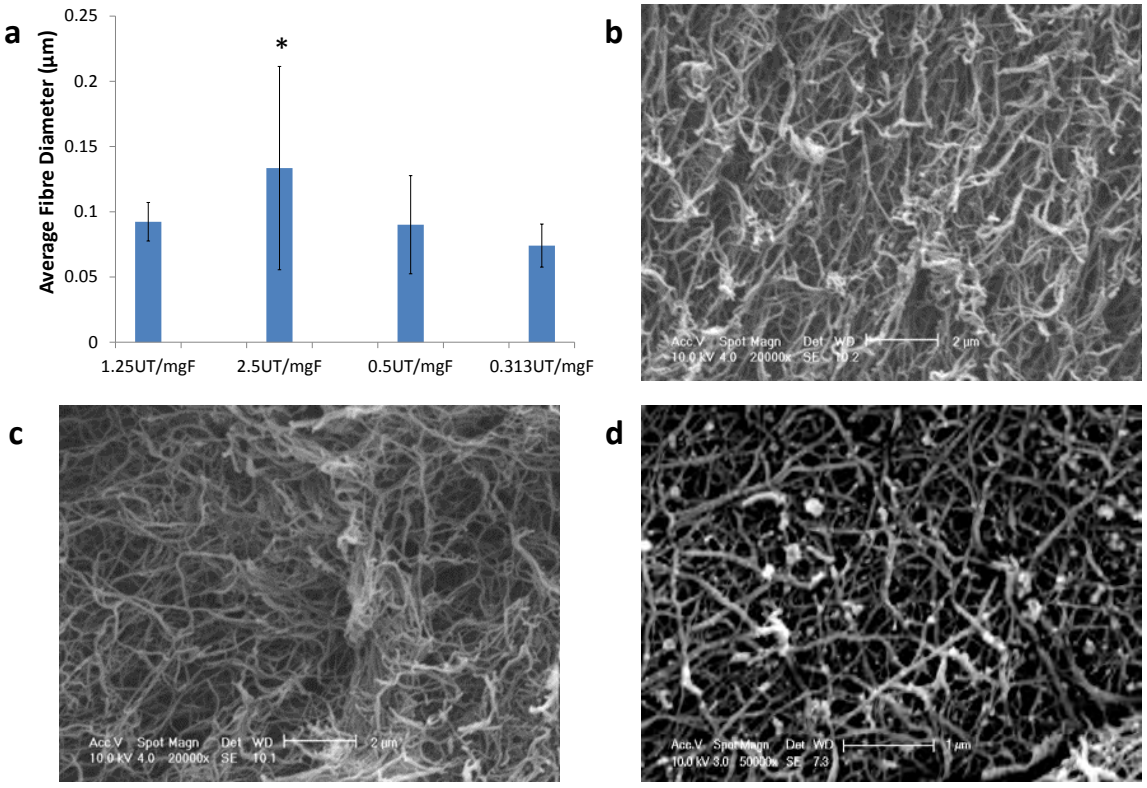

FIGURE 5.11: Analysis of fibrin fibre diameters. a) No statistically significant differences were observed between fibre diameters. SEM images of a) Control (1.25UT/mgF) gels , b) 2.5UT/mgF gels and c) 0.313UT/mgF gels. *Scale bar is 2µm for b & c and 1µm for d.*

relevant variances between the 0.313UT/mgF and 1.25UT/mgF control (p=0.000) and 2.5UT/mgF (p=0.031) groups. 0.313UT/mgF had an average pore size of 195 ± 223μm^2 (p<0.05), whilst that of 1.25UT/mgF control was 66 ± 58 μm^2 and 2.5UT/mgF was 127 ± 223μm^2 (Figure 5.12). Differences between the control and the 2.5UT/mgF group were not statistically significant (p=0.064). However, because the number of pore sizes above 400μm^2 increased in the stiffer gels of decreasing thrombin, this was in line with the literature, which report that stiffer gels are more porous.

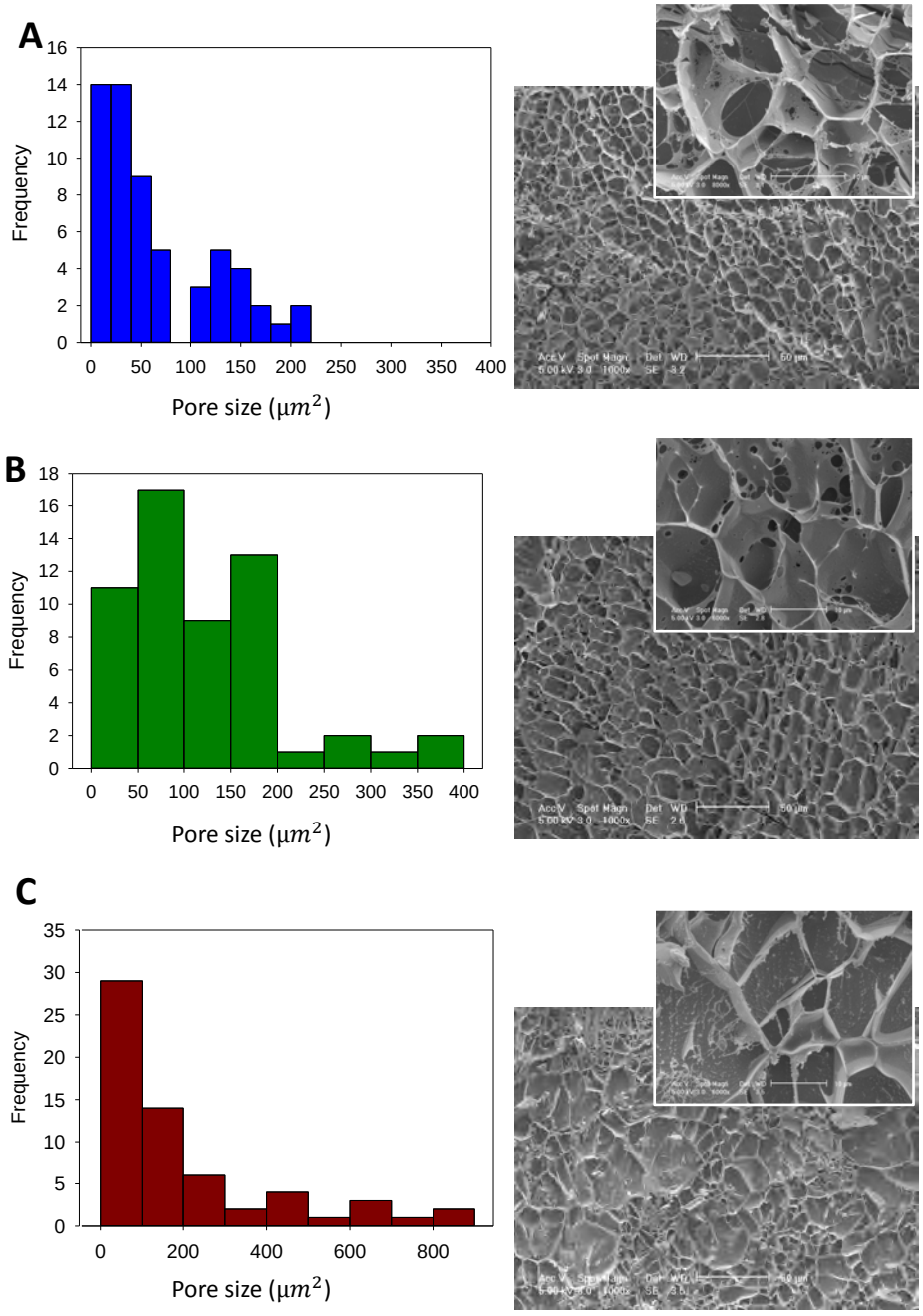

FIGURE 5.12: Analysis of fibrin pore sizes. Images of cryo-fractured fibrin gels were used to measure scaffold pore sizes: A) Control 1.25UT/mgF gels, B) 2.5UT/mgF gels and C) 0.313UT/mgF gels. Increase in fibrin gel stiffness resulted in a number of pore sizes above 400μm^2.

5.3.4.4 Gelling kinetics of fibrin gels of varying thrombin to fibrinogen ratio

Gelling kinetics of fibrin gels where quantities of thrombin and fibrinogen were altered were investigated. This was done to observe differences in stiffness during polymerisation and completion of gelation at the 1 hour time point, which is the about the time when cells are seeded on the gels during construct formation.

It was observed that gelation began to occur almost instantaneously upon mixing as G' was higher than G" at time t=13s (Figure 5.13). For all gels, there appeared to be an increase in G' until an initial stable plateau was reached, which was followed by a second steady increase in storage modulus. This phenomenon was more readily noticeable in 1.25UT/mgF and 0.313UT/mgF gels. The points at which these plateau were reached were at approximately 12Pa, 14Pa and 18Pa for gels 2.5UT/mgF, 1.25UT/mgF and 0.313UT/mgF, respectively, at times 2500s, 2900s and 2300s, in aforementioned order. Referring to the review by Weisel (2004), this is likely the gel point, which is reached when at least 10% of the fibrinogen has polymerized, followed by further branching to increase the stiffness of the gel. After an hour, the storage modulus of 0.313UT/mgF was higher than for 2.5UT/mgF and 1.25UT/mgF gels (Table 5.6). No significant differences were seen between 2.5UT/mgF and 1.25UT/mgF.

TABLE 5.6: G' of gels of varying thrombin to fibrinogen ratio at t=3600s.

Group	2.5UT/mgF	1.25UT/mgF	0.313UT/mgF
G' (Pa)	19.605 ± 2.51	16.625 ± 6.34	32.295 ± 8.493

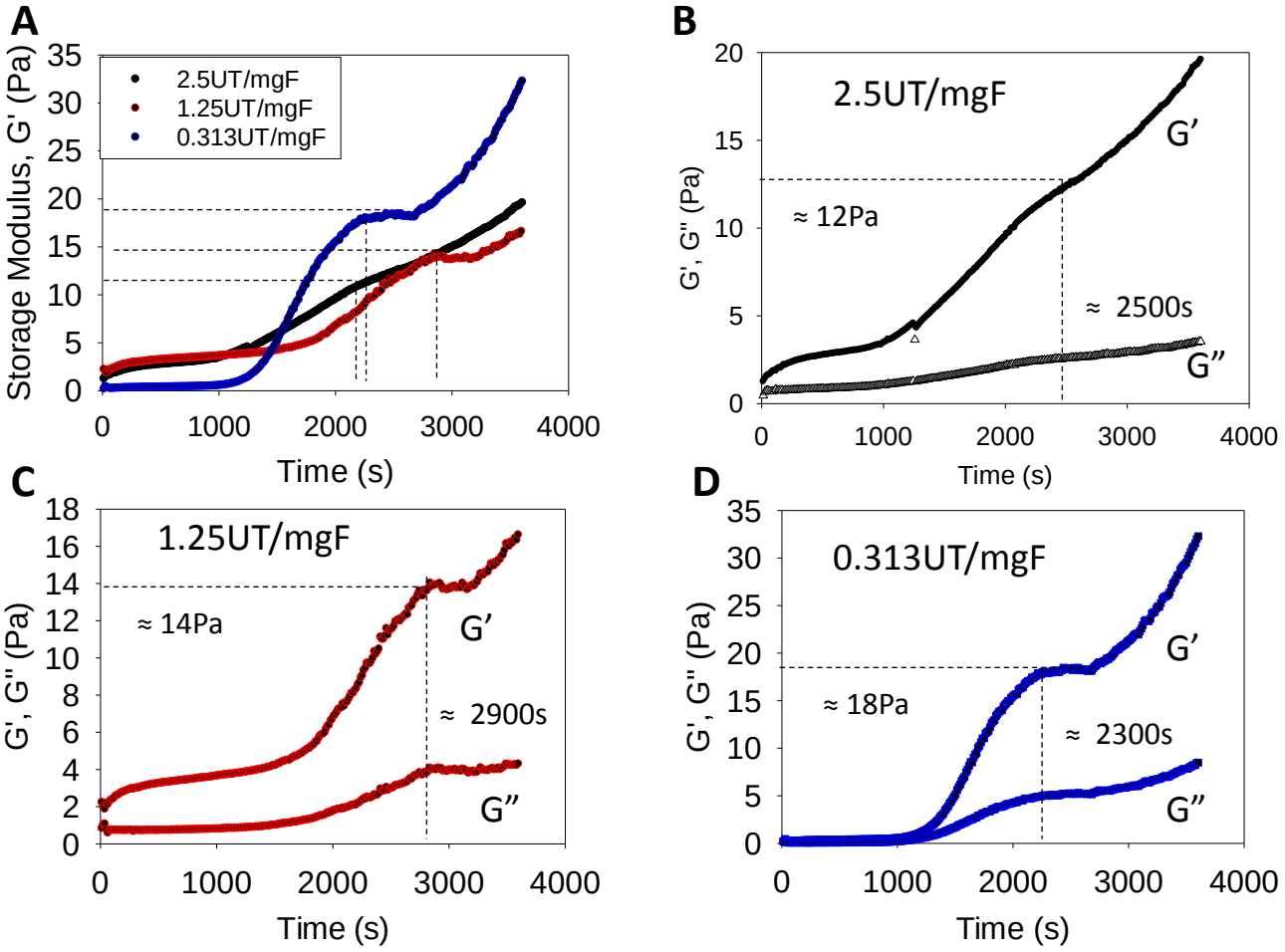

FIGURE 5.13: Time sweeps of gels. A) Gelation profiles of prepared using varying thrombin to fibrinogen ratios. An initial peak was reached, followed by further increase in stiffness. This occurred at close time points. Individual gelation curves are shown from B to D. (n=3)

In-situ strain sweeps of gels (following time sweep), showed gels had strain-dependent stiffening behaviour at very low strain <0.5% (Figure 5.14). This LVR was lower than of gels pre-gelled in the incubator before testing shown in the above section 5.3.3.3.

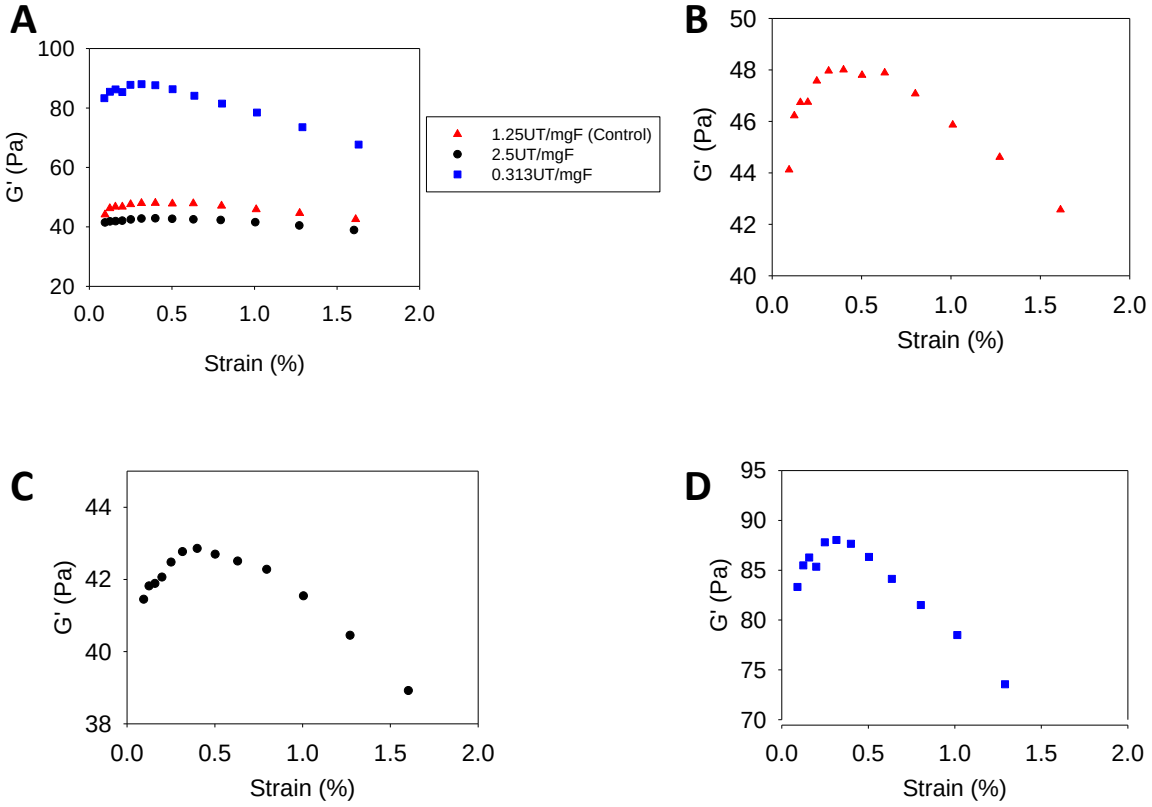

FIGURE 5.14: Strain stiffening behaviour at low % strain. A) In-situ strain sweeps following gelation. The strain stiffening behaviour is more apparent in the separate plots B) to D).

5.3.4.5 Mechanical behaviour of acellular fibrin gels of varying thrombin to fibrinogen ratios

Rheology tests were conducted on fibrin gels of varying thrombin to fibrinogen ratios, which were gelled in an incubator.

Strain sweeps

Response of acellular fibrin gels to deformations of increasing amplitude indicated that 2.5UT/mgF and 1.25UT/mgF gels were linear at strains <5% although 0.313UT/mgF appeared to almost immediately slowly deform (Figure 5.15).

At 1% strain, G' for gels were 20.27 ± 4.41Pa, 50.90 ± 1.74Pa and 121.67 ± 10.46Pa for gels 2.5UT/mgF, 1.25UT/mgF and 0.313UT/mgF respectively. The G' for 0.313UT/mgF gels was over 2-fold greater than that of the control gels (1.25UT/mgF).

Corresponding G" were 2.02 ± 0.66Pa, 5.16 ± 1.74Pa and 14.64 ± 2.28Pa. Cross over of G' and G" occurred at about 65% strain for 2.5UT/mgF and 1.25UT/mgF gels and 50% strain for 0.313UT/mgF gels. G' at these points were 1.73 ± 1.03Pa (2.5UT/mgF), 6.71 ± 2.46Pa (1.25UT/mgF) and 13.96 ± 1.03Pa (0.313UT/mgF).

Frequency sweeps

There were no interactions between G' spectra of all groups depicting statistically significant differences. The response was linear, further emphasising the robustness of the gels to deformation (1% strain). However, G" response to increasing angular frequency for 2.5UT/mgF and 1.25UT/mgF gels were almost identical whereas G" for 0.313UT/mgF gels was significantly higher than for other groups.

5.3.4.6 Effect of cell presence on fibrin gel rheological response

To determine whether the presence of CTF cells altered fibrin gel response either by stiffening or softening the gels, possibly due to the secretion of MMPs, frequency sweeps were conducted on gels 5 days post cell seeding. Similar to gels in the previous section, the gels were relatively frequency independent. The presence of cells on the fibrin gels did not affect the stiffness of the gel in the first 5 days as G' of cell seeded and acellular 1.25UT/mgF gels did not differ in magnitude (Figure 5.17).

5.3.4.7 Cell morphology on fibrin gels

Fibrin gels of varying thrombin to fibrinogen ratios, fixed in place to prevent contraction of the gel, were seeded with CTF cells and left to incubate for 3 days, to evaluate the effect of gel mechanics on cell morphology and proliferation. Light microscopy images of the gels at 4X magnification suggested proliferation was highest in gels of highest thrombin to fibrinogen ratio (2.5UT/mgF) and lowest in the stiffest gels (0.313UT/mgF) (Figure 5.18). At higher magnification (10X), cells on 2.5UT/mgF

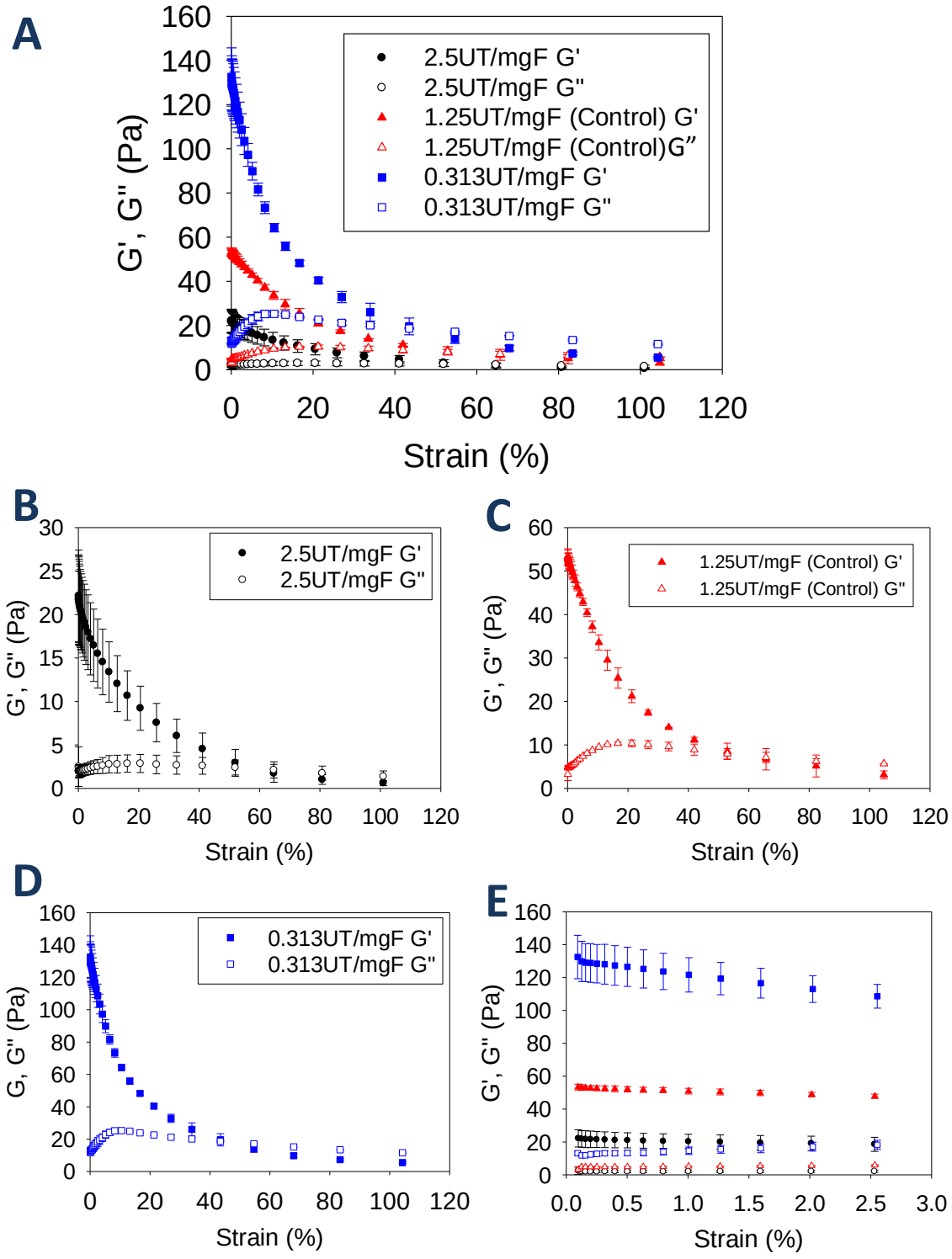

FIGURE 5.15: Strain sweeps of gels of varying thrombin to fibrinogen ratios. A) At zero shear, G' of gels differed significantly. Behaviour of all gels B) – C) was non-linear at high strains and linear only at very low strains <5% (E). (n=3)

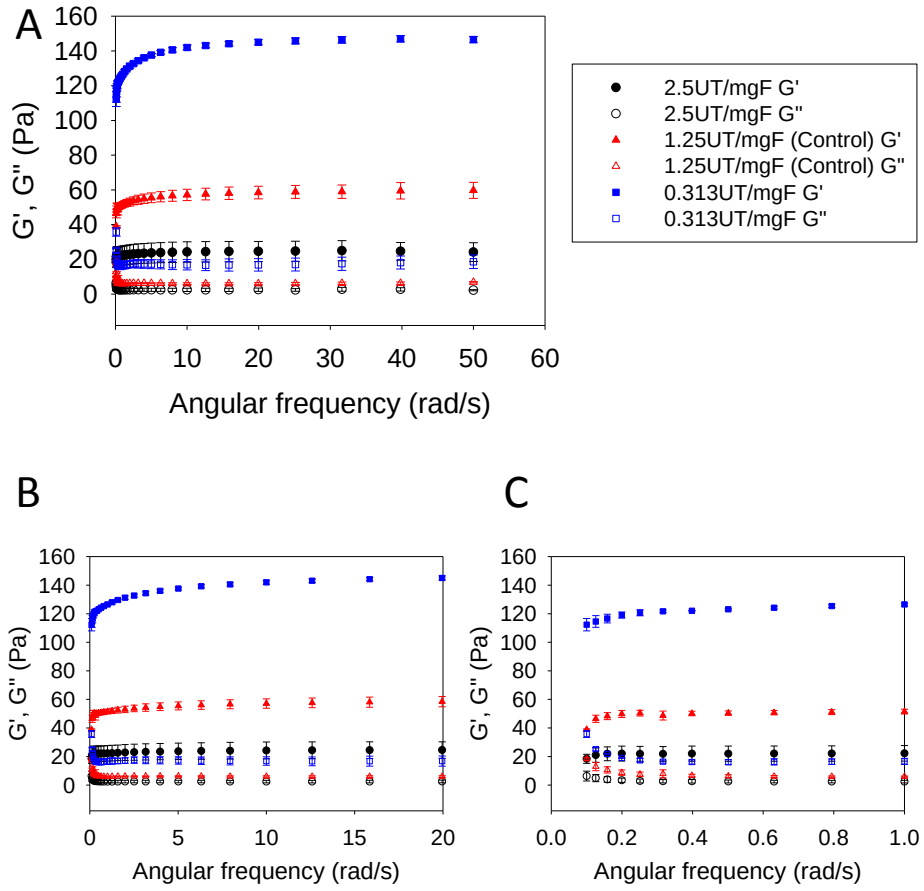

FIGURE 5.16: Frequency sweeps of gels of varying thrombin to fibrinogen ratios. A) Gels were fairly robust over the frequency range at a low strain of 1% and the results confirmed that lowering UT/mgF significantly increased gel stiffness. B) Frequency independence at high frequency as well as (C) low frequency (<1rad/s). (n=3)

appeared elongated or more spindle shaped. On the 1.25UT/mgF and 0.313UT/mgF fibrin gels, cells possessed slight dendritic extensions though some cells on the stiffest gels also appeared smaller and rounded. Using live/dead staining, contrasting results were seen, with 2.5UT/mgF showing the least amount of proliferation, however, cell morphology was in agreement with that seen using light microscopy. Live/dead staining of cells on 0.313UT/mgF gels, showed a mixture of rounded and elongated cells as well as directional alignment. Cell viability was high in all gel groups and no significant amount of dead (red) cells were seen.

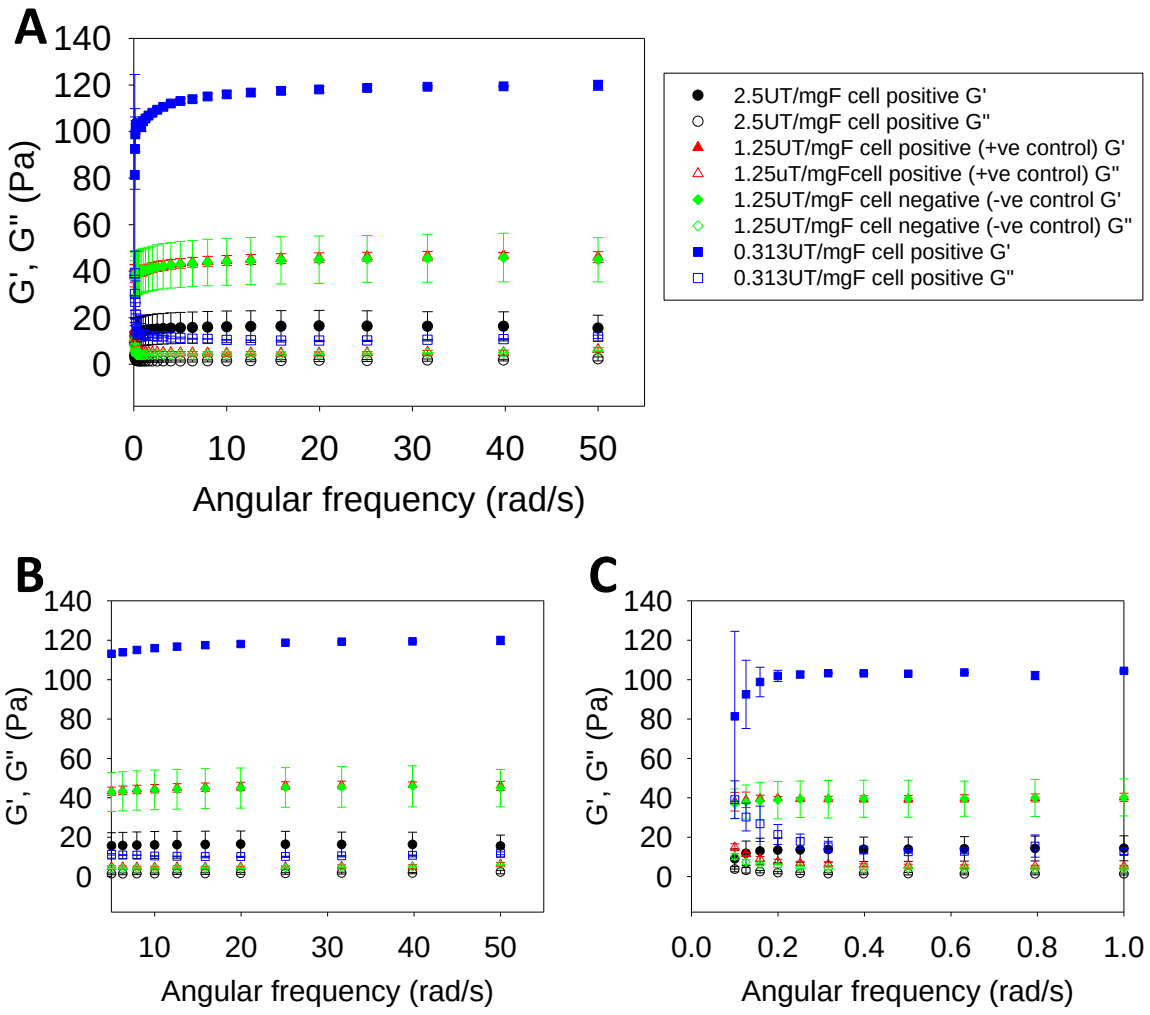

FIGURE 5.17: Frequency sweeps of gels of varying stiffness seeded with cells. A) Frequency sweeps of gels seeded with CTF cells following 5 days of incubation. B) No differences were observed between acellular and cell seeded control/ 1.25UT/mgF. C) Gels were frequency independent even at <1rad/s. (n=3)

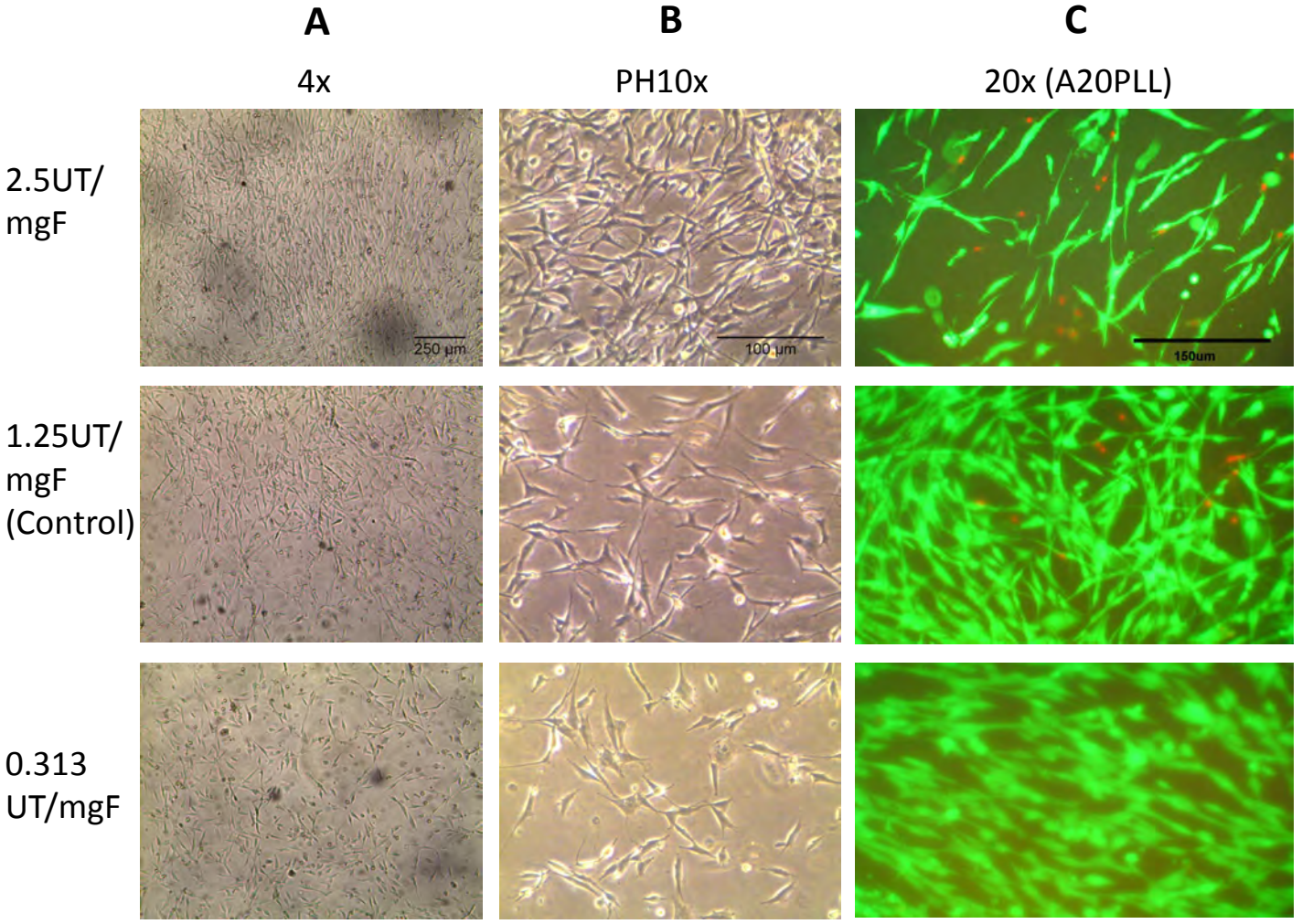

FIGURE 5.18: CTF cell proliferation on contraction inhibited fibrin gels on day 3. A) Light microscopy images of cell. B) Images taken using light microscopy with phase contrast showed greater proliferation in softer gels than stiffer gels. C) Conversely, confocal images of calcein-AM and propidium iodide (live/dead) stained gels indicated greater proliferation in stiffer matrices. *Scale bars are 250µm, 100µm and 150µm for 4X, PH10X and 20X, respectively.*

5.3.4.8 Cell proliferation within constructs

Due to the contrasting results seen in section 5.3.4.7 regarding cell proliferation, it was necessary to detach the cells from gels/ constructs. To determine how cells proliferate on gels of varying stiffness during TE L/T formation, constructs were allowed to form TE sinews by permitting contraction of the fibrin hydrogel. Day 3 results showed the number of live cells on 2.5UT/mgF gels to be lowest at $2.6 \times 10^5 \pm 5.1 \times 10^4$ cells and significantly different ($p<0.05$) when compared to groups 1.25UT/mgF ($3.6 \times 10^5 \pm 1.0 \times 10^5$ cells), 0.5UT/mgF ($3.0 \times 10^5 \pm 1.6 \times 10^5$ cells) and 0.313UT/mgF ($4.1 \times 10^5 \pm 1.3 \times 10^5$ cells).

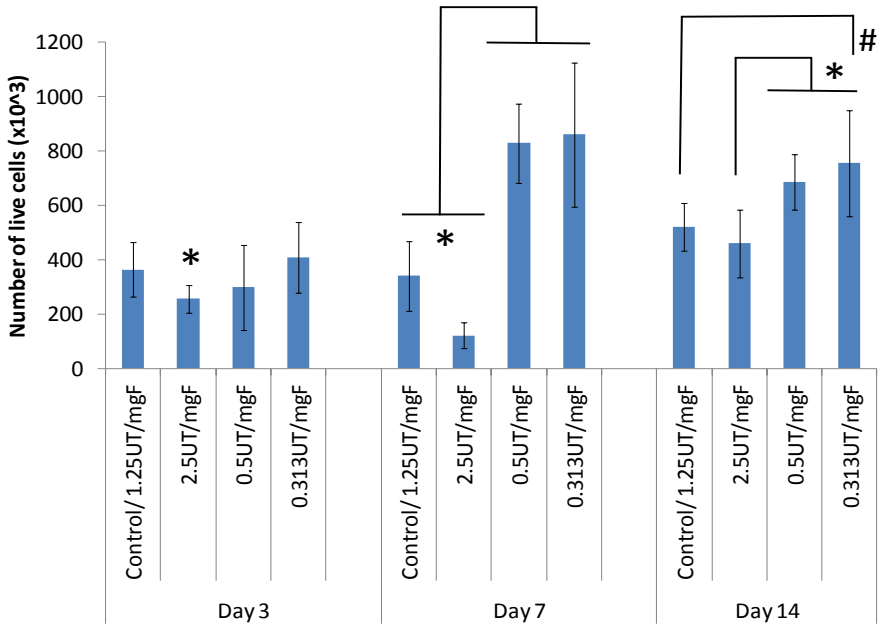

FIGURE 5.19: Proliferation of CTF cells seeded on gels of varying stiffness. Generally, cell proliferation increased with increasing gel stiffness.

Proliferation was highest for the stiffer gels 0.5 & 0.313 UT/mgF on day 7, with live cell numbers of $8.3 \times 10^5 \pm 1.5 \times 10^5$ cells and $8.6 \times 10^5 \pm 2.7 \times 10^5$ cells, respectively. These cell numbers were approximately 250% greater than those of 1.25UT/mgF (control) constructs ($3.4 \times 10^5 \pm 1.3 \times 10^5$ cells) and approximately 700% higher than live cell numbers of the softest gel 2.5UT/mgF ($1.2 \times 10^5 \pm 4.8 \times 10^4$ cells) ($p<0.05$).

Day 14 saw a decline in live cell numbers in the 0.5UT/mgF and 0.313UT/mgF by 17% and 12%, to $6.9 \times 10^5 \pm 1.0 \times 10^5$ cells and $7.6 \times 10^5 \pm 1.9 \times 10^5$ cells, in that order. Live cell numbers on the softer gels increased by 53% for 1.25UT/mgF ($5.2 \times 10^5 \pm 8.8 \times 10^4$ cells) and by and 281% for 2.5UT/mgF ($4.6 \times 10^5 \pm 1.2 \times 10^5$ cells). Differences in live cell number on day 14 between 2.5UT/mgF and both 0.5UT/mgF and 0.313UT/mgF were statistically significant as were differences between 1.25UT/mgF and 0.313UT/mgF ($p<0.05$). Generally, a stiffer gel formulation promoted cell proliferation in the early stages of contraction, but after prolonged culture attenuated growth.

5.3.4.9 Histological morphology of constructs

Figures 5.20A and B show longitudinal sections of 0.313UT/mgF and 1.25UT/mgF (control) constructs, respectively, stained with H&E. Similar to constructs in chapter 4, a larger number of cells were present on the periphery of the constructs (nuclei stained dark blue). Cells appeared to be aligned in the central portion of the control constructs, along the direction of tension (Figure 5.20B). At the pinned end of a control construct, it can be seen that the cells aligned themselves following the curvature of where the pin was placed (Figure 5.20D). Upon closer magnification of 0.313UT/mgF constructs, cells also appeared to align themselves in the direction of tension although the constructs were less densely packed with cells; in addition, the greatest alignment and density of cells occurred within the folds of the 0.313UT/mgF constructs, indicating that the increase in fibrin gel stiffness had not impacted cell migration and proliferation (Figure 5.20C). Cross-sectional images (Figures 5.20E to H) also revealed constructs to be surrounded by a thin layer rich in cells. Fibrillation was present within the constructs although perhaps this may have been a result of processing artefacts or due to the folding nature of formation (Figure 5.20G and H). The rolling mechanism that occurs during TE L/E formation was particularly prominent in 0.313UT/mgF constructs (Figure 5.20E).

5.3.4.10 Construct collagen content

Chapter 4 results suggested there was a relationship between construct collagen content and fibrin gel contraction. To determine whether fibrin gel stiffness played a role

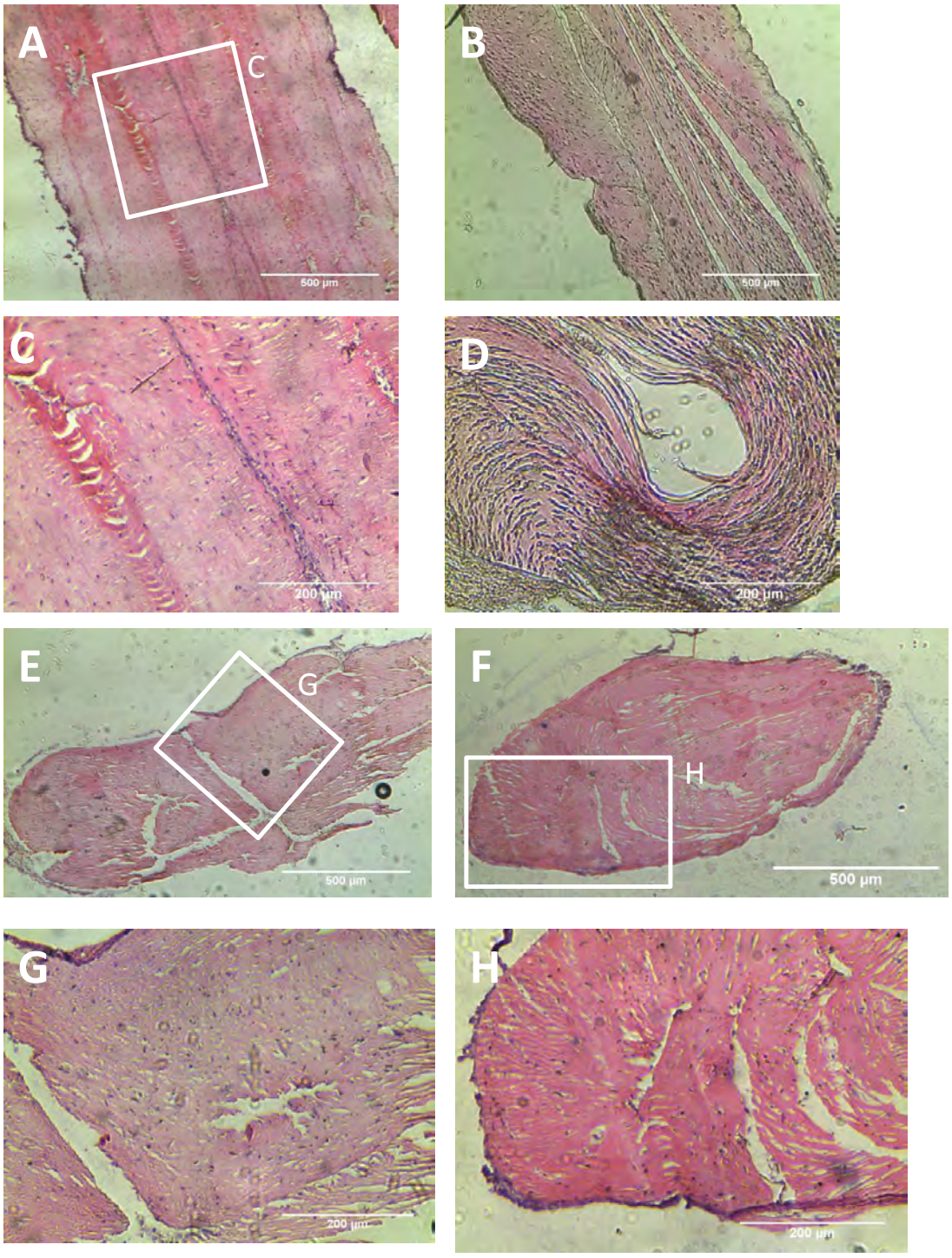

FIGURE 5.20: Histology of 0.313UT/mgF and control (1.25UT/mgF) constructs. A) Longitudinal section of 0.313UT/mgF construct. Cells were aligned in the mid-substance along the direction of tension (C) and cross-sections (E) revealed the presence of the rolling mechanism seen during formation resulting in a central fold (G). Cells were observed throughout the construct. Control (1.25UT/mgF) longitudinal section (B) showed the presence of aligned cells. Where pins were used, cells aligned around the pin edge (D). Cross-sections of control constructs (F) and (H) showed folds within the sinew and cell presence.

in cell collagen synthesis, collagen content of week 5 sinews was evaluated. No statistically significant differences were found between the collagen contents of all groups, which had collagen contents of 17.89 ± 7.54% (1.25UT/mF / control), 22.38 ± 13.65% (2.5UT/mgF), 19.36 ± 3.54% (0.5UT/mgF) and 20.51 ± 2.86% (0.313UT/mgF) per dry mass.

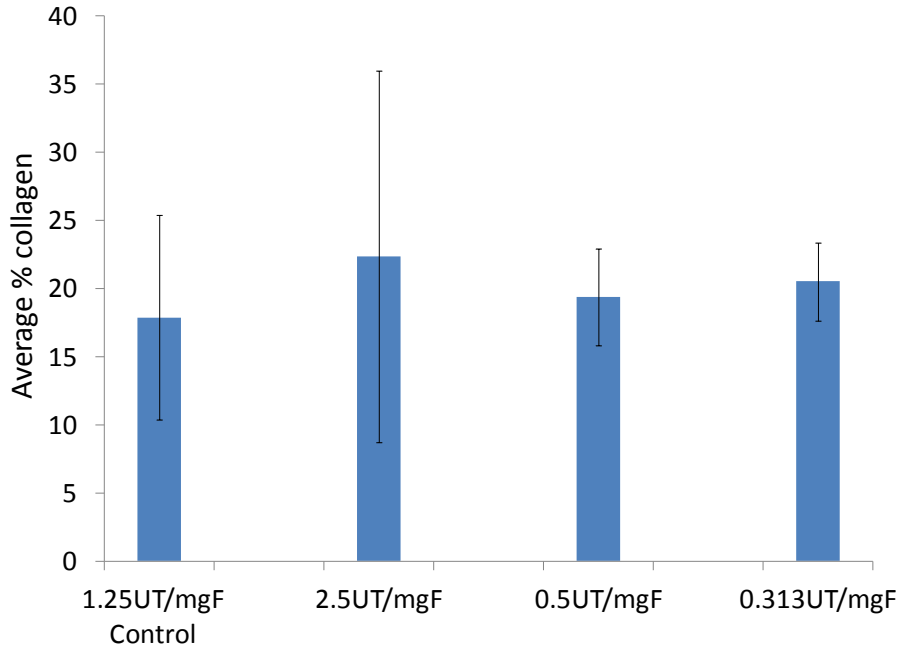

FIGURE 5.21: Collagen content of constructs.

5.3.4.11 Construct tensile strength

Figure 5.22 shows the load vs. extension curves of constructs prepared using fibrin gels of varying stiffness. The stiffest constructs had the highest maximum load of 201 ± 32mN, which showed statistical variation from the maximum load of constructs of the softest fibrin gel of 136 ± 30mN (Figure 5.22C). No significant differences were observed when compared to the control group (1.25UT/mgF) whose maximum load was 182 ± 26mN or compared to 0.5UT/mgF at 188 ± 37mN.

As the constructs varied in dimensions (maximum and minimum widths), these were taken to be a factor that would affect maximum/ minimum stresses withstood by the constructs (see section 5.3.4 on construct max/min widths). 2.5UT/mgF constructs being smallest in width had the highest maximum and minimum tensile stresses

of 122.05 ± 25.13kPa and 80.71 ± 27.94kPa (Figure 5.22B). Maximum stresses of groups 1.25UT/mgF, 0.5UT/mgF and 0.313UT/mgF were 73.96 ± 5.83kPa, 59.89 ± 13.39kPa and 75.23 ± 12.18kPa, whilst the minimum stresses were 37.75 ± 16.00kPa, 33.59 ± 14.74kPa and 60.12 ± 11.87kPa, in stated group order. The maximum stress of the 2.5UT/mgF group differed significantly from all other maximum stresses, whilst its minimum stress varied significantly only from 1.25UT/mgF and 0.5UT/mgF minimum stresses. Strain at ultimate load/ stress showed a slight decrease with increasing fibrin gel stiffness although differences were only significant between groups 1.25UT/mgF (1.29 ± 0.51) and 0.313UT/mgF (0.34 ± 0.19).

The Young's (elastic) modulus of the constructs was calculated from the initial linear portion of the stress/strain curves (Figure 5.23). Group 1.25UT/mgF appeared to have the lowest elastic modulus (based on the minimum stress profile, which would be the limiting case) of 132 ± 106kPa. Elastic modulus values for groups 2.5UT/mgF, 0.5UT/mgF and 0.313UT/mgF were 281 ± 84kPa, 200 ± 110kPa and 335 ± 196kPa, respectively. Due to the large standard deviations in these results, no statistically relevant differences were observed.

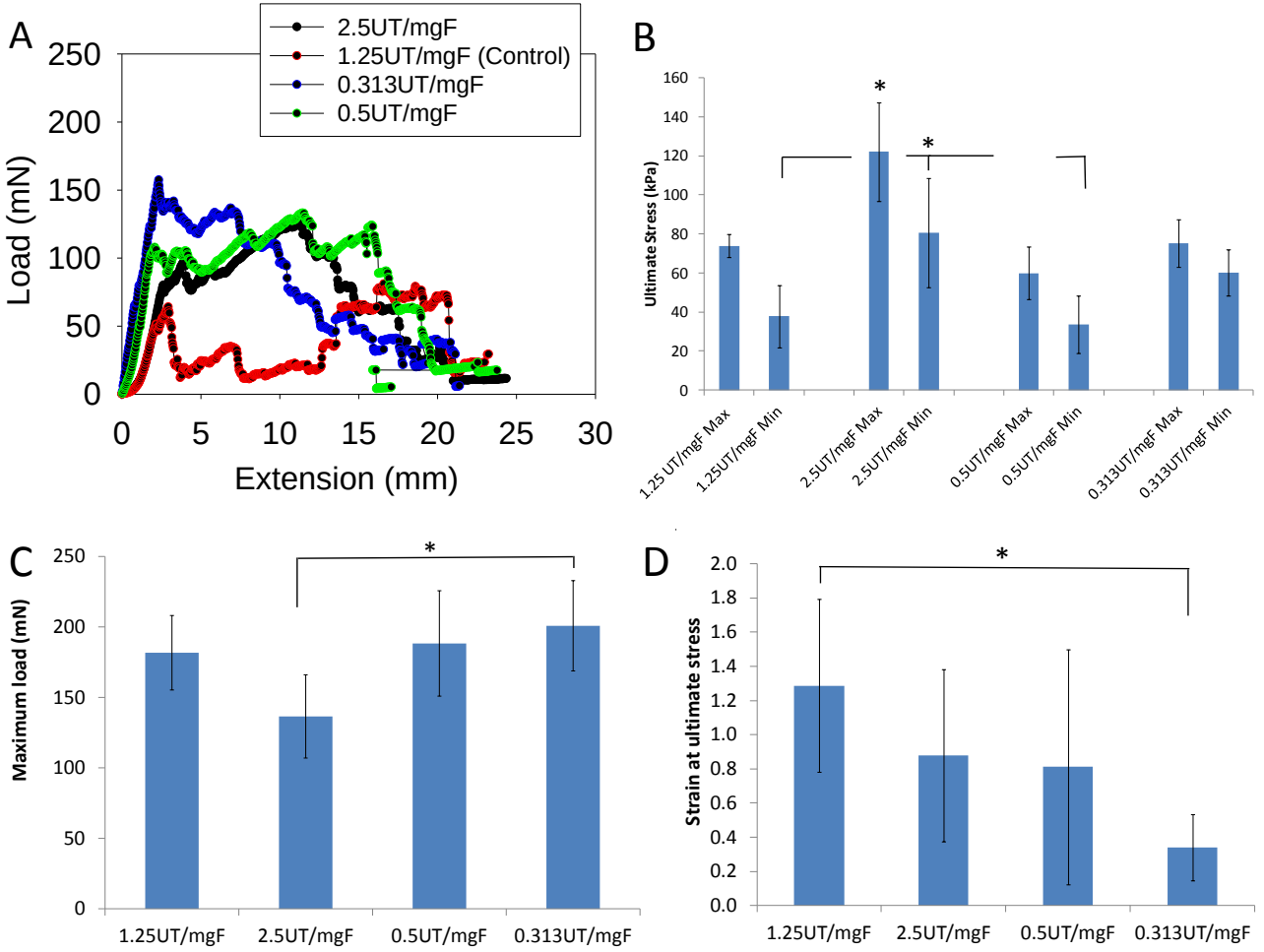

FIGURE 5.22: Tensile test results. A) Load vs extension curves of constructs. B) Stresses are dependent to geometry of constructs whereas maximum loads (C) can be quoted irrespective of construct maximum or minimum widths. D) 0.313UT/mgF had lower strains and significantly differed from the controls. ** represents significant difference at $p<0.05$.*

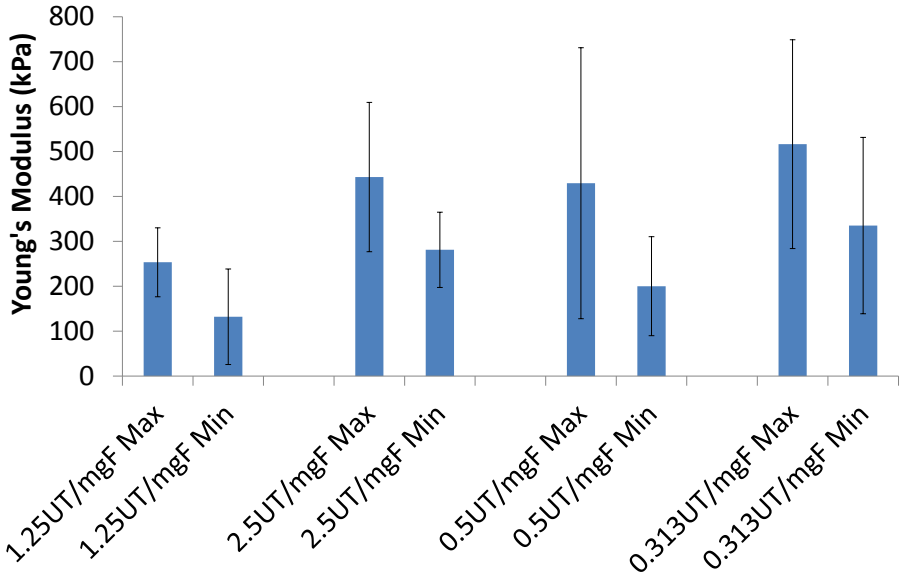

FIGURE 5.23: Young's Modulus of constructs due to scaffold stiffness. Increasing fibrin gel stiffness did not increase stiffness of constructs after 5 weeks of culture.

5.4 Discussion

AA+P supplementation of acellular gels did not affect gel stiffness

Rheological tests suggested that AA+P had no effect on the stiffness of acellular fibrin gels. This suggested that differences observed between AA+P treated constructs and the control where largely due to cell mediated processes. In Chapter 4 it was shown that AA+P treated constructs contracted the fibrin hydrogel to a greater extent and contained significantly higher quantities of collagen than non-treated control constructs. The relationship between ascorbic acid and fibrin(ogen) needs to be further studied as AA has been shown to polymerise fibrinogen without thrombin (Marx and Chevion, 1985). Studies are also available, which show that AA enhances fibrinolysis, but these were in the presence of endothelial cells (Kojima et al., 1986). As a result, since AA+P supplementation showed no direct effects on fibrin mechanical strength, further evaluation into the influence of other cell variables with or without AA+P was required.

Increasing fibrinogen volume and stiffness did not limit TE ligament formation

Degradation rates of TE scaffolds are known to be crucial to providing cells with sufficient time for new extracellular matrix deposition (Wu and Ding, 2004). Increasing the volume of fibrinogen used to prepare constructs resulted in considerable differences in the rates of contraction of the fibrin hydrogel, particularly between the gel of the lowest fibrinogen volume (100μL) and the highest volume (800μL) (Section 5.3.2, Figure 5.3). The widths of the lowest volume constructs visibly resembled constructs treated with AA+P, however, they were not significantly different from the controls (Figure 5.4). Surprisingly, at almost double the total volume of reagents used in the standard protocol (700μL) at 1300μL and a fibrin gel thickness of 1.35mm, cells were still able to contract and form a ligament-like sinew between the anchors. This suggested that the increase in fibrinogen volume to 800μL was not limiting to the formation of TE ligaments although correct biological morphology was not assessed at this point. It was visualized that since cells were seeded on top of the fibrin gels rather than entrapped within the gels, nutrient diffusion distances would be lower than for the latter case and still provide adequate mass transfer, additionally due to the replenishment of medium every two to three days (Figure 5.24). The assumption was: if the cells were able to migrate to a certain distance within the gel, then nutrient transfer would also be possible to/from that location.

The data suggested that increasing stiffness had a greater effect on contraction than increasing volume

In order to uncouple the effects of changing volumes and stiffness, constructs were prepared at constant ratios of thrombin to fibrinogen as per standard protocol but with changing total volumes. The results indicated that fibrin volume alone could be used to control the rate of fibrin depletion and consequently construct dimensions. When compared with results from section 5.3.2 on day 3, the percentage gel area of the 800μL fibrinogen group was 8.28 times larger than the 100μL group (Figure 5.3). However, where only the volume was altered the increase in percentage gel areas between lowest and highest volume was only 4.31 fold. This suggested that stiffness played a greater role on fibrin gel contraction rates, especially considering that the 800μL group had a higher average fibrin percentage gel area of 90.19 $\pm$

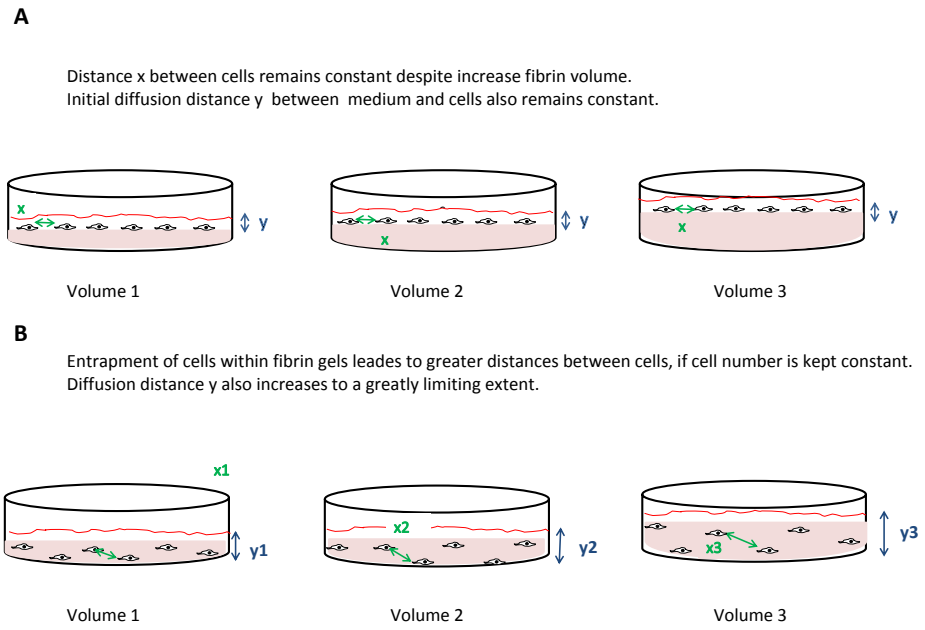

FIGURE 5.24: Visualized effect of increasing fibrin volume on diffusion distances.

6.41% yet a lower total fibrin volume of 1300μL when compared to the 1500μL group where only the total volume was altered at constant stiffness. Day 22 showed similar relationships between the effect of volume and stiffness due to changing fibrinogen volume. The difference in percentage gel areas between the highest volume of 1500μL was only 2.19 times greater in percentage gel area than the lowest volume group (500μL), however, when compared with changing fibrinogen groups, the percentage gel area of 800μL fibrinogen (of total volume 1300μL) was 6 fold greater than that of the 100μL fibrinogen group (total volume 600μL), again suggesting that at the particular stiffnesses and volumes used, stiffness had an additional effect on rates of contraction at those high volumes.

When the stiffness of the gels was altered whilst maintaining a constant volume (using similar ratios of thrombin to fibrinogen as in section 5.3.2, where fibrinogen volume was increased), no differences were seen between the percentage gel areas of the two softest gel groups compared to the two stiffest gels in the first week, suggesting that differences in the stiffnesses of groups 2.5UT/mgF and 1.25UT/mgF had no effect of the rate of contraction (see section 5.3.4). However, as expected, the result showed

that increasing the stiffness of the gel slowed the rate of fibrin gel contraction and consequently increased the final maximum and minimum widths of the constructs, at stiffnesses above 0.5UT/mgF. Final average maximum widths of the experiment were fibrinogen volumes (and stiffness) were increased, were 41.4% larger at 4.37mm ± 0.55mm for 800μL fibrinogen (Figure 5.4) than those were stiffness alone was altered at constant volume, 3.09mm ± 0.38mm for 0.313UT/mgF. Minimum widths of the 800μL group were also larger than for 0.313UT/mgF, though only by 29%. These results further suggested that although the 800μL group was at nearly double the volume of the 0.313T/mgF group, the effect of volume alone on construct maximum and minimum widths was smaller.

Although the data was not shown, it is important to note that at higher stiffness the 500μL and 800μL, were thicker than standard constructs prepared at total fibrin volumes of 700μL and of a more rectangular shape rather than circular. As such, there was a dimension neglected, in order to preserve sterility during tissue culture.

Comparison of contraction data further suggested that increasing total fibrin volume or increasing stiffness (lowering thrombin to fibrinogen ratios) have the same effect

Figure 5.25 compared results of all the contraction experiments in this chapter and it appeared to indicate that generally, increasing fibrinogen volume had the same effect as increasing volume at constant stiffness, which in turn had the same effect as increasing stiffness at constant volume. The red highlighted groups were the control groups, all at similar stiffness and volume, and as their percentage fibrin gel areas and maximum/minimum widths, seem to vary from one experiment to another, made it difficult to form definitive conclusions about variations between experiments, although differences between groups within each experiments were very clear.

Extent of contraction is proportional to total quantity of fibrinogen

Within experimental groups, increasing the volume of fibrin or increasing stiffness or both would naturally increase the amount of fibrin matter present, which would result

	Percentage fibrin gel area		
	Altering fibrinogen volume (and stiffness)	**Altering volume at constant stiffness**	**Stiffness at constant volume**
Group order	100µL fibrinogen 200µL fibrinogen 500µL fibrinogen 800µL fibrinogen	500µL volume 700µL volume 1000µL volume 1500µL volume	2.5UT/mgF 1.25UT/mgF 0.5UT/mgF 0.313UT/mgF
Day 3	10.89% ± 2.50% 13.31% ± 2.56% 61.66% ± 18.30% 90.19% ± 6.41%	18.01% ± 4.49% 37.00% ± 5.06% 60.32% ± 6.62% 77.58% ± 8.44%	25.21% ± 8.70% 40.65% ± 6.28% 58.96% ± 9.11% 77.68% ± 20.09%
Day 22	1.22% ± 0.17% 2.24% ± 0.45% 7.68% ± 4.01% 7.38% ± 0.54%	2.78% ± 0.25% 3.42% ± 0.13% 4.41% ± 0.29% 6.10% ± 0.42%	2.76% ± 0.20% 2.83% ± 0.46% 5.45% ± 0.30% 6.16% ± 0.25%
Day 35	1.10% ± 0.10% 2.09% ± 0.38% 7.36% ± 4.98% 6.63% ± 0.58%		1.68% ± 0.30% 2.13% ± 0.36% 3.07% ± 0.42 3.52% ± 0.41%
	Maximum widths		
	Altering fibrinogen volume (and stiffness)	**Altering volume at constant stiffness**	**Stiffness at constant volume**
Day 3	8.14mm ± 2.53mm 8.20mm ± 1.40mm 26.15mm ± 5.84mm 33.73mm ± 2.07mm	9.40mm ± 2.00mm 17.35mm ± 2.94mm 23.56mm ± 1.80mm 35mm ± 0.00mm	12.24mm ± 2.37mm 17.40mm ± 2.17mm 21.00mm ± 2.84mm 32.21mm ± 4.42mm
Day 22	1.14mm ± 0.04mm 1.68mm ± 0.20mm 5.28mm ± 2.26mm 5.19mm ± 0.35mm	1.82mm ± 0.27mm 2.24mm ± 0.25mm 2.71mm ± 0.16mm 4.22mm ± 0.48mm	2.01mm ± 0.22mm 2.83mm ± 0.35mm 3.61mm ± 0.33mm 3.87mm ± 0.23mm
Day 35	0.98mm ± 0.08mm 1.51mm ± 0.21mm 4.33mm ± 2.59mm 4.37mm ± 0.55mm		1.81mm ± 0.35mm 2.54mm ± 0.30mm 2.72mm ± 0.28mm 3.09mm ± 0.38mm
	Minimum widths (mm)		
	Altering fibrinogen volume (and stiffness)	**Altering volume at constant stiffness**	**Stiffness at constant volume**
Day 3	6.00mm ± 1.27mm 6.98mm ± 1.05mm 20.78mm ± 9.42mm 31.55mm ± 2.30mm	7.42mm ± 1.67mm 12.70mm ± 1.92mm 21.74mm ± 2.20mm 33.00 ± 0.00mm	8.96mm ± 1.50mm 15.40mm ± 1.81mm 19.98mm ± 2.81mm 30.33mm ± 4.43mm
Day 22	0.69mm ± 0.09mm 1.42mm ± 0.19mm 3.66mm ± 1.41 3.84mm ± 0.26mm	1.35mm ± 0.28mm 1.74mm ± 0.03mm 2.26mm ± 0.23mm 3.37mm ± 0.39mm	1.25mm ± 0.12mm 1.98mm ± 0.14mm 2.58mm ± 0.12mm 3.11mm ± 0.54mm
Day 35	0.64mm ± 0.14mm 1.19mm ± 0.22 3.51mm ± 1.70mm 3.14mm ± 0.14mm		1.19mm ± 0.14mm 1.58mm ± 0.13mm 2.05mm ± 0.19mm 2.44mm ± 0.36mm

FIGURE 5.25: Comparison of percentage fibrin gel areas, maximum and minimum widths of experimental groups. *The control groups are shown in red.*

in the constructs taking longer to contract. However, cell processes such as proliferation, cell mediated contraction and cell enzymatic digestion, which could increase or decrease in response to scaffold and other extracellular environment signals could not be predicted, making these experiments necessary. By quantifying the actual mg of fibrinogen present and using equations from Wufsus et al. (2013) (equations 5.1 and 5.2) to determine the overall fibrin fibre volume fraction ϕ_f, it was found that there were correlations between the rates and extents of contraction with the total mg of fibrinogen used to prepare the fibrin gels (Table 5.7, an example calculation is shown in Appendix A).

$$\Phi_{int} = 0.015ln(c_{Fbg}) + 0.13 \tag{5.1}$$

where Φ_{int} *is the internal solid fraction of individual fibres*

$$\phi_f = \frac{c_{Fbg}}{\rho_m \Phi_{int}} \tag{5.2}$$

where c_{Fbg} *is fibrinogen concentration,* ρ_m *is fibrinogen density*

TABLE 5.7: Estimated fibrin fibre volume fraction in experimental groups. *The control groups are shown in red.*

Experiment 1			Experiment 2			Experiment 3		
Fibrinogen vol	**Fibrinogen (mg)**	**Vf (ϕf) (%)**	**Fibrin volume**	**Fibrinogen (mg)**	**Vf (ϕf) (%)**	**Stiffness**	**Fibrinogen (mg)**	**Vf (ϕf) (%)**
100µL	2.00	1.61	500µL	2.86	2.62	2.5UT/mgF	2.34	1.61
200µL	4.00	2.61	700µL	4.00	2.61	1.25UT/mgF	4.00	2.61
500µL	10.00	4.34	1000µL	5.72	2.62	0.5UT/mgF	7.00	4.34
800µL	16.00	5.24	1500µL	8.58	2.62	0.313UT/mgF	8.62	5.25

The increase in ϕ_f of experiment 1 and constant ϕ_f of experiment 2, explain why, dramatic differences in percentage gel areas/ widths were observed between the 800μL and 100μL fibrinogen groups and more moderate variances occurred between the 1500μL and 500μL fibrin volume groups. The stiffest groups (800μL and 0.313UT/mgF) had twice the fibrin fibre volume fraction of the controls (shown as red). Considerable increases in fibrinogen content and consequently ϕ_f, were more readily achieved by increasing stiffness (*i.e.* lowering thrombin to fibrinogen ratio) than by increasing fibrinogen volume – the former also potentially reduces the amounts of reagents

used. This suggested that mechanical strength and dimensions of TE tissues could be tailored to a certain extent by altering the stiffness of fibrin scaffold or increasing the fibre volume fraction by modulating only the stock concentrations, whilst maintaining the thrombin to fibrinogen ratio. This could potentially be applicable to various branches of tissue engineering. For example, if larger/ broader tissues are desired then only the total volume would need to be altered at a specific thrombin to fibrinogen ratio/ fibrinogen concentration, provided the volumes are not limiting to cell survival. Alternatively, gel stiffness could be increased by adjusting thrombin to fibrinogen ratios or increasing the concentrations of both stock solutions to increase the fibrin fibre volume fraction as shown in Table 5.7. Possibly culture periods could also be adjusted to control sinew mechanics and dimensions.

Gel mechanical characteristics

Gels possess very low LVRs (<5%) and are frequency independent

Cells have been shown to respond to the stiffness of the matrix or scaffold resulting in variations of cell shape, gene expression and myosin dependent contractility (Discher et al., 2005; Solon et al., 2007). As a result, the stiffness of the matrix was of interest here as it not only determined the rates and extension of contraction by the cells but also the morphology of the TE ligaments/tendons (sections 5.3.4.7 and 5.3.4.9). Fibroblasts have been shown to achieve maximal spreading on stiffer surfaces around 10kPa (Solon et al., 2007). To determine if the increasing volumes of fibrin gels at constant thrombin to fibrinogen ratio (or stiffness) used to prepare constructs in section 5.3.3, were in fact at constant stiffness, the storage (G') and loss (G") moduli were rheologically measured.

According to Shen et al. (1974), elastic modulus as a measure of fibrin gel stiffness due to molecular networks and as a determinant of the extent of branch points in the network was developed by Ferry et al. (1951). Dynamic measurements of viscoelastic moduli revealed that gel storage modulus G' increased with increasing volume, most likely due to the higher total fibrin fibre quantity. Again this supported findings that adjusting volume or stiffness perhaps had the same effect. However, the highest volume gel (15X) was weaker as it began to deform at very low strains of >0.3% strain (Figure 5.6B). The gels also exhibited frequency independence and paralleled

other studies, which have shown frequency independent behavior of fibrin gels (Shah and Janmey, 1997; Wen et al., 2007; Weisel, 2007). Frequency independence of G' indicates that mechanical energy is not lost or stored as a result of molecular motions during the test (Janmey et al., 1991), in addition, it signifies interconnectedness of the fibrin fibres (Shah and Janmey, 1997).

Where the ratios of thrombin to fibrinogen were altered, time sweep studies showed that stiffness increased with decreasing thrombin amounts, as expected. The G' for gels was lower than expected <35Pa at 3600s (1 hour), though G' for 0.313UT/mgF gels was double that of 1.25UT/mgF. The gelation profile also showed that gels reached a plateau at between 2300s and 2900s, however, thereafter a second increase in gel stiffness was observed. It was not clear, whether this was due to further networks and branching forming within the gel or drying out of the gel on the machine as very low sample volumes were used (700μL) at 37°C. Following, the time sweeps, in-situ strain sweeps revealed the strain stiffening behavior of the fibrin gels noted by researchers such as Shah and Janmey (1997), which occurred at strains <5%. Such strain stiffening behaviour was not observed in pre-formed gels, gelled in the incubator. This suggested that how the gels are prepared affects response to oscillatory shear and measured G' values.

Strain sweeps of gels of changing thrombin to fibrinogen ratios (Figure 5.15) that were gelled in an incubator prior to analysis, showed a similar response to increasing deformations as with gels of varying volume and thickness (Figure 5.6), with an LVR below 5% strain. It was expected that increasing the stiffness by decreasing thrombin concentrations used would improve the robustness of the gels and the stiffer 0.313UT/mgF had an initial G' twice that of the control 1.25UT/mgF gels.

Presence of cells, incubated over a period of 5 days, did not appear to affect the stiffness of the gels, though it should be noted that the volumes were 6X greater than those used for TE L/T preparation but the seeding density was maintained at 100,000cells/mL. The purpose of seeding the cells, was to determine if they would secrete matrix degrading enzymes in response to the fibrin gel stiffness that would

alter its mechanical strength.

Reducing thrombin to fibrinogen ratio showed no effect on fibrin fibre diameter but increased porosity

Characterisation of the fibrin hydrogels showed that there were no significant differences in fibrin fibre diameters, with increasing stiffness (Section 5.3.4.3). This was surprising as increasing fibrin gel stiffness has been attributed to larger fibre diameters and increased porosity (Shen et al., 1974; Wolberg and Campbell, 2008). Reasons for this, may have been due to processing methods such as ethanol dehydration and critical point drying, used in preparing the gels for SEM. Additionally, *in vivo*, concentrations of thrombin fluctuate, which affect the structure of the fibrin clot (Shen et al., 1974) along with other variables such as pH, ionic strength and calcium concentration (Mosesson, 2005). SEM images of cryo-fractured gels, suggested that at lower thrombin concentrations, 0.313UT/mgF showed larger variation in pore structure with clusters of small pores surrounding some larger ones. The amount of solid fibrin matter present in the gels 2.46 $\pm$ 0.05%, was consistent with estimated fibrin fibre volume fractions determined using equations 5.1 and 5.2 of 2.61%.

It is important to note, studies on purified fibrin are likely to differ from plasma fibrin due to their structural differences (Weisel, 2004). In addition, the effects of plasmin, an enzyme synthesized in the liver which more readily digests fibrin clots, may differ from MMPs and consequently the degradation of fibrin gels produced *in vitro*.

Stiffness enhances cell alignment and proliferation

Morphological evaluation showed that increasing stiffness increased CTF cell proliferation in TE ligament and tendon (Figure 5.19). This is likely due to higher percentage fibrin gel areas with increasing stiffness, resulting in greater scaffold availability. A study by Cox et al. (2004), showed similar results with their formulations 6 and 9 at 0.2UT/mgF and 1.68UT/mgF (closest to UT/mgF shown here) resulting in higher and lower proliferation, respectively. On contraction impeded gels, light microscopy and fluorescent imaging of calcein-AM stained gels showed that the stiffest gels (0.313UT/mgF) had a mixture of rounded and spread cells. This was contrary

to literature, where increasing stiffness has been shown to improve cell attachment and result in a spread morphology of the cells (Discher et al., 2005; Solon et al., 2007; Mason et al., 2012; Wells, 2008). However, cells seeded on the stiffer gels of 0.313UT/mgF stained with calcein-AM appeared to align themselves in a particular direction (Figure 5.18). This was possibly due to higher tensions occurring in the gel due to cell contractile forces, which were likely greater in the stiffer gels than in the control and 2.5UT/mgF groups.

H&E staining of 5 week sinews confirmed that the increase in fibrin gel stiffness to 0.313UT/mgF was not limiting to cell migration, proliferation or construct formation as cells were present throughout the length and breadth of the constructs. In addition, the images also showed that sinews of the stiffest gel also formed using the rolling mechanism previously shown in Chapter 4 and by Paxton et al. (2012) (Appendix D). More individual cells were present within the the 0.313UT/mgF sinews, greater cell densities and alignment occurring mostly in the folds, whereas control sinews had a greater extent of cell alignment throughout the constructs.

Increasing stiffness did not increase sinew collagen content or sinew tensile strength

Although increase in fibrin gel stiffness increased CTF cell proliferation, this did not result in significant increases in collagen content (Figure 5.21). This demonstrated that collagen synthesis is not proportional to cell number or gel stiffness but dependent on other factors, particularly the presence of chemical cues such as AA+P as shown by Paxton et al. (2010a, 2012). As there was not a significant increase in collagen content seen between the sinews, tensile strength (load in mN) also showed no major differences, with statistical significance ($p<0.05$) only occurring between constructs 2.5UT/mgF (softest) and 0.313UT/mgF (stiffest) (Figure 5.22). Sinews of smaller geometry experienced greater stress or load per unit area, therefore as the sinews showed varying widths, comparing the maximum loads withstood by the constructs conferred fairer comparisons.

Factors leading to variability in fibrin gels

Owing to variations observed between fibrin gel mechanical behaviour of incubator gelled and rheometer gelled samples as well as contraction of control constructs

shown in previous chapters, factors that may have led to variation in the fibrin gel mechanical properties were evaluated. Fibrinogen sterilisation methods and freeze-thaw cycles up to 8 cycles showed no significant effect on the varying rates of fibrin gel contraction and construct maximum and minimum widths. However, fibrinogen powder dissolution time did, the optimum being >3 hours. In addition, the number of thrombin freeze thaw cycles affected contraction, as greater numbers of freeze-thaw cycles were shown to lower fibrin gel mechanical strength. These results are shown in Appendix C.

5.5 Conclusion

These results demonstrated that both fibrin gel volume and fibrin gel stiffness could be used to control the rates of fibrin gel contraction and its extent. Fibrin rates of contraction and its extent appeared to be largely dependent on the amount of fibrin or volume fraction of fibrin fibres present within the gel or its stiffness in terms of thrombin to fibrinogen ratios. Unexpectedly, increasing fibrin gel stiffness did not increase construct collagen content or improve tensile strength. This was perhaps testament to the importance of AA in collagen synthesis.

Characterisation into fibrin fibre diameters and porosity confirmed that enhancing fibrin fibre volume fraction reduced extent of contraction as no differences were observed in fibre diameters, their quantity must have increased. This chapter also quantitatively demonstrated that the G' of 0.313UT/mgF gels was twice that of 1.25UT/mgF and 6-fold that of the 2.5UT/mgF at low strains or low angular frequencies. In addition, gels were generally stable at low strains <5% and exhibited frequency independence, which was in line with the literature regarding the mechanical behaviour of biopolymers. Differences between construct contraction at constant UT/mgF, using the standard control gel formulation of 1.25UT/mgF must depend largely on the cells and cell mediated processes.

Chapter 6

Optimisation of ascorbic acid + proline treated constructs

6.1 Introduction

Chapter 4 showed that AA+P resulted in enhanced contraction of the fibrin gel as well as upregulation of MMP-2. Increasing the stiffness of the fibrin gel in Chapter 5 reduced the extent of fibrin gel contraction and constructs were wider although no AA+P supplementation was used.

In this chapter, it was therefore of interest to establish if supplementation of constructs prepared using the stiffest 0.313UT/mgF fibrin gel formulation with AA+P would result in constructs that were wider that also had a similar or higher collagen content compared to supplemented constructs prepared using the standard 1.25UT/mgF fibrin gels. Since, AA+P treatment enhanced MMP-2 expression, treatment with protease inhibitors would likely be necessary. Normally, ϵ-aminohexanoic acid (AH) and aprotinin (AP) are added to thrombin in sDMEM during fibrin gel preparation (see Chapter 3 section 3.2.4). Both these enzyme inhibitors have been shown to reduce fibrinolysis (Krishnan et al., 2003). As a result, this chapter investigated the effect of adding AH and AP directly to growth medium to determine if this reduced fibrin gel contraction rates. Cross-linking of collagen would likely make it more resistant to degradation (Even-Ram and Yamada, 2005). Lysyl oxidases are

responsible for collagen cross-linking and require Zn^{2+} and Cu^{2+} as cofactors, whilst Mn^{2+} is a cofactor necessary for collagen glycosylation and is involved in collagen fibril formation (Leccia, 1996). The effects of Zn^{2+} and Mn^{2+} metal ions on contraction, construct collagen content and tensile strength, in combination with AA+P supplementation, were also evaluated.

6.2 Materials and Methods

6.2.1 Construct preparation

For AP/AH and EDTA MMP inhibition studies as well as supplementation with $ZnSO_4$ and $MnSO_4$, constructs were prepared using the standard fibrin gel formulation of 1.25UT/mgF as described in Chapter 3 section 3.2.

Where the stiffest fibrin gel formulation of 0.313UT/mgF was used, this was prepared by spreading 270μL of enzymes (Thrombin, AP and AH) in sDMEM on a 35mm well and adding 431μL fibrinogen to initiate the polymerisation process. After gelling for 1 hour in an incubator at 37°C, CTF cells were seeded on top of the gels at a density of 100,000 cells/mL.

In all instances, CTF cells were used.

6.2.2 Construct supplementation

6.2.2.1 Combined AH and AP treatment

Fibrin gels were prepared as previously described. Groups were divided as control or AH + AP treated groups. When cells were seeded onto gels, 2μL/mL of each of the 200mM aminohexanoic Acid (AH) and 10mg/mL Aprotinin (AP) solutions were added to the media. Constructs were incubated for three days, after which supplementation with AH and AP was suspended and constructs were fed only with sDMEM, as with the control group.

6.2.2.2 Supplementation with AH, AP or EDTA

Constructs were prepared to be either non-treated controls or supplemented with AH, AP (quantities as above) or 1mM EDTA at 1μL/mL of medium. Supplementation was performed every 2 to 3 days on feeding with DMEM.

6.2.2.3 Supplementation with $ZnSO_4$ and $MnSO_4$

1mM of $ZnSO_4$ (102994, Analar) and $MnSO_4$ (Fluka) solution were prepared in PBS solution. Constructs were prepared as previously described and received either no treatment or were supplemented with either $ZnSO_4$ and AA+P, $MnSO_4$ and AA+P or AA+P only on feeding with sDMEM every 2 to 3 days.

All constructs were imaged and percentage gel areas and widths quantified as previously described in Chapter 3 section 3.3.

6.2.3 Collagen quantification

Procedure was detailed in Chapter 3 section 3.4.

6.2.4 Histology

Samples were prepared for histology as decribed in Chapter 3 section 3.9.

6.2.5 Confocal microscopy

Constructs were prepared as described in Chapter 3 and left overnight ($\geq$ 18 hours) for cells to attach. The following day, the constructs were fixed in 4% formaldehyde in PBS solution for 1 hour. Thereafter, samples were incubated in 0.1% Triton-X for 15 minutes. A 1% BSA in PBS solution was prepared and 5μL phalloidin stain (Alexa Fluor 4888, Life Technologies) was added to 200μL of the PBS solution. The stain was added to the samples and incubated at 37°C for 1.5 hours. After washing

in PBS, the samples were counter-stained in DAPI (D1306, Life Technologies), as decribed in Chapter 3 section 3.7.1. Samples were imaged using a confocal fluorescence microscope (Leica DM 2500).

6.2.6 RT-PCR

Generally, cells were detached from the matrix as detailed in Chapter 3 section 3.6.2 and RT-PCR was performed as detailed in section 3.10. The mRNAs investigated in this chapter are referred to according to the genes they regulate and/or the proteins encoded for by those genes.

6.2.7 Interface strength testing

The tensile testing system set up as shown in Chapter 3 was used. Constructs were cut in half and each half of the TE soft tissue was glued between two pieces of waterproof sandpaper such that only the interface was visible (Figure 6.1). The brushite cement anchor was not removed but gripped in the bottom of the water bath. The TE soft tissue was attached to the top grip. The mechanical tester (Instron 5800) was fitted with a 10N load cell (Instron) and set at an extension rate of 0.4mm/s.

6.3 Results

6.3.1 Use of MMP inhibitors to reduce rates of matrix degradation

AP and AH are normally added to the fibrin reagents prior to gelation as they inhibit the action of MMPs and slow the degradation of the fibrin hydrogel.

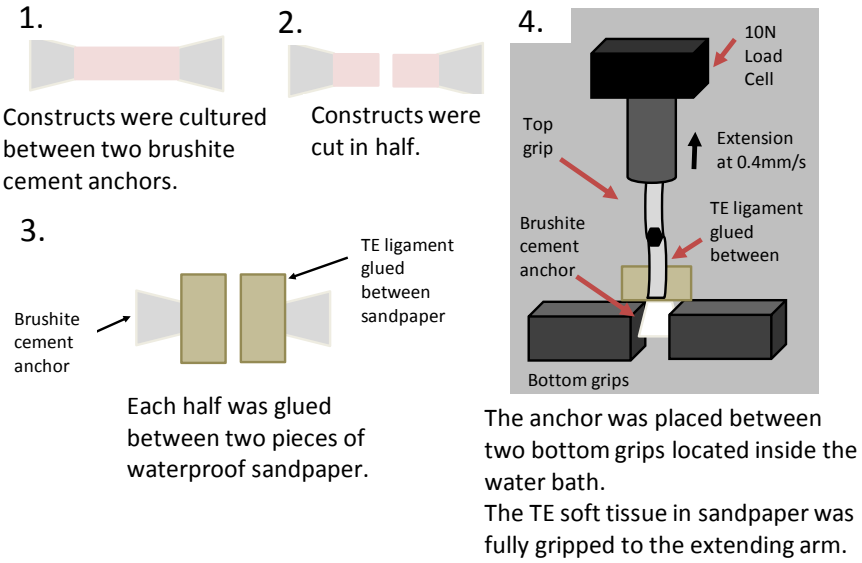

FIGURE 6.1: Method for tensile testing construct interface strength.

6.3.1.1 Supplementation with both AH and AP

To determine if supplementation of the medium with MMP inhibitors retarded initial contraction, AP and AH were added to the medium at construct preparation only (day 0). Addition of AP and AH in combination to sDMEM resulted in an increased rate of contraction of the fibrin gel in the first two days (Figure 6.2). From day 3, when supplementation was withdrawn, control and AP-AH treated constructs appeared almost identical in width and percentage gel areas showed no significant difference from each other.

6.3.1.2 Supplementation with AH, AP or EDTA

In the above section, AH and AP were added to the culture medium on seeding and then withdrawn. It was therefore necessary to determine the effects of prolonged supplementation. The effects of EDTA on delaying fibrin gel contraction was also investigated due to its ability to inhibit MMPs. Measurements were taken from day 7 where the control and AP supplemented percentage fibrin gel areas were greater and differed significantly from AH and EDTA supplemented groups as well as each other (Figure 6.3A).

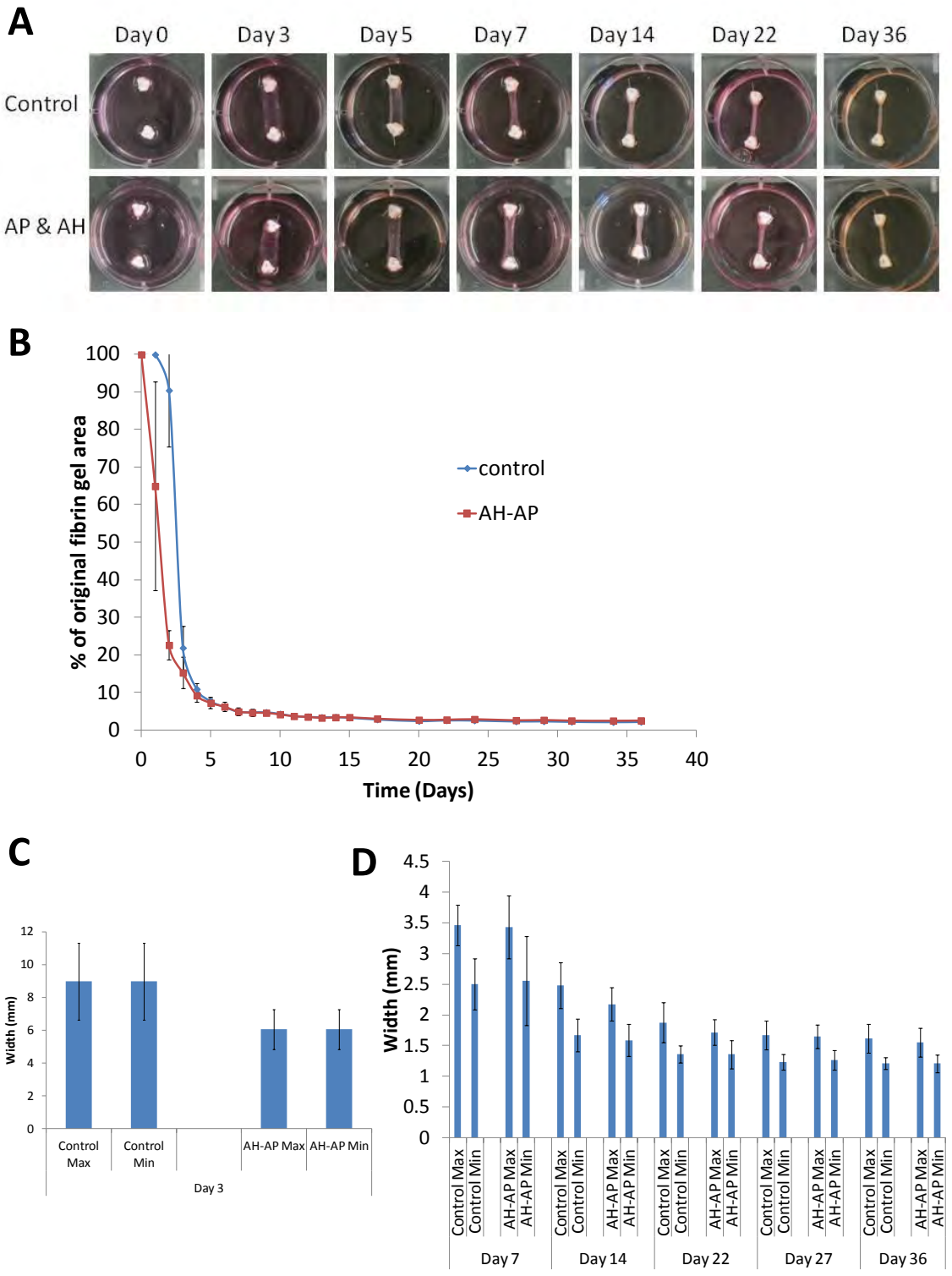

FIGURE 6.2: Contraction inhibition using AP and AH in combination. Addition of AP and AH to growth medium on seeding day did not retard the initial rates of fibrin gel contraction. A)– C) fibrin percentage gel areas and widths of AP and AH treated constructs were smaller that non-treated controls on day 3. Withdrawal of AP-AH treatment resulted in fibrin percentage gel areas and widths matching those of the controls.

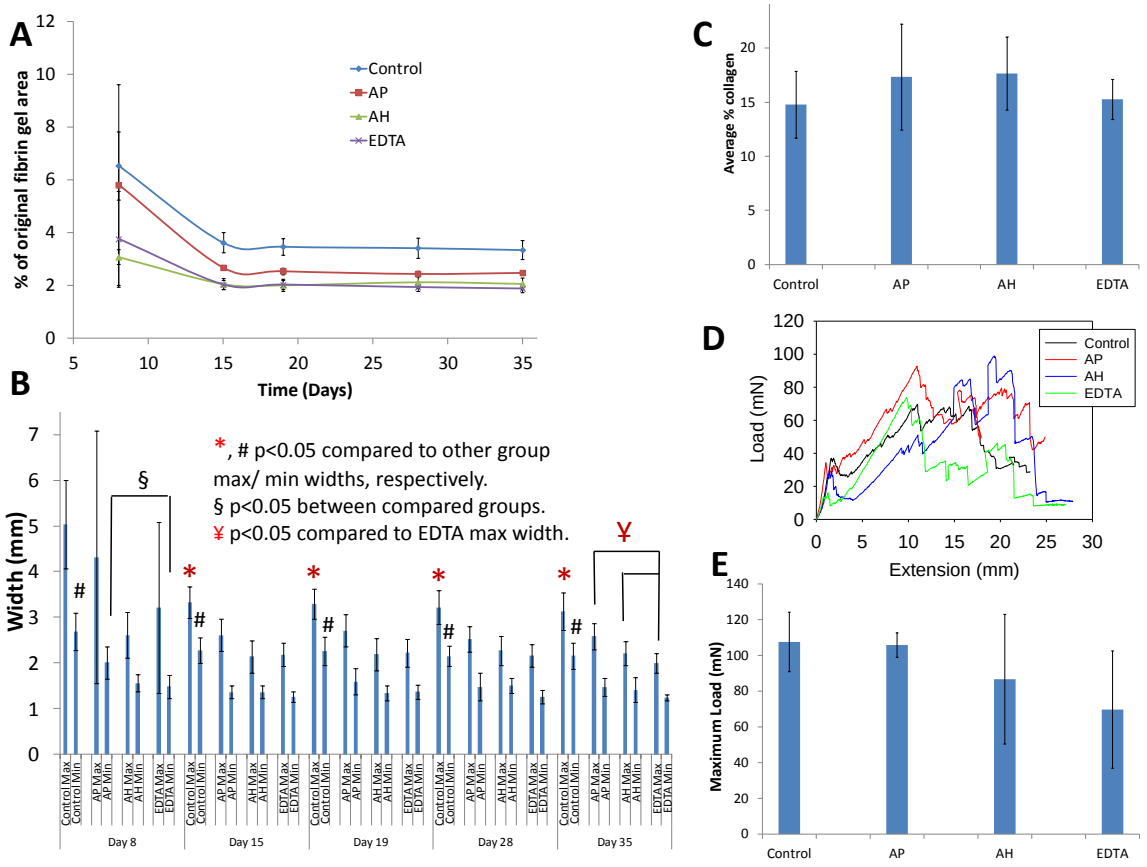

FIGURE 6.3: Effect of MMP inhibitors on contraction and sinew mechanics. A) Supplementation with AP, AH or EDTA resulted in increased rates of contraction from week 2 to week 5, compared to control constructs. B) As a results, widths of control constructs were wider than of treated constructs. C) Collagen content did not differ significantly although average values of AP and AH supplemented constructs were slightly higher. D) & E) Maximum loads were not affected by supplementation.

From the 2^{nd} to 5^{th} week of culture, the control group had significantly greater widths than all other groups (Figure 6.3B). AH and AP group maximum widths were thinner than control and also differed significantly from the EDTA group at week 5. Although the percentage gel areas and widths of the supplemented groups were smaller than of the control group, average collagen content between the groups did not differ greatly (Figure 6.3C). The average values for AP and AH were slightly higher than for the control at 17.34 ± 3.88%, 17.65 ± 3.37% and 14.78 ± 3.10%, respectively, however, differences were not statistically significant. Yet, this was still interesting because, it suggested that inhibiting MMPs did increase construct collagen content. Tensile tests indicated that the constructs resembled each other in mechanical strength (Figure

6.3D and E).

These results and those in section 6.3.1.1 further suggested that fibrin contraction and fibrinolysis were two separate mechanisms that do not necessarily have to occur together. However, considering that MMPs may not have been completely inhibited, if the concentrations of the inhibitors were insufficient, then an alternative hypothesis would be that reducing rates of fibrinolysis resulted in increased rates of contraction as a compensatory means of remodelling the matrix.

6.3.2 Effect of collagen cross-linkers on contraction and collagen synthesis

As previously mentioned, zinc and manganese are cofactors required during collagen synthesis. Zinc and manganese are present in medium specifically designed for chick cells such as MCDB-201 as well as in Ham's F12 (see Appendix C on comparisons of media components used for chick fibroblast cell culture).

To evaluate the effects of Zn^{2+} and Mn^{2+} on fibrin gel contraction and collagen synthesis, they were added in sulfate form to growth medium.

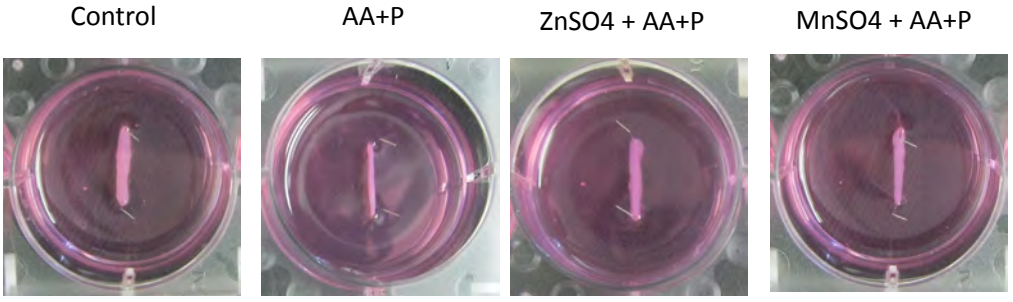

FIGURE 6.4: Images of constructs treated with combinations of ZnSO4, MnSO4 and AA+P on Day 35. Control constructs were widest whilst AA+P only treated constructs were thinnest. Combined treatment of $ZnSO_4$ or $MnSO_4$ with AA+P resulted in constructs whose widths were somewhere in between that of the control and AA+P only constructs.

Figure 6.4 shows that supplementation with $ZnSO_4$ or $MnSO_4$ in combination with AA+P reduced the extent of fibrin contraction and degradation as these constructs were wider than those treated with AA+P alone.

6.3.2.1 Fibrin percentage gel areas and widths

Percentage fibrin gel areas of the control and AA+P only supplemented groups differed significantly ($p<0.05$) from each other as well as from groups treated with $ZnSO_4$ or $MnSO_4$ in combination with AA+P (Figure 6.5A). On day 35, percentage gel areas of the control, AA+P only, $ZnSO_4$ and $MnSO_4$ groups were 2.81 ± 0.12%, 1.38 ± 0.33%, 2.23 ± 0.38% and 2.09 ± 0.20%, respectively. In the first 3 weeks of culture, maximum and minimum widths of the control (non-treated) group were broadest and differed significantly from all groups ($p<0.05$), (Figure 6.5B). Widths of the $ZnSO_4$ and $MnSO_4$ groups were also significantly greater than of constructs treated with only AA+P. Day 35 widths of the control group were 2.86 ± 0.20mm for the maximum and 1.87 ± 0.27mm for the minimum. Of the supplemented groups, $ZnSO_4$ constructs were broadest with max/min widths of 2.43 ± 0.46mm and 1.54 ± 0.28mm, followed by the $MnSO_4$ with widths of 2.23 ± 0.19mm and 1.41 ± 0.15mm. The AA+P constructs were thinnest with max/min widths of 1.32 ± 0.34mm/ 0.95 ± 0.12mm.

6.3.2.2 Construct collagen content and tensile strength

Mechanical testing showed that there were no differences in the maximum loads withstood by the constructs (Figure 6.5C). Although the maximum loads did not vary between the groups, constructs treated with AA+P only had the highest average collagen content of 34.12 ± 13.00% (Figure 6.5D). The group with the second highest average collagen content was $ZnSO_4$ of 29.26 ± 9.84%. Both the AA+P only and $ZnSO_4$ AA+P groups showed statistical significant difference from the control group with 14.44 ± 4.67% ($p=0.000$, for both instances). The $MnSO_4$ AA+P group with 21.79 ± 3.65% collagen only differed from constructs treated with AA+P only ($p=0.001$ and $p=0.079$, $p=0.071$ when Mn group was compared to AA+P only, control and Zn groups, respectively). AA+P only constructs were significantly stiffer than all other groups (Figure 6.5E).

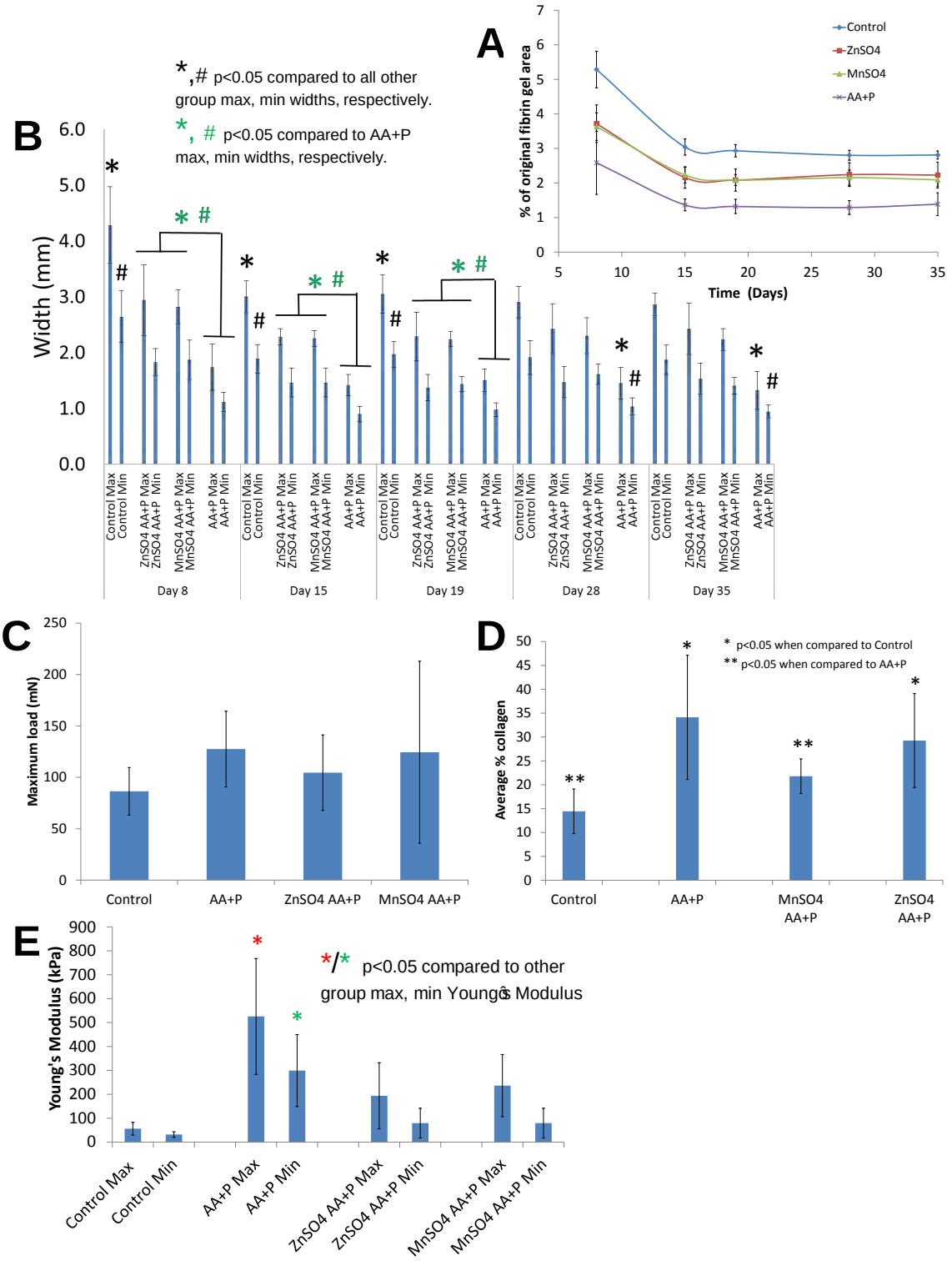

FIGURE 6.5: Effects of $ZnSO_4$ and $MnSO_4$ on fibrin contraction and construct mechanical properties. A) Percentage gel area of the control and AA+P only supplemented groups differed significantly from $ZnSO_4$ and $MnSO_4$ treated constructs and this was similarly reflected in the construct widths (B). Maximum loads were similar for all groups (C) although collagen content showed variation (D). AA+P only treatment resulted in the stiffest constructs (E).

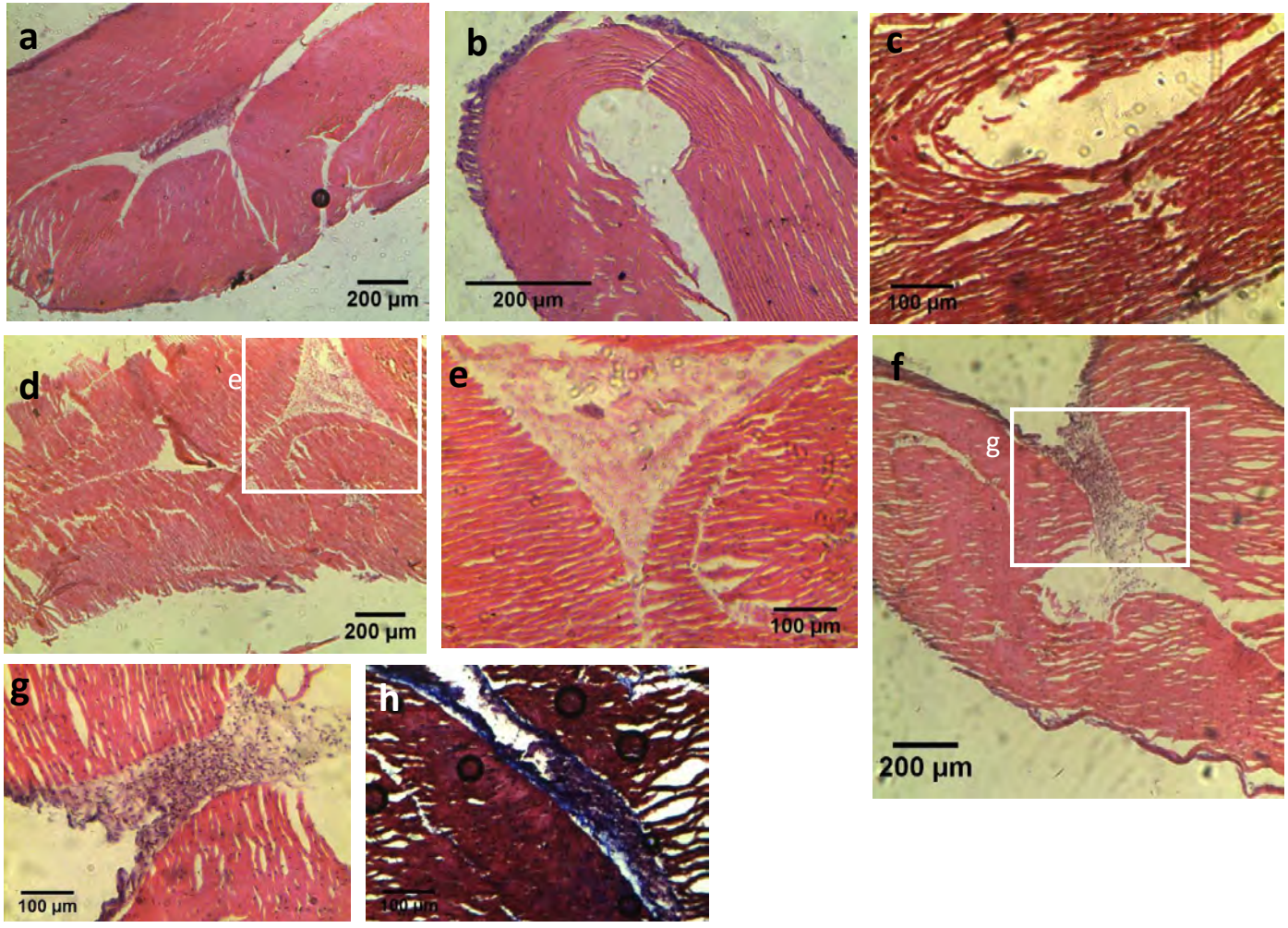

.

FIGURE 6.6: Histological staining of constructs treated with $ZnSO_4$ and $MnSO_4$. a) & b) H&E staining of control constructs showing folds and cell alignment in direction of tension. c) Massons trichrome staining showed fibre alignment but no significant collagen content. H&E staining of $ZnSO_4$ (d & e) and $MnSO_4$ treated constructs showed fibres to be aligned across rather than along construct. f) Masson's Trichrome of $MnSO_4$ showed greater presence of collagen in comparison to the control.

6.3.2.3 Construct morphology

Longitudinal sections of the control $ZnSO_4$ and $MnSO_4$ groups were stained with H&E or Massons Trichrome (Figure 6.6). The control constructs had one main central fold along the length of the construct. Where formation was not disrupted by further folding, cells were seen to align along fibres aligned in the direction of tension/ length of tissue (Figure 6.6a and b). In $ZnSO_4$ or $MnSO_4$ the fibres seemed to extend cross-wise from the centre of the constructs (Figure 6.6e and g). Masson's staining for collagen did not reveal significant collagen presence in control constructs (Figure 6.6) compared to $MnSO_4$ supplemented constructs, which were significantly darker and had large quantities of collagen in the main middle fold (Figure 6.6h).

6.3.3 Effect of Ascorbic Acid + Proline treatment on constructs prepared on stiffest gel formulation

6.3.3.1 Tensile strength and collagen content

In Chapter 5 section 5.3.4 it was shown that fibrin gels of the stiffest formulation 0.313UT/mgF did not contract to the same extent as control gels of 1.25UT/mgF and were significantly broader in width. It was also demonstrated that AA+P supplementation of constructs of a 1.25UT/mgF fibrin gel formulation produced constructs that were very thin but with increased collagen content in comparison to controls receiving no supplementation in Chapter 4. Here, the 0.313UT/mgF gel formulation was supplemented with AA+P to determine if the extent of fibrin contraction after 5 weeks would be reduced in comparison to 1.25UT/mgF AA+P constructs. An additional aim was to optimise construct collagen content and tensile strength.

AA+P supplementation of constructs prepared from 0.313UT/mgF fibrin gels resulted in constructs that were visibly wider than constructs prepared using the standard formulation of 1.25UT/mgF and supplemented with AA+P (Figure 6.7A). The maximum load of 0.313UT/mgF AA+P constructs was double that of all other groups at 218 ± 84mN (Figure 6.7B and C). Control constructs had a maximum load of 113 ± 17mN, AA+P treated maximum load was 110 ± 30mN and untreated

0.313UT/mgF was 88 ± 3mN. AA+P supplementation resulted in constructs that were stiffer, achieving lower strains than non-treated groups (Figure 6.7D).

Average collagen content of the control, AA+P, 0.313UT/mgF and 0.313UT/mgF AA+P constructs were 16.97 ± 2.08%, 25.64 ± 3.25%, 20.99 ± 1.74% and 35.57 ± 10.61%, respectively (Figure 6.7E). The collagen content of 0.313UT/mgF AA+P constructs was the highest and differed significantly from all groups ($p < 0.05$). AA+P treated constructs differed significantly from controls 1.25UT/mgF ($p=0.001$) but not from 0.313UT/mgF ($p=0.207$). The 0.313UT/mgF group only differed significantly from 0.313UT/mgF AA+P ($p=0.000$).

6.3.3.2 Construct morphology

Histological staining of constructs revealed variations in morphology due to supplementation and fibrin gel stiffness. One large central fold between two halves was visible in the H&E stained control sections along with other visible contraction fold in each half (Figure 6.8a and b). The rolling mechanism of AA+P treated constructs was clearly visible in Figure 6.8d and e. Stratified fibres were visible along the periphery and middle section of AA+P treated constructs. Rolling formation was also apparent in 0.313UT/mgF (Figure 6.8g). It was also clear that 0.313UT/mgF AA+P constructs were composed of two main folds (Figure 6.8j).

Masson's Trichrome staining revealed patchiness of pink and red in the controls, with red occurring mostly on the outer edges and inside construct folds (Figure 6.8c and i). AA+P treated constructs were darker in colour than the controls. AA+P constructs of the softer gel formulation showed collagen to be largely concentration around the edges of the construct (Figure 6.8f). 0.313UT/mgF AA+P constructs were darker in colour than the AA+P group. Longer strands of collagen running across the construct were detected (Figure 6.8l).

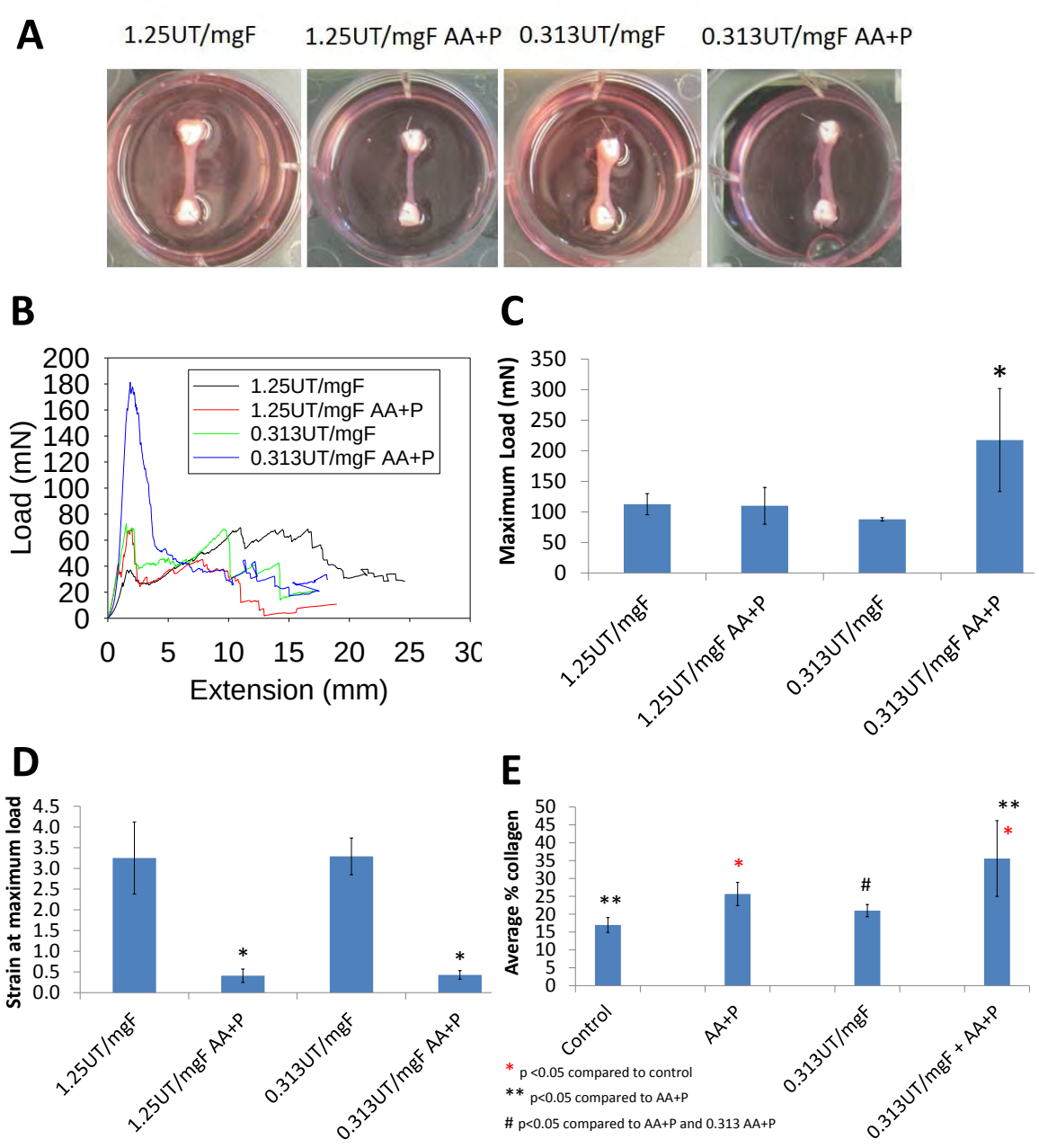

FIGURE 6.7: AA+P supplementation of constructs prepared using the stiffest gel formulation. A) 0.313UT/mgF AA+P constructs appeared significantly broader than AA+P only treatment. B) & C) There was an increase in the maximum loads of the constructs compared to non-treated and AA+P only constructs. D) However, both AA+P treated groups were stiffer than their controls. E) 0.313UT/mgF AA+P constructs had the highest collagen content, $p<0.05$ compared to all other groups.

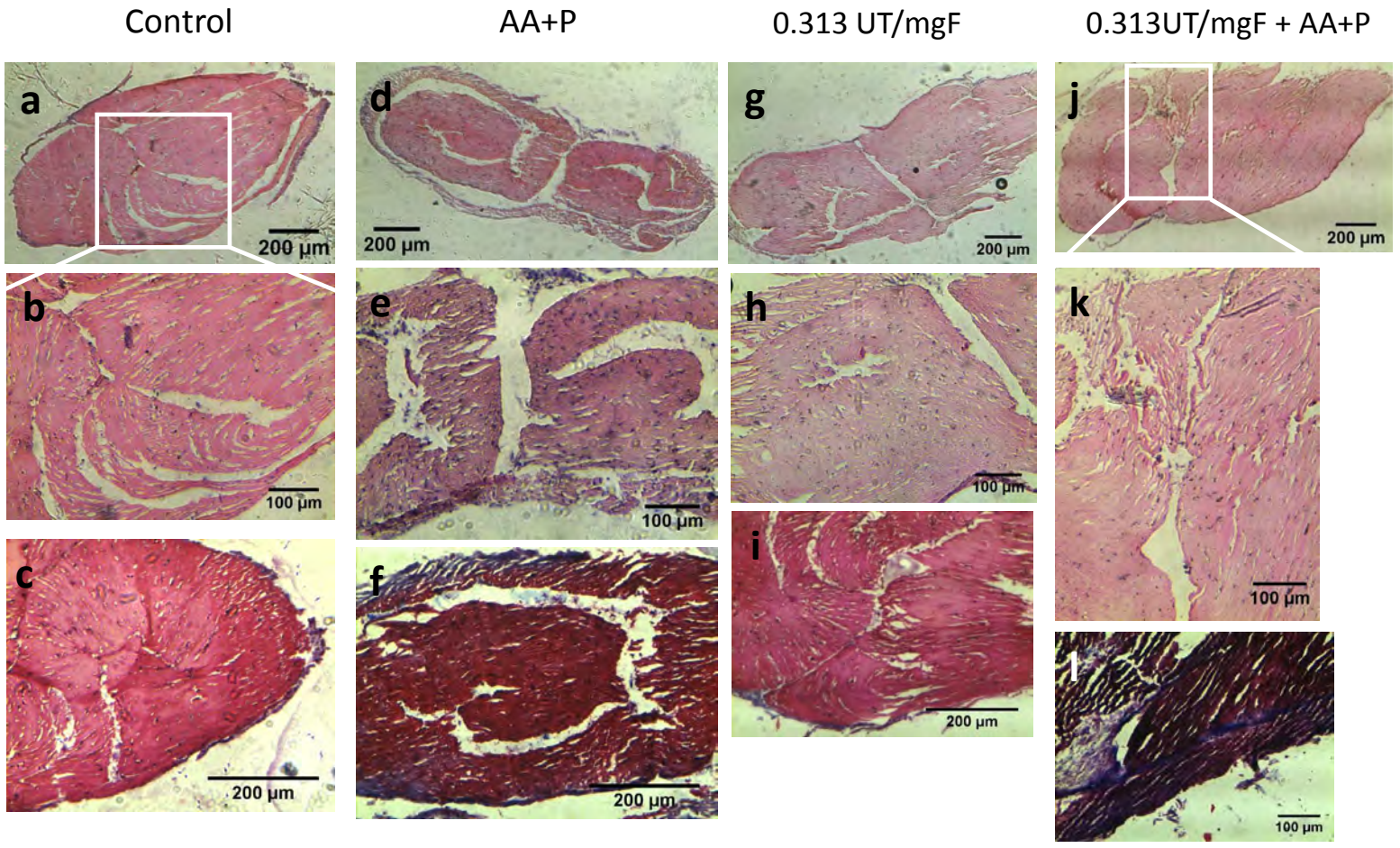

FIGURE 6.8: Histological staining of construct cross-sections prepared using the stiffest gel formulation and treated with AA+P. H&E staining showed presence of cells throughout cross-sections of control (a & b), AA+P (d & e), 0.313UT/mgF control (g & h) and 0.313UT/mgF AA+P (j & k) constructs. Masson's Trichrome stained 0.313UT/mgF AA+P constructs (l) significantly darker than all other groups (c, f & i) and collagen fibres were detected. *Some of the control, AA+P and 0.313UT/mgF images were shown in previous chapters and are repeated here for clarity.*

Masson's Trichrome staining of construct longitudinal sections also showed that cells were aligned along fibres on the length of the constructs (Figure 6.9). Most of the collagen present in control constructs was located on the edges (Figure 6.9a) although small quantities were also present in the mid-section of the constructs (Figure 6.9b). The darker staining in 0.313UT/mgF AA+P constructs was likely due to the higher collagen content (Figures 6.9d and e). Closer magnification of 0.313UT/mgF AA+P constructs revealed extensive collagen "threads" within the constructs (Figure 6.9). These were likely collagen fibrils as their appearance differed from the "specks" or collagen subunits seen in Chapter 4.

6.3.3.3 Confocal microscopy

Actin staining for stress fibres showed that cells in the 0.313UT/mgF AA+P group expressed greater amount of actin than the control and 0.313UT/mgF groups (Figures 6.10).

6.3.3.4 RT-PCR detection of transcripted mRNAs

The expression of 9 target mRNAs was evaluated using RT-PCR (Figure 6.11). At weeks 2 and 3 no target mRNAs were detected and these results are for constructs at week 4. Comparisons between the AA+P and control groups were previously shown Chapter 4 section 4.3.8 and are repeated here for clarity. The results indicated that COL1A1 expression in 0.313UT/mgF AA+P constructs was 32% higher than in standard AA+P constructs and ACTA expression was 38% higher, which supported the results in Figure 6.7E and Figure 6.10. MMP-2 expression was highest in AA+P treated constructs and $MnSO_4$ AA+P constructs also expressed higher quantities of MMP-2 than the control group. Constructs were AA+P was included also expressed higher amounts of RhoA, when compared with both unsupplemented control groups. MMP-3 and MMP-9 were highest in 0.313UT/mgF AA+P constructs, although expression of both their mRNAs fell below GAPDH. MMP-1 expression was highest in the control and $MnSO_4$ AA+P group. Tenascin-C expression was highest in the AA+P group and lowest in the control group.

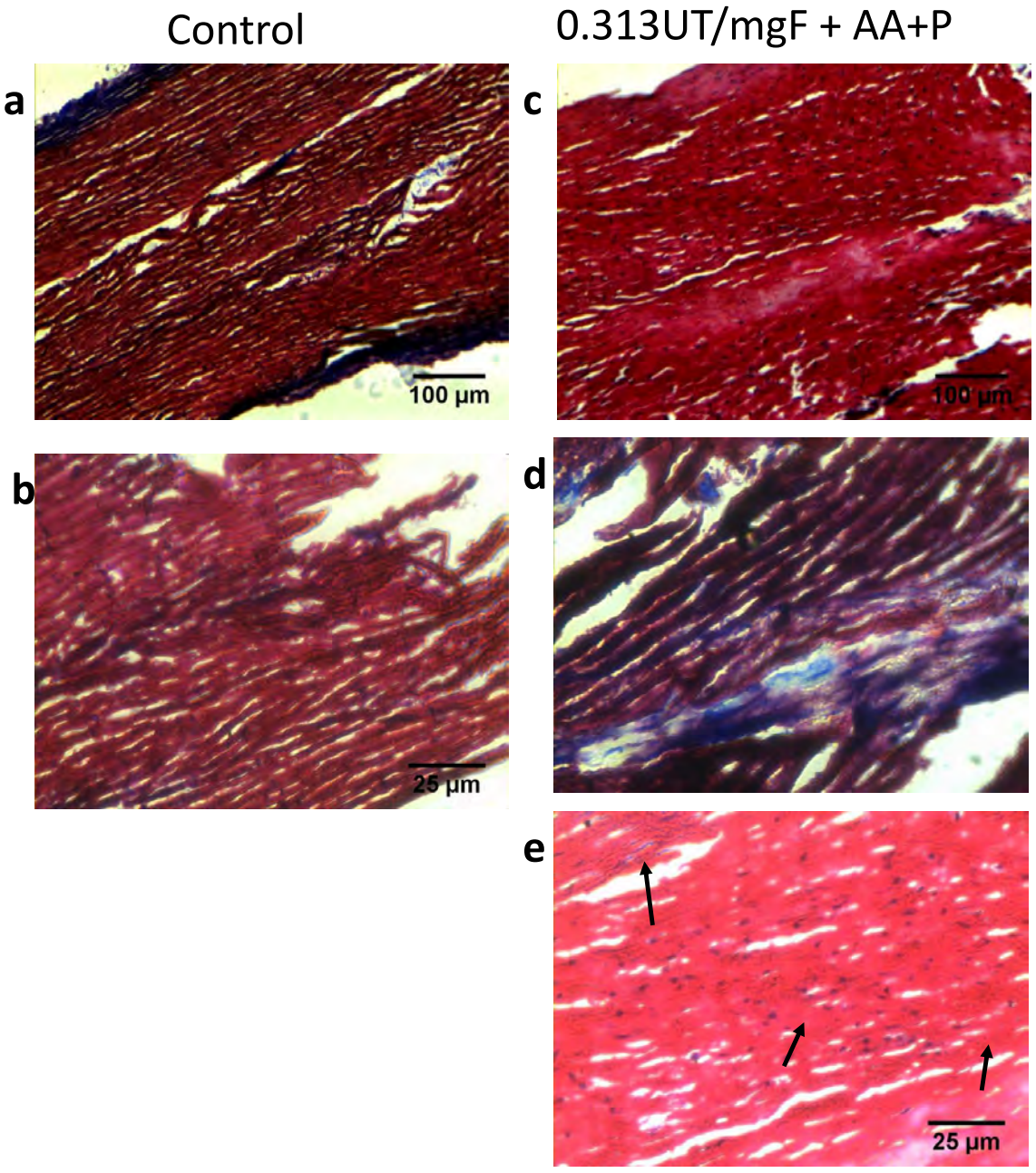

FIGURE 6.9: Histological staining of construct long-sections prepared using the stiffest gel formulation and treated with AA+P. a) Collagen was mainly located on the edges of control constructs although a few collagen strands were present towards the middle (b). 0.313UT/mgF AA+P had significant amounts of collagen (c & d) and small strands within the sinew (d) proximal to cells.

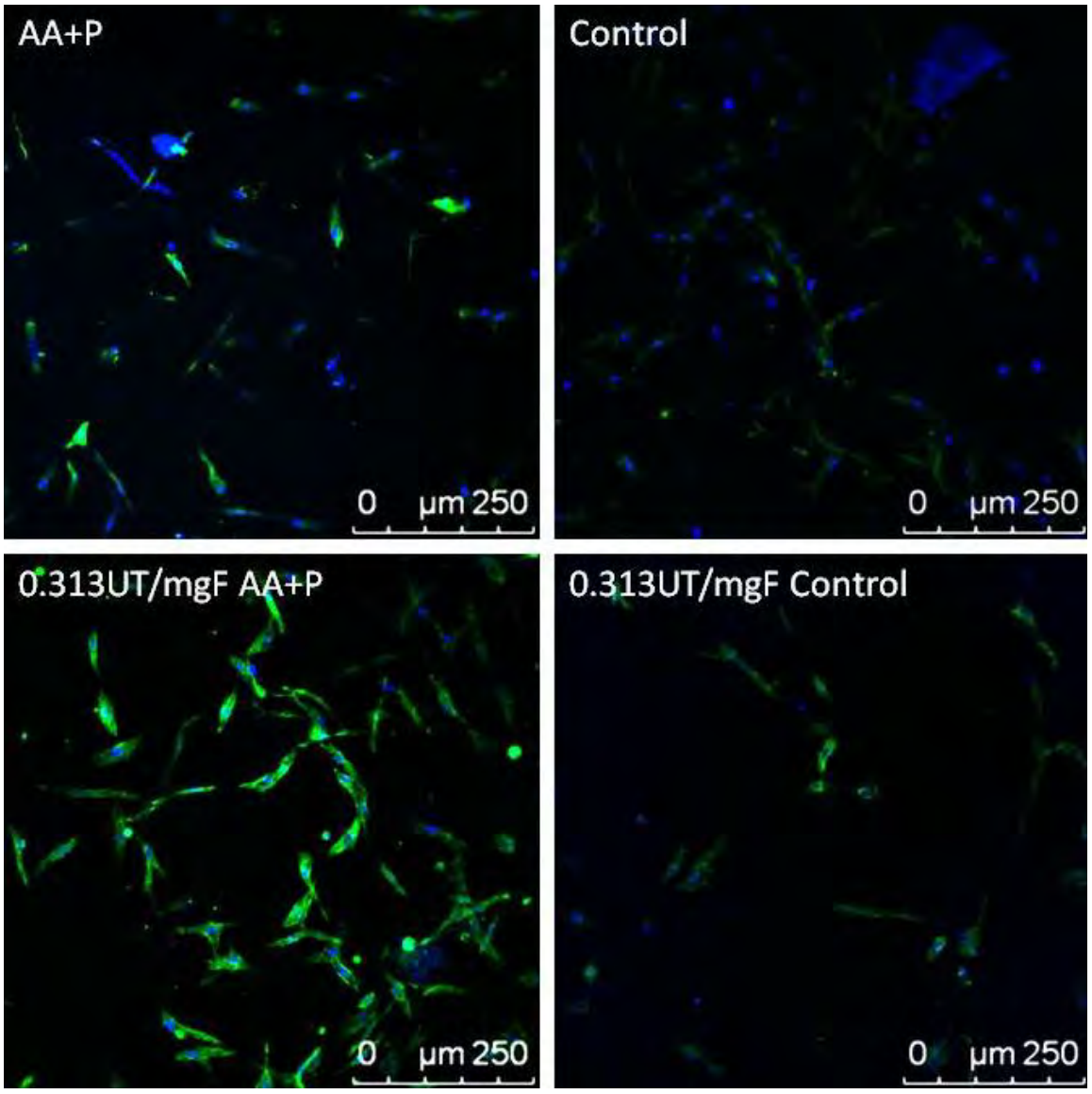

FIGURE 6.10: Actin staining of constructs treated with AA+P. A greater concentration of actin filaments (green) were seen in cells on the 0.313UT/mgF gels supplemented with AA+P.

6.3.3.5 Interface mechanical strength

The strength of the interface was tested for control, AA+P and 0.313UT/mgF AA+P treated groups (Figure 6.13). On average, complete detachment of the TE soft tissue from the brushite anchor required about 15s. Figure 6.13A suggests that control constructs had the weakest interface as they detached first. Surprisingly, the loads required to initiate interface detachment were significantly lower for the control and

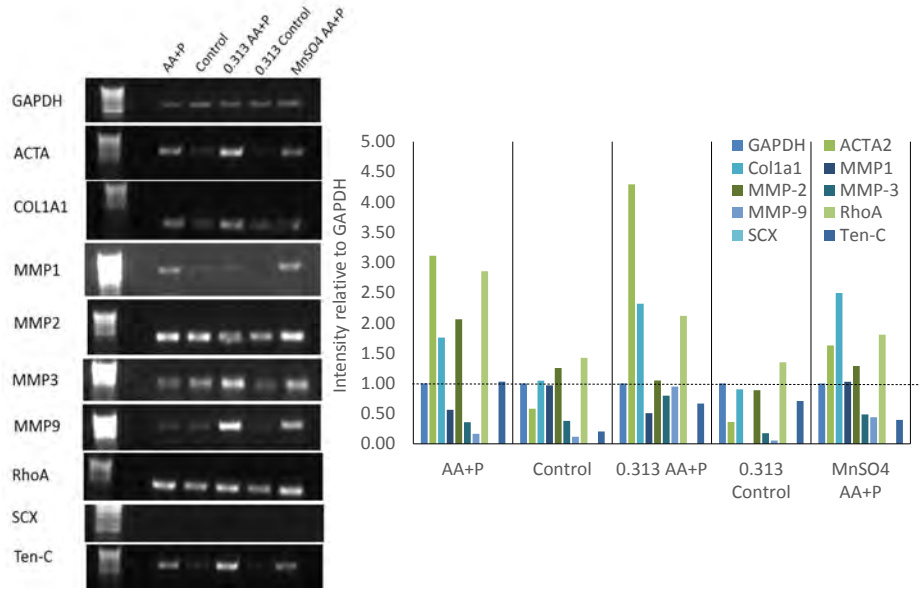

FIGURE 6.11: RT-PCR results showing mRNA expressions of constructs treated with AA+P. Compared to AA+P only constructs, the 0.313UT/mgF AA+P group expressed higher levels of ACTA2, COL1A1, MMP-3 and MMP-9. However, MMP-2, RhoA and Ten-C were downregulated. Interestingly, treatment with $MnSO_4$ also enhanced COL1A1 expression, higher than AA+P only and 0.313UT/mgF AA+P groups.

0.313UT/mgF AA+P groups at 0.08mN and 0.052mN, respectively, than for the AA+P group (5.4mN). However, after 10s, control and AA+P interfaces had completely detached whereas the 0.313UT/mgF AA+P required longer to reach ultimate failure. These preliminary results suggest that interface attachment improved with increasing gel stiffness and AA+P treatment (Figure 6.13B and C) although differences were not statistically significant.

6.4 Discussion

At concentrations used, AH, AP and EDTA increased rate of fibrin gel contraction and moderately enhanced average collagen content

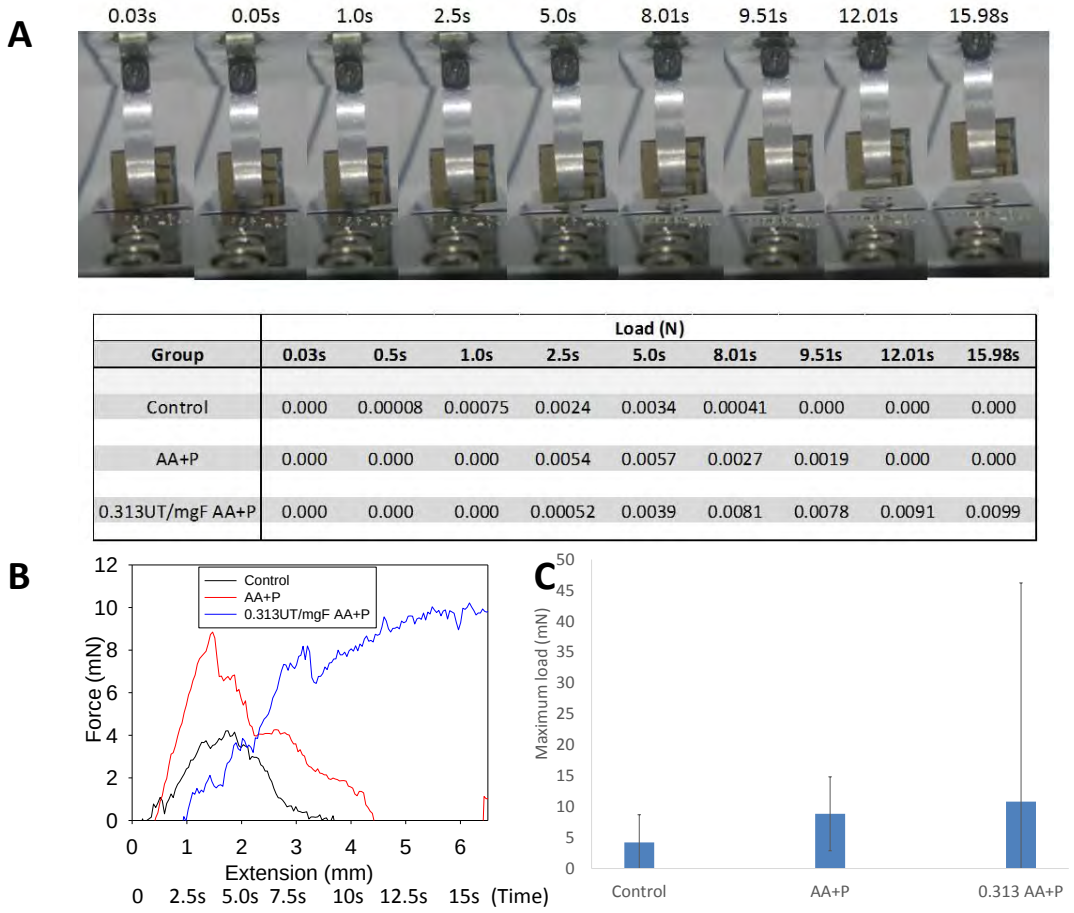

	Load (N)								
Group	0.03s	0.5s	1.0s	2.5s	5.0s	8.01s	9.51s	12.01s	15.98s
Control	0.000	0.00008	0.00075	0.0024	0.0034	0.00041	0.000	0.000	0.000
AA+P	0.000	0.000	0.000	0.0054	0.0057	0.0027	0.0019	0.000	0.000
0.313UT/mgF AA+P	0.000	0.000	0.000	0.00052	0.0039	0.0081	0.0078	0.0091	0.0099

FIGURE 6.12: Interface tensile strength of AA+P treated constructs. A) Extension to failure loads of control and AA+P treated constructs over 15 seconds. B) Load-extension curves of data shown in (A). The results indicated that the interface of AA+P constructs remained attached for longer than controls. In addition, 0.313UT/mgF AA+P construct interfaces also attached for longer than those of the AA+P only group. C) Maximum loads of 0.313UT/mgF AA+P construct differed considerably from each other. ($n \geq 4$).

Aminohexanoic acid (ϵ-aminocaproic acid) inhibits plasmin degradation of fibrin and its addition to growth medium has been shown to decrease the rate of fibrin degradation in a concentration dependent manner (Grassl et al., 2002). Results by Grassl et al. (2002) went further to show that at high concentrations of aminohexanoic acid construct collagen content decreased. Aprotinin is considered an inhibitor of a wide range of MMPs (Kupcsik et al., 2008). In section 6.3.1, combined supplementation of Aminohexanoic acid (AH) and Aprotinin (AP) increased the rate of fibrin contraction and constructs were smaller in width than the controls, though results were not statistically significant. Individual supplementation with AH, AP as well as EDTA,

which is an MMP inhibitor (Ashcroft et al., 1997), expressed similar results, though average collagen content with AH and AP treatment was slightly higher (Figure 6.3). Treatment with AA+P would still be required to enhance construct collagen content. These findings suggest that MMP inhibition could be further optimised either through determining the optimum concentrations for AH and/or AP supplementing regimes or exploration of alternative MMP inhibitors such galardin (GM6001), which has shown efficacy in preventing fibrin degradation (Ahmed et al., 2007).

Moreover, this data presents fascinating parallels when compared to findings in Chapter 4 where inhibiting collagen synthesis did not stop but actually slightly increased the initial rates of contraction. The results shown here and in Chapter 4 suggested that contraction was a separate phenomenon that does not have to occur with collagen matrix deposition or fibrinolysis although these phenomena can occur simultaneously. Why increased initial rates of contraction are observed is unclear but may have been due to cells using contraction to compensate for impeded proteolysis. Martin-Martin et al. (2011) studied the effects of GM6001 on contraction of collagen matrices of varying stiffness using fibroblasts from different parts of the human body as well as mouse fibroblasts. They found that fibroblasts used two different modes to remodel the collagen matrices, namely, contraction and proteolysis and that this depended on intrinsic cell properties. In addition, high concentrations of GM6001 also showed varying efficacy in inhibiting contraction and could not overcome intrinsic cell contractile properties. Interestingly, their results also showed that the presence or absence of serum in growth medium affected rates of contraction (see Appendix C).

To further support the hypothesis that contraction and MMP degradation can act independently of one another, Phillips et al. (2003) demonstrated that inhibition of MMPs with garlardin did not alter cell generated contraction forces, when compared to the uninhibited group and similar to results by Martin-Martin et al. (2011) extent of inhibition by galardin varied by cell type.

These findings support results in thesis regarding the influence of matrix stiffness, cell type and growth medium on contraction and emphasize the necessity in determining factors that impact cell contraction and/or MMP mediated remodelling on formation

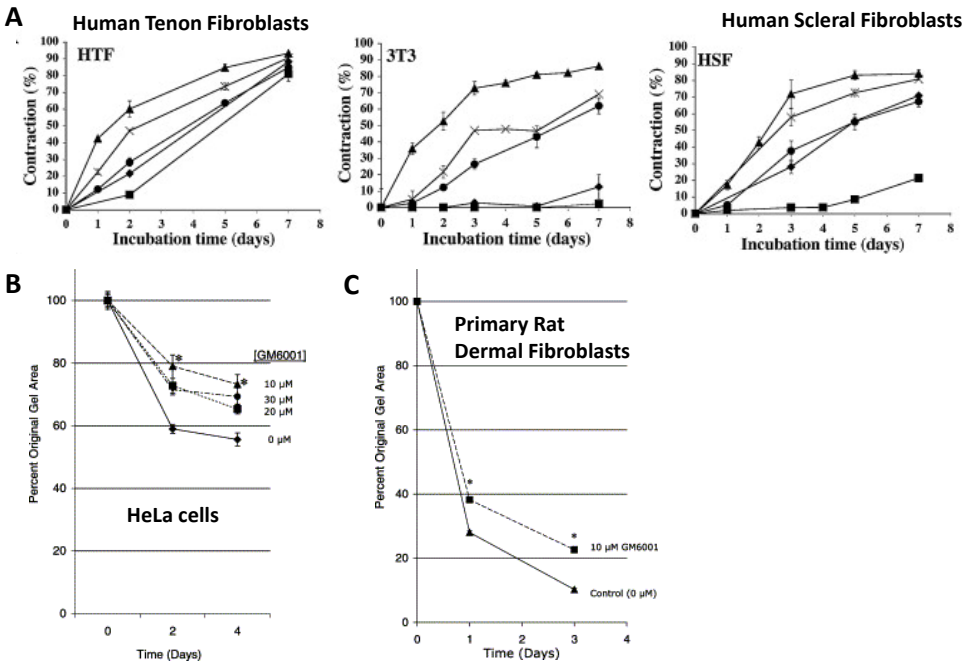

FIGURE 6.13: Effect of 100μM galardin on inhibiting contraction in matrices of differing stiffness or employing different cell types. A) Extent of contraction differed depending on the stiffness of the collagen matrix (triangle = softest, squares=stiffest) (Martin-Martin et al., 2011). Similarly, Phillips et al. (2003) showed that galardin significantly reduced extent of contraction of collagen matrix by B) HeLa cells, though increasing concentrations reduced extent of inhibition whereas C) rat dermal fibroblasts showed higher rates of contraction than HeLa cells. In all cases, inhibtion of MMPs by galardin did not completely stop contraction. *Images used with permission.*

of engineered (L/T) tissue.

Supplementation with $ZnSO_4$ and $MnSO_4$ in combination with AA+P decreased extent of fibrin gel contraction and $ZnSO_4$ maintained collagen content similar to AA+P only supplementation.

Supplementation with $ZnSO_4$ and $MnSO_4$ along with AA+P decreased the rate of fibrin contraction and construct average collagen content in comparison to AA+P only treated constructs (Figure 6.5). Histological images confirmed a higher collagen content in Zn and Mn supplemented constructs compared with non-treated sinews (Figure 6.6). The catalytic active site of MMPs contains Zn^{2+} (Lansdown et al., 2007) and surprisingly, this did not increase the rate of fibrin degradation and no differences

in collagen content were observed in comparison to AA+P only constructs (Figure 6.5D), suggesting that there were other cell processes dependent on the zinc supplementation. Mn supplementation however, resulted in a significantly lower collagen content when compared to AA+P only constructs. This may be due to additional requirements of manganese by mitochondria and antioxidant enzymes that control cell superoxide free radical levels (Craven et al., 2001) and may explain why contraction and degradation of the fibrin gel was decreased. Nevertheless, RT-PCR results indicated that $MnSO_4$ treatment resulted in the highest expression of collagen of the groups investigated, however, the collagen amino acid may not have been in a form detectable by the test (Figure 6.11).

Supplementation of stiff gels (0.313UT/mgF) with AA+P significantly increased construct widths and collagen content compared to AA+P only treatment

In Chapter 5 section 5.3.4, it was shown that fibrin gels of the formulation 0.313UT/mgF were significantly stiffer and wider than the control fibrin gels of 1.25UT/mgF, however, no statistically significant differences were observed in the average collagen content or maximum loads withstood (Figures 5.21 and 5.22). As 0.313UT/mgF constructs were wider than 1.25UT/mgF control constructs, it was investigated whether supplementation with AA+P would lead to constructs that were broader and with higher collagen content than AA+P constructs prepared using the standard gel formulation 1.25UT/mgF.

The stiffest gels had a similar yet magnified response to AA+P treatment. 0.313UT/mgF AA+P constructs appeared significantly broader than AA+P constructs (Figure 6.7). The average collagen content of the 0.313UT/mgF AA+P group was about 10% greater than for AA+P and the maximum loads withstood by 0.313UT/mgF AA+P was 2-fold that of AA+P constructs (Figure 6.7C and E). Masson's Trichrome staining indicated a significantly darker extent of blue colouring in the 0.313UT/mgF AA+P group (Figure 6.8f and l). At higher magnification, threads or thin strands of collagen were detected throughout the 0.313UT/mgF AA+P constructs (Figure 6.9e). Because the increase in collagen content and maximum loads withstood by the 0.313UT/mgF AA+P group only occurred when both the stiffness was increased and constructs were supplemented with AA+P, **the results suggest that construct**

collagen content can be optimised by altering the scaffold matrix stiffness whilst administering the necessary chemical cues.

Supplementation of 0.313UT/mgF constructs with AA+P also altered the expression of targeted mRNAs when compared to 1.25UT/mgF AA+P constructs. 0.313UT/mgF AA+P expressed greater amounts of actin, as shown by confocal fluorescence images in Figure 6.10C. This was confirmed by RT-PCR results, which indicated that ACTA2 expression was over 30% higher in 0.313UT/mgF AA+P constructs than in the AA+P group (Figure 6.11). Alpha smooth muscle actin is a marker for the myofibroblast cell type; fibroblast differentiation to myofibroblast requires tension, which activates RhoA, which in-turn is involved in the organization of cytoskeletal actin and its contraction (Hinz and Gabbiani, 2003b). However, RhoA expression in the 0.313UT/mgF AA+P was 35% lower than in AA+P constructs. Perhaps this was an experimental anomaly. Alternatively, the results suggest lower matrix tension in 0.313UT/mgF AA+P constructs. Possibly, reduced extent of contraction caused lower tension in the matrix and as a result Tenascin-C expression, a marker for tendons was 31% lower in 0.313UT/mgF AA+P than AA+P constructs. However, Tenascin-C expression was still 72% greater in 0.313UT/mgF AA+P than in controls.

MMP-1 is known to degrade collagen type I and its expression was higher in control constructs than in both AA+P supplemented groups. On the other hand, MMP-2 is implicated in collagen I matrix degradation and indirectly to fibrin through MT1-MMP, which degrades fibrin and activates MMP-2. Unfortunately, MT1-MMP was not evaluated at this stage, but due to its importance in connective tissue remodelling (Page-McCaw et al., 2007), its expression will need to be determined in future work. MMP-2 in the stiffer gel constructs was significantly downregulated and MMPs 3 and 9 were upregulated in comparison to AA+P constructs. This is likely why 0.313UT/mgF AA+P exhibited reduced extents of fibrin contraction and higher collagen content, when compared to AA+P, where MMP-2 was upregulated. MMP2, MT1-MMP and Rho have been shown to depend on each other as MMP-2 is also activated/deactivate by RhoGTPases (Zhuge and Xu, 2001). Using cardiac fibroblasts (Schram et al., 2011) demonstrated that inhibition of Rho attenuated MMP-2 expression.

MMP-2 and MMP-9 are also involved in activating TGF-β (Egeblad and Werb, 2002), which is a growth factor involved in wound healing and collagen type I production by fibroblasts (Clark et al., 1995) as well as other ECM components (Roberts et al., 1992). This suggests that in the stiffer gels supplemented with AA+P, TGF-beta may have been upregulated along with the mRNA expression of other ECM proteins. A study by Kim et al. (2004) showed that TGF-β stimulated the expression of MMP-3 and MMP-9 in corneal epithelial cells, in a TGF-β concentration dependent manner, however, TGF-β showed no such effect on MMP-2 expression.

0.313UT/mgF AA+P treatment may increase cement-tissue interface strength

The interface strength of the constructs was tested and no statistical differences were seen in the maximum loads withstood (Figure 6.13). However, 0.313UT/mgF AA+P constructs remained attached for longer than AA+P, which were also attached longer than control constructs. The results suggest that supplementation of 0.313UT/mgF constructs with AA+P may improve interface duration of attachment. Duration of attachment is equally as important as strength because time dependent behaviour is a key component of viscoelastic materials such as ligament and tendons (Provenzano et al., 2001).

6.5 Conclusion

AA+P enhanced contractility by increasing actin expression due to increased tension in the matrix, in both AA+P and 0.313UT/mgF AA+P groups. Increasing gel stiffness in combination with AA+P supplementation significantly raised construct collagen content, whilst retaining width. RT-PCR investigation also suggested that MMP-2 and possibly MT1-MMP were responsible for matrix degradation of constructs prepared using the softer standard gel formulation 1.25UT/mgF and AA+P treatment as MMP-2 was downregulated in stiffer gel constructs. Possibly, TGF-beta expression may have been upregulated in 0.313UT/mgF AA+P, which will need to be investigated further. The brushite cement anchor to TE L/T interface strength was tested and although the results showed no statistical significance, the findings suggest

that 0.313UT/mgF AA+P improved attachment in comparison to AA+P and control constructs. Attempts to use MMP inhibitors to reduce the extent of contraction were unsuccessful at the concentrations of AP, AH and EDTA used. However, the results suggested that collagen degradation may be reduced. It would be interesting to investigate the use of MMP inhibitors along with AA+P treatment on stiffer fibrin gel constructs to determine if this would lead to yet further increases in collagen content.

Chapter 7

Influence of cell properties on sinew formation

7.1 Introduction

Ascorbic acid and proline supplementation was shown to significantly enhance construct collagen content (Chapters 4, 5 and 6) though it led to greater reductions in the fibrin gel areas. The expression of several targeted mRNAs were upregulated including matrix degrading MMPs and mRNAs associated with stress fibre formation. The internal morphology of control and AA+P supplemented constructs were shown to be dissimilar. However, direct treatment of acellular fibrin gels with AA+P did not affect gel mechanical strength. As a result, cell properties and activities had a greater effect on construct formation, especially with AA+P treatment. Altering fibrin volume and thrombin to fibrinogen ratios used to prepare fibrin gels, affected rate of fibrin gel contraction and resultant sinew maximum and minimum widths (Chapter 5). However, sinew collagen content was not enhanced and no differences in tensile strengths were observed unless supplemented with AA+P (Chapter 6). Since there were variations in the initial contraction rates of several non-supplemented controls groups presented in this thesis, other cell factors such as variations in cell passage number or cell seeding density may have been responsible. These parameters are important for TE, as reflected by the copious literature investigating their effects on a number of conditions.

Cell seeding density has been shown to affect scaffold depletion as well as cell viability and formation of engineered tissue (Dvir-Ginzberg et al., 2003; Holy et al., 2000; Mauck et al., 2002; Wang et al., 2008). Viability of cells is greatly influenced by molecular diffusion of nutrients and waste through the constructs posing limitations on construct dimensions and cell seeding densities. For oxygen sensitive cells, diffusion of oxygen dissolved in medium has been shown to be limited to construct outer layers approximately only 100μm thick (Radisic et al., 2003). Constructs 1 – 5mm thick seeded with cells at high densities showed a decrease in cell viability within the initial 4.5 hours by 55%, which was overcome by direct perfusion, reducing loss of viability to only 20%, (Radisic et al., 2003). Mature tendons and ligaments are composed of few cells and are largely avascular, with oxygen requirements 7.5 times less than for skeletal muscles (Sharma and Maffulli, 2006). Nutrition is supplied through diffusion of the synovial fluid rather than blood vessel perfusion (Fenwick et al., 2002). In contrast, developing ligaments have high cell densities, which originate at the enthesis (Tozer and Duprez, 2005). Three dimensional culture of tenocytes at high density is attractive as continuous two dimensional culture results in a loss of tenocyte characteristics and decreased collagen I production with increasing passages (Schulze-Tanzil et al., 2004).

Age has been shown to determine L/T morphology as older joints become broader and stiffer due to increases in collagen content and anatomical changes within the joints (Carlstedt, 1987; Woo et al., 1986; Feland et al., 2001). Response of human embryonic fibroblasts to chemical cues of conditioned medium was shown to decline steadily after passage 25 (Albini et al., 1988). Adult cells taken from donors between the ages of 10 and 60 years became less responsive to chemoattractants much earlier, from passage 15 (Albini et al., 1988). Almarza et al. (2008) evaluated the effect of fibroblast passage number sourced from Long Evans rats on collagen gene expression and determined that with increasing passage numbers, cells took longer to reach confluency, cell numbers decreased and from passage 2 collagen expression also decreased, with additional variation in collagen expression observed between MCL, ACL and patellar tendon cell sources.

Ge et al. (2005) compared the suitability of rabbit MSCs, ACL and MCL fibroblasts for ACL tissue engineering and found that due to inherent differences between the cells types, concluding that MSCs were better suited for ACL tissue engineering than

ACL or MCL fibroblasts. MSCs proliferated better *in vitro*, survived longer *in vivo* and excreted higher quantities of collagen (Ge et al., 2005). According to Almarza et al. (2008) MCL fibroblast proliferate better, migrate faster and produce more ECM than ACL fibroblasts. However, Ge et al. (2005) found that MCL fibroblasts secreted less ECM than ACL fibroblasts and in contrast to Almarza et al. (2008), MCL and ACL fibroblasts began to show reduced proliferation, exhibiting morphological changes such as increased size and irregular shape. These results emphasise the differences in cell type behaviour sources from different tissue within the same organism as well as additional variances stemming from organism to organism.

This chapter investigated the influence of cell properties such as passage number and minor fluctuations in cell seeding density that may have occurred were not previously investigated as contributing factors on rates and extent of fibrin gel contraction. It was also of interest to determine whether the TE L/T model was applicable for use with other cell types.

7.2 Materials and Methods

7.2.1 Construct preparation

Construct fibrin gels were prepared using the standard fibrin gel formulation of 1.25UT/mgF as described in Chapter 3 section 3.2.4.

7.2.1.1 Varying passage number

CTF cells were thawed at various intervals such that cells at passages 2, 3, 4 and 5 were simultaneously available to seed on fibrin hydrogels.

7.2.1.2 Cell seeding density

The cell seeding density of 100,000 cells/mL was halved and doubled so that experimental groups had cell seeding densities of 50,000 cells/mL (50K), 100,000 cells/mL (100K) and 200,000 cells/mL (200K).

7.2.1.3 Cell type for construct formation

Fibrin gels were seeded with CTFs (chick), 3T3s (mouse) or PFBs (rat tail tendon) to determine differences in construct formation due to cell type.

7.2.2 Supplementation

7.2.2.1 Determining effect of ascorbic acid + proline on constructs seeded with rat tail tendon fibroblasts

Constructs seeded with PFBs were supplemented with AA, P or AA+P or received no treatment (NT) (Control group). AA was supplemented at a concentration of 250μM and P at 50μM every two to three days on feeding with sDMEM.

7.3 Results

7.3.1 Effect of passage number on rates and extent of fibrin gel contraction

Chick tendon fibroblast cells between Passages 2 to 5 were used. Contraction due to passage numbers showed variations in extent of contraction by day 1. However, percentage gel areas were not statistically significant until day 3, where percentage gel areas increased with increasing passage number (Figure 7.1).

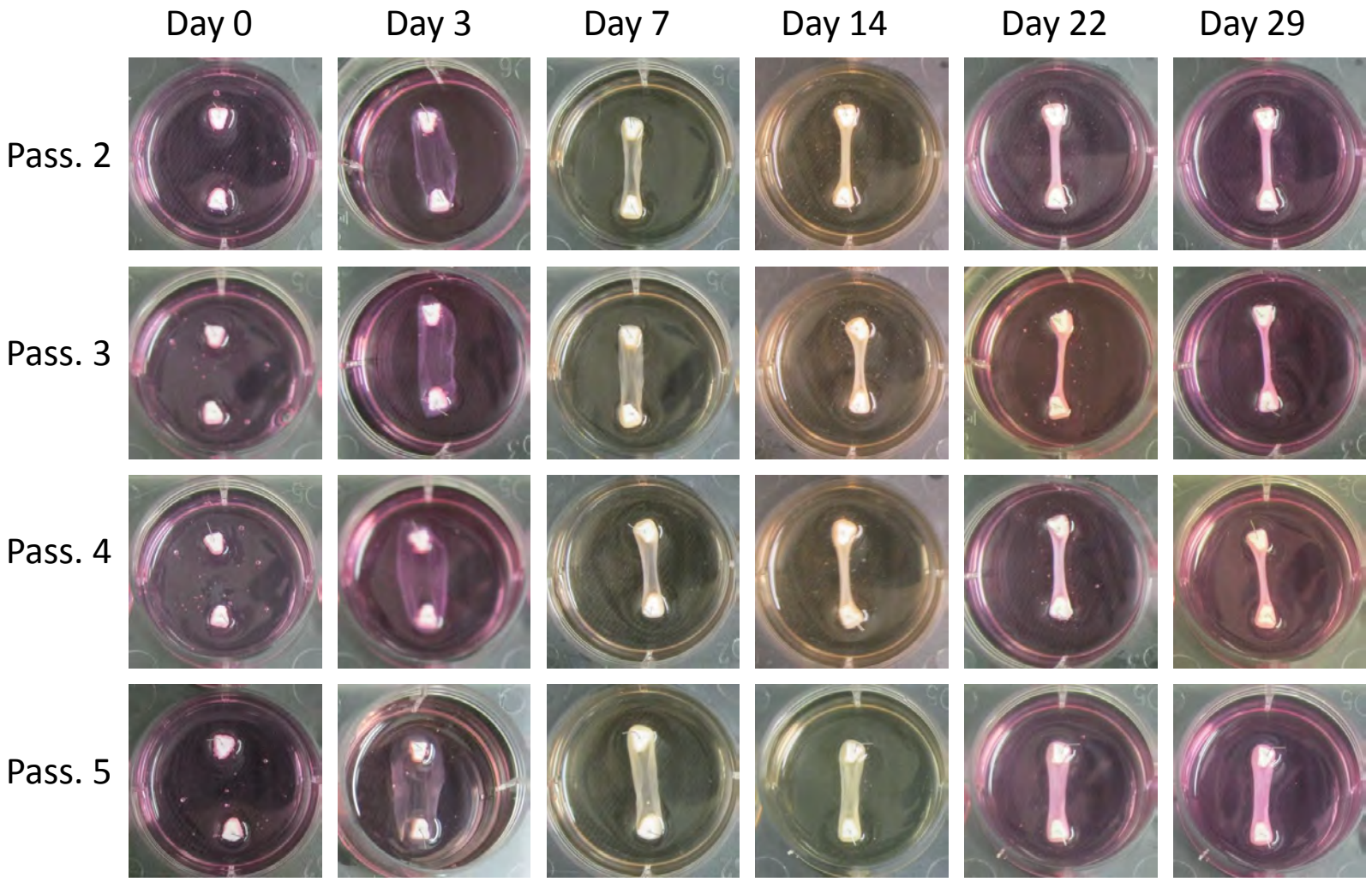

FIGURE 7.1: Images of constructs prepared using cells at differing passage stages. On day 29, passage 5 constructs had a greater percentage of original fibrin gel area remaining and were significantly broader in width.

Percentage gel areas on day 3 were 11.52 ± 3.71%, 17.28 ± 7.61%, 21.47 ± 15.64% and 30.83 ± 12.78% for passages 2, 3, 4 and 5, in that order, significant difference occurring between passages 2 and 5 (p=0.029). By day 7, passage 2 and 4 percentage gel areas of 6.26 ± 1.26% and 5.68 ± 0.73% differed significantly from that of passage 5, which had the highest percentage gel area of all groups at 9.39 ± 3.30% (Figure 7.2B).

On day 12, passage 5 percentage gel area was 6.04 ± 0.92% and this differed significantly from all groups. Passage 5 continued to differ significantly from all groups to day 31, the end of the study. Final percentage gel areas on day 31 were 3.05 ± 0.46%, 2.96 ± 0.45%, 3.07 ± 0.42% and 4.92 ± 0.69% for passages 2, 3, 4 and 5, respectively.

Despite the significant difference in percentage gel areas between passage 2 and passage 5 constructs on day 3, no differences were observed between all construct maximum and minimum widths (Figure 7.3A).

Day 7 maximum and minimum widths for passage 5 were 5.31 ± 1.72mm and 4.30 ± 0.92mm and day 14 maximum and minimum widths were 3.87 ± 0.47mm and 3.05 ± 0.51mm, respectively (Figure 7.3B). Passage 5 maximum/minimum widths differed significantly from passage 2 max/min widths of 3.67 ± 0.63mm/ 3.01 ± 0.68mm and passage 4 max width of 3.65 ± 0.66mm/ 2.60 ± 0.47mm, on day 7.

On day 14, passage 5 maximum widths were significantly greater than all groups, whereas the minimum widths of passages 2 and 4 were significantly smaller than passage 5 minimum widths only. Towards the remainder of the study, passage 5 max/min widths were broadest and differed significantly from all groups.

7.3.2 Effect of cell seeding density on fibrin contraction

In the first week, there was a correlation between cell seeding density and extent of fibrin gel contraction as the 50K cell group showed the least amount of contraction and the 200K contracted the most (Figure 7.4A). The percentage original fibrin gel areas of the 50K group expressed statistically significant difference from the 100K and 200K groups in the first seven days (Figure 7.5A).

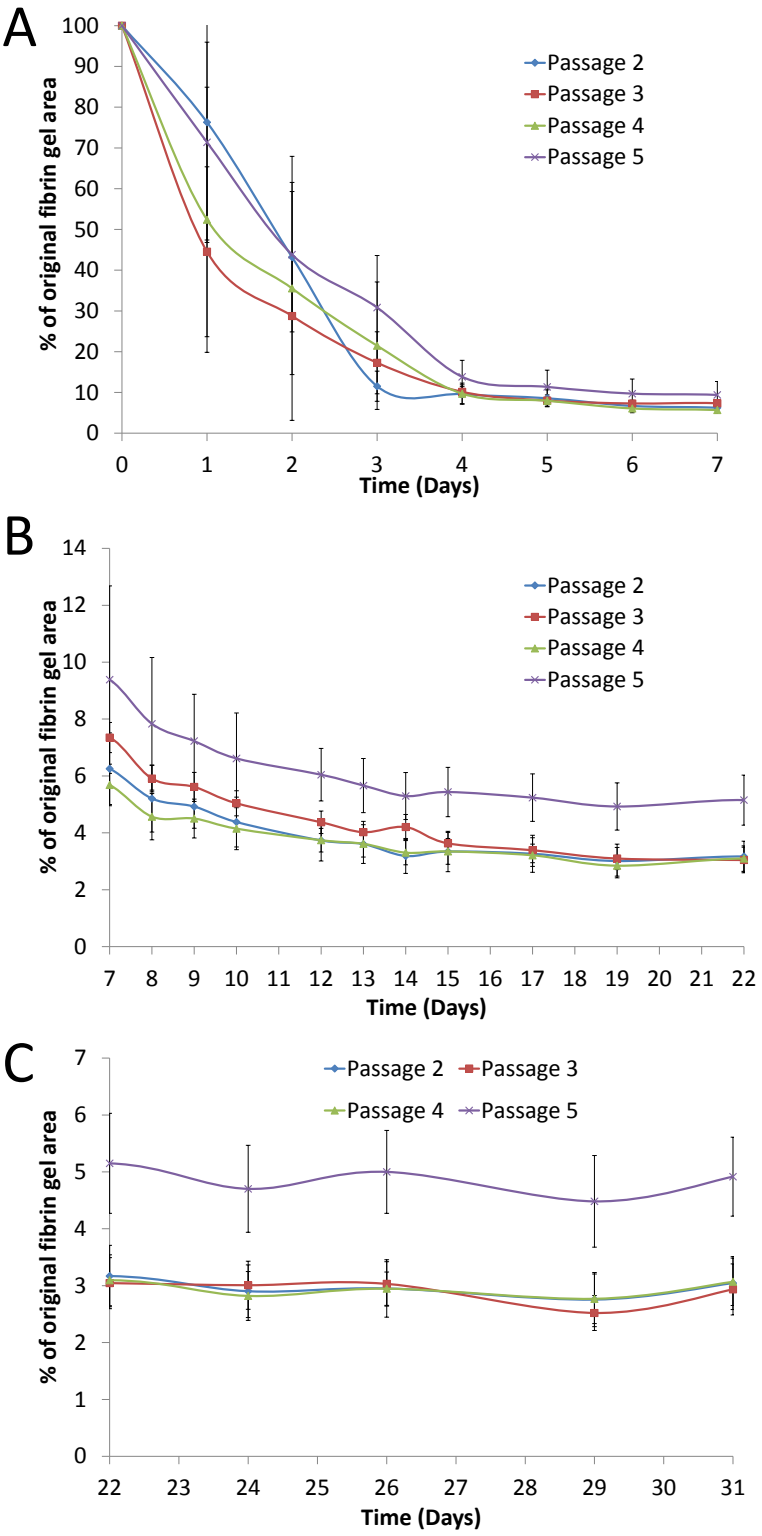

FIGURE 7.2: Effect of CTF cell passage number on fibrin gel contraction. (A) In the first week, passage 2 differed significantly from passage 5 on day 3. (B) From day 12 Passage 5 differed significantly from all other groups until the end of the study on day 31 (C).

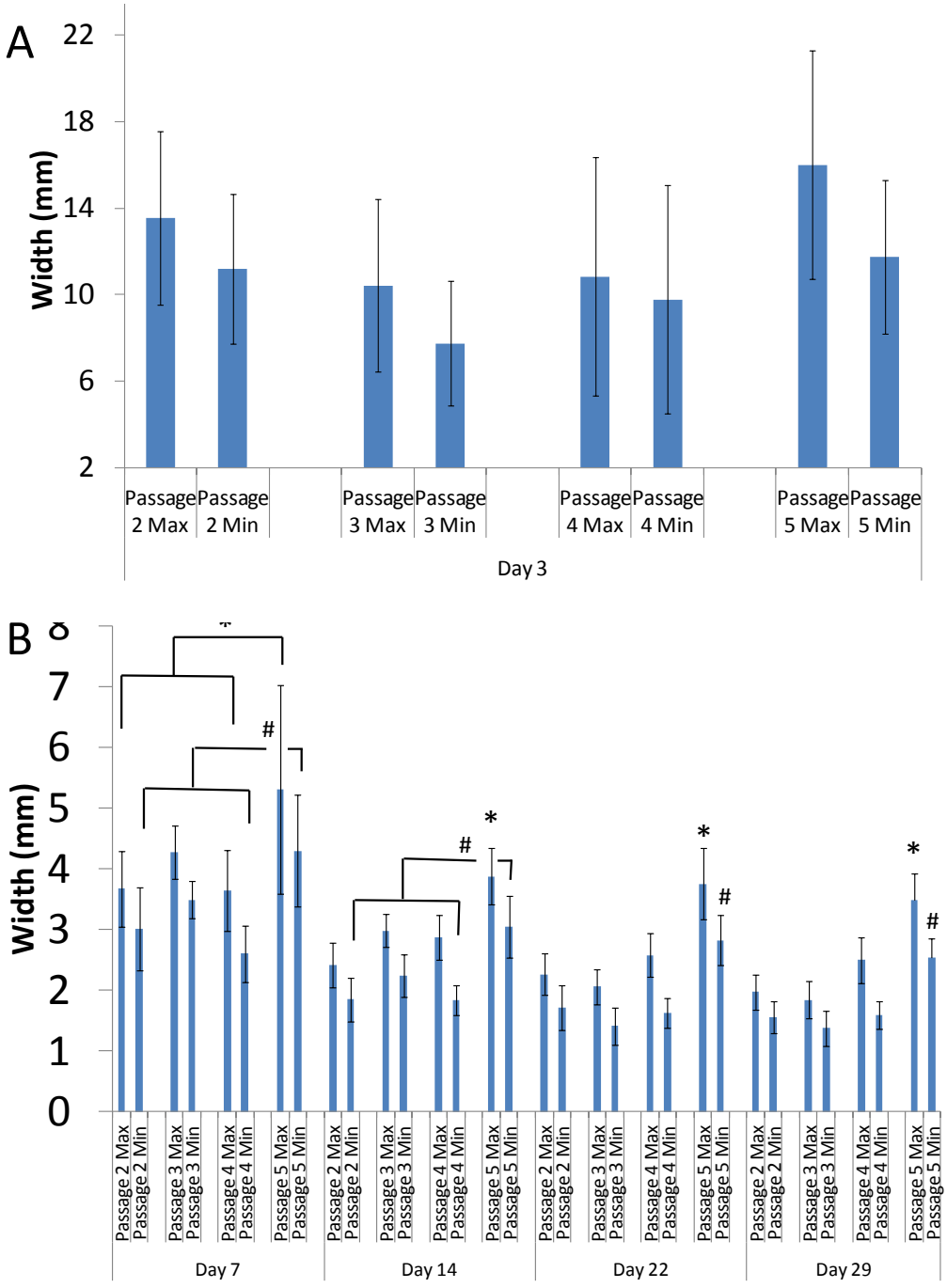

FIGURE 7.3: Effect of CTF cell passage number on sinew maximum and minimum widths. There were no significant differences in construct widths on day 3 (A). Passage 2 and 4 had significantly smaller maximum and minimum widths when compared to passage 5 on day 7. Thereafter passage 5 maximum width was broader those than all other groups ($p<0.05$). *Significant difference denoted by * for max widths and # for min width.*

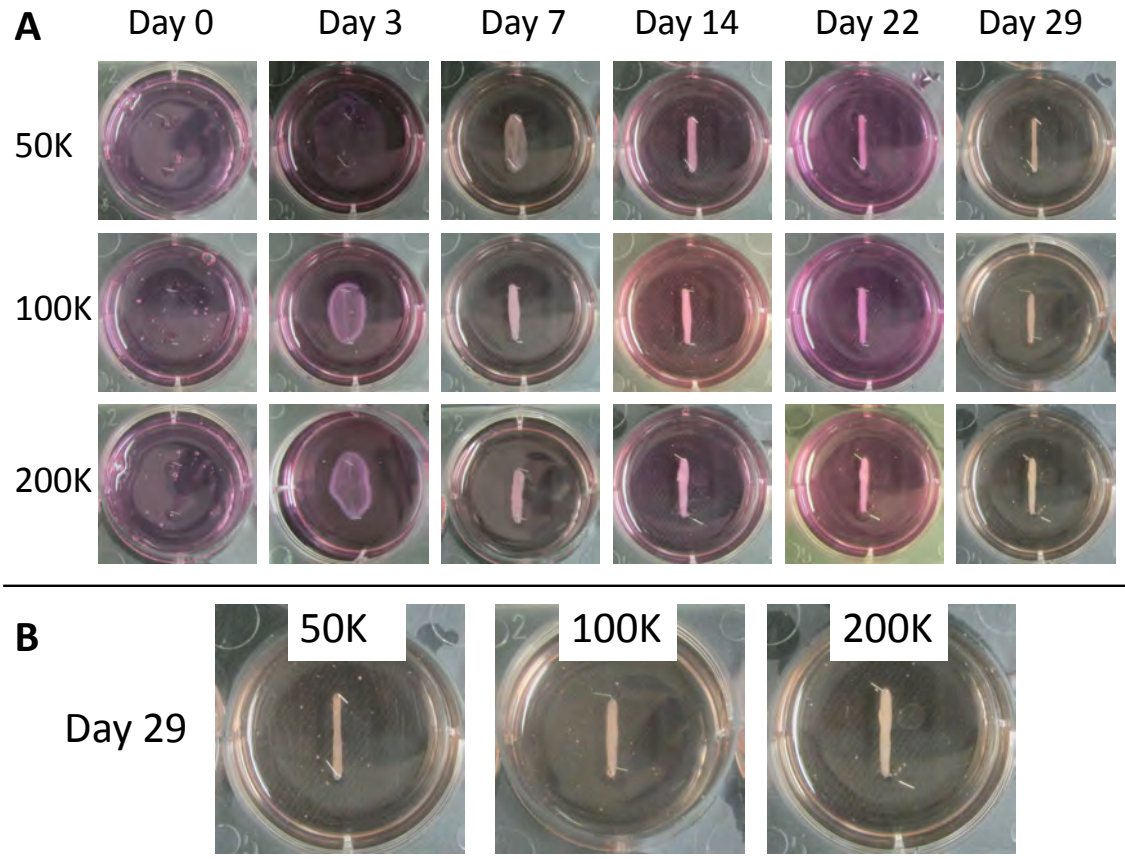

FIGURE 7.4: Effect of cell seeding density on fibrin gel contraction. Contraction of the 50K group was slow in the first week, though no visible differences were apparent between 100K and 200K on day 7 (A). By 29, the 50K group constructs were significantly thinner in width than both 100 and 200K groups.

Day 7 percentage areas were 5.65 ± 0.93%, 3.27 ± 0.28% and 3.36 ± 0.53% for 50K, 100K and 200K, respectively (Figure 7.5B). On day 14, percentage gel areas of all groups were almost identical at 2.71 ± 0.23% for 50K, 2.53 ± 0.26% for 100K and 2.70 ± 0.36% for 200K. This indicated an increased rate in fibrin gel contraction in constructs with a 50K cell density between the 1st and 2nd week. The maximum and minimum widths of the 50K group reflected percentage gel area results seen on day 7 at 5.30 ± 0.84mm (max) and 3.19 ± 0.58mm (min), which were greater than max/min widths of group 100K of 3.26 ± 0.70mm/ 1.82 ± 0.13mm and 3.20 ± 0.77mm/ 1.95 ± 0.33mm for 200K (Figure 7.6).

The changes in fibrin gel percentages areas from day 14 to day 29 continued to be small for 100K and 200K, with final values of 2.13 ± 0.18% and 2.14 ± 0.19%, respectively, on day 29. The 50K group continued to contract the fibrin gel and had

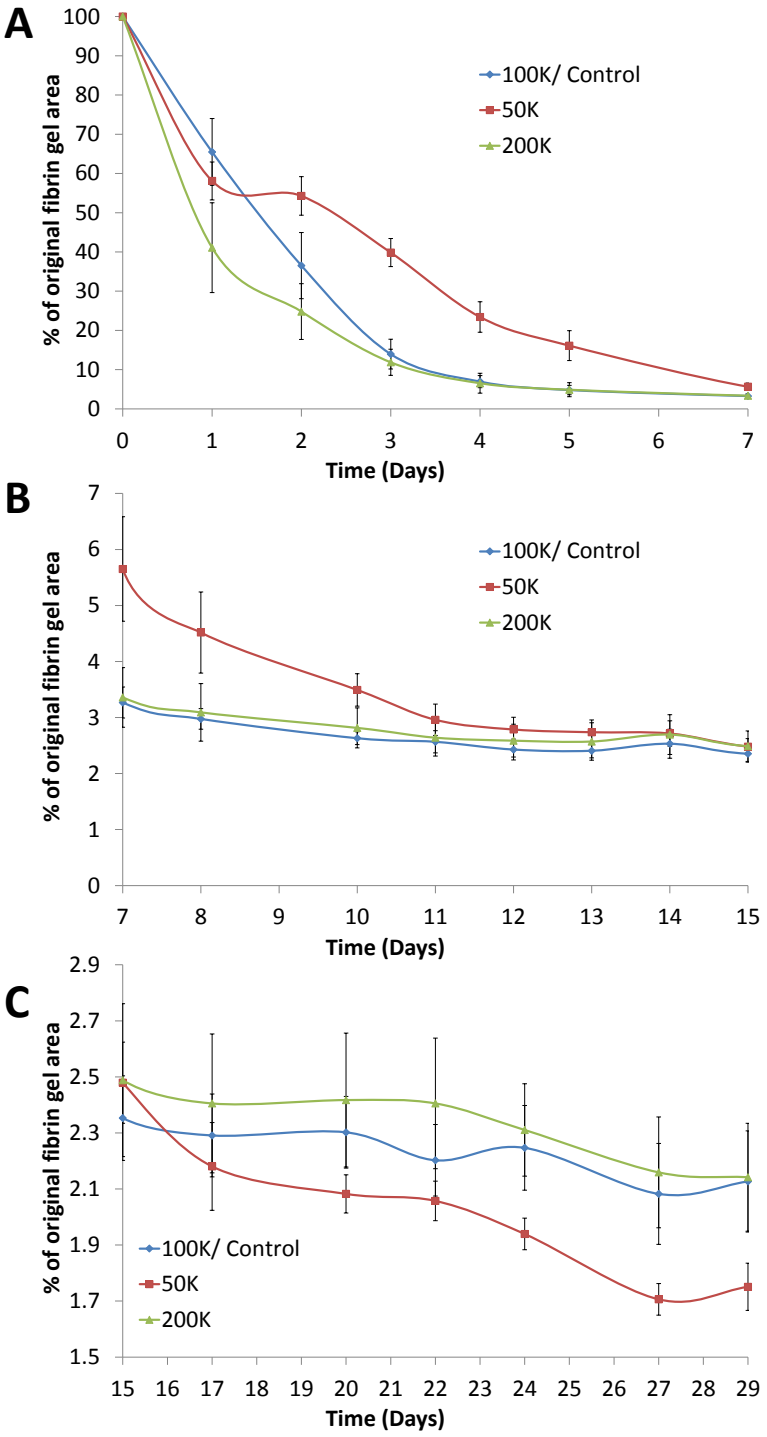

FIGURE 7.5: Contraction of fibrin gels due to cell seeding density. Halving the cell seeding density to 50K had a greater effect on contraction than doubling it to 200K. 50K constructs had higher percentage gel areas up to day10 (A & B). From day 15, the contraction rate of the 50K group rapidly increased, resulting in the greatest reduction of original fibrin gel area compared to 100K and 200K constructs ($p<0.05$). Groups 100K and 200K were not significantly different.

a percentage gel area of 1.75 ± 0.08% on day 29 ($p<0.05$) (Figures 7.4B & 7.5C). Day 29 max/min widths further supported fibrin percentage gel areas and were 1.56 ± 0.09mm/ 1.26 ± 0.12mm, 2.01 ± 0.20mm/ 1.32 ± 0.09mm and 2.01 ± 0.18mm/ 1.36 ± 0.19mm for 50K, 100K and 200K, in that order. With prolonged culture, over 4 weeks, a low cell density of 50K cells actually increased the extent of fibrin gel contraction observed.

7.3.3 Suitability of different cell sources for TE L/T

To determine if the TE L/T model could be used with varying sources of fibroblast cells, constructs were seeded with 3T3 cells, CTFs or PFBs. Constructs seeded with PFBs contracted the most in the first 3 days (Figure 7.7).

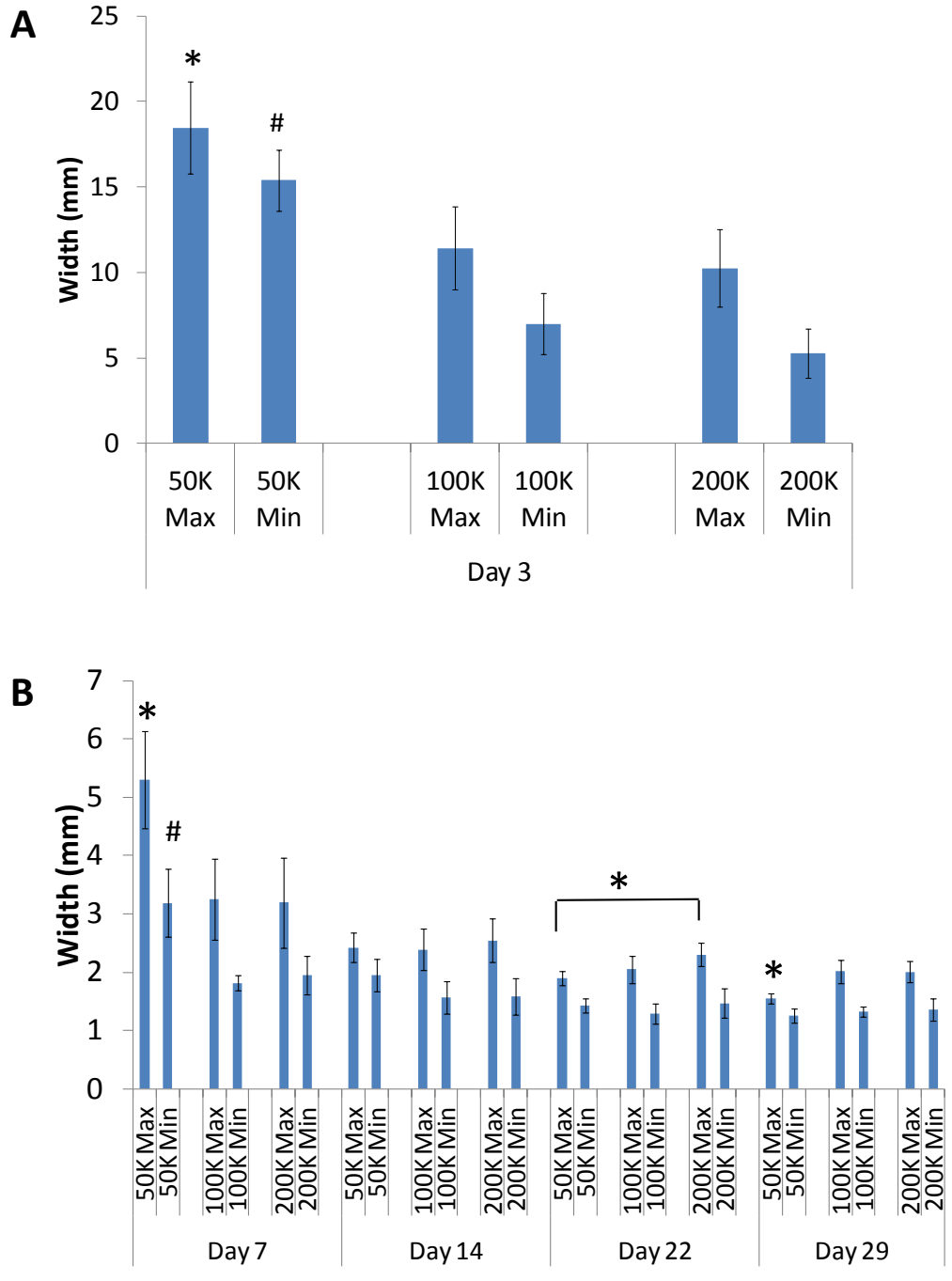

FIGURE 7.6: Effect of cell seeding density on maximum and minimum widths. Max/min widths of the 50K constructs were significantly broader than those of groups 100K and 200K in the first week. The opposite was true by day 29, as the 50K constructs were significantly thinner than all other groups. *Significant difference denoted by * for max widths and # for min width.*

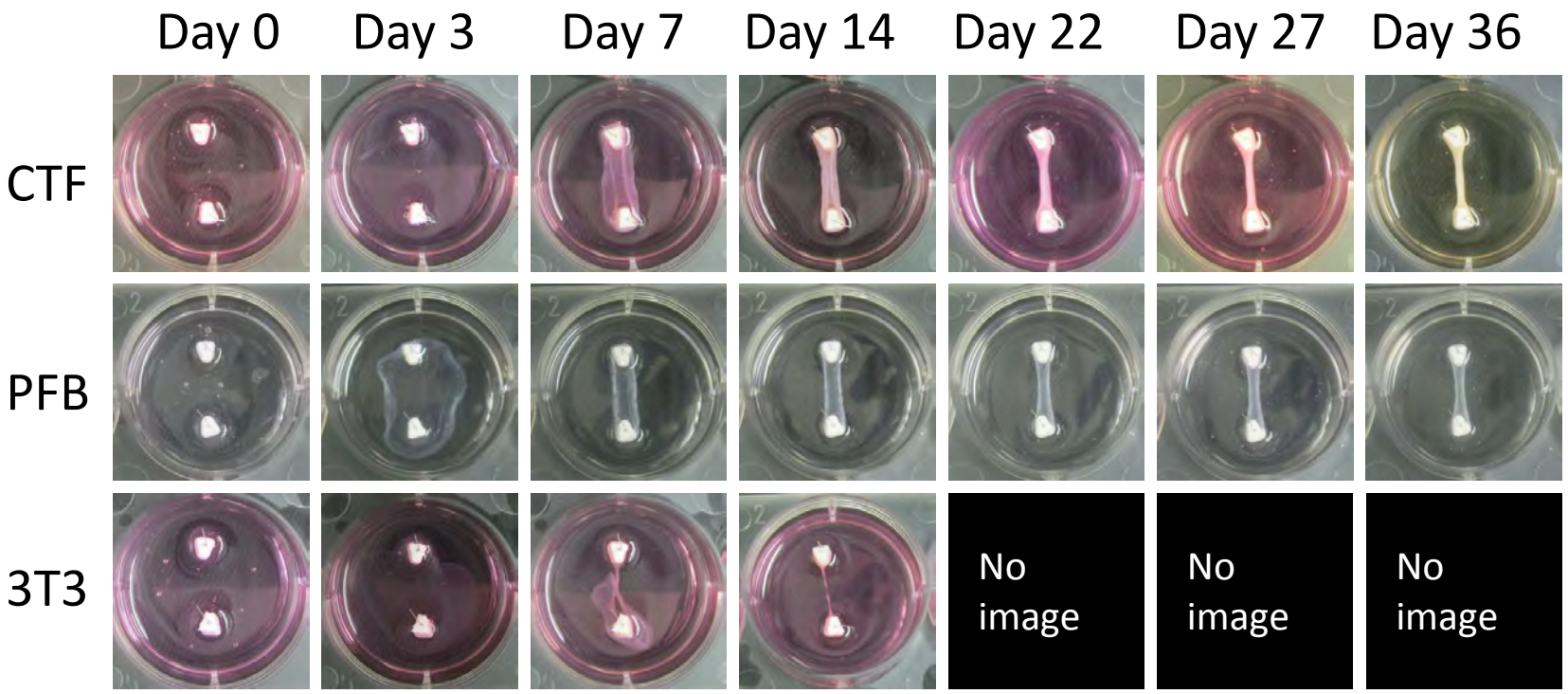

FIGURE 7.7: Images showing contraction of fibrin due to different cell types. 3T3s did not contract very well around the anchors and the fibrin gel had completely disappeared after the second week. PFBs initially contracted the fibrin gel faster than CTF constructs though from the second week contraction appeared to have halted. PFB constructs also appeared more translucent than CTF constructs.

3T3s did not contract the gel uniformly between the anchors and after the first week exhibited a rapid rate of fibrin gel contraction. After the second week, 3T3 cells had completely degraded the fibrin matrix. PFBs formed sinews in between the two anchors, as with CTF cells, though they appeared more translucent than CTF constructs. After day 11, PFB constructs showed slower rates of fibrin gel contraction remaining broader than CTF constructs over the rest of the study.

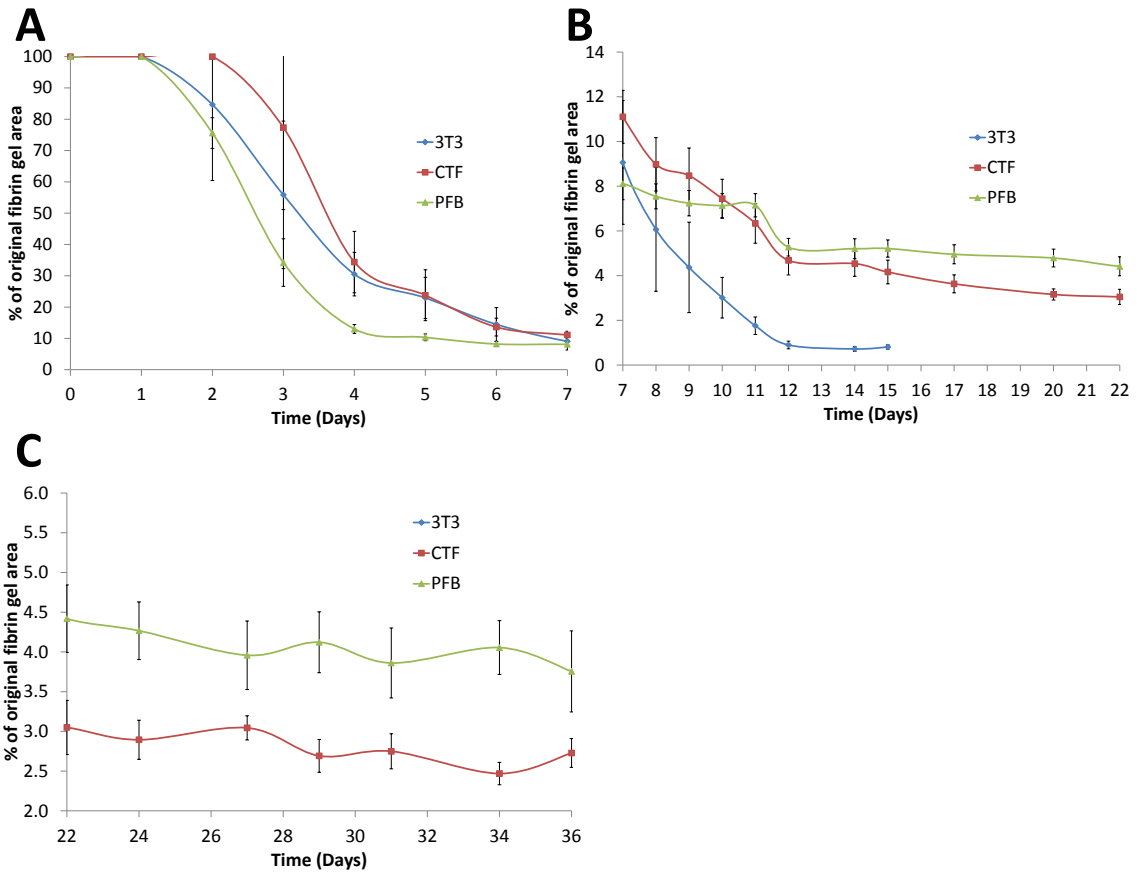

FIGURE 7.8: Rate of fibrin contraction dependent on cell type. (A) PFB constructs showed a greater extent of fibrin contraction in the first 4 days, which then remained constant and decreased only slightly on day 11 (B) and plateaued once more (B & C). PFB constructs had higher percentage gel areas than CTF constrcts. 3T3s had completely degraded the matrix by day 17 (B).

The percentage gel area of the 3T3s was 3.01 ± 0.91% on day 10. This was about 60% less than the percentage gel areas of PFB constructs 7.13 ± 0.54% and the CTF group 7.44 ± 0.87%. Maximum and minimum widths of 3T3 constructs were also

significantly smaller at 2.13 ± 1.46mm/ 0.35 ± 0.12mm than for PFBs at 4.77 ± 0.38mm/ 3.79 ± 0.36mm and for CTFs 4.48 ± 0.36mm/ 3.79 ± 0.62mm.

It is worth noting that on day 10 maximum and minimum widths of PFB and CTF constructs were near identical. By the next day, day 11, 3T3 percentage gel areas had further reduced by 40% to 1.76 ± 0.39% whereas PFB were 7.15± 0.52% and CTF were 6.33 ± 0.88%. PFB constructs continued to have higher percentage gel areas than CTF until day 36, with values of 3.75 ± 0.51% and 2.73 ± 0.18%, in order mentioned. Maximum and minimum widths of PFB sinews of 3.32 ± 0.33mm and 2.28 ± 0.29mm were also significantly greater than CTFs of 1.76 ± 0.13mm and 1.40 ± 0.12mm.

7.3.4 Effect of ascorbic acid and proline on contraction of PFB seeded constructs

Figure 7.10A shows contraction of PFB seeded constructs over 29 days. During the first two days, the control group contracted the least and differed significantly from AA and AA+P treated groups, which had the lowest percentage gel areas but not from Proline treated group. The P only group differed significantly from the most contracted AA group.

From day 3 to day 16 no significant differences were observed between the percentage gel areas of the groups (Figure 7.10B & C). No clear trend was seen between the maximum and minimum widths of the sinews though the proline group max width of 5.05 ± 0.23mm were smaller than those of the controls of 6.23 ± 0.98mm ($p<0.05$) on day 7 (Figure 7.10E). On day 17, the AA+P group differed from AA ($p=0.029$) and P ($p=0.042$) as it had the largest percentage gel area of 5.00 ± 0.58%. The control group had contracted to 4.48 ± 1.27% whereas AA was at 3.62 ± 0.77% and P at 3.57 ± 0.53%. From day 24 to day 29, AA+P treatment resulted in significant difference when compared with all other groups as it exhibited a lesser extent of contraction. The percentage gel area of the AA+P group was 4.27 ± 0.41% on day 29. For the control group this was 2.84 ± 1.19%, 2.98 ± 0.83% for AA and 2.81 ± 0.49% for P. The proline group had the smallest minimum width of 1.86 ± 0.38mm, which differed

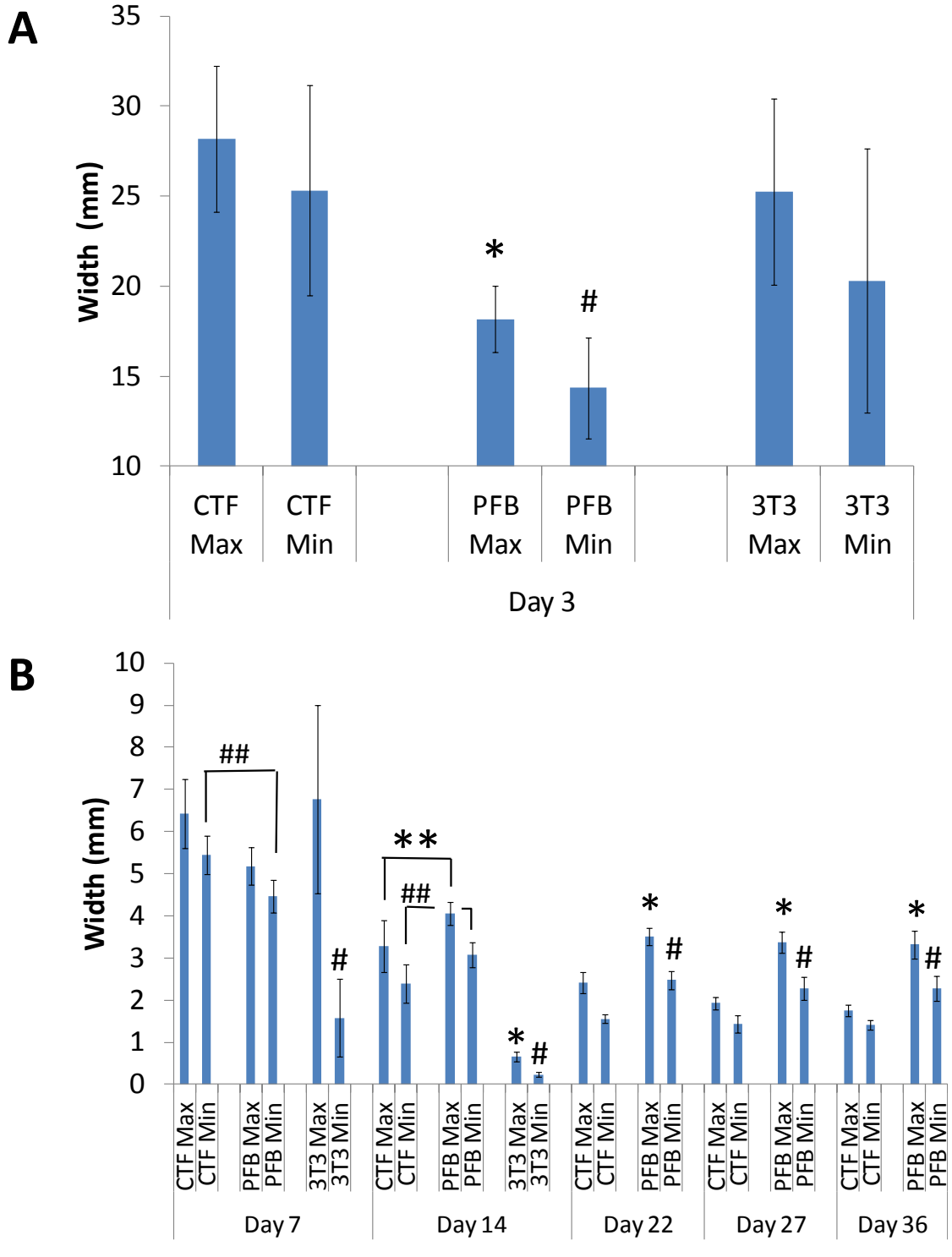

FIGURE 7.9: Maximum and minimum widths of constructs of varying cell type. PFB maximum and minimum widths were significantly smaller than other groups on day 3. From the third week in culture, PFB max/min widths were significantly broader than CTF construct widths.

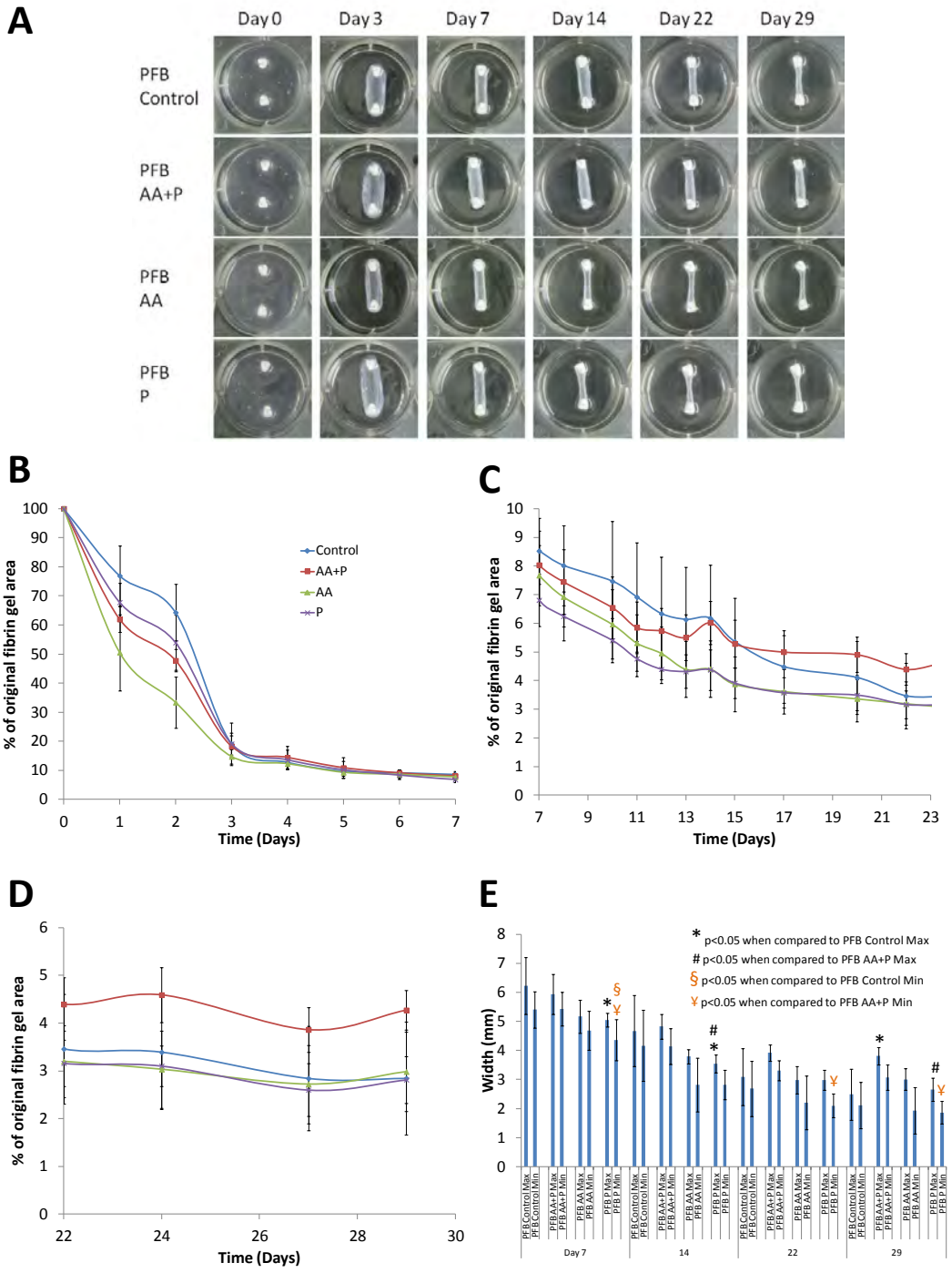

FIGURE 7.10: Contraction of PFB seeded constructs due to AA/P treatment. (A) Images showing contraction due to supplementation. AA+P treatment resulted in constructs that were visibly broader than other constructs, whilst P constructs were smallest in width. (B) and (C) The control group percentage gel areas differed from AA & AA+P treated in the first two days but from day 3 to 16 all constructs showed no significant differences. (D) By the end of the study, AA+P had contracted the fibrin gel the least. (E) Generally, P group max/min widths were significantly smaller than AA+P treated constructs.

significantly from that of the AA+P group, which had the broadest minimum width of 3.06 ± 0.43mm, on day 29.

During culture it was observed that AA only treatment resulted in fissures within the sinews, possibly due to the treatment enhancing degradation of the matrix (Figure 7.11).

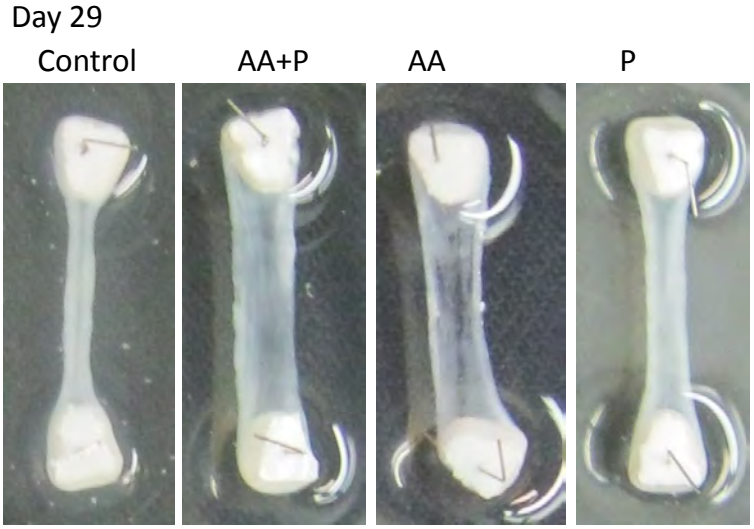

FIGURE 7.11: Digestion of fibrin matrix due to AA treatment. Fissures were apparent within the AA treated sinews likely due to enhanced fibrin degradation, a separate phenomenon from contraction.

These fissures were not present in sinews of the other groups though AA+P treated constructs had areas of greater thinness and translucence within.

7.3.5 Effect of ascorbic acid + proline on chick and rat fibroblast cell proliferation

Both treated and non-treated CTF constructs exhibited a lesser extent of proliferation than the PFB groups. The CTF control and AA+P treated groups had $3.6 \times 10^5 \pm 1.0 \times 10^5$ cells and $2.6 \times 10^5 \pm 3.7 \times 10^1$ cells, respectively, on day 3, which differed significantly from PFB control with $9.5 \times 10^5 \pm 2.4 \times 10^2$ cells and PFB AA+P with $1.6 \times 10^6 \pm 5.8 \times 10^5$ cells (Figure 7.12).

AA+P treatment appeared to have opposing effects on CTF and PFB cells as CTFs treated with AA+P had the lowest live cell number, whilst PFB supplemented with

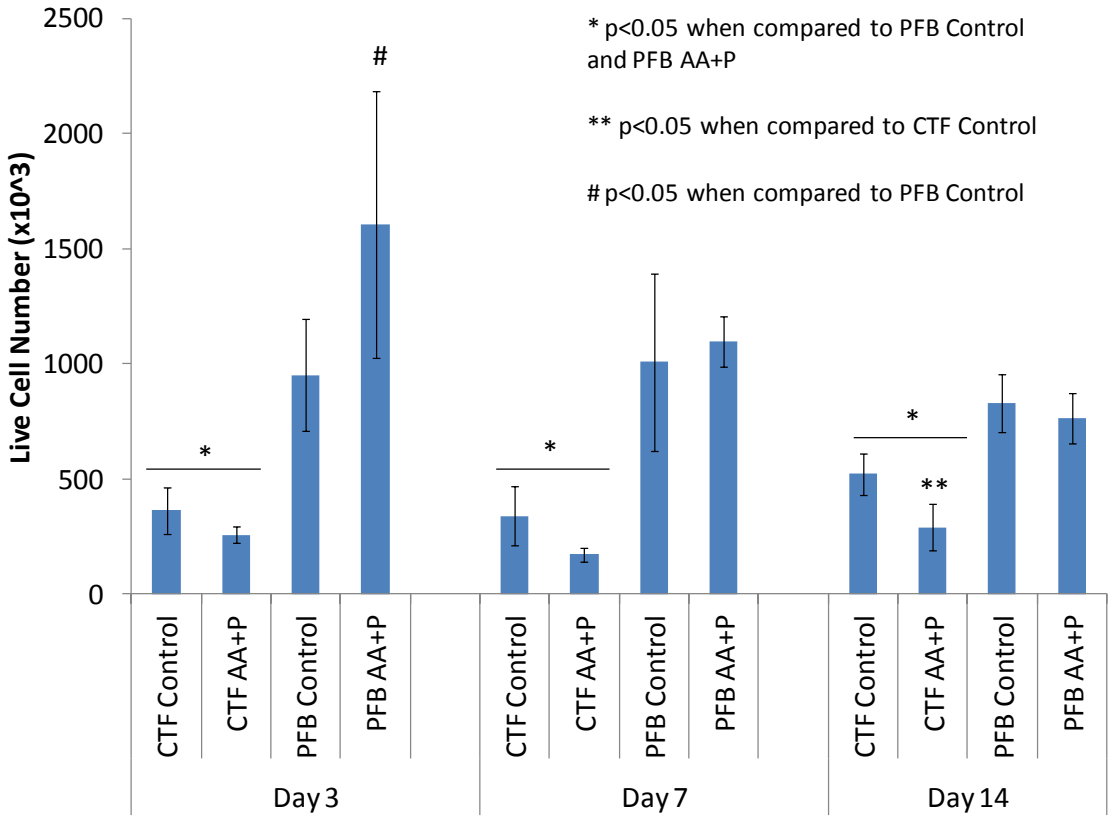

FIGURE 7.12: Proliferation of constructs supplemented with AA/P. CTFs showed a lesser extent of proliferation than both AA+P treated and control PFB groups.

AA+P had the greatest number of live cells about 6-fold that of the CTF AA+P group. On day 14, both CTF cell group live cell numbers were significantly less when compared to the PFB groups. In addition, the CTF AA+P group had a significantly reduced number of live cells, $2.9 \times 10^5 \pm 9.9 \times 10^1$ cells, in comparison to the control group with $5.2 \times 10^5 \pm 8.8 \times 10^1$ cells.

7.3.6 Morphology of rat tail PFB cells on fibrin gels

To determine if supplementation altered gel properties and cell morphology, contraction impeded gels seeded with cells were stained with calcein-AM and propidium iodide (Figure 7.13). Day 3 results supported the proliferation study (Figure 7.12), indicating that PFB cells receiving no treatment proliferated to a lesser extent than AA+P treated PFB cells (Figure 7.13A). Similarly, AA only treatment of PFB cells

resulted in greater proliferation than P only supplementation. For the CTF cells, P only supplementation appeared to retard proliferation. Supplementation with AA or AA+P resulted in cell alignment.

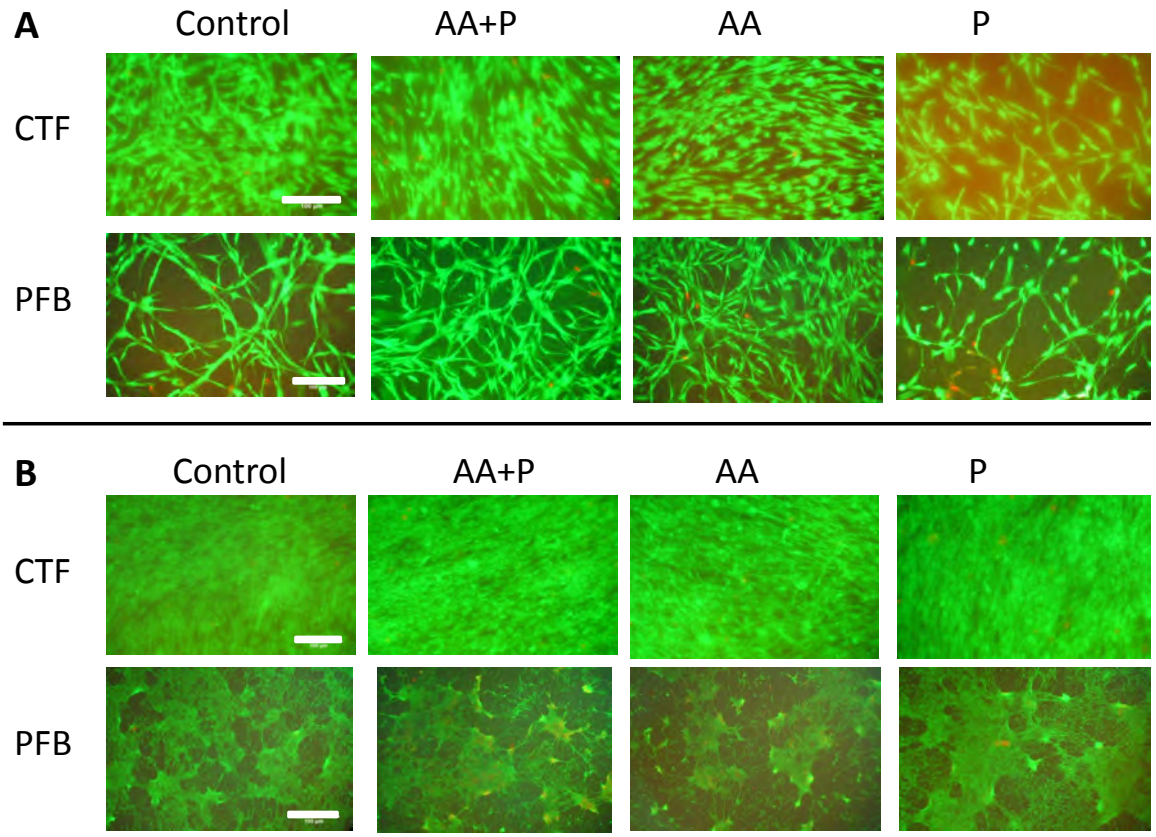

FIGURE 7.13: Variation in cell proliferation between CTF and PFB cells over 7 days. Live/dead staining of gels seeded with CTFs or PFBs on days 3 (A) and day 7 (B). On day 3, CTFs treated with P did not appear to have proliferated well. AA and AA+P resulted in alignment of the CTF cells. AA and AA+P supplementation also increased PFB cell proliferation. By day 7, all CTF groups exhibited profound proliferation whereas the morphology of PFBs appeared altered. *Scale bars are 100μm.*

By day 7, all CTF cell groups showed no distinguishable difference in proliferation. This was also in agreement with results from Figure 7.12, which showed no differences in live cell numbers between CTF control and CTF AA+P. The morphology of PFB cells appeared drastically altered by day 7, having formed thin vastly interconnected clustered networks (Figure 7.13B). AA treatment of PFB cells also appeared to enhance digestion of the matrix.

7.3.7 Construct collagen content and tensile strength

7.3.7.1 Comparison of CTF and PFB construct collagen content

The collagen content of experimental groups in this chapter was evaluated. After 5 weeks of culture, average percentage collagen of passage 2, 3, 4 and 5 constructs were 13.15 ± 5.23%, 6.85 ± 2.17%, 12.34 ± 2.59% and 8.81 ± 2.45%, in order mentioned (Figure 7.14A). Passage 3 constructs had the least amount of collagen, which differed significantly from passage 2. Cell seeding density did not have an effect on the amount of collagen present (Figure 7.14B).

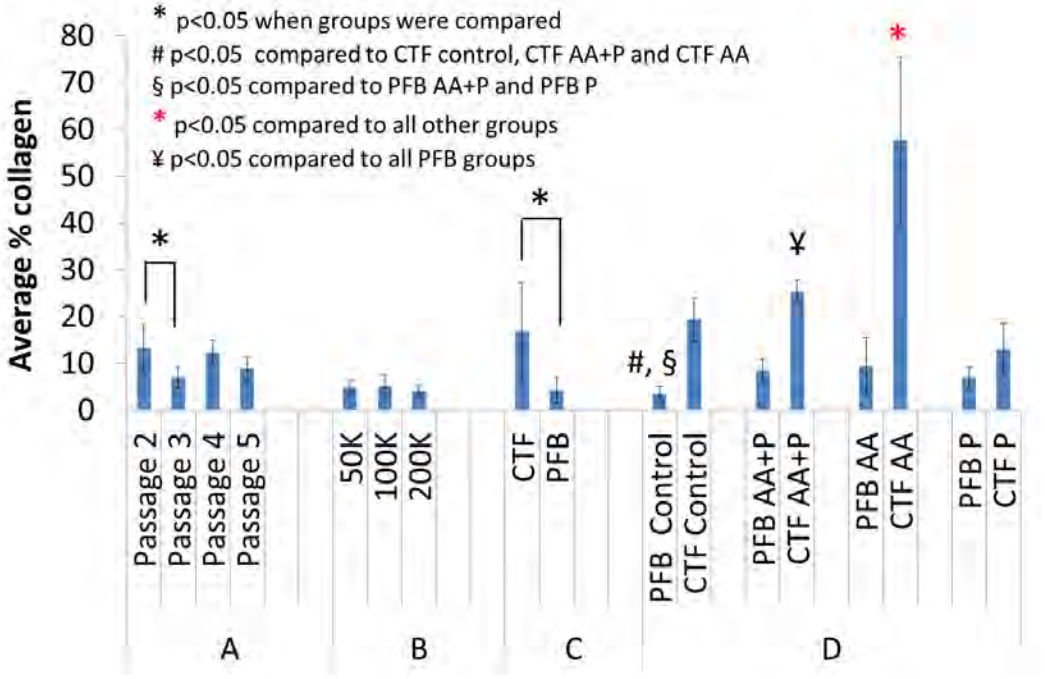

FIGURE 7.14: Collagen content of constructs due to cell properties. (A) Passage 3 had the lowest % collagen, whilst passage 2 cells expressed the highest amount. (B) Cell seeding density did not affect sinew collagen content. (C) PFB cells produced significantly less collagen than CTF cells. (D) Supplementation resulted in CTF AA constructs, containing the highest amount of collagen, which differed from all groups. CTF AA+P collagen content was significantly greater than all PFB groups. Again PFB control collagen differed from CTF control and also from PFB P.

These constructs where cell seeding density was varied were prepared using cells at passage number 5, however, the average % collagen differed significantly from passage number experiments. Generally, CTF cells expressed higher quantities of collagen

than PFB cells (Figure 7.14C). Here, CTF constructs treated with AA only had a collagen content of 57.67 ± 17.79%, which differed significantly from all other groups (Figure 7.14D). Supplementation of CTF cells with AA+P resulted in a significant difference between CTF AA+P (25.19 ± 2.60%) and all treated and non-treated PFB groups, which all contained an average percentage collagen less than 10%.

7.3.7.2 Comparison of CTF and PFB construct tensile strength

The tensile test curves for constructs of varying cell passage number, cell seeding density and cell type with/without supplementation are shown in Figure 7.15A–D. For passage 3, the load vs extension curve differed from those of passages 2, 4 and 5 and had the lowest maximum load of 131 ± 21mN (Figure 7.15A). Out of the passages investigated, passage 3 constructs possessed the least amount of collagen (section 7.3.7). Passage 2, 4 and 5 had similar maximum loads of 244 ± 31mN, 232 ± 42mN and 237 ± 72mN, in that order. Passage 5 constructs were stiffest although they did not contain the highest collagen content, with highest Young's Modulus of 37.13 ± 8.28kPa. This differed significantly from passages 3 and 4 of Young's Modulus 12.21 ± 2.94kPa and 17.35 ± 6.38kPa, respectively.

Despite 100K and 200K cell seeding densities having 2-fold and 4-fold the initial number of cells of the 50K group, this did not affect the total amount of collagen present in the constructs but resulted in the 50K group having smallest percentage of original fibrin gel area on day 29. The 50K group also had lowest tensile strength, withstanding only 52 ± 18mN ($p<0.05$) (Figure 7.15B and E). The 100K group had a maximum load of 110 ± 42mN, whilst the 200K load had a maximum load of 120 ± 30mN. Increasing the cell seeding density from 100K to 200K, did not appear to affect construct tensile strength.

PFB constructs were weaker than CTF constructs and achieved maximum loads <80mN. The PFB control and PFB P groups had similar maximum loads of 73 ± 17mN and 71 ± 18mN, respectively. Groups PFB AA+P and PFB AA had lower maximum loads of 46 ± 15mN and 42 ± 25mN, respectively. Supplementation did not affect collagen synthesis as no differences were observed between the PFB groups, however, tensile tests indicate that AA+P and AA supplemented PFB constructs

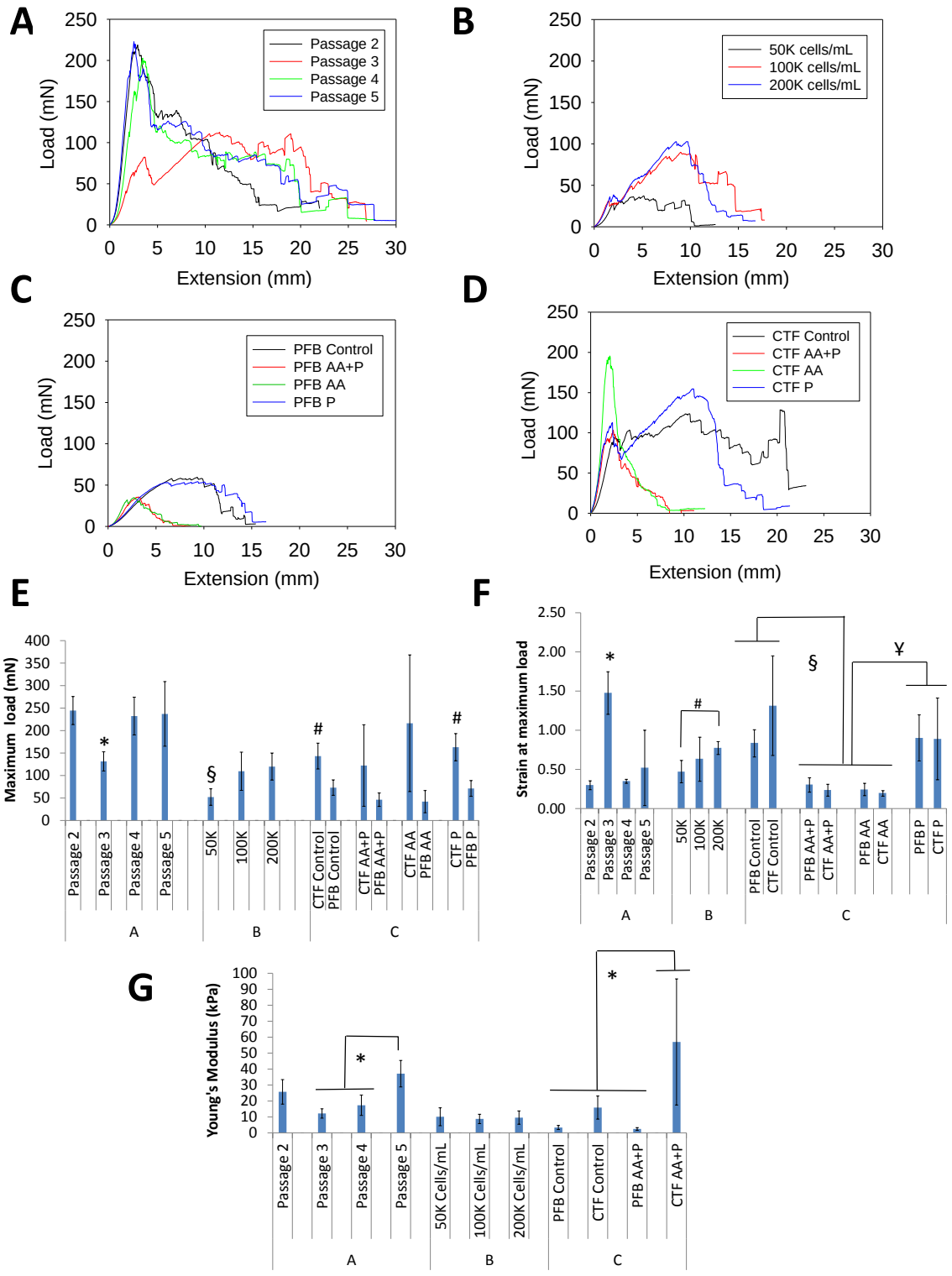

FIGURE 7.15: Construct tensile test results. Load to strain curves of constructs at different CTF passage number (A), CTF cell seeding density (B), supplemented PFB constructs (C) and supplemented CTF constructs (D). (E) shows sinew maximum loads and (F) the corresponding strains at maximum loads. (G) Young's modulus of constructs. *Symbols represent significance at $p<0.05$. In (E) # is when compared to all PFB groups.*

were more fragile than the non-treated or proline only supplemented constructs, failing at lower strains. Similarly, supplementation with AA+P/AA resulted in CTF constructs that were more brittle, the maximum load and failure strains occurring at very low strains <1.0 strain (Figure 7.15D, E and F). This was further reflected in the Young's Modulus of CTF AA+P of 57 ± 40kPa, which was significantly larger than CTF control, PFB control and PFB AA+P, with values of 16 ± 7.0kPa, 3.4 ± 1.3kPa and 2.5 ± 0.8kPa, in order mentioned. Although CTF AA had the highest percentage collagen, differences in the maximum loads of the CTF constructs were not significant. CTF Control and CTF P maximum loads of 143 ± 29mN and 163 ± 30mN, respectively, did vary from all the proline groups.

7.4 Discussion

Increasing cell passage numbers and cell history affect fibrin gel contraction and resulting sinew mechanical strength

Cells at passage number 5 exhibited decreased fibrin gel contractility and were generally wider in width than passage 2 and 4 in the first weeks and then significantly different from all groups by the end of the study. This indicated that increasing passage numbers decreased cell responsiveness to the matrix and affected cell mediated contraction. This was not surprising but it was unexpected that the decrease in contractility would be observed at such an early passage. With age, fibroblasts from the human skin become quiescent, have endoplasmic reticulum that is not well developed and are less responsive to the matrix and chemotactic signals (Ashcroft et al., 2002). Foetal and adult fibroblasts have been been shown to vary in their capacity to contract wounds during healing, with *in vivo* and *in vitro* results varying between cell types/sources and experimental protocols (Moulin and Plamondon, 2002).

The effects of experimental protocols or cell history were further demonstrated by the behavior of passage 3 constructs, which did not differ significantly from passage 5 in the first three weeks, despite being "younger". The cells used for the passage 3 group, were thawed from a different batch of cells, frozen at a different time point. Passage 3 expressed the least amount of collagen and had a load-extension curve that

varied from the other passage numbers. Chang et al. (2002) investigated genome expressions of human fibroblasts sourced from 10 different parts of the body such as the arm, scalp, toe, gum, to name a few, from 16 different donors, looking at both foetal and adult cells and determined that fibroblasts should be considered a class of distinct differentiated cell types. They determined that the fibroblasts from different body locations and passages maintained their distinct phenotypes and expressed gene related to their origin, an important characteristic for tissue engineering cell sourcing. In a lung undergoing tissue repair and remodelling, several distinct types of fibroblasts have been identified within the same lung (Phan, 2008).

Low seeding density increases extent of fibrin contraction and may promote differentiation into myofibroblasts

The ability of fibroblasts to contract the fibrin matrix is due to complex cell-matrix interactions and environmental cues that lead to the expression of smooth muscle actin (α-sma) mRNA (see Chapter 2, section 2.3.1.2). Adult differentiated fibroblast are quiescent, with slow rates of proliferation, matrix turnover and absent actin filaments (Ashcroft et al., 2002; Gabbiani, 2003). During wound healing, fibroblasts differentiate into myofibroblasts, which have two-fold the contractile capacity of fibroblasts and are able produce *de novo* extracellular matrix (Hinz et al., 2007). The expression of α-sma by myofibroblasts is said to be dependent on mechanical stress such as matrix rigidity, the presence of particular ECM proteins and the TGF-β growth factor, which is often released during wound healing as it also promotes collagen type I synthesis (Gabbiani, 2003; Hinz et al., 2007). *In vivo*, once fibroblasts have differentiated into myofibroblasts tissue remodeling will continue until the wound is healed, after which α-sma expression ceases due to ERK pathway downregulation, leading to cell apoptosis (Desmouliere, 1995; Hinz, 2007; Grinnell, 2000). Other factors are likely to be involved in wound contraction as some open wounds have been shown to spontaneously contract suggesting that granulation tissue and myofibroblasts may not be the only requirements for contraction(Grinnell, 2000; Gross et al., 1995; Tomasek et al., 2002). Masur et al. (1996) demonstrated that fibroblasts differentiation into myofibroblasts was also dependent on cell density. Plating corneal fibroblasts at low cell seeding density impeded cell to cell contacts resulting in 70-80% differentiation into myofibroblasts whereas at high cell seeding densities, only a

5-10% conversion was achieved (Masur et al., 1996). Further, passaging of corneal myofibroblasts at high density resulted in a loss of α-sma expression, the marker for myofibroblasts. The results from Masur et al. (1996) may explain why increased contraction of the fibrin gel was observed at the low seeding density of 50K cells/mL. Alternatively, seeding at low density may have enhanced proliferation as the cells strived to increase cell-cell contacts, which may also have increased collective contractile forces or increased cumulative MMPs present. *In vitro*, human articular chondrocytes seeded at low densities redifferentiated more readily and had a 3-fold greater extent of proliferation than cells seeded at higher densities (Gagne et al., 2000).

Fibroblasts from varying sources respond differently to AA+P treatment

Although cell mediated contraction of the fibrin gel has been focused on thus far, cell-matrix interactions also involved enzymatic digestion of the fibrin gel by cell secreted MMPs, which contributed to reduction in percentage fibrin gel areas, sinew widths and final collagen content. The complete depletion of the fibrin gel by murine 3T3 cells suggested that distinct fibroblast cell types express varying levels of MMPs that digest the fibrin gel and possibly any synthesized collagen. The stiffness of the fibrin gel may have been unfavourable for 3T3s as different cell types have been shown to prefer matrices of different stiffness (Discher et al., 2005), with the optimum stiffness for fibroblast dendritic morphology being about 10kPa (Solon et al., 2007). Selection of cell and scaffold type need to be considered for the tissue to be engineered (Dado and Levenberg, 2009) and these results suggest that several L/T TE models may need to be developed for different individuals or age groups.

Although PFB cells contracted to form ligament-like tissues, they remained fairly translucent in comparison to CTF constructs which appeared denser (Figure 7.8), which suggested that less collagen was deposited. Upon handling, PFB constructs were flimsy and not as robust as CTF constructs (data not shown). The tensile tests and collagen content results supported these statements as TE PFB control sinews had significantly less collagen and a lower maximum load strength than CTF control sinews (Figures 7.14 and 7.15).

Supplementation of PFB constructs with AA+P led to surprising results as supplementation did not significantly increase collagen content and actually resulted in sinews of lower mechanical strength than non-treated sinews. Treatment with AA enhanced fibrin degradation rather than fibrin contraction as fissures appeared within AA treated sinews (Figure 7.11). Arrigoni and De Tullio (2000) state that AA's roles extend past its function as an anti-/pro-oxidant or as a cofactor for collagen synthesis because AA is required for the expression of several genes and it cofactors many other enzymes. A study by Esteban et al. (2010) investigating the reprogramming of mouse and human fibroblasts into induced pluripotent stem cells (iPSCs) highlights such additional functions of AA. Fibroblast become quiescent during *in vitro* culture, partly due to the increase in reactive oxygen species (ROS), which Esteban et al. (2010) found also increased during the reprogramming of mouse fibroblasts. They explored the use of several antioxidants to reduce ROS but only treatment with AA resulted in a significant improvement in reprogramming efficiency, a result they concluded was not solely due to AA's antioxidant capacity as similarly active antioxidants showed no such effect (Esteban et al., 2010). The researchers noted that AA reduced cell idleness though they were unclear about the exact mechanism, which could have been due to AA's involvement with collagen proly hydroxylases, HIF-prolyl hydroxylases, and histone dimethylases (Esteban et al., 2010). Further research on the extensive functions of AA on biological systems are much needed.

Growth medium type affects fibrin gel mechanics, construct collagen content and tensile strength

Because PFB cells do not grow well when cultured in DMEM, Ham's F12 medium was used instead. As a result, this was an additional variable between CTF and PFB constructs. Acellular fibrin gels prepared using either DMEM or Ham's F12 Ham, suggested that Ham's F12 led to the formation of stiffer fibrin gels. To evaluate this further, CTF cells were seeded on gels prepared using Ham's F12 media and PFB's were seeded on fibrin gels containing DMEM. Constructs were fed with the medium corresponding to that making up the fibrin gels, with or without AA+P supplementation. After 5 weeks of culture, CTF constructs fed with Ham's F12 had a significantly higher collagen content and greater tensile strength. The results suggested that the culture medium used had an effect on cell collagen synthesis.

Medium formulations differ and to optimise protein synthesis, separate or additional factors need to be considered as, in this thesis, enhanced collagen synthesis is equally important as maintaining cell proliferation and viability. For example, some media contain proline, hydroxyproline or ascorbic acid as well as differing concentrations of calcium, which could contribute to varying the stiffness of the fibrin gel or altering the amount of collagen produced. These results and the various formulation of growth media used for chick fibroblast cells are are shown in Appendix C.

7.5 Conclusion

What is clear from these results is that there are several cell specific parameters that affect cell mediated contraction and remodelling of the fibrin hydrogel scaffold and consequently the dimensions and mechanics of the TE L/T. Alterations to the model or several models may need to be developed for tissue engineering various ligaments and tendons for different people/ animals.

Chapter 8

Conclusions and Future Work

8.1 Conclusions

The results presented in this thesis have quantitatively demonstrated the effects of AA+P supplementation and effects of fibrin hydrogel stiffness on cell mediated scaffold contraction and the resultant TE tissue dimensions. In addition, possible modes of action behind AA+P supplementation have been elucidated. It was also shown that scaffold stiffness and supplementation in combination could be exploited to control construct widths, whilst increasing collagen content and improving the mechanical strength of the TE tissue as well as prolonging attachment at the brushite cement interface. The main findings from chapters in this thesis are described below.

Proline reduced initial rates of contraction.

In Chapter 4 it was shown that proline supplementation had a dominant effect on contraction rates and that initial rates of contraction of the AA+P group were largely dependent on the presence of P. It was also shown that the rates of AA contraction were largely similar to the control group over the course of the study. Altering the concentrations of either AA or P whilst maintaining one or the other constant revealed that P had no significant effects on construct collagen content, however, increasing AA increased collagen significantly. AA and P clearly had different modes of action. Further, constructs with enhanced collagen content also had higher rates of fibrin gel

contraction and smaller widths suggesting a correlation between construct collagen content and contraction rates.

Control constructs had collagen subunits with less fibril formation and lacked organisation. AA+P treatment led to extensive remodelling due to the upregulated collagen synthesis, contraction and MMP-2 expression.

Biological characterisation using histological, microscopy and RT-PCR techniques in Chapter 4 offered further insight into the differences between control and AA+P treated constructs. Histology and TEM images indicated that although control constructs sythesize collagen precursors, formation of collagen fibrils was limited. AA+P led to greater extent of fibrin gel remodelling, resulting in a dense matrix with collagen fibrils. Cells were seen to be actively involved in protein synthesis as they had prominent endoplasmic reticula. RT-PCR confirmed the upregulation of collagen type I in AA+P supplemented constructs as well as stress fibre activator RhoA and contractile actin. MMP-2, a gelatinase that degrades degraded collagen I (gelatin) and is linked to fibrin degradation, was also upregulated.

Fibrin fibre volume fraction can be used to control rates of contraction and construct widths

Fibrin gel stiffness was increased in Chapter 5 to determine if collagen content would be enhanced either due to the increased collagen gene expression or due to delayed fibrin contraction rates, which would increase cell number and therefore possibly collagen. Additionally, if contraction was delayed this would result in constructs that were broader in width. Indeed, increasing fibrin gel properties such as volume and stiffness, reduced the rates of fibrin gel contraction and constructs were broader. Increases in volume and/or stiffness did not limit construct formation and cells were seen to align along the direction of tension. However, comparisons of contraction data revealed that increasing fibrin volume or increasing fibrin stiffness produced constructs with similar fibrin percentage gel areas and widths.

As a result, fibrin total volume, stiffness or fibre volume fraction are parameters that can be used to control construct dimensions such as width. The findings also showed that increasing the scaffold volume or stiffness was insufficient in raising collagen content. Thereby emphasising the necessity of collagen cofactors or other stimulatory agents.

Reducing thrombin to fibrinogen ratios to 0.313UT/mgF doubled fibrin gel stiffness (G'). No difference was observed in fibre diameters although porosity increased suggesting increase in stiffness was due to greater quantity of fibrin fibres.

The structure and mechanical performance of the fibrin gels used in Chapter 5 were characterised. No difference was observed in fibrin fibre diameters of varying stiffness though 0.313UT/mgF gels had larger pores not seen in the other formulations. Increasing fibrin total volume also increased stiffness though to a more moderate extent than altering thrombin to fibrinogen ratio, likely due to increased number of fibres. Gelling kinetics were also observed and fibrin gels polymerised in-situ, on the rheometer, showed strain stiffening behaviour, which was not observed in gels pre-gelled in the incubator before testing.

There is an optimum stiffness required for collagen sythesis and only in combination with AA+P supplementation

Because constructs of the stiffest gel formulation 0.313UT/mgF were broader than constructs of the control gels of 1.25UT/mgF, the effect of stiffness combined with AA+P treatment was investigated in Chapter 6. As expected, 0.313UT/mgF AA+P constructs were broader than AA+P constructs prepared using the control gel formulation. In addition, collagen content and sinew mechanical strength increased dramatically. Attachment at the interface was prolonged in comparison to AA+P only and the control constructs. The results suggested that there is an optimum stiffness at which AA+P collagen production is most efficient.

Distinct models may need to be developed for different cell types. Growth medium may affect gel stiffness and consequently construct collagen content when supplemented with AA+P.

Chapter 7 investigated the use of different cell sources and their potential to form TE L/T. The results showed that fibroblast cells have an inherent affinity for fibrin that varies between cell types. 3T3s completely degraded the fibrin gel within 2 weeks. Supplementation of PFB constructs with AA/P or AA+P had the opposite effect to that observed using CTF cells. AA and AA+P reduced extent of PFB construct contraction whilst no treatment and P supplementation increased it. In addition,

PFB constructs generally contained significantly lower quantities of collagen than CTF constructs.

The compositions of various media including DMEM and Ham's F12 were detailed in Appendix C. Because PFB and CTF constructs were cultured using different media this presented an additional variable. Stiffness of the fibrin gels was shown to be affected by the type of medium used (Ham's F12 or DMEM), suggesting medium choice to be a factor determining construct collagen content.

8.2 Recommendations for future work

8.2.1 Increasing fibrin fibre volume fraction

The results presented in this thesis have shown that fibrin contraction rates were significantly reduced by increasing fibrinogen volume or fibrin stiffness (Figure 8.1). The fibre volume fraction can be increased by raising the concentration of the thrombin and fibrinogen stock solutions. Fibrin fibre diameters and pore spaces will need to be evaluated to ensure they do not become limiting. Optimum fibrin gels are those that balance fibre lengths, diameters, quantity and extent of branching without extremes in one parameter (Weisel, 2007). In some instances, cell encapsulation within the firbin gel, will assist cell permeation as opposed to cell seeding on the gel surface. In addition, cell encapsulation would assist the formation of 3D TE L/T with improved attachment to the brushite cement anchors. This will likely eliminate the rolling mechanism observed in this thesis and promote uniform formation with fewer folds, which may have limited construct strength.

8.2.2 Optimising fibrin gel stiffness with AA+P supplementation

The results in this thesis showed that increasing stiffness together with AA+P supplementation increased final fibrin gel percentage areas, constructs widths, collagen content and maximum loads. Using DOE software (Design Expert, Stat Ease), Figure

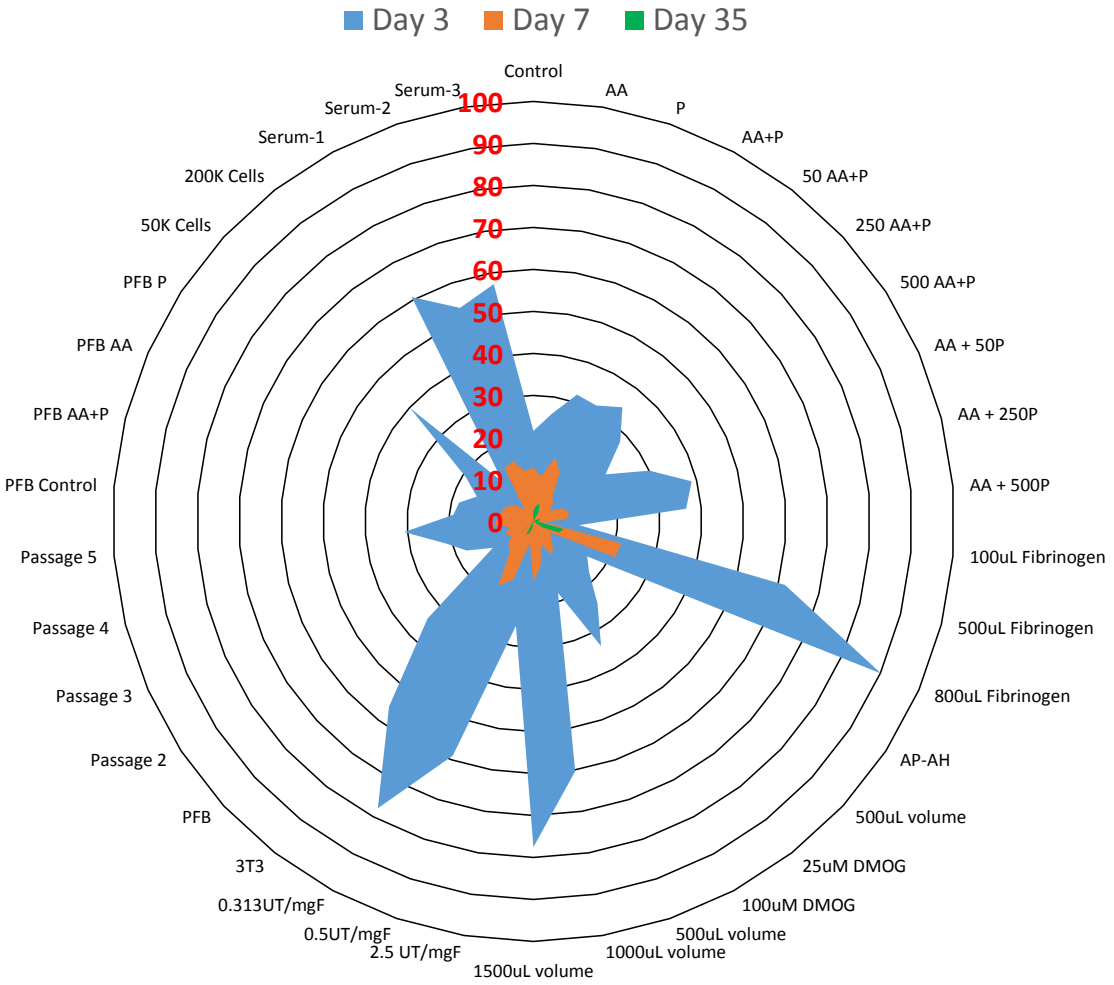

FIGURE 8.1: Multiple factor comparison of percentage gel areas.

8.2 was produced. From data presented in this thesis, the optimum condition at the stiffnesses investigated was to use the stiffest formulation 0.313UT/mgF with supplementation (where 1 = treated, 0= non-treated) in order to maximize the responses: fibrin percentage gel area, maximum load and collagen content.

Increasing concentrations of the stock solutions will allow the stiffness of the gels to be increased further whilst adjusting thrombin to fibrinogen ratios. And it would be of interest to evaluate the effects of varying concentrations of AA and P and the stiffer gels on construct morphology and mechanical properties.

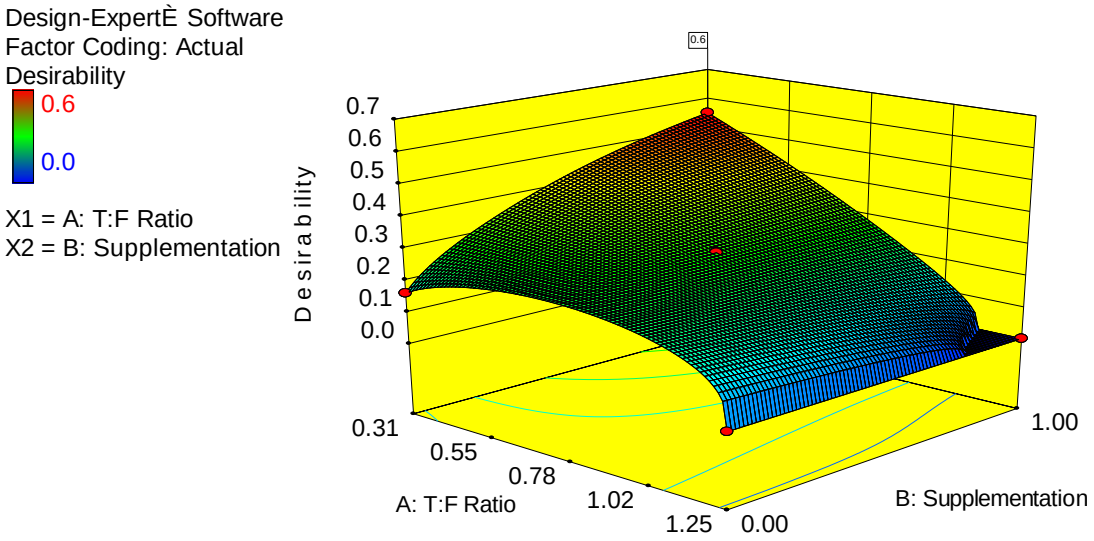

FIGURE 8.2: Effect of fibrin UT:mgF ratio and supplementation on maximizing construct properties. Conditions were set to optimise construct percentage gel areas, maximum load and collagen content.

8.2.3 Cross-linking fibrin

In the body, fibrin clots are cross-linked by the enzyme transglutaminase or Factor XIIIa, which reduces the degradative effects of MMPs (Janmey et al., 2009a). Addition of $CaCl_2$ to fibrinogen has been shown to increase fibrin stiffness by allowing the formation of cross-links (Shen et al., 1974). Use of cross-linked fibrin hydrogels may help reduce the rates of fibrin gel contraction. Increasing the rigidity by cross-linking whilst supplementing with AA+P may further improve construct collagen content.

8.2.4 Quantifying degraded fibrin

Although MMP-2 upregulation suggested degradation of both newly formed collagen and fibrin, through the action of MT1-MMP (MMP-14) the amount of fibrin actually degraded will need to be quantified in order to determine if differences between the control and AA+P supplemented constructs are due to enhanced contraction and not enhanced proteolytic activity. Fibrin degradation products (FDPs) are produced during fibrinolysis and can be measured using biological assays. Hoelzel Diagnostika supply Bovine Fibrinogen Degradation Product ELISA kits for the cost of 576 Euros each (price January 2013).

8.2.5 Interface

In this thesis one of the aims was to improve interface strength and attachment by enhancing properties of TE soft tissue. Further work needs to be conducted in characterising the effects of fibrin gel stiffness with AA+P treatment on the interface strength. In addition, as stated in Chapter 2 strategies for regenerating the enthesis include co-culture (Lu et al., 2010) of cells capable of forming bone, cartilage and the TE soft tissue.

8.2.6 Mechanical loading

Mechanical loading implementing intermittent stretch regimes has also been shown to enhance collagen content and improve the strength of the interface (Paxton et al., 2011). It would be of interest to determine whether increased fibrin gel stiffness along with AA+P supplementation and stretching would further enhance construct collagen content and mechanical strength, as well as the strength of the interface.

8.2.7 RT-PCR

Preliminary RT-PCR results indicated the upregulation of several MMPs. No scleraxis was detected, which is a marker for tendons, highly expressed by fibroblasts and even more so by myofibroblasts. Myofibroblasts are known to be highly contractile, which makes the absence of scleraxis questionable as RhoA and actin were upregulated, whilst Tenascin-C expression was higher in supplemented constructs than non-treated controls. Reasons for the lack of scleraxis detection may have been due to a low signal from low cDNA concentrations. As a result, further work needs to be conducted to investigate scleraxis expression. Further, the results implied that constructs prepared on 0.313UT/mgF gels and supplemented with AA+P expressed other small GTPase proteins such as Ras and that TGF-β expression may also have been upregulated. Additional work needs to be conducted to determine the upregulation of these proteins. Although MMP-2 was seen to be upregulated or downregulated for AA+P or 0.313UT/mgF AA+P, respectively, as MMP-2 is activated by MT1-MMP, the expression of MT1-MMP itself will need to be explored.

8.2.8 Studying contraction

To better study the influence of supplementation or fibrin gel stiffness on cell contractile activities, future work could implement time lapse microscopy with microbeads to quantify actual cell forces generated, observe migratory processes and physical mechanisms of remodelling the matrix. Dikovsky (2008) used such a system, incorporating microbeads in a PEGylated-Fibrin gel to study the effects of matrix stiffness on cell morphology and proteolytic activity. Techniques such as AFM could also be used to measure cell-matrix adhesion strength. Work was begun aimed at exploring contractile behaviour of cells on matrices of differing stiffness, with or without supplementation using micropost arrays as per protocol developed by Yang et al. (2011). Unfortunately, due to time constraints it was not possible to measure cell contractile forces using this method in this thesis. However, work on fabricating the pillars was begun and we were supplied with the Matlab code relating to their protocol, therefore this study should be continued in future work.

8.2.9 Supplementation

AA, P, $ZnSO_4$ or $MnSO_4$ supplements were used in this thesis. Combined treatment of $ZnSO_4$ or $MnSO_4$ with AA+P reduced the extent of fibrin gel contraction. Zinc (Kaplan et al., 2004) and manganese are cofactors for enzymes involved in collagen synthesis (Leccia, 1996). RT-PCR results showed that supplementation with $MnSO_4$ and AA+P upregulated collagen expression to a higher extent than both AA+P only and 0.313UT/mgF AA+P constructs, however, the assay for testing collagen content suggested collagen content of $MnSO_4$ AA+P was below that of AA+P or 0.313UT/mgF AA+P. The mechanism behind the mode of action of Zn^{2+} and Mn^{2+} on collagen synthesis therefore needs to be further evaluated.

There may be room to further optimize AA+P supplement concentrations. Using the DOE software and data from Chapter 4 where AA or P were varied whilst maintaining one of them constant, a suggested supplementation regime to enhance fibrin percentage gel area and collagen content, was to increase concentrations of AA and P in **combination** to 340μM AA with 185μM P (Figure 8.3A). However, the actual optimum design, based on the range of concentrations used, would be 316μM AA

without P (Figure 8.3B). Experiments can be setup in the future to determine the validity of such models.

The results presented in this thesis suggested that collagen synthesis was not significantly increased by raising P concentration at constant AA. Perhaps this is because a combination of several co-factors may be required to maximize collagen synthesis such as iron and α-ketoglutaric acid, which along with AA are required for proline hydroxylation. Iron is already present in cell culture medium (as shown in Appendix C), however, it may be worth determining optimum concentrations for collagen production. In addition, although α-ketoglutaric acid is a product of metabolism, its inhibition with increasing concentrations of DMOG (Chapter 4) suggested that it is important for collagen synthesis and fibrin gel contraction. A longer study utilizing DMOG should be conducted to determine construct fibrin percentage gel areas, collagen content and tensile strength.

8.2.10 Cell proliferation

This thesis used enzymatic digestion methods to detach cells from the matrix. Quantification using calcein-AM relied on cells remaining viable. Although it was shown that the reagents did not lead to significant cell apoptosis (see Chapter 3, Figure 3.7), the use of Hoechst Assay would allow quantification of total cell DNA, including both live and dead cells thereby offering a more accurate means of determining cell proliferation within the constructs.

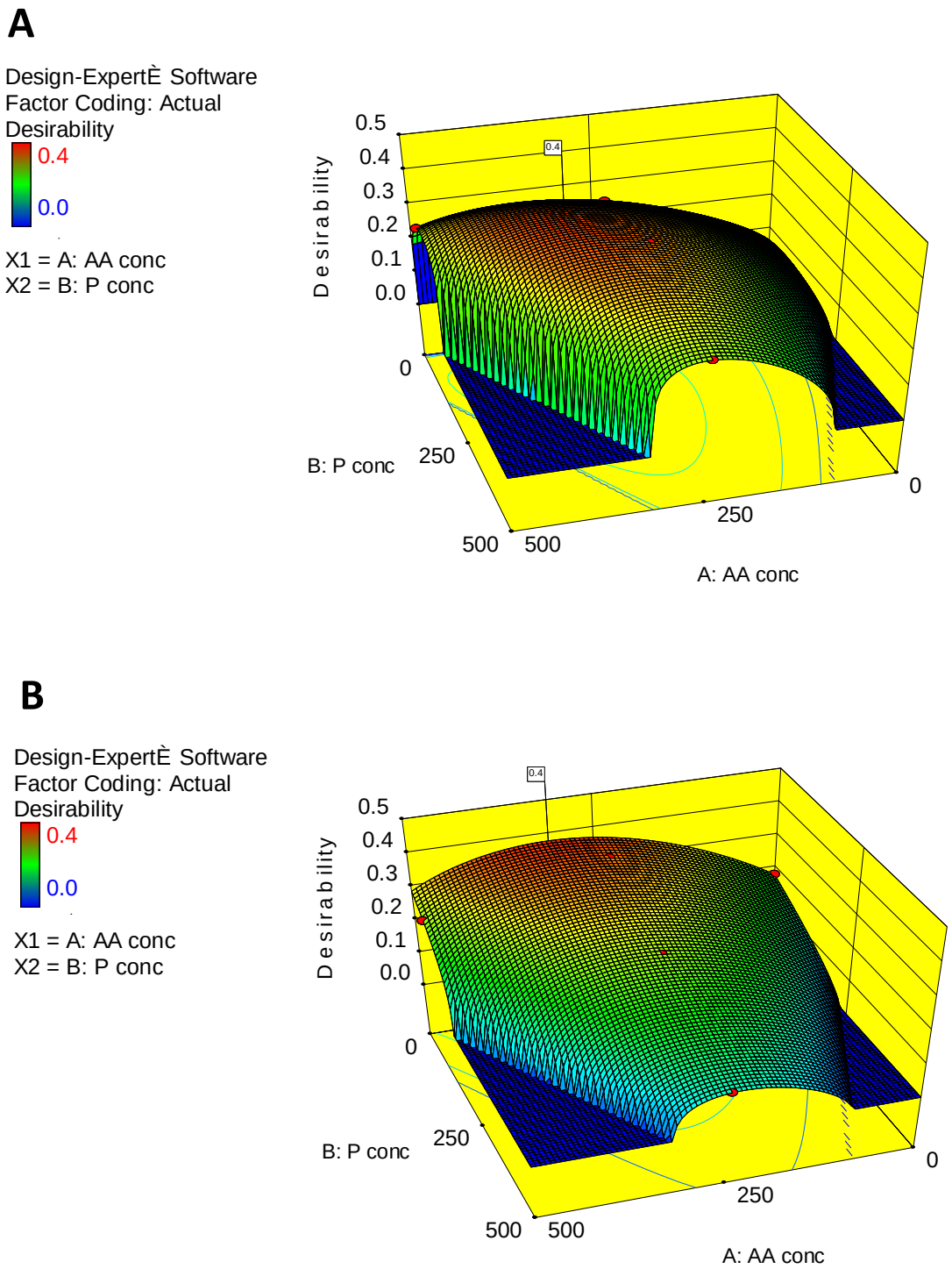

FIGURE 8.3: Optimizing AA+P concentrations. A) When the design was set to find the optimum maximum concentrations of AA and P in combination, suggested concentrations were 340μM AA + 185μM P. To increased both fibrin percentage gel areas and collagen content within the ranges of concentrations used, the suggested optimum concentrations were B) 316μM AA, without proline. (Note: *The position of the flag (optimum condition) in A moved backwards in B, to zero Proline.*)

Appendix A

Example calculations

A.1 Determining UT/mgF of control gels

Fibrinogen stock solution = 20mg/mL
Thrombin stock solution = 200UT/mL

Fibrinogen

Per 35mm petri-dish / well plate:
Fibrinogen = 200μL added

Fibrinogen per petri-dish = (200/1000) mL * 20mg/mL = 4mg

Thrombin

Enzymes: Thrombin and MMP inhibitors AP and AH are added to sDMEM first at volumes of 50μL Thrombin, 2μL AP and 2μL AH per 1mL of medium.
For example, 20mL would contain 1000μL Thrombin, 40μL AP and 40μL in 18.92mL sDMEM $\longrightarrow$ total 20mL.

500μL of these enzymes are added to each petri dish/ well.

UT in 500μL = 5UT [from: 200UT/mL * (50/1000)mL * (0.5mL/1.0mL)]

Therefore UT/mgF = 5UT/4mg = 1.25UT/mgF

A.2 Estimating fibrin gel thickness

petri dish diameter = 35mm
petri dish radius (PDR)=17.5mm
PDR=0.0175 m

Control volume, V_0 = 700μL (from 500μL sDMEM with Thrombin + 200μL fibrinogen)
=0.7 mL
=0.0000007 m^3

Using V=π r^2 h
at control V_0, h_0 = 0.000727565m
h_0= 0.73mm

A.3 Estimating fibrin fibre volume fraction

From:
The hydraulic permeability of blood clots as a function of fibrin and platelet density (Wufsus 2013)

cfbg = fibrinogen concentrations (valid for 1–40mg/mL)
mass density of fibrinogen protein, rho m = 1.4 g/mL = 1400 mg/mL

phi int = internal fibre volume fraction = 0.015 ln(cfbg) + 0.13

overall fibre volume fraction = phi f = cfbg/ (rho m * phi int)

Fibrinogen stock = 20 mg/mL
Units thrombin per well/ petri dish = 5 UT

Fibrinogen Groups
mg Fibrinogen in μL of fibrinogen solution

mg Fibrinogen = volume fibrinogen in mL * stock concentration (20mg/mL)

Table A.1: mg Fibrinogen in increasing fibrinogen volumes.

μL Fibrinogen	mL Fibrinogen	mg Fibrinogen
100	0.1	2
(control)200	0.2	4
500	0.5	10
800	0.8	16

Table A.2: mg Fibrinogen in UT/mgF.

UT/mgF	μL Fibrinogen	mL Fibrinogen	mg Fibrinogen
2.5	117	0.12	2.34
(control) 1.25	200	0.20	4.00
0.5	350	0.35	7.00
0.313	431	0.43	8.62

Table A.3: Fibre volume fractions (ϕ_f) of fibrin gels of increasing fibrinogen volumes or of varying UT/mgF

Fibrinogen mL	UT/mg	mg/mL (cfbg)	phi int	phi f	phi f %
0.1	2.5	3.34	0.15	0.016	1.61
0.2	1.25	5.71	0.16	0.026	2.61
0.5	0.5	10.00	0.16	0.043	4.34
0.8	0.313	12.31	0.17	0.052	5.25

mg/mL (cfbg) were calculated by dividing mg fibrinogen with total volume in petri-dish (given that total volume in petri-dish = mL fibrinogen + mL thrombin in sDMEM).
For example:
mg/mL fibrinogen (cfbg) for 1.25UT/mgF = 4.00mg / 0.7mL = 5.71mg/mL
mg/mL fibrinogen for 800μL fibrinogen (cfbg) = 16mg / 1.3mL = 12.31mg/mL

Note for changing fibrinogen volumes, thrombin in sDMEM was kept constant at 500μL (or 0.5mL), so total petri-dish volume for 800μL fibrinogen volume group would be 800μL fibrinogen + 500μL thrombin in sDMEM = 1300μL (1.3mL).
For changing thrombin to fibrinogen ratios, volumes were made up to a total of 700μL. For the 0.313UT/mgF group, mL fibrinogen = 0.43mL, therefore thrombin in sDMEM was 0.7mL - 0.43mL = 0.27mL.

A.4 Quantifying collagen from standard curve

From the calibration curve prepared from known hydroxyproline concentrations, the sample hydroxyproline contents were obtained using their absorbance readings at 550nm (Figure A.1).

μg/mL hydroxyproline (known) = absorbance (known - used to plot curve)
μg/mL hydroxyproline in sample (unknown, X) = absorbance (known from sample readings)

From best fit line equation: y = mx + c
Sample absorbance (unitless) = (gradient of calibration curve)x + constant
Where x = sample hydroxyproline content

Units check, for sample hydroxyproline:

Using, x =(y - c)/m
x (μg/mL)= (y - constant) * (μg/ mL)
x (μg/mL) = μg/mL

However, of the known hydroxyproline concentrations standards only 50μL was used. Same for the sample.
So actual amount of hydroxyproline in sample:

0.05mL * x μg/mL = μg/mL * 0.05mL
μg = μg

Therefore using basis that hydroxyproline = 13.4% of total collagen then:

μg hydroxyproline in sample * (100/13.4) = sample μg collagen

sample μg collagen/ sample weight μg * 100

OR as equation shown in Chapter 3:

$$\frac{\mu\text{g hydroxyproline in lysate}}{0.134} \times \frac{1}{\mu\text{g dry construct}} \times 100 \qquad \text{(A.1)}$$

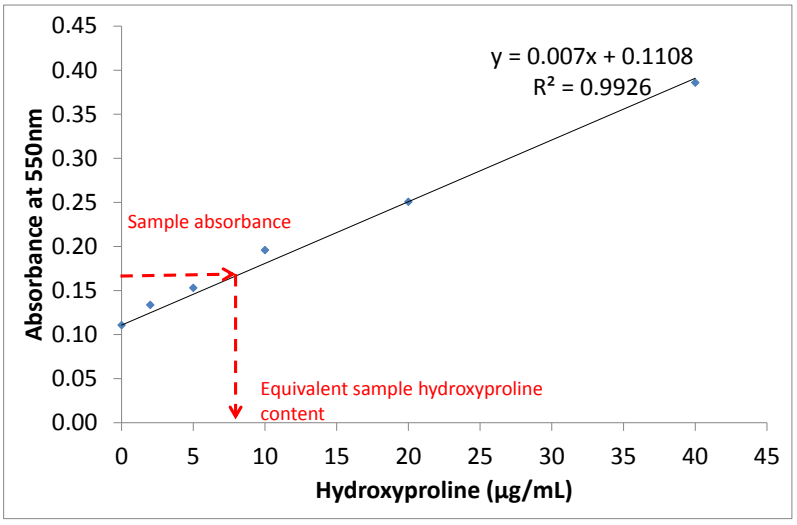

FIGURE A.1: A CTF construct hydroxyproline caliberation curve.

Appendix B

Construct uniformity and anchor parameters

The results in chapter 4 indicted differences in fibrin gel contraction and maximum and minimum widths. To fully attribute the difference in contraction to the supplements, potential sources of error had to be eliminated.

In sections 4.3.1.2 and 4.3.5 maximum and minimum width measurements indicated that constructs did not form uniformly. The ratio of maximum to minimum width was determined to better illustrate this and determine if construct irregularity varied significantly in certain experimental groups and how this difference in construct width differed with culture duration.

Additionally, anchor positioning is necessary to provide tension required for the formation of TE sinew, as without them, the extensive contraction and depletion of the fibrin gel occurs resulting in the formation of small spherical ball.

The distance between the anchors is a parameter that if varied significantly between groups, would lead to inaccurate comparisons. For example, if the anchors are too close together, then it is likely that construct widths would be broader. Conversely, if they are too far apart, this may lead to excessive tension in the middle of the constructs, causing them to snap and contract around each individual anchor. Distances between the anchors from section were measured using day 0 images (see Figure B.1) and no significant differences were observed between the groups. As differences between the percentage gel areas and max/min widths of the constructs were small, especially after 4 weeks in culture then

even minor differences in placing the anchors could have affected the results. Thus a truer measure for comparison was thought to be aspect ratio as this would relate the length and width of individual constructs.

However, anchor distance was not the only factor that could have affected construct fibrin gel area and maximum/minimum widths measurements. Fibrin percentage gel area measurements were conducted such that the area of the anchors at the measurement plane were subtracted from the total area, to give only the area of the fibrin gel (see Chapter 3 section 3.3). As a result, differences in anchor areas could have potentially been the cause of observed differences between supplemented groups rather than the supplements themselves.

B.1 Determining construct length to width (aspect) ratios

The distance between the anchors was measured and divided by the average width to give the construct aspect ratios. The average width was taken to be the the mean of the maximum and minimum width. Measurements and calculations were conducted for each construct (n=7 per group).

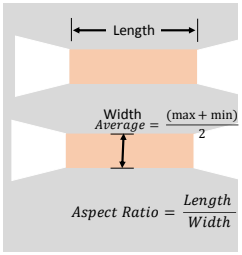

Control

Construct	1	2	3	4	5	6	7	Average	SD
Length	11.68	12.07	10.72	11.85	13.40	11.92	12.51	12.02	0.81

AA+P

Construct	1	2	3	4	5	6	7	Average	SD
Length	12.59	13.16	11.65	12.79	12.22	11.62	12.34	12.34	0.57

AA

Construct	1	2	3	4	5	6	7	Average	SD
Length	11.87	11.03	11.21	11.01	12.87	12.30	11.94	11.75	0.70

P

Construct	1	2	3	4	5	6	7	Average	SD
Length	12.26	13.20	11.94	12.06	11.54	12.88	10.92	12.11	0.77

FIGURE B.1: Dimensions measured for aspect ratio and initial distances (lengths) between anchors. The lengths shown are of constructs in Sections 4.3.1 and 4.3.1.2.

B.2 Construct anchor area measurements

Areas of the anchors (A_i) were calculated using Image J as described in Chapter 3 for fibrin gel percentage areas. Average areas and standard deviations were determined per group as per equations in Figure B.2.

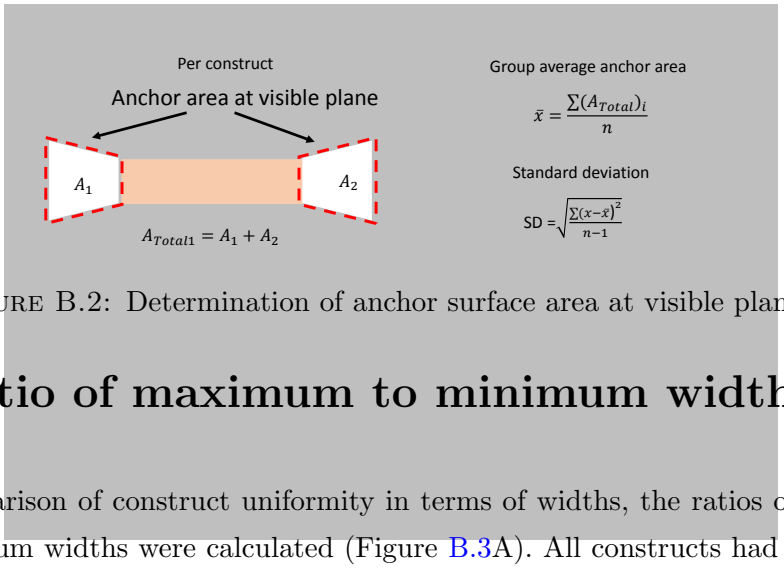

FIGURE B.2: Determination of anchor surface area at visible plane.

B.3 Ratio of maximum to minimum widths

To allow comparison of construct uniformity in terms of widths, the ratios of their maximum to minimum widths were calculated (Figure B.3A). All constructs had maximum to minimum width ratios greater than 1, indicating the non-uniform formation of the constructs and differences were not statistically significant. However, during the first week supplementation with AA+P and AA only resulted in constructs with the lowest ratios of 1.30 ± 0.29 and 1.23 ± 0.16, respectively, suggesting greater uniformity as their average values tended towards 1. The ratio of the control group was 1.74 ± 0.93 and that of the P only group was 1.49 ± 0.34 on day 7. Over the course of the study, supplementation appeared to influence construct widths as treated constructs showed less variability in widths than control constructs. On day 52, the control constructs had the greatest max to min ratio of 1.97 ± 1.31 and showed the greatest variation in width between constructs. Ratios of AA+P, AA and P were 1.64 ± 0.30, 1.53 ± 0.57 and 1.53 ± 0.39, respectively.

B.4 Aspect ratio

To determine the effect of anchor distance on construct widths, the aspect (length to width) ratios were calculated and are shown in Figure B.3B. However, no statistically significant differences were observed between the groups. Construct lengths between the anchors remained constant during the study and as expected the average widths of the constructs contributed to the greatest difference between the groups.

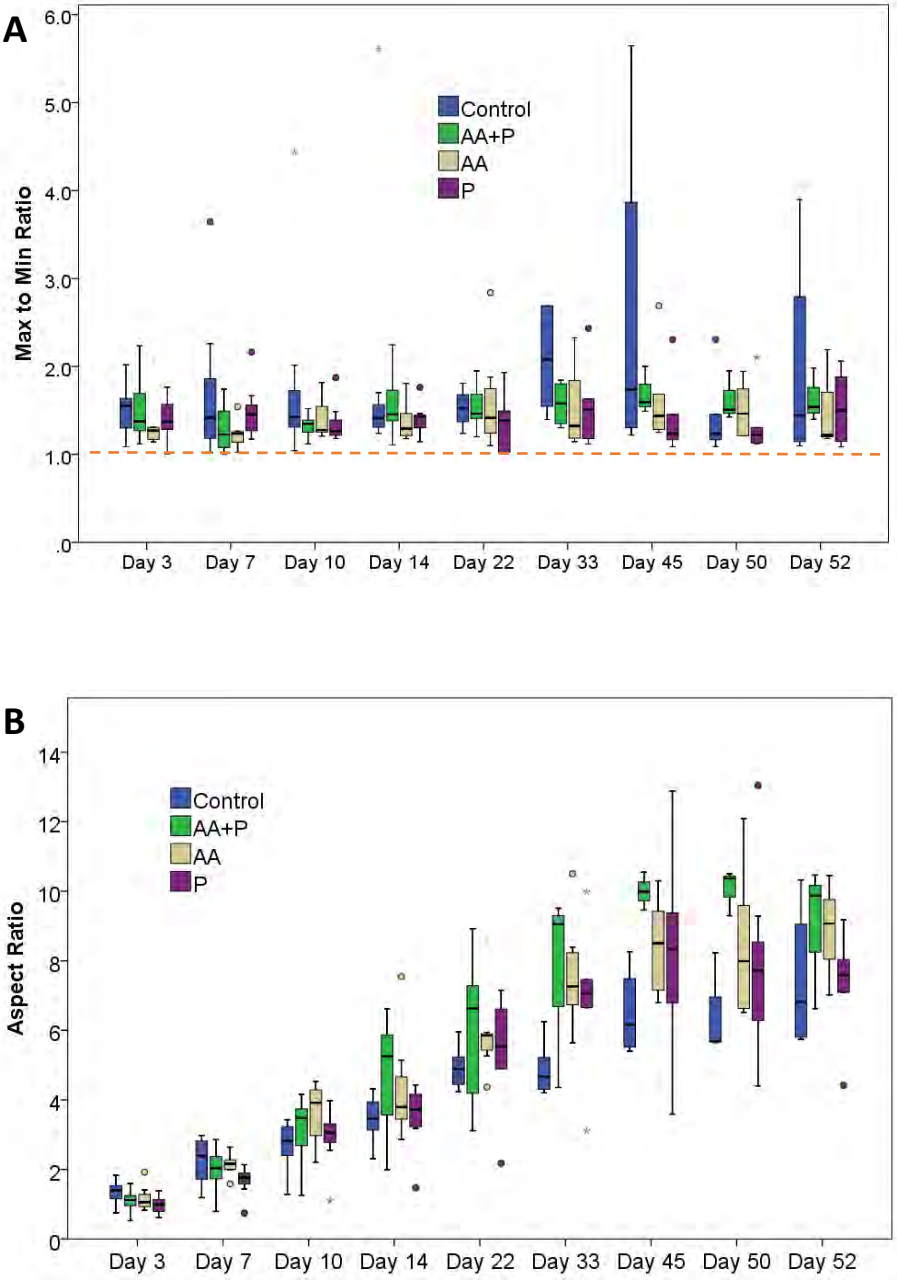

FIGURE B.3: Comparison of construct dimensions. A) Ratio of maximum to minimum widths. A greater tendency towards 1 suggests greater uniformity in construct widths. B) Construct aspect ratio, the relationship between anchor distance and construct width.

B.5 Effect of anchor planar surface area

Figure B.4 shows that there were no significant difference between visible anchor surface areas within individual experiments. Between experiment comparisons indicated that anchors of the initial study, supplementing with AA/ P or AA+P, differed significantly from anchors of the other experiments ($p<0.05$).

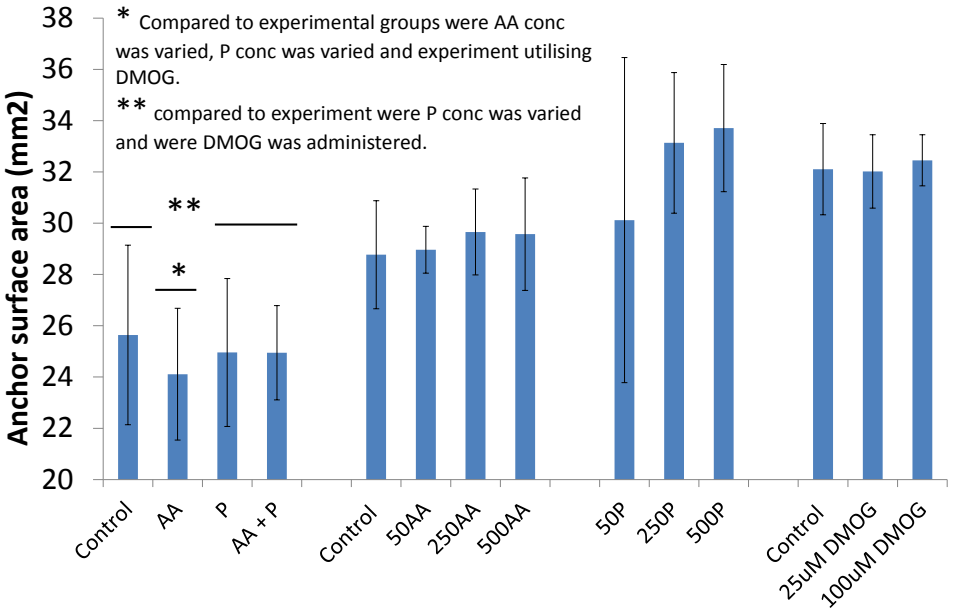

FIGURE B.4: Comparison of average anchor surface areas at visible plane. 2D surface areas of the anchors measured and subtracted from fibrin contraction quantification experiments.

Appendix C

Influence of extrinsic factors on fibrin gel contraction

Cells cultured *in vitro* require the supply of nutrients for growth, which are provided in the form of artificial growth media. According to Freshney (2005), the development of cell culture media began with the use of serum and lymph fluids until Eagle's Minimal Essential Medium (EMEM) was developed in the 1959. Different cell types have varying nutritional needs resulting in the demand for media with compositions that vary. EMEM was developed from the nutritional requirements of mouse L-strain fibroblasts and human uterine carcinoma (HeLa) cells, which required 12/13 similar amino acids and 7 vitamins for survival and growth (Eagle, 1955). EMEM was modified by Dulbecco et al. to DMEM, containing greater amounts of vitamins and glucose. DMEM is considered a general cell culture medium and it also has higher quantities of amino acid and vitamins than the F12 Ham medium (Freshney, 2005). Early research using embryonic chick heart and fibroblast cells for a period of 4 to 5 weeks led to the synthesis of Medium 199 by (Morgan et al., 1950), intended for cell culture without serum. Morgan's analysis of cell culture media available at the time concluded that Medium 199 was suitable for chick fibroblast cell survival rather than growth as significant cell growth was seen only when serum was combined with media such as investigations by Eagle et al. (Morgan, 1958). Due to experimental variability posed by the use of serum, (Ham, 1965) also sought to produce serum free synthetic medium in the form of Ham's medium to culture CHO cells as well as human fibroblasts and chick embryo fibroblasts (Shipley and Ham, 1981). Medium MCDB-201, was specifically developed for chicken fibroblast cells (McKeehan and Ham (1976) as cited by Ham and McKeehan (1978)).

Apart from medium and serum, preparation methods such UV sterilisation affect biopolymer structure and reduce cell adhesion (Fischbach et al., 2001) and freeze-thaw cycles have also been shown to lead to protein degradation and loss of protein activity (Cao et al., 2003; Pikal-Cleland et al., 2000).

Chapter 5 investigated the effects of the fibrin gel mechanics and cell properties such as cell seeding density, passage number and cell type on the rates and extent of contraction of the fibrin hydrogel, collagen content and mechanics of the sinews. These properties were intrinsic to the formation of the TE L/T. This Appendix demonstrates external factors, which do not directly become a physical part of the TE L/T itself affect fibrin contraction. Factors that were investigated include the choice in growth culture medium, which as mentioned above, could affect the activities of the cells; the selection and preparation methods used for fibrinogen, thrombin and serum reagents; and whether duration of TE L/T culture affects sinew mechanics.

C.1 Effect of fibrin reagents and preparation methods

Fibrinogen is purchased in powder form and is dissolved in F12K medium, swirling intermittently, in a water bath at 37°C. It was noted that dissolution time of the fibrin powder can vary. In addition, two types of sterilisation methods were used for fibrinogen, namely, syringe filtration and overnight UV sterilisation. To determine if fibrinogen powder dissolution time at 37°C and sterilization using UV irradiation affected fibrin gel contraction, the percentage gel areas and maximum and minimum widths of the constructs were measured at intervals during the first week. Further, the fibrinogen solutions for UV sterilisation were prepared from fibrinogen powders left to dissolve for 1 hour in the waterbath before leaving to sterilise under UV, whilst the dissolution time fibrinogens were syringe filtered, thereby allowing a comparison of sterilisation methods

C.1.1 Fibrin gel contraction

A fibrinogen powder dissolution time of only 1 hour resulted in the fastest rate of fibrin gel contraction, in comparison to the 3 hour and 6 hour groups. By day 4, the 1 hour constructs had a percentage gel area of $12.62 \pm 1.74\%$ whereas the 3 hour and 6 hour group constructs

had contract to 28.98 ± 7.66% (p=0.000, compared to 1hr) and 25.83 ± 8.93% (p=0.002), respectively (Figure C.1A). Constructs prepared from UV treated fibrinogen showed the greatest extent of contraction. Day 4, percentage gel areas were 6.41 ± 0.62%, 7.09 ± 1.18% and 8.94 ± 5.55%, in that order. Interestingly, the 1 hour fibrinogen dissolution group did not differ significantly from the UV sterilisation groups on day 4, although dissolution groups of 3 and 6 hours did. By day 6, no significant differences were observed between the percentage gel areas of the groups. Maximum and minimum widths on days 4, 6 and 8 also showed no statistically significant differences from each other (Figure C.1B).

As proteins are known to be denatured by repeated freeze-thaw (FT) cycles, the effect of fibrinogen freeze-thaw cycles on fibrin gel contraction was investigated. Percentage gel areas of fibronogen that had undergone 1, 2, 5 and 8 FT cycles were 17.96 ± 3.21%, 15.30 ± 5.10%, 16.32 ± 4.47% and 14.23 ± 7.37%, respectively, on day 3 (Figure C.1C). A 5- to 6-fold reduction in fibrin gel areas occured between days 3 and 8 to 2.90 ± 0.40%, 2.75 ± 0.22%, 3.19 ± 0.37% and 2.24 ± 1.30% for FTs 1,2,5 and 8, in that order. Differences in percentage gel areas of the groups were not statistically relevant and neither were differences in the maximum and minimum widths (Figure C.1D).

C.1.2 Rheology of fibrin gels due to FT cycles and UV sterilisation

The stiffness of fibrin gels from section C.1.1 were quantified to determine if there were differences in stiffness either due to fibrinogen freeze thaw cycles or fibrinogen UV sterilisation times. Fibrin gel stiffness due to thrombin freeze thaw cycles was also evaluated.

C.1.2.1 Fibrin gel mechanical response due to FT cycles or UV sterilisation

At low strains, there were large variation in the G' of all gels signified by the large standard deviations (Figure C.2a and d).

At 1% strain, G' was 6.76 ± 2.35Pa for 1 FT, 12.91 ± 7.06Pa for 5 FT, 23.26 ± 7.63Pa for overnight UV sterilisation, 27.53 ± 6.62Pa for 5 hours UV treatment and 22.90 ± 16.05Pa for 7 hours under UV light. No statistically significant differences were seen between the groups at 1% or 10% strain (Table C.1).

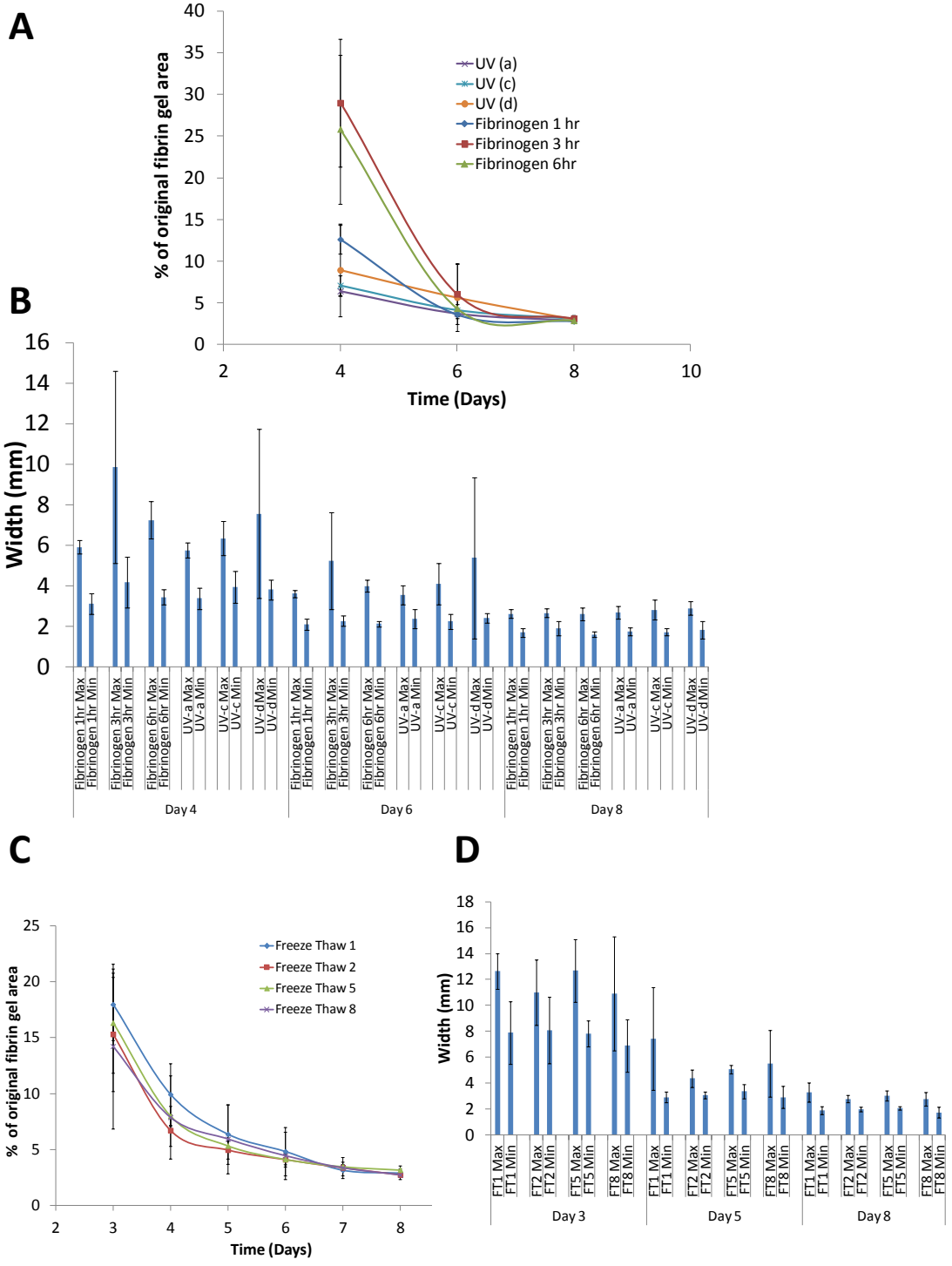

FIGURE C.1: Effect of fibrinogen powder dissolution time, sterilisation method and freeze-thaw cycles on fibrin gel contraction. (A) Percentage gel areas due to fibrinogen preparation methods varied greatly before day 6. However, by day 8, no significant differences were observed between percentage gel areas or max/min widths (B). The investigated freeze-thaw cycles also did not affect construct percentage gel areas (C) or max/min widths (D). *Note: UV(a), UV(b) and UV(c), represent overnight UV sterilisation, 5 hours UV and 7 hours UV, respectively.*

TABLE C.1: G' values at low strain and low frequency.

	G' (Pa)				
	1 FT	**5 FT**	**UV Overnight**	**UV 5.0hrs**	**UV 7.0 hrs**
1% Strain	6.76 ± 2.35	12.91 ± 7.06	23.26 ± 7.63	27.53 ± 6.62	22.90 ± 16.05
10% Strain	6.45 ± 2.45	10.71 ± 4.89	21.29 ± 8.14	20.36 ± 4.99	17.83 ± 13.02
Frequency 1 rad/s	6.98 ± 2.58	11.98 ± 6.29	23.07 ± 7.54	28.26 ± 5.94	23.36 ± 16.60
Frequency 10 rad/s	10.19 ± 4.07	16.80 ± 3.16	26.60 ± 8.67	31.75 ± 6.89	26.49 ± 18.51

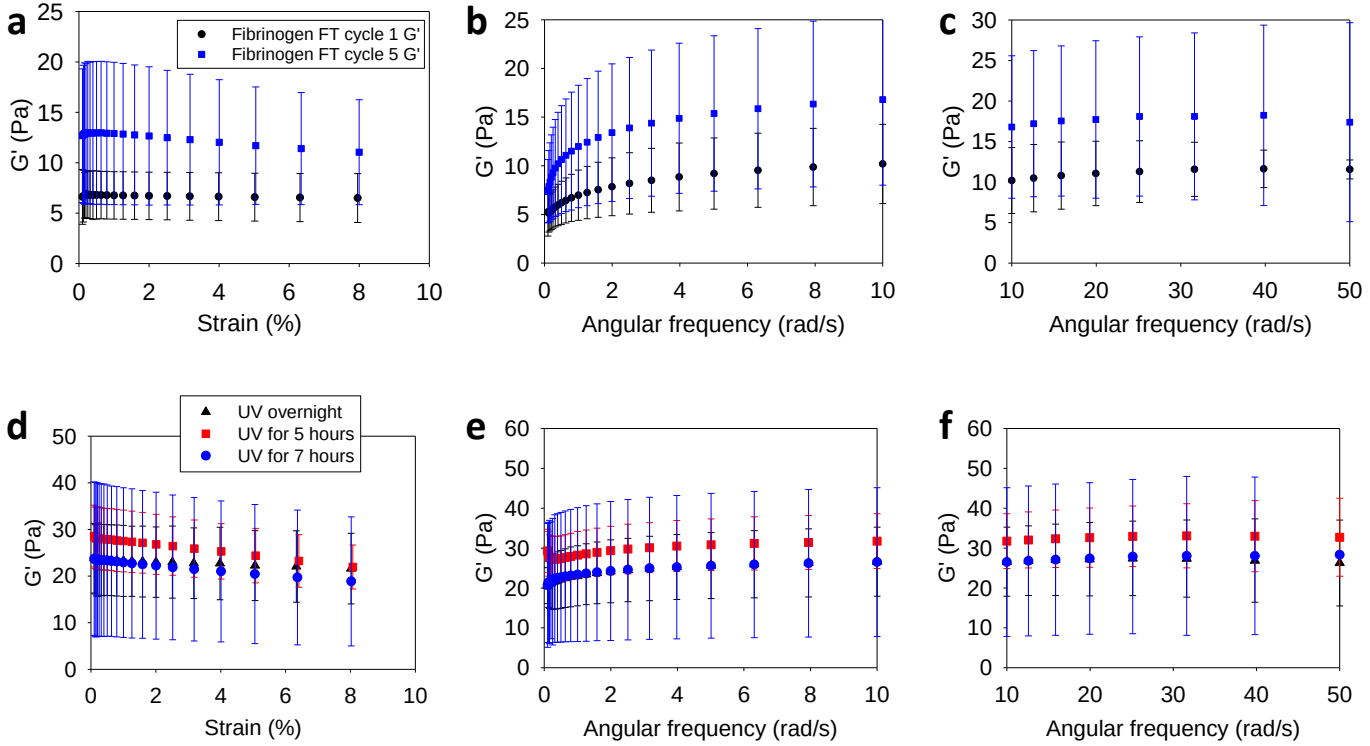

FIGURE C.2: Rheology of fibrin gels of differing freeze thaw cycles and UV sterilisation times. a) Strain sweeps: fibrin gels had a linear response up to 10% strain, b) Freeze -thaw cycles 1–5 did not appear to adversely affect fibrin gel robustness and gels were showed frequency independence, particularly at >50rad/s (c). Fibrin gels sterilised under UV were within the LVR at strains <10% (d). Gels were also robust over the frequency range 0.1–50rad/s (d & e).

Frequency sweeps showed that the gels were frequency independent as no statistical differences were seen at 1rad/s or at 10rad/s for all groups (Table C.1). The freeze-thaw cycles and time under UV irradiation investigated did not appear to affect gel mechanical strength. However, the fibrinogens for freeze thaw cycles experiments were sterilised by syringe filtration from the same stock solutions that were used to prepared fibrinogens for UV sterilisation.

C.1.2.2 Thrombin

Figure C.3A shows the time sweep profiles of gels prepared from varying thrombin freeze-thaw cycles. There was a relationship between the number of thrombin FT cycles and gel storage modulus following gelation for 1 hour as G' was 95.19Pa for 1FT, 76.14Pa for 5FTs and 61.80Pa for 8FTs cycles. In-situ strain sweeps showed the gels exhibited strain hardening behavior. The 5FT strain curve varied from those of 1FT and 8FT, peaking at a G' of 128.6Pa and a lower strain of 15.15% whereas 1FT had a maximum G' at 206Pa and 24.71% strain and 8FT's maximum G' was 143.4Pa and 24.7% strain (Figure C.3B). The gels were also frequency dependent at low frequencies, however, 1FT and 5FT did not differ significantly from each other and were fairly linear between 10-50 rad/s (Figure C.3C). The 8FT gels were not as strong as FT1 and FT5 gels over the frequency range investigated.

C.2 Effect of culture medium type

CTF and PFB constructs in Chapter 7 were fed with different types of media – F12Ham for PFB cells and DMEM for CTFs. As a result, additional variations, apart from that due to cell type, may have occured due to the type of growth medium used to prepare the gels and feed the constructs. To determine if culture medium type affected construct fibrin gel contraction, widths, collagen content and tensile strength, PFB and CTF constructs were prepared using DMEM or F12Ham, for each cell type. In addition, the shear modulus of acellular gels was measured.

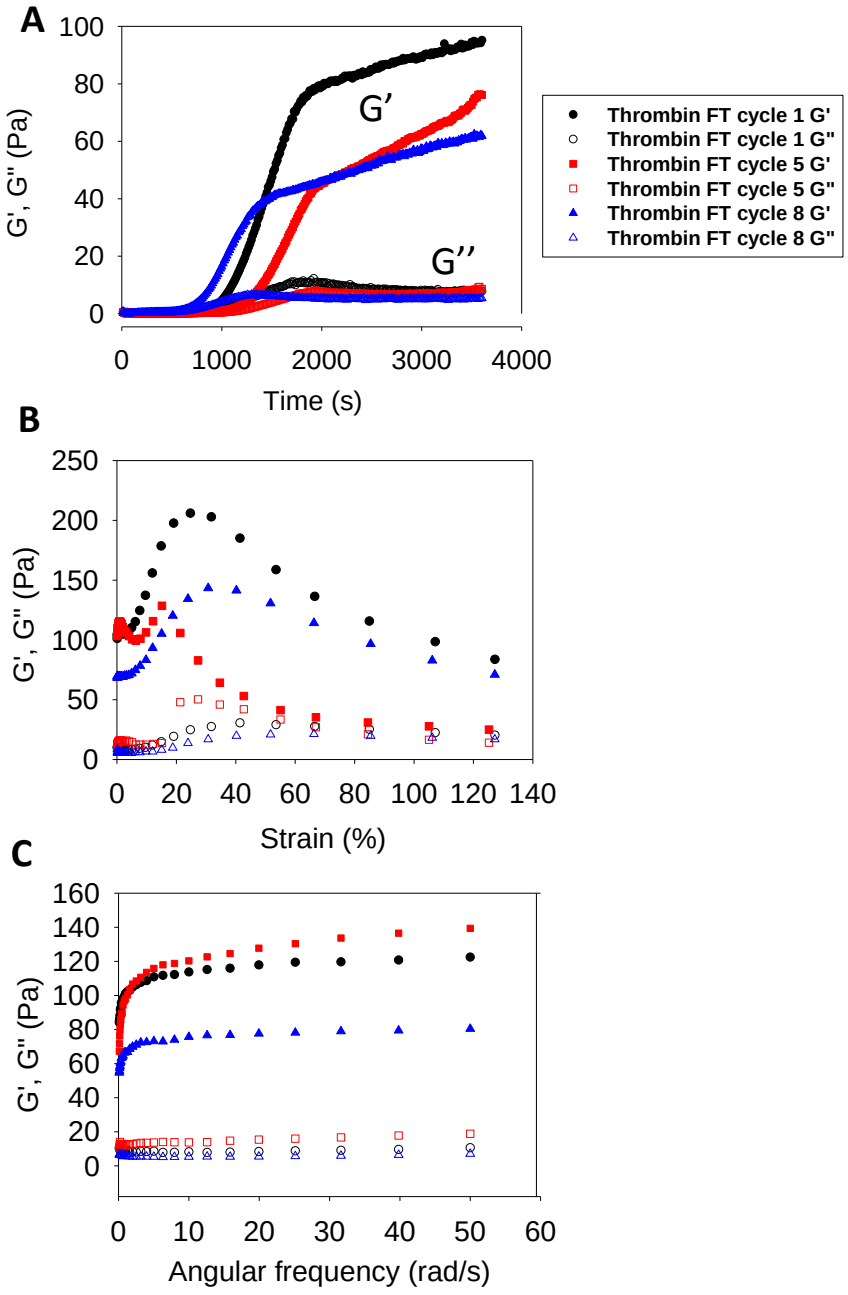

FIGURE C.3: Effect of thrombin FT on fibrin gel mechanical strength. A) Thombin gelation profiles over 1 hour. Increasing freeze-thaw cycles, reduced gel stiffness. B) Strain stiffening non-linear behaviour observed in the gels. C) Gels were fairly robust over frequency range investigated.

C.2.1 Fibrin gel contraction

CTF constructs cultured in either DMEM or F12 Ham appeared denser than PFB constructs (Figure C.4A). PFB constructs did not form well in DMEM and were visibly weaker and more transluscent.

C.2.1.1 Fibrin percentage gel areas

On day 3, no contraction of the fibrin gel was observed for CTF constructs whereas PFB DMEM had contracted the fibrin gel to 17.65 ± 8.55% of its original area and PFB F12 Ham gel areas had reduced to 23.78 ± 9.52%. By day 5, no statistically significant differences were observed in the fibrin gel areas of all groups.

The percentage gel areas of the PFB DMEM group were significantly different from all other groups on day 26 (Figure C.4B) at 1.89 ± 0.28% and 1.13 ± 0.40% on day 28 (p=0.000 in all instances). Fibrin percentage gel areas of groups PFB F12Ham, CTF F12 Ham and CTF DMEM were 3.41 ± 0.38%, 3.52 ± 0.35% and 3.16 ± 0.20% on day 26 and 2.51 ± 0.23%, 2.75 ± 0.22% and 2.34 ± 0.19%, respectively.

C.2.1.2 Maximum and minimum widths

The maximum width of the PFB DMEM group was 2.42 ± 0.38mm on day 26 and this differed only from the CTF F12 Ham group, which had a maximum width of 3.30 ± 0.57mm (p=0.020) (Figure C.4C). PFB DMEM maximum widths of 2.28± 0.36mm on day 28 also differed significantly from the maximum widths of PFB F12 Ham and CTF F12 Ham of 3.00 ± 0.40mm (p=0.026) and 3.12 ± 4 0.46mm (p=0.009). Similarly on day 35, PFB DMEM max width of 2.19 ± 0.34mm was the smallest of groups, differing from the F12 Ham fed groups with maximum widths of 2.90 ± 0.34mm (PFB, p=0.020) and 3.00 ± 0.44mm (CTF, p=0.007).

C.2.2 Sinew collagen content and mechanical strength

Analysis of collagen content in the sinews at 5 weeks revealed that the PFB DMEM group had the lowest collagen content of 4.95 ± 3.01% (Figure C.5). This was 3-fold lower than PFB constructs cultured in F12 Ham, which had an collagen quantity of 15.09 ± 5.56%.

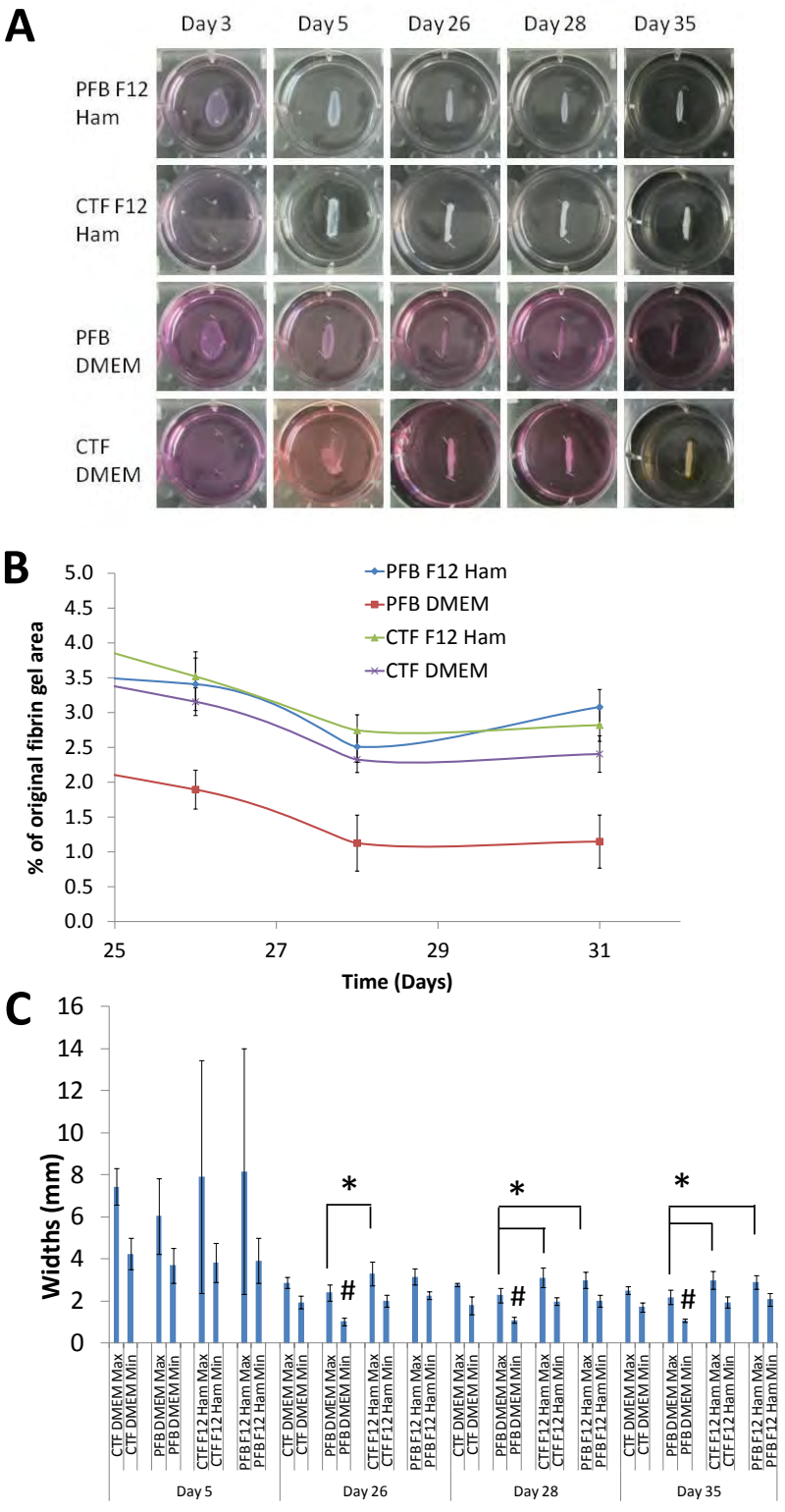

FIGURE C.4: Effect of medium. A) shows images of constructs cultured in DMEM or F12 Ham. B) Percentage gel areas of PFB constructs cultred in DMEM were lowest in week 4. CTF cells grew well in both F12 Ham and DMEM. C) PBF DMEM constructs max/min widths were significantly smaller than for constructs cultured in F12 Ham.

Interestingly, feeding CTF constructs with F12 Ham increased the collagen content from 12.79 ± 3.21% (DMEM) to 17.34 ± 3.76% (p=0.006).

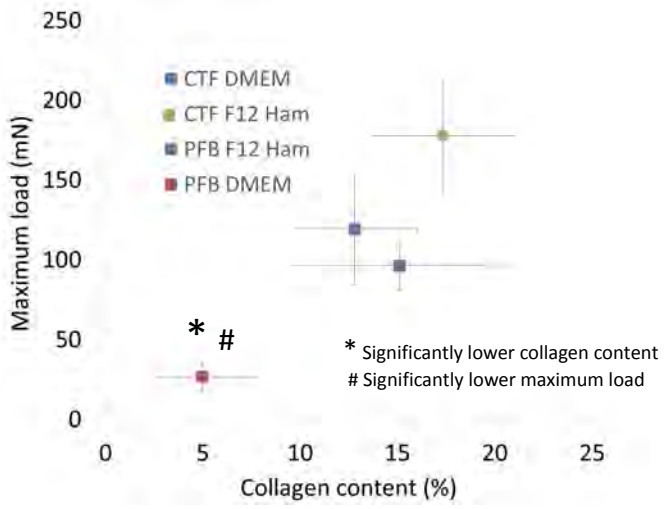

FIGURE C.5: Effect of medium type on construct collagen content and maximum loads. CTF constructs cultured in F12 Ham had a significantly higher collagen content. The maximum load of CTF F12 Ham constructs was also greater than for other groups.

Tensile test results showed PFB DMEM to be weakest, likely due to the low collagen content, as the average maximum load endured by the sinews was only 27 ± 9mN (Figure C.5). The PFB F12 Ham had a maximum load of 97 ± 16mN. The maximum loads of CTF DMEM and CTF F12 Ham were 119 ± 35mN and 178 ± 37mN ($p < 0.05$), respectively.

C.2.3 Rheology of fibrin gels prepared using different media

As the fibrin gels were prepared using different media, it was of interest to determine whether the medium affected the mechanics of the fibrin gel. Strain sweep results indicated that fibrin gels prepared using DMEM were fairly robust at strains <10%, although both DMEM and F12 gels generally exhibited non-linear responses to strain over the range investigated (Figure C.6A and B). G' and G" of gels prepared using F12 Ham were significantly greater than those of the DMEM group. At 1% strain F12 Ham gels had a G' of 36.03 ± 9.31Pa and for DMEM gels G' was 17.4 ± 5.50Pa.

At low frequencies <10rad/s, both gels showed frequency dependent stiffening although differences in G' between data points per group were not statistically significant. At 1

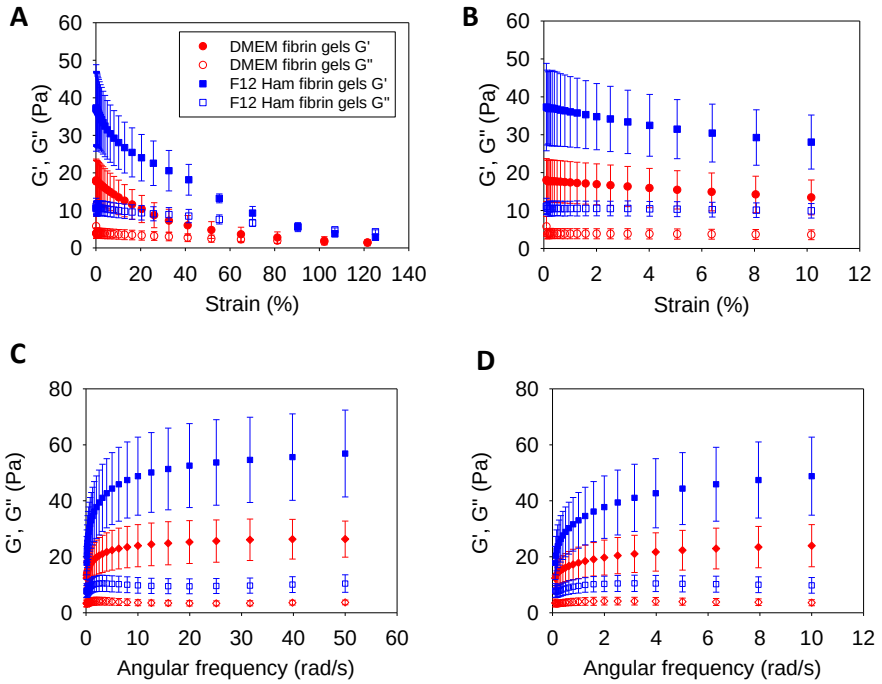

FIGURE C.6: Effect of medium - mechanical performance of gels. (A) shows G' over 0.1 - 120% strain. At low strains <10%, the gels were fairly robust and had a linear response (B). Low freequency dependene was observed, which stabilised after 10 rad/s (C & D).

rad/s, the results wer in correlation with those seen at 1% strain. G' of the F12 Ham fibrin gels was 33.01 ± 9.97Pa and for the DMEM gels G' was 17.85% ± 5.60Pa.

C.2.4 DMEM and Ham's F12 media composition

Table C.2: DMEM and F12 Ham media composition.

Component	Culture Medium		
	DMEM (Sigma D6546) g/L	DMEM (Sigma D5796) g/L	F12 Ham (Sigma N4888) g/L
Inorganic Salts			
Calcium Chloride (CaCl2)	0.2	0.2	0.0333
Fe(NO3)3 • 9H2O	0.0001	0.0001	----
MgSO4	0.09767	0.09767	----
KCl	0.4	0.4	0.224
NaHCO3	3.7	3.7	1.176
NaCl	6.4	6.4	7.599
NaH2PO4	0.109	0.109	0.14204
Cupric Sulfate • 5H2O			0.0000025
Ferrous Sulfate • 7H2O			0.000834
Magnesium Chloride			0.0576
Zinc Sulfate • 7H2O			0.000863
Amino Acids			
L-Alanyl-L-Glutamine	----	----	----
L-Arginine • HCl	0.084	0.084	0.211
L-Cysteine • 2HCl	0.0626	0.0626	----
L-Glutamine	----	----	0.146
Glycine	0.03	0.03	0.00751
L-Histidine • HCl • H2O	0.042	0.042	----
L-Isoleucine	0.105	0.105	0.00394
L-Leucine	0.105	0.105	0.0131
L-Lysine • HCl	0.146	0.146	0.0365
L-Methionine	0.03	0.03	0.00448
L-Phenylalanine	0.066	0.066	0.00496
L-Serine	0.042	0.042	0.0105
L-Threonine	0.095	0.095	0.0119
L-Tryptophan	0.016	0.016	0.00204
L-Tyrosine • 2Na • 2H2O	0.10379	0.10379	0.00778
L-Tyrosine	----	----	----
L-Valine	0.094	0.094	0.0117
L-Alanine			0.009
L-Asparagine • H2O			0.01501
L-Aspartic Acid			0.0133
L-Cysteine • HCl • H2O			0.035
L-Glutamic Acid			0.0147
L-Histidine • 3HCl • H2O			0.02096
L-Proline			0.0345
Vitamins			
Choline Chloride	0.004	0.004	0.01396
Folic Acid	0.004	0.004	0.00132
myo-Inositol	0.0072	0.0072	0.018
Niacinamide	0.004	0.004	0.000037
D-Pantothenic Acid • ½Ca	0.004	0.004	0.00048
Pyridoxal • HCl	----	----	----
Pyridoxine • HCl	0.004	0.00404	0.000062
Riboflavin	0.0004	0.0004	0.000038
Thiamine • HCl	0.004	0.004	0.00034
D-Biotin			0.0000073
Vitamin B12			0.00136
Other			
D-Glucose	4.5	4.5	1.802
HEPES	----	----	----
Phenol Red • Na	0.0159	0.0159	0.0013
Pyruvic Acid • Na	0.11	----	0.11
Hypoxanthine			0.00408
Linoleic Acid			0.000084
Putrescine • HCl			0.000161
Thioctic Acid			0.00021
Thymidine			0.00073
ADD			
NaHCO3	----	----	----
L-Glutamine	0.584	----	----
Glucose	----	----	----

C.2.5 Evaluation of media used during chick fibroblast cell culture

TABLE C.3: Media used during culture of embryonic chick cells.

Cell type	Medium	Serum	Reference
CTF	DMEM	10% New born bovine serum	Gunn and Ehrlich (2012)
CEF	DMEM	10% New born bovine serum	Hazard et al. (2011)
CEF	EMEM with Earle's Salts	10% FBS	Hernandez and Brown (2010)
CTF	DMEM	10% Fetal calf serum	Kapacee et al. (2008)
CSF	DMEM	10% Fetal calf serum	Chiquet et al. (2004)
CEF	MEM or RPI 1640 Medium	10% Fetal calf serum	Hornemann et al. (2003)
CEF	DMEM	8% Fetal calf serum + 2% chick serum	Edom-Vovard et al. (2002)
CEF	Medium 199	2% calf serum + 1% chick serum	Yang and Hawkes (1992)
CEF	EMEM	10% FBS	Rifkin et al. (1979)
CEF	F12 Ham	Fetal calf serum	Conrad et al. (1977)
CHC	EMEM	15% FBS	Schneider et al. (1965)

C.2.6 Composition of different types of media used for chick fibroblast cell culture

Medium 199, RPMI-1640 and MCDB-201 all contain L-Proline, Medium 199 also includes ascorbic acid, RPMI-1640 has L-hydroxyproline and MCDB contains cupric, manganese and zinc sulfates and several other trace elements. In terms of medium costs, Medium 199 is slightly more expensive than DMEM, though RPMI-1640 and MCDB-201 work out slightly cheaper (Table C.5), which suggests medium choice to be performance based although there are few studies to support this.

C.3 Serum sensitivity of CTF cells and effects on fibrin gel contraction

Due to reported contamination of the regular serum brand used during previous TE L/T, it was necessary to find an alternative serum brand. Three types of serum were evaluated blind as serum 1, serum 2 and serum 3 and the fibrin contraction results were compared to the control group of previously published data (see Chapter 4 and Appendix D) and controls of two other experiments (reported as UNW-X, where X refers to experiment number).

All three serum types contracted the fibrin gel at similar rates though serum 3 constructs appeared denser than the other two types (Figure C.7A).

C.3.0.1 Fibrin percentage gel areas

When fibrin gel contraction data were compared, there was variation in the initial rates of contraction, not solely attributable to serum (Figure C.7B). Day 7 percentage gel areas were 14.83 ± 2.31%, 15.67 ± 1.86%, 12.57 ± 3.44% and 12.36 ± 5.64% for serum 1, serum 2, serum 3 and unw-3 control group, respectively. Percentage gel areas of serum 1-3 and unw-3 published data showed no statistically significant differences on days 7 and 9.

C.3.0.2 Maximum and minimum widths

Maximum widths of the unw-3 control group were 11.41 ± 3.12mm and minimum widths were 7.93 ± 3.39mm, which were significantly lower than for serum 1, 2 and 3, whose

TABLE C.4: Comparison media used during culture of chick embryo cells.

Component	Medium 199 Sigma M2154 g/L	Component	RPMI-1640 Sigma R0883 g/L	Component	MCDB-201 Sigma M6770 g/L
Inorganic Salts		**Inorganic Salts**		**Inorganic Salts**	
CaCl2 • 2H2O	0.2	Ca(NO3)2 • 4H2O	0.1	Ammonium Metavanadate	0.000000006
Fe(NO3)3 • 9H2O	0.00072	MgSO4 (anhydrous)	0.04884	Calcium Chloride(anhydrous)	0.2219
MgSO4 (anhydrous)	0.09767	KCl	0.4	Cupric Sulfate•5H2O	0.00000025
KCl	0.4	NaHCO3	2	Ferrous Sulfate•7H2O	0.001668
KH2PO4	---	NaCl	6	Magnesium Sulfate (anhydrous)	0.18057
Na • Acetate (anhydrous)	0.05	Na2HPO4 (Anhydrous)	0.8	Manganese Sulfate	0.000000075
NaHCO3	---			Molybdic Acid•4H2O (ammonium)	0.000000618
NaCl	6			Nickel Chloride•6H2O	0.0000000012
Na2HPO4	----			Potassium Chloride	0.22365
NaH2PO4 (anhydrous)	0.122			Sodium Chloride	7.599
				Sodium Metasilicate•9H2O	0.000142
				Sodium Phosphate Dibasic (anhydrous)	0.07099
				Sodium Selenite	0.000000865
				Zinc Sulfate•7H2O	0.000028744
Amino Acids		**Amino Acids**		**Amino Acids**	
L-Alanine	0.025	L-Alanyl-L-Glutamine	----	L-Alanine	0.00891
L-Arginine • HCl	0.7	L-Arginine • HCl	0.2	L-Arginine•HCl	0.0632
L-Aspartic Acid	0.03	L-Asparagine • H2O	----	L-Asparagine•H2O	0.15
L-Cystine • HCl • H2O	0.00011	L-Asparagine	0.05	L-Aspartic Acid	0.01331
L-Cysteine • 2HCl	0.026	L-Aspartic Acid	0.02	L-Cysteine•HCl•H2O	0.03513
L-Glutamic Acid	0.0668	L-Cystine • 2HCl • H2O	0.0652	L-Glutamic Acid	0.01471
L-Glutamine	0.1	L-Glutamic Acid	0.02	L-Glutamine	0.14615
Glycine	0.05	L-Glutamine	----	Glycine	0.00751
L-Histidine • HCl • H2O	0.02188	Glycine	0.01	L-Histidine•HCl•H2O	0.02097
Hydroxy-L-Proline	0.01	L-Histidine • HCl • H2O	0.015	L-Isoleucine	0.01312
L-Isoleucine	0.02	Hydroxy-L-Proline	0.02	L-Leucine	0.03935
L-Leucine	0.06	L-Isoleucine	0.05	L-Lysine•HCl	0.03654
L-Lysine • HCl	0.07	L-Leucine	0.05	L-Methionine	0.00448
L-Methionine	0.015	L-Lysine • HCl	0.04	L-Phenylalanine	0.00496
L-Phenylalanine	0.025	L-Methionine	0.015	L-Proline	0.00576
L-Proline	0.04	L-Phenylalanine	0.015	L-Serine	0.03153
L-Serine	0.025	L-Proline	0.02	L-Threonine	0.03574
L-Threonine	0.03	L-Serine	0.03	L-Tryptophan	0.00613
L-Tryptophan	0.01	L-Threonine	0.02	L-Tyrosine•2Na•2H2O	0.01135
L-Tyrosine • 2Na • 2H2O	0.05766	L-Tryptophan	0.005	L-Valine	0.03513
L-Valine	0.025	L-Tyrosine • 2Na • 2H2O	----		
		L-Tyrosine	0.02184		
		L-Valine	0.02		
Vitamins		**Vitamins**		**Vitamins**	
Ascorbic Acid • Na	0.0000566	D-Biotin	0.0002	D-Biotin	0.00000733
D-Biotin	0.00001	Choline Chloride	0.003	Choline Chloride	0.01396
Calciferol	0.0001	Folic Acid	0.001	Folinic Acid (calcium)	0.00000512
Choline Chloride	0.0005	myo-Inositol	0.035	myo-Inositol	0.01802
Folic Acid	0.00001	Niacinamide	0.001	Niacinamide	0.00611
Menadione (sodium bisulfite)	0.000016	p-Aminobenzoic Acid	0.001	D-Pantothenic Acid (hemicalcium)	0.000477
myo-Inositol	0.00005	D-Pantothenic Acid • ½Ca	0.00025	Pyridoxine•HCl	0.0000617
Niacinamide	0.000025	Pyridoxine • HCl	0.001	Riboflavin	0.000113
Nicotinic Acid	0.000025	Riboflavin	0.0002	Thiamine•HCl	0.000337
p-Amino Benzoic Acid	0.00005	Thiamine • HCl	0.001	Vitamin B-12	0.000136
D-Pantothenic Acid • ½Ca	0.00001	Vitamin B12	0.000005		
Pyridoxal • HCl	0.000025				
Pyridoxine • HCl	0.000025				
Retinol Acetate	0.00014				
Riboflavin	0.00001				
DL-a-Tocopherol Phosphate • Na	0.00001				
Thiamine • HCl	0.00001				
Other		**Other**		**Other**	
Adenine Sulfate	0.01	D-Glucose	2	Adenine•HCl	0.000172
Adenosine Triphosphate • 2Na	0.001	Glutathione (reduced)	0.001	D-Glucose	1.441
Adenosine Monophosphate • Na	0.0002385	Phenol Red • Na	0.0053	Linoleic Acid	0.0000841
Cholesterol	0.0002			Putrescine•2HCl	0.000000161
Deoxyribose	0.0005			HEPES	7.149
Glucose	1			Phenol Red•Na	0.001242
Glutathione (reduced)	0.00005			Pyruvic Acid•Na	0.055
Guanine • HCl	0.0003			Thioctic Acid	0.00000206
HEPES	----			Thymidine	0.0000727
Hypoxanthine	0.0003				
Phenol Red • Na	0.0213				
TWEEN	0.02				
Ribose	0.005				
Thymine	0.0003				
Uracil	0.0003				
Xanthine • Na	0.000344				
ADD		**ADD**		**ADD**	
L-Glutamine	0.1	L-Glutamine	0.3	Required supplements	
Sodium Bicarbonate	----	NaHCO3	----	-----	
Serum for long-term culture		Required supplements			

TABLE C.5: Comparison of tissue culture medium costs.

Cat. No.	Medium	Cost (£) per 500mL bottle
D6546	DMEM (without L-Glutamine and pyruvate)	21.00
D5796	DMEM (with L-Glutamine)	18.10
M2154	Medium 199 with Earle's salts	28.30
M6770	MCDB 201 (sold as powder for 1L at a cost of £37.90)	18.95
R0883	RPMI-1640	18.00

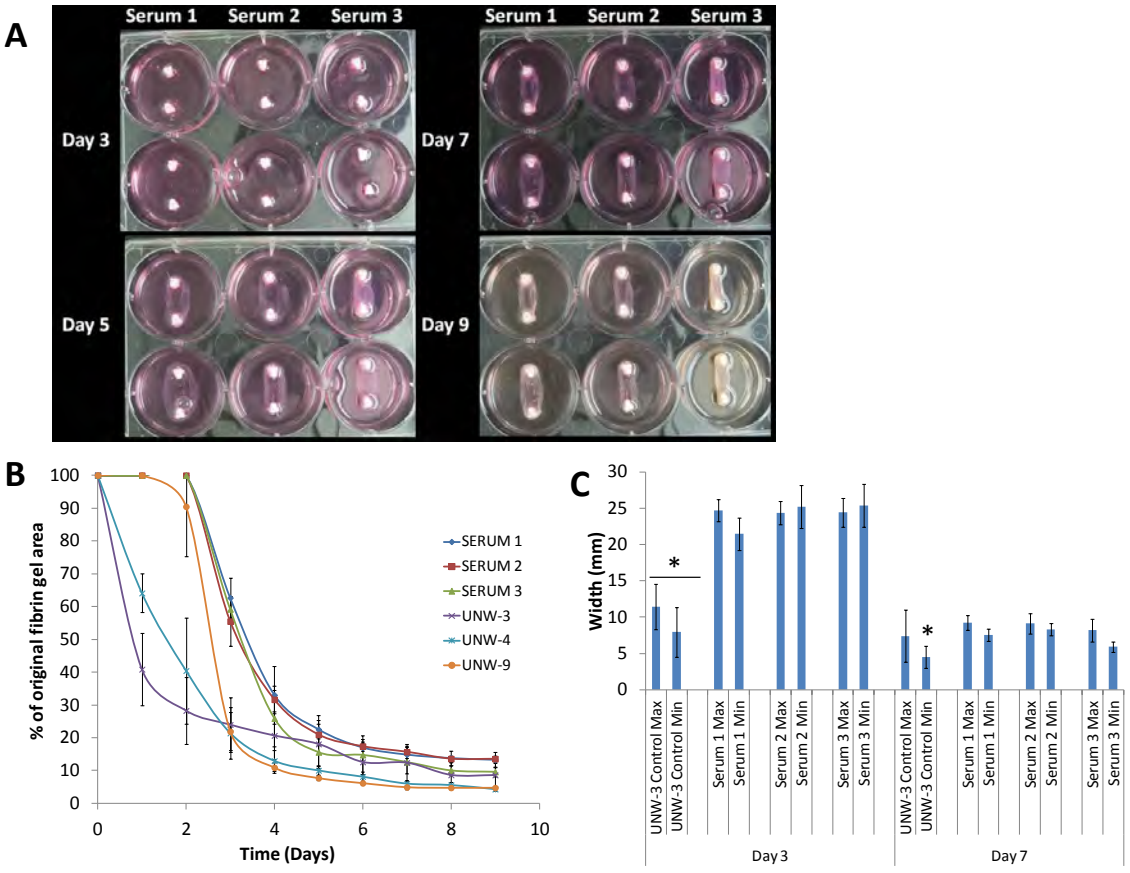

FIGURE C.7: Serum type effects on contraction. (A) Images of constructs fed with media containing different types of serum. (B) Variation in percentage gel areas in the first 4 days did not appear to be related to serum as groups UNW-3, UNW-4 and UNW-9 were prepared using the same type. No statistically significant differences were observed. (C) Max/min widths of constructs fed with serum 1, 2 and 3, diiffered from that of published data on day 3 and 7 for the min width.

average maximum widths were all about 24 ± 2mm on day 3 (Figure C.7C). On day 7, all maximum widths were not significantly different from each other.

C.4 Effect of temperature

Generally, constructs were maintained in an incubator at 37°C and reagents/media were pre-warmed to this temperature before use. Care was taken to avoid drastic drops in temperature. However, it was of interest to determine how minor temperature fluctuations would affect fibrin gel mechanical strength.

At 25°C, the gels were stiffer with a G' of 15.14 ± 3.24Pa. With increasing temperature, G' fell to 13.58 ± 2.57Pa at 28°C, 10.74 ± 1.53Pa at 28°C, 10.74 ± 1.53Pa at 35°C, 9.47 ± 1.47Pa at 37°C and 8.97 ± 1.40Pa at 38°C. Between 35°C and 38°C, differences in G' were not statistically significant, however, G' at these temperatures varied from the G' at 25°C ($p < 0.05$).

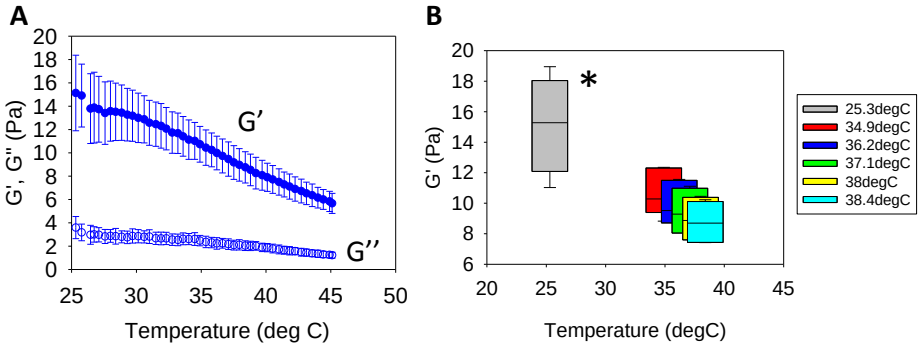

FIGURE C.8: Effect of temperature fluctuations of fibrin gel mechanics. (A) Gel stiffness fell with increasing temperature. (B) G' at 25°C differed signifcantly with G' between 35°C and 38°C.

C.5 Effect of culture duration on construct mechanical strength

Generally, constructs for contraction studies were maintained in culture for a period of 5 weeks. However, to determine if duration of culture affected construct mechanical strength, particularly at weeks 4 or 5, tensile tests of NT constructs were conducted.

Generally, maximum loads withstood by the sinews increased with increasing culture duration. Week 3 maximum loads were 99 ± 54mN, week 4 maximum loads were 112 ± 45mN and 120 ± 27mN at week 5, however, increases in load were not statistically significant (Figures C.9A). Sinew stiffness did increase with culture time as average strains at the maximum load at week 5 were lower at 2.39 ± 1.12 than at week 3 at 2.94 ± 0.69, p >0.05, (Figure C.9B). Young's Modulus values reflected this, with values of 15 ± 10kPa, 25 ± 11kPa and 31 ± 23kPa for weeks 3, 4 and 5, respectively (Figure C.9C). The duration of culture had a significant effect on collagen content in the sinews (Figure C.9D). Week 5 construsts had the highest collagen content of 15.60 ± 4.28%, which varied considerably from week 4 with 10.50 ± 4.34% (p=0.002, compared to week 5) and week 3 with 9.25 ± 3.07% (p=0.000).

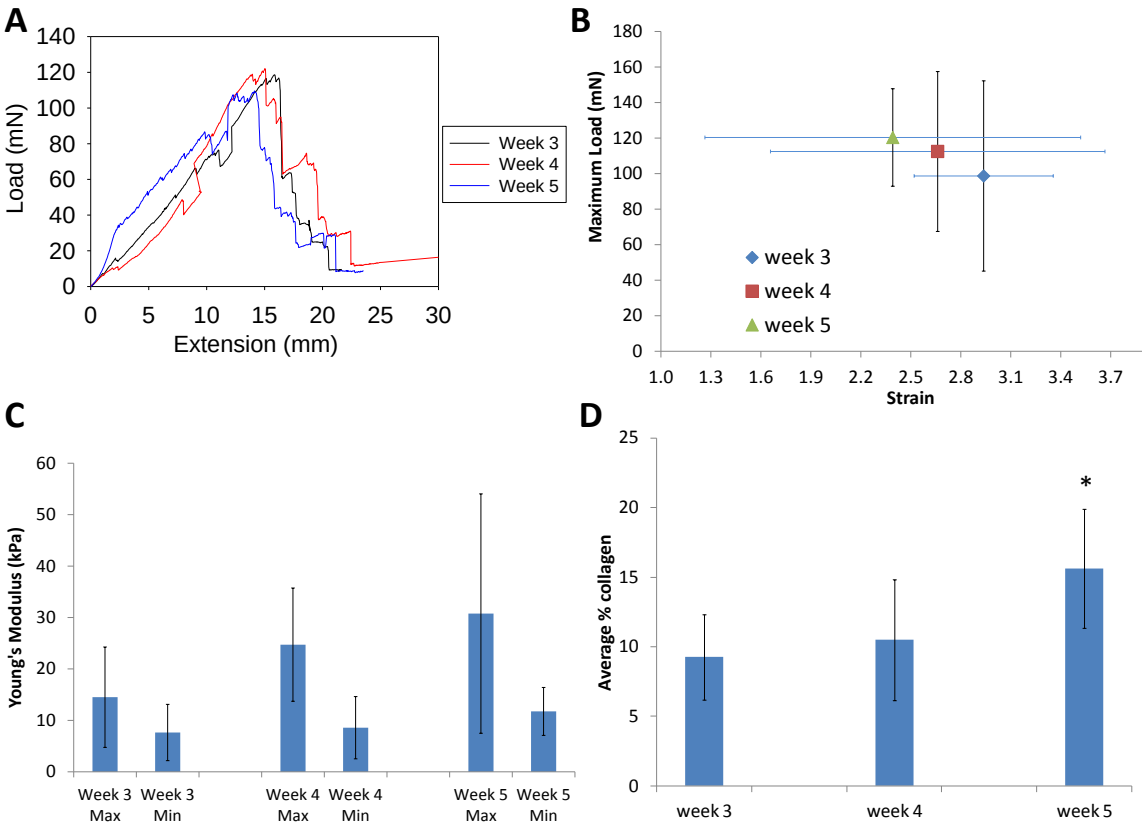

FIGURE C.9: Effect of culture time on construct mechanics. No significant differences were observed in the maximum loads achieved by 3, 4 or 5 week old sinews although at week 5, constructs were slightly stiffer (B) and (C). Week 5 had a significantly higher collagen content than weeks 4 or 3 (D).

Appendix D

Publication

D.1 Monitoring Sinew Contraction During Formation of Tissue-Engineered Fibrin-Based Ligament Constructs

TISSUE ENGINEERING: Part A
Volume 18, Numbers 15 and 16, 2012

DOI: 10.1089/ten.tea.2011.0535

Original Article

Monitoring Sinew Contraction During Formation of Tissue-Engineered Fibrin-Based Ligament Constructs

Jennifer Z. Paxton, Ph.D.,[1] Uchena N.G. Wudebwe, M.Eng.,[1] Anqi Wang, Ph.D.,[1,2] Daniel Woods, Ph.D.,[3] and Liam M. Grover, Ph.D.[1]

The ability to study the gross morphological changes occurring during tissue formation is vital to producing tissue-engineered structures of clinically relevant dimensions *in vitro*. Here, we have used nondestructive methods of digital imaging and optical coherence tomography to monitor the early-stage formation and subsequent maturation of fibrin-based tissue-engineered ligament constructs. In addition, the effect of supplementation with essential promoters of collagen synthesis, ascorbic acid (AA) and proline (P), has been assessed. Contraction of the cell-seeded fibrin gel occurs unevenly within the first 5 days of culture around two fixed anchor points before forming a longitudinal ligament-like construct. AA + P supplementation accelerates gel contraction in the maturation phase of development, producing ligament-like constructs with a higher collagen content and distinct morphology to that of unsupplemented constructs. These studies highlight the importance of being able to control the methods of tissue formation and maturation *in vitro* to enable the production of tissue-engineered constructs with suitable replacement tissue characteristics for repair of clinical soft-tissue injuries.

Introduction

In vitro engineering of connective tissues for surgical implantation is an active field of research. In particular, the manufacture of suitable artificial tissues for replacement of the anterior cruciate ligament (ACL) is receiving much interest, as each year an estimated 80,000 to 100,000 ACL ruptures occur in the United States alone.[1] The majority of these injuries occur in young, active individuals,[2] and failure to repair the injured tissue will result in joint instability,[3] pain,[1] injury to other structures within the knee joint,[3] muscle weakness,[4] and the subsequent development of osteoarthritis.[5,6] While attempts have been made to repair the ACL with synthetic graft replacements (e.g., Gore-tex, Dacron, and carbon fibers), problems resulting from the mechanical breakdown of the grafts mean that transplantation of an autograft to the injured site remains the most successful method of ACL repair. However, because of problems such as pain,[7,8] muscle weakness,[4] patellar tendonitis,[9] and donor-site morbidity[10] after autograft treatment, tissue-engineered constructs are now being investigated for implantation.

We have recently shown that complete bone-ligament-bone constructs for potential implantation and repair of the ACL can be formed *in vitro* using brushite anchors and a cell-seeded fibrin gel.[11] However, little attention has been given to the three-dimensional (3D) morphology of the soft-tissue portion of the graft during construct formation and the effects of anabolic supplementation on morphology. Such information is desirable to predict the long-term size and shape of construct grafts for implantation. While conventional imaging techniques, such as histology, usually allow only visualization of the tissue using destructive methods, we have used the nondestructive optical coherence tomography (OCT) imaging technology alongside conventional digital imaging to visualize the morphology of constructs during their formation and maturation phases.

OCT is an emerging imaging technology for the biological and medical sciences. It enables imaging of 1–2-mm inside opaque tissue without any special preparation, making it an ideal nondestructive adjunct to histology. Also, the use of low-power infrared light means that OCT is also noncontact, noninvasive, and capable of providing high-resolution images at a video rate. OCT works by focusing a beam of light inside a sample, and the depth positions of multiple subsurface structures are then determined by performing frequency-domain time-of-flight measurements on the backscattered light, resulting in a tomographic depth-reflectivity profile (A-scan). One- and two-dimensional (2D) scanning of

[1]School of Chemical Engineering, College of Physical Sciences and Engineering, University of Birmingham, Edgbaston, Birmingham, United Kingdom.
[2]School of Dentistry, College of Medical and Dental Sciences, University of Birmingham, St Chad's Queensway, Birmingham, United Kingdom.
[3]Michelsons Diagnostics, Orpington, Kent, United Kingdom.

the focused beam can then be used to make 2D and 3D images of the sample. Recently, OCT has been used within many different fields of research from cancer biology[12,13] and development[14–16] to clinically within cardiology[17] and ophthalmology[18–20] owing to the nondestructive nature of the technique and the ability to visualize inside tissues and organisms. Furthermore, it has also received great attention within the tissue engineering field, having been described as a technique with great promise for visualizing engineered tissues.[21] Many groups have utilized this imaging technique to study scaffold morphologies,[21–26] collagen gel remodeling,[27] and collagen fiber alignment.[28]

The aim of this study was to investigate the morphological changes occurring during the early-stage formation and maturation of tissue-engineered bone-to-bone ligament-like constructs manufactured from fibroblast-seeded fibrin gels. Digital imaging, OCT, and histological techniques were used to evaluate construct development over time.

Materials and Methods

β-Tricalcium phosphate manufacture

The β-tricalcium phosphate (β-TCP; $Ca_3(PO_4)_2$) was manufactured by reactive sintering of a powder containing $CaHPO_4$ (Mallinckdrodt-Baker) and $CaCO_3$ (Merck), with a theoretical calcium to phosphate molar ratio of 1.5. The powder mixture was suspended in absolute ethanol and mixed for 12 h. After this, the suspension was filtered and the resulting cake heated in an alumina crucible to 1400°C for 12 h and 1000°C for 6 h before quenching in a dessicator in ambient conditions. The resulting sinter cake was then crushed using a pestle and a mortar, and was passed through a 125-μm sieve.

Brushite cement formation

The brushite cement was made by incrementally combining β-TCP ($Ca_3(PO_4)_2$) with 3.5 M orthophosphoric acid (H_3PO_4; Sigma-Aldrich) at a ratio of 3.5 mg/mL to form a paste. Citric acid (200 mM; Sigma-Aldrich) and sodium pyrophosphate (200 mM; Sigma-Aldrich) were added to the H_3PO_4 before combination with β-TCP. The paste was consolidated into a custom-made silicone mold,[29] and mold-filling was improved with the use of a vibrating platform (Denstar 500; National Dental Supplies) for 60 s. Stainless steel insect pins (0.2-mm diameter; Fine Science Tools) were inserted into each anchor before setting occurred, and cement anchors were left to set within their molds overnight at 37°C. Final cement anchors were trapezoidal in shape, measuring $\sim 4 \times 4$ mm at the widest points and 3 mm in height as described previously.[11,29]

Ligament-like construct formation

Thirty-five-millimeter Petri dishes were coated with 1.5 mL of Sylgard (type 184 silicone elastomer; Dow Corning Corporation) and left to polymerize for at least a week before use. Cement anchors were removed from their molds and pinned to the sylgard layer ~ 12 mm apart, and the anchors and plate were sterilized by soaking in 70% ethanol for 20 min. The Sylgard layer was used to allow immobilization of the cement anchors and to provide a non-cell-adhesive surface underneath the fibrin gel. Five hundred microliters of the Dulbecco's modified Eagle's medium (DMEM; Invitrogen) supplemented with 10% fetal bovine serum (FBS; Biosera), 1% penicillin/streptomycin (P/S; Invitrogen), 50 U/mL thrombin (Calbiochem), 400 μM aminohexanoic acid (Sigma-Aldrich, UK), and 20 μg/mL aprotinin (Roche) solution was used to coat the Sylgard layer. Two hundred microliters of 20 mg/mL fibrinogen (Sigma-Aldrich) was then added dropwise, and the fibrin gel was left to polymerize at 37°C for 1 h. Embryonic chick tendon fibroblasts were isolated from the flexor tendons of 13.5-day-old chick embryos by a 1.5-h digestion in the collagenase type-II solution (in serum- and antibiotic-free DMEM) at 37°C. After digestion, the solution was passed through a 100-μm cell strainer (BD Biosciences) to remove any insoluble material. The cell solution was spun at 2500 rpm for 3 min. The resulting cell pellet was suspended in the DMEM supplemented with 10% FBS and 1% P/S (Invitrogen). Chick tendon fibroblasts were cultured and split routinely, and used between passages 2 and 5. Cells were seeded on top of the polymerized fibrin gel at a concentration of 100,000 cells in 1 mL. The growth medium (DMEM + 10% FBS + 1% P/S) was replenished on day 3 after seeding, and then every 2–3 days for the duration of the experiments. On day 7 of formation, half the ligament-like constructs received supplementation with 250 μM ascorbic acid 2-phosphate (AA; Sigma-Aldrich) and 50 μM L-proline (P; Sigma-Aldrich) added to the growth medium. Day 7 was chosen, as it was in line with previous work.[11,29] This supplementation regime was continued on every day of medium replenishment in the AA + P-treated samples. Over time, the fibrin gel contracts around the two brushite cement anchors to form a cement-cellularized fibrin gel–cement (bone-ligament-bone) construct.

Optical coherence tomography

Ligament-like constructs were scanned using a high-resolution EX1301 MultiBeam OCT microscope daily from day 0 to day 7, followed by day 10, day 14, and then every 7 days until day 35 ($n = 16$ in each treatment group). The day-0 scans were taken after the addition of cells in the growth medium. The microscope was equipped with a Santec HSL-2010 swept-source laser with a spectral range of 150 nm spectrum centered at 1310 nm. The measured resolution was < 9 μm axially (depth) and < 7.5 μm laterally. The frequency of A-scans was at a rate of 10,000/s. Optical B-Scans comprising 1188 A-Scans and spanning ~ 5 mm laterally and 1.9 mm in depth (1188×460 pixels) were captured showing cross sections of the ligaments in the longitudinal orientations. For transverse orientations, B-scans comprised 242–1118 A-scans depending on the diameter of the construct at the time of scanning. Multiple parallel B-Scan image sets with fixed spatial periodicity were also acquired by moving the sample orthogonally to the B-Scan direction on an automated translation stage in 4-μm steps. Using this technique, 3D volumes of ligament-like constructs can be digitally reconstructed with dimensions up to $5 \times 25 \times 1.9$ mm for fly-through examination. Constructs were scanned in their Petri dishes, in the growth medium, with the Petri dish lid removed. Consequently, each sample could only be used for one time point per scan. Images of the constructs were also taken using a digital camera (Optio V10; Pentax Corporation) at the same time points as the scans. Constructs that have not been assigned for time-point scans were kept in

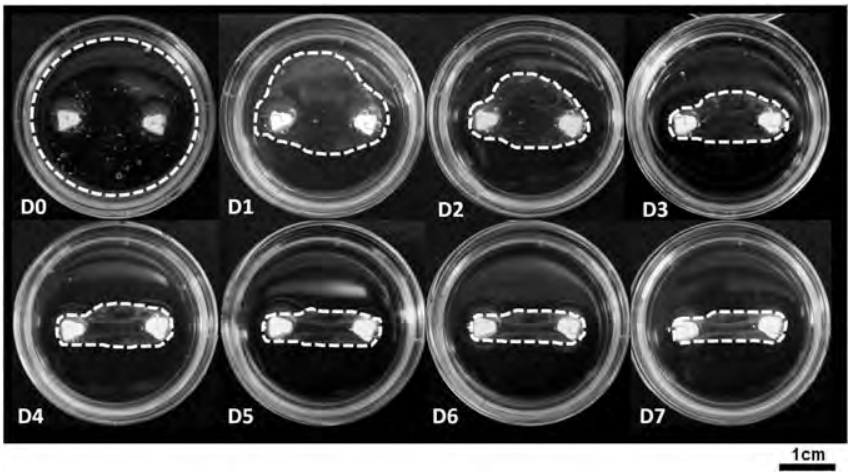

FIG. 1. Early-stage formation of the ligament-like constructs. Digital images of the constructs were taken each day from day 0 (D0) to day 7 (D7) after cell seeding. The outer edges of the fibrin gel have been marked for clarity (white-dashed line). Over the course of the 7 days, the fibrin gel contracts unevenly around the two fixed anchor points. Constructs are formed in 35-mm Petri dishes.

the same culture conditions until the 2.5-month time point, where 3D scans were taken ($n=1$ each condition).

Gel contraction analysis

To investigate and quantify the effect of supplementation with AA+P on gel contraction, constructs were formed and supplemented with or without AA+P from day 0 of culture ($n=7$ in each group). The decision to supplement from day 0 was to investigate the effect of AA+P on gel contraction from the beginning of formation, rather than from day 7 as described earlier. Digital images were taken of each construct every day until day 15, and then every other day thereafter. Gel surface areas were quantified using image analysis software (ImageJ; NIH) to calculate percentage reduction in gel area over time. Further to this, the maximum and minimum widths of the ligament-like constructs transverse to the longitudinal length were also measured ($n=7$ in each group; ImageJ; NIH.). All measurements were taken in between the anchors to ensure consistency.

Histology

The ligament-like constructs were removed from their culture media at the 5-week and 10-week time points ($n=2$) and fixed in 4% formaldehyde buffer in phosphate-buffered saline at 4°C for 24 h. Samples were then dehydrated in a series of ethanol solutions from 35% to 100% followed by 100% xylene. The specimen was then transferred to a 60°C paraffin wax bath (HISTO WAX 514409) overnight, and then placed under vacuum (Citadel 1000; Thermo Shandon) for 4 h to allow wax infiltration. The sample was later embedded in paraffin wax, and a LEICA RM 2035 microtome was used to cut 5–7-μm sections. The sections were picked up on glass coverslips (four per slide and two slides per construct) that were left in a 60°C oven for 30 min before they were stained using hematoxylin and eosin (H&E; SHANDON Linistain GLX) per the manufacturer's instructions. Stained sections were viewed on a light microscope (Inverso 3000, Ceti; Progen Scientific) and images taken using Image Capture (Ceti; Progen Scientific).

Collagen content

The collagen content of ligament-like constructs was measured over time using a hydroxyproline assay, as hydroxyproline accounts for ~13% of total collagen and is released after tissue hydrolysis.[30,31]

Briefly, ligament constructs ($n=4$ each time point and group) were removed from their cement anchors and left to dehydrate at 37°C for at least 72 h. The dry mass of each sample was then measured, and the dry sample was hydrolyzed in 200 μL of 6 M HCl at 130°C for 3 h. The liquid was removed by allowing the HCl to evaporate for 30 min in a fume hood at 130°C. The resulting pellet was re-suspended in 200 μL of hydroxyproline buffer. Samples were further diluted 1:8 in hydroxyproline buffer. About 150 μL of chloramine T solution was added to each sample, vortexed, and left at room temperature for 20 min. About 150 μL of aldehyde–perchloric acid solution was then added to each tube before the tubes were vortexed and incubated in a preheated water bath at 60°C for 15 min. After incubation, tubes were left to cool for 10 min, and then samples/standards were read at 550 nm on a Glomax Multi Detection System Plate reader (Promega). Hydroxyproline was converted to collagen using a factor of 13.34%.

Statistical analysis

Where appropriate, data are presented as means ± standard error of the mean. Differences in mean values were compared within groups, and significant differences were determined by analysis of variance with the *post hoc* Tukey-Kramer Honestly Significant Difference test using BrightStat.[32] The significance level was set at $p<0.05$. The gel contraction data were analyzed using independent one-tailed tests (IBM SPSS Statistics 19) on a day-by-day basis. To determine the effect size of the data, Pearson's correlation r was used such that r values <0.1 represented a small effect; 0.3, a medium effect; and 0.5 or greater, a large effect. The Cohen's d method was also used, with categories being 0.2 is small, 0.5 is medium, and 0.8 is large. Pearson's r and Cohen's d effect sizes are referred to as ES r and ES d, respectively. *Post hoc* power analyses were also conducted (DSS Research Statistical Power Calculator).

Results

Early-stage formation of ligament-like constructs

Over the course of 7 days, the cell-seeded fibrin gel contracted around the two fixed brushite anchor points (Fig. 1).

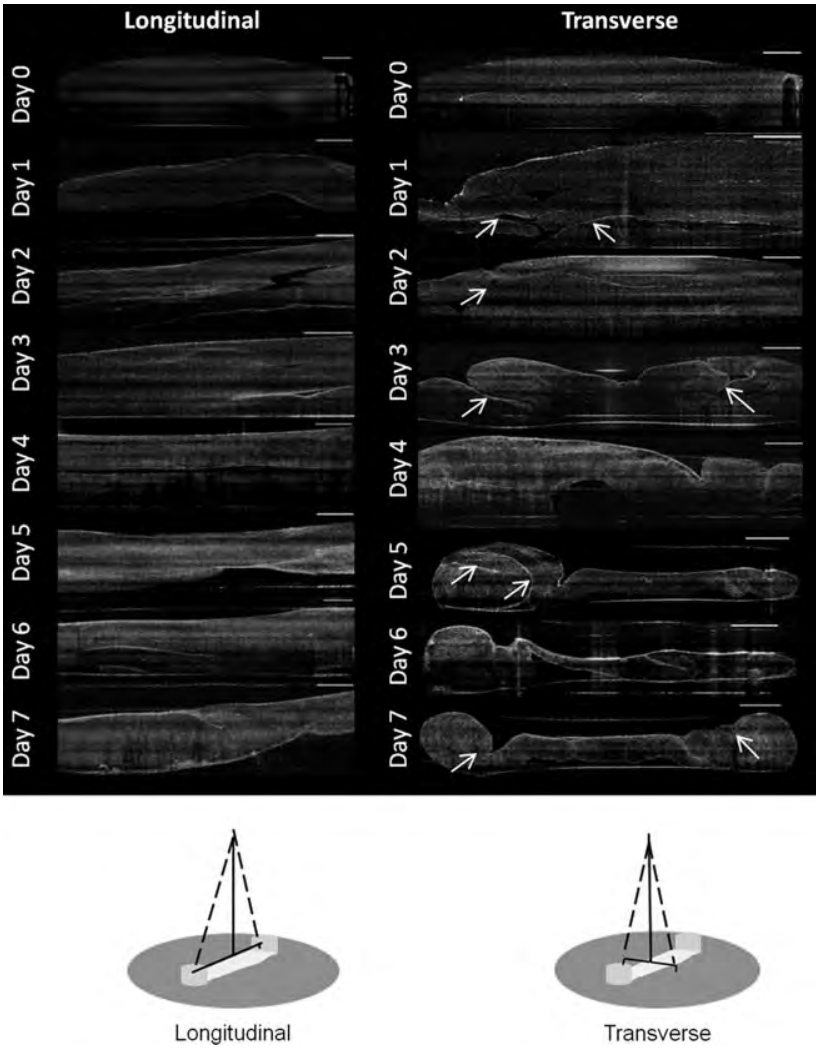

FIG. 2. Optical coherence tomography (OCT) scans in the longitudinal and transverse orientations during early-stage formation of the ligament-like constructs. OCT scans were performed daily. Fibrin gel contraction is evident from day 1 after cell seeding and continues over the course of the week. Folds in the fibrin gel are marked with arrows. Scale bar represents 1 mm in all images. Schematic diagrams depict the scanning direction in both orientations.

The fibrin gel began to contract rapidly and unevenly within 5 days after cell seeding, continuing rapid contraction until day 5, when the contraction rate noticeably reduced (Fig. 1).

The OCT scans demonstrate the method of gel contraction in the ligament constructs. Folds of the fibrin gel can be seen in the transverse scans from day 1 onward (Fig. 2, arrows), becoming clearly evident at day 3 (Fig. 2). The uneven nature of gel contraction demonstrated in Figure 1 can also be observed in Figure 2. By day 7, both sides of the fibrin gel have contracted around the anchor points evenly, and the folds have coalesced into a single solid mass (Figs. 1 and 2).

Maturation of ligament-like constructs

Contraction of the ligament constructs continues over several weeks of maturation (Fig. 3). Supplementation of the

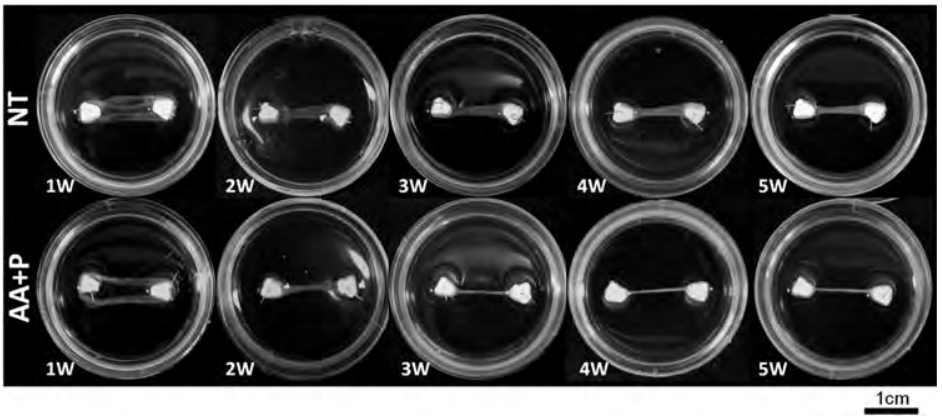

FIG. 3. Maturation of the ligament-like constructs. Digital images of the ligament-like constructs over a 5-week period in unsupplemented and supplemented groups (250 μM ascorbic acid 2-phosphate [AA] + 50 μM proline [P]). Supplementation causes increased contraction from week 2 (2W) onward. Constructs are formed in 35-mm Petri dishes. NT, no treatment.

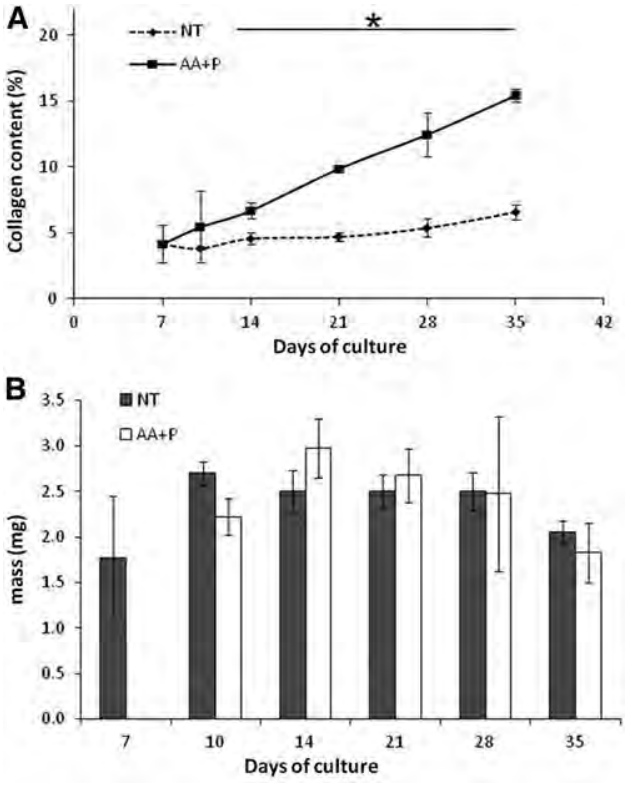

FIG. 4. Collagen content of ligament-like constructs. **(A)** AA + P causes a significant increase in the collagen content when compared to unsupplemented samples at all time points from 14 days. $*p < 0.05$ when compared to the unsupplemented group. $n = 6$ in all groups. **(B)** Dry mass of constructs does not significantly differ between supplemented and unsupplemented groups. $n = 6$ in all groups.

culture medium with AA + P has a marked effect on contraction of the constructs, with supplemented constructs continuing to contract beyond the boundaries of the cement anchors as seen in the unsupplemented group (Fig. 3). Notably, in both the unsupplemented and supplemented groups, the constructs became white and appeared to increase in opacity over time, which is indicative of increased matrix deposition in the samples (Fig. 3). To confirm this, the hydroxyproline content constructs were measured at each time point (Fig. 4). As anticipated, the supplemented group continued to produce collagen, with the collagen content rising significantly from 4.16% ± 1.42% at 1 week to 15.45% ± 0.49% per construct after 5 weeks of culture ($p > 0.00$). In the unsupplemented samples, however, the collagen content stayed relatively constant, with no significant difference observed between week 1 and week 5 of culture at any time point measured ($p > 0.05$ at all time points). Furthermore, the dry weights of the constructs do not significantly differ at any time point measured (Fig. 4B).

Figure 5A displays the longitudinal scans of the constructs using OCT in the maturation phase of development. Over the course of 5 weeks, the constructs became thinner and more opaque, markedly so in the AA + P-treated samples (Fig. 5A). The transverse scans of the constructs clearly demonstrated gross morphological changes occurring during construct maturation (Fig. 5B). In both the AA + P-treated samples and the unsupplemented group, the constructs display a rolled-up appearance after 1 week of formation. Gradually, the two sides of the construct contracted and joined to form a tubular structure by week 2 (Fig. 5B). Notably, this occurred faster in the AA + P-treated group (Fig. 5B). Cross-sectional areas of the transverse OCT scans were measured and plotted against time (Fig. 5C). At all time points after 14 days, unsupplemented samples possess a larger cross-sectional area than supplemented constructs (Fig. 5C), reaching significance on day 14 ($p = 0.001$), day 28 ($p = 0.01$), and day 35 ($p = 0.0001$). Over the course of the following weeks, constructs in both groups contracted further, became more opaque, and displayed a more uniform tissue distribution. Continued culture of the ligament-like constructs for several months in culture maintains this gross morphology as shown in the 3D reconstructions of constructs with dense constructs with distinct morphologies produced (Fig. 6). As shown previously in the digital images (Fig. 3), constructs in the AA + P-treated group underwent significant contraction, becoming < 2 mm in width by 4 weeks of culture. To investigate the effect of supplementation of AA + P on the contraction of cell-seeded fibrin gels, constructs were photographed every day after cell seeding for 2 weeks and then every other day for the duration of the experiment. Gel areas were then calculated using digital imaging software (ImageJ; NIH). The percentage reduction in the gel area is displayed in Figure 7. Overall, it appears that supplementation has no prominent effect on gel contraction. However, to allow for better comparison of the gel contraction, percentage area reductions were plotted for specific time periods of the experiment—the early-stage contraction period (0–7 days, Fig. 7B), maturation of the ligament-like constructs (7–35 days, Fig. 7C), and late-stage maturation (35–52 days, Fig. 7D). Figure 7B demonstrates that at the initial stage of gel contraction, unsupplemented constructs contract faster than supplemented, reaching a similar gel area by 7 days. Unsupplemented constructs contract to 40.83% ± 4.12% of their original area in the first 24 h after seeding (Fig. 7B) compared to AA + P-supplemented reduction to 45.52% ± 4.95%. Conversely, as contraction continues after day 7, AA + P-supplemented constructs display a faster rate of contraction with the difference between groups stabilizing at around day 14 (Fig. 7C). The most noticeable difference between groups is observed in the late-stage formation of ligament-like constructs, where from day 33 to day 36, AA + P-supplemented constructs contract more and then exhibit a smaller area at the remaining time points, with values of 2.72% ± 0.11% and 3.41% ± 0.47%, respectively (Fig. 7D). Statistical analysis revealed that while this difference was not significant ($p > 0.05$), it represented a large effect size (an indication of the strength of the relationship between the groups).[33,34]

To further quantify the differences observed between the constructs, the maximum and minimum transversal widths were measured. As with the construct gel area measurements, the largest change in widths was observed between day 0 and day 1 (Fig. 8). The no treatment (NT) group exhibited a greater extent of contraction in comparison to the AA + P group. The maximum width of the NT constructs reduced from 35 to 13.98 ± 4.45 mm, and the maximum width of the AA + P supplemented maximum width reduced to

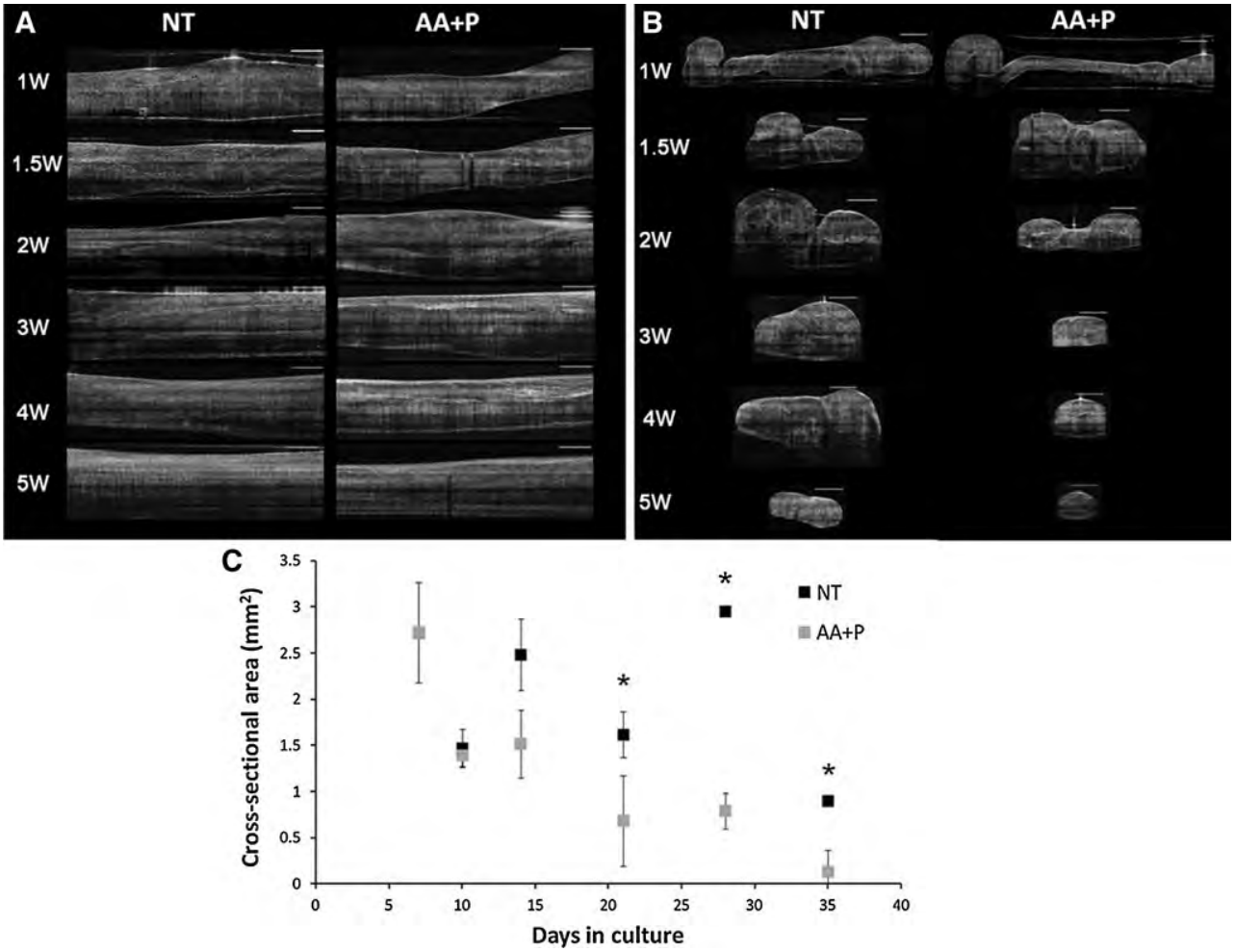

FIG. 5. OCT scans of ligament-like construct maturation: **(A)** longitudinal and **(B)** transverse orientations of the constructs. The difference in the construct morphology on addition of AA + P is evident in the transverse OCT scans. Scale bar represents 1 mm in all images. **(C)** Cross-sectional measurements of ligament-like constructs as measured by ImageJ software. Data are represented as mean ± standard deviation of three measurements per individual scan. $^*p < 0.05$.

22.23 ± 5.49 mm ($p = 0.0045$, ES $r = 0.67$, ES $d = 1.78$). The minimum widths for NT and AA + P were 10.41 ± 4.46 mm and 17.36 ± 7.41 mm, respectively ($p = 0.0275$, ES $r = 0.52$, ES $d = 1.22$). From day 33 to day 52, the average maximum and minimum widths of the NT group were almost double than those of the AA + P group, with the NT group widths being ~1.6 times larger than the AA + P-treated widths (Fig. 8 and Table 1). For example, on day 52, the maximum widths were 2.41 ± 0.48 mm for NT and 1.48 ± 0.15 mm for AA + P, ($p = 0.012$, ES $r = 0.82$, ES $d = 1.63$), while the minimum widths for NT and AA + P were 1.47 ± 0.51 mm and 0.91 ± 0.1 mm, respectively (Fig. 8). All the maximum widths were found to be significant between days 33 and 52 ($p < 0.05$); however, the minimum widths were not. The effect–size statistics,

FIG. 6. Three-dimensional reconstructions of the ligament constructs after 2.5 months in culture, with and without AA + P supplementation.

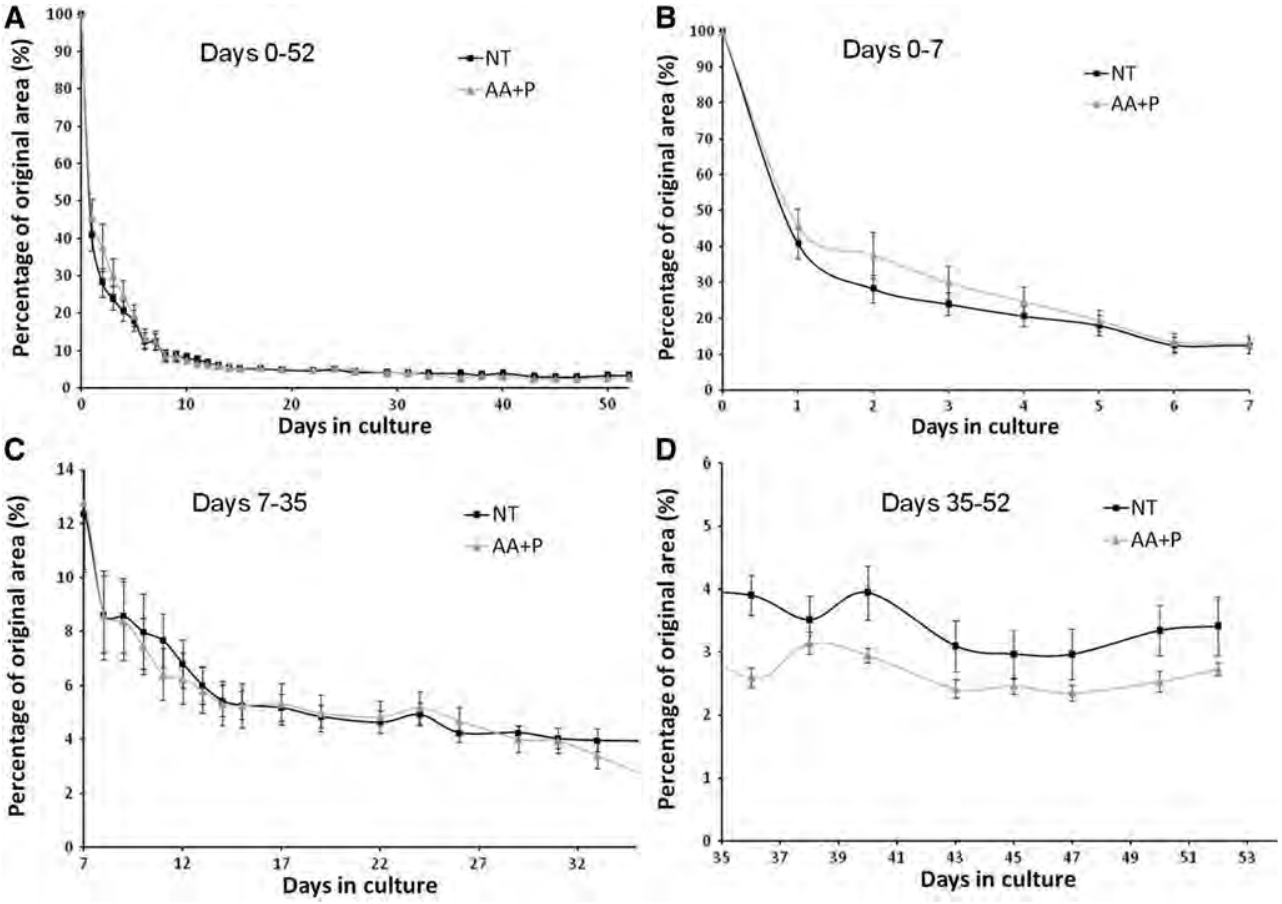

FIG. 7. Quantification of contraction of ligament-like constructs. **(A)** Global percentage reduction in the fibrin gel area over time. **(B)** Early-stage formation of ligament constructs (0–7 days), **(C)** maturation stage (7–35 days), and **(D)** late-stage maturation (35–52 days). $n=7$ for each time point and group.

which is an indication of the strength of the relationship between the groups, was calculated using Cohen's *d* and Pearson's Correlation Coefficient *r*. Both methods resulted in large effect–size statistical values on day 1 and in the period between days 33 and 52, meaning that although the minimum widths failed to give significant results, there was strong separation between means due to the AA+P treatment (Fig. 8C, D).

The transversal maximum-to-minimum width ratios within each group were also determined to observe if there were any extremes in the construct dimensions (Table 2). Although the magnitude of contraction differed between the groups, the maximum-to-minimum width ratios of the constructs were almost identical by day 52, at 1.64 and 1.62 for NT and AA+P-supplemented, respectively (Table 2). Using the average widths, the aspect ratio of the constructs was calculated (Table 3). The final aspect ratio of the constructs treated with AA+P was larger, at ~10, than for those unsupplemented with an aspect ratio of about 6 (Table 3), again indicating that AA+P changes the final dimensions of the ligament-like constructs.

Histological sections of supplemented ligament-like constructs were taken after 5 and 10 weeks of culture (Fig. 9). H&E staining of the sections shows that in cross section, the folds of the fibrin gel can be seen in the center of the construct (Fig. 9A, small arrows) and where the fibrin gel attaches to the cement anchor (Fig. 9B). Furthermore, a cell layer can be seen on the outside of the tubular structure (Fig. 9A, large arrows) with limited cells visible in the inside of the structure. However, in longitudinal sections at 10 weeks in culture, cells are present throughout the ligament-like construct, and the tissue displayed a fiber-like appearance (Fig. 9C, D). Figure 9C and D also revealed a thick layer on the outer edges of the scaffold, in line with the cortex layer that can be observed in the 3D reconstructions in the AA+P-treated group (Fig. 6).

Discussion

In this study, we have examined the morphological changes occurring during early-stage formation and maturation of tissue-engineered bone-to-bone ligament-like constructs. We have used conventional digital imaging alongside OCT imaging with anticipation that by combining these techniques, we could gain an understanding of construct formation and matrix deposition by nondestructive means, improving our understanding of how these tissues form and develop *in vitro*. Furthermore, we have combined the OCT scans with the digital image analysis of the constructs to study the effect of AA+P supplementation on

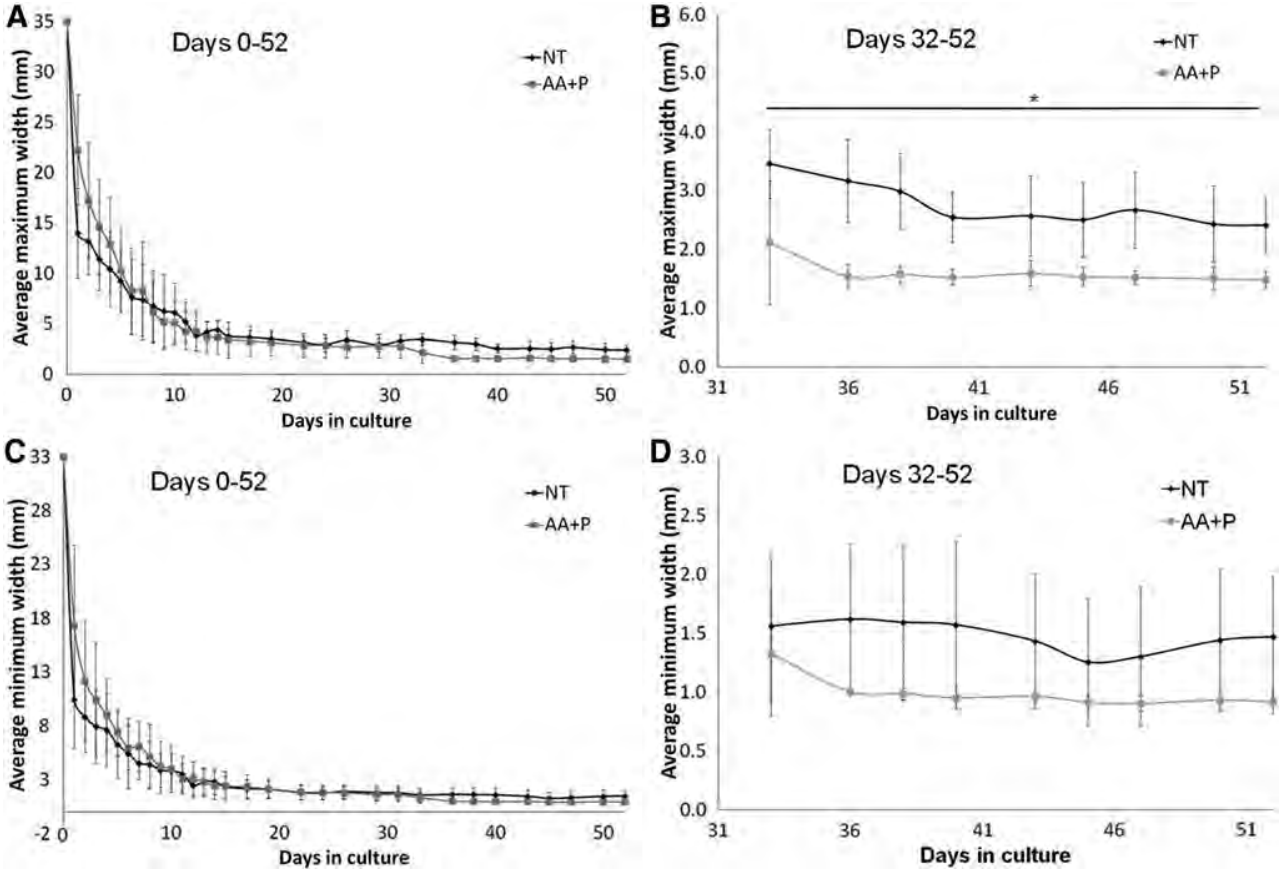

FIG. 8. Transversal maximum and minimum widths of the ligament-like constructs. **(A)** Maximum widths for no treatment (NT) and AA + P constructs over time. **(B)** Maximum widths from 33 to 52 days. **(C)** Minimum widths for NT and AA + P constructs over time. **(D)** Minimum widths from 33 to 52 days. $n = 7$ for each time point and group. $^*p < 0.05$ between groups.

fibrin gel contraction and tissue-engineered ligament construct formation.

Although the standard histological analysis of tissue-engineered constructs has advantages, such as the ability to determine matrix components and determine cell distribution within tissues, it also has several drawbacks. First, a histological analysis can require the fixation and freezing of tissue constructs. Both these procedures can damage the specimen and therefore may not provide a true representation of tissue morphology. Second, owing to the limitations of light microscopy, constructs need to be sectioned into slices of several micron thicknesses, and therefore it remains difficult to obtain a 3D view of the specimen. This can be problematic if, as is the case here, the gross morphology during formation is of interest. In this study, OCT has allowed an in-depth view of the tissue morphology in both the transverse and the longitudinal orientations that is not possible using digital imaging alone. The use of OCT allowed visualization of the gross cross-sectional morphology of the ligament-like constructs during formation and has permitted a far better understanding of the mode of construct formation. However, it is also apparent that the use of OCT to determine matrix composition by images alone is not ideal and requires further analysis. Some researchers have demonstrated the use of polarization-sensitive OCT to visualize collagen fiber alignment within tendon,[35] cartilage,[36] and tissue-engineered structures.[28] By this method, the polarization of backscattered light is measured after it has passed though the sample, and this can be directly related to the alignment of the collagen fibers. Such an analysis should be performed on the ligament-like construct samples to confirm an increase in

Table 1. Ratio of NT-to-AA + P Maximum and Minimum Widths of Ligament-Like Constructs Over 33–52 Days

		Day								
Description	*Ratio*	*33*	*36*	*38*	*40*	*43*	*45*	*47*	*50*	*52*
Max. width	NT:AA + P	1.63	2.05	1.90	1.67	1.61	1.63	1.75	1.61	1.63
Min. width	NT:AA + P	1.18	1.62	1.62	1.65	1.49	1.38	1.44	1.55	1.61

NT, no treatment; AA + P, ascorbic acid and proline.

Table 2. Ratio of Maximum-to-Minimum Widths of Ligament-Like Constructs in NT- and AA+P-Treated Samples Over 33–52 Days

		Day								
Group	*Ratio*	*33*	*36*	*38*	*40*	*43*	*45*	*47*	*50*	*52*
NT	Max:min	2.22	1.96	1.88	1.62	1.79	1.99	2.05	1.69	1.64
AA+P	Max:min	1.60	1.54	1.60	1.61	1.66	1.69	1.69	1.62	1.62

collagen deposition and alignment in the samples over an extended culture period.

The transverse OCT scans clearly demonstrate the manner in which the fibrin gel contracts around the two anchor points and rolls into a tubular structure (Figs. 2 and 5B). Eventually, the two sides of the construct come into contact and fuse together to form a single longitudinal ligament-like structure by approximately week 2 of culture (Fig. 5B). Another research group has recently reported the formation of tendon-like constructs using a similar method, although they embedded the ACL cells into the fibrin gel before polymerization.[37] It would also be interesting to compare the methods of formation of those constructs using OCT, to establish their mode of formation. Furthermore, it seems likely that the two modes of formation could result in a distinct mechanical behavior between the two and may provide evidence to establish which method is conducive to forming engineered tissues with greater mechanical integrity.

The decision to supplement the ligament-like constructs with AA+P was made through our previous work that demonstrates that the addition of AA+P to the culture media of the constructs resulted in an increased deposition of collagen within the fibrin matrix after only 1 week of supplementation.[11] As expected, the supplementation of AA+P over the 5-week culture period resulted in a continuous increase in the collagen content of the constructs (Fig. 4A). AA is an essential cofactor for prolyl-4-hydroxylase, and its presence is required for the hydroxylation of collagen chains during collagen fibril assembly.[38] In addition, as proline is a major constituent of the collagen protein, it is not surprising that increasing both AA and proline availability augments collagen production. Here, we have also demonstrated the effect that AA+P supplementation has on contraction of the ligament-like constructs, with supplemented groups displaying increased contraction in the digital images (Fig. 3), OCT scans (Fig. 5B), and the evaluation of contraction by digital imaging (Figs. 7 and 8). Although there were no statistically significant differences between the gel areas of the NT- and AA+P-supplemented constructs, the maximum widths of the constructs differed significantly between the groups between days 33 and 52 (Fig. 8B). The ratios calculated from the results (Table 1) do show that there is some inherent pattern in the formation of the constructs with regard to the maximum and minimum widths achieved. The ratios of the maximum-to-minimum width of the supplemented group appeared to stabilize from day 33 onward, at a value of about 1.6. The max/min ratio for the NT group is not as consistent, but reaches a similar value of 1.64 on day 52. A possible explanation for the stability seen in the max/min ratio of the AA+P group, in the final stages of the study, could be that treatment with AA+P causes a more uniform and controlled type of contraction of the gel as a result of increased deposition of collagen matrix (Fig. 4A).

However, it must also be noted that with the digital images and resulting contraction data, the area measured does not take the depth of the construct into account. As observed in the transverse OCT scans, AA+P-supplemented constructs display distinct cross-sectional areas (Fig. 5B) with unsupplemented constructs remaining broad and flat and AA+P-supplemented constructs becoming thin and round. Cross-sectional area was less in supplemented constructs than in unsupplemented constructs from day 14 onward (Fig. 5C) reaching values of 0.132 and 0.9 mm^2 respectively at the 35-day time point (Fig. 5C). Native ligaments are typically described as broad, flat tissues; in particular, the ACL has an average length and width range in humans from 22 to 41 mm and 7 to 12 mm, respectively.[39] Based on this information, although collagen content improves, the increased contraction observed on addition of AA+P is not ideal for our intended application, as it results in the production of thin, tubular structures, vastly different from the native ligament tissue morphology. The fact that supplemented constructs display greater contraction is not unexpected, since AA addition has been shown to increase wound contraction in mouse[40] and guinea pig models.[41–43] It is important to note that even though the AA+P constructs contract to a greater degree, the dry weight of the constructs does not significantly differ at any time point (Fig. 4B). Furthermore, it is critical to mention that while the cross-sectional area of the construct was measured, these measures were made at only one point in the graft. In hindsight, since the constructs are not completely uniform, it would have been beneficial to obtain several scans along the full length of the construct. Future work should focus on obtaining a

Table 3. Ratio of Length to Width of Ligament-Like Constructs in NT and AA+P Samples Over 33–52 Days

		Day								
Group	*Ratio*	*33*	*36*	*38*	*40*	*43*	*45*	*47*	*50*	*52*
NT	Length:width	4.79	5.03	5.25	5.84	6.01	6.40	6.06	6.22	6.20
AA+P	Length:width	7.18	9.71	9.64	9.96	9.66	10.08	10.18	10.13	10.32

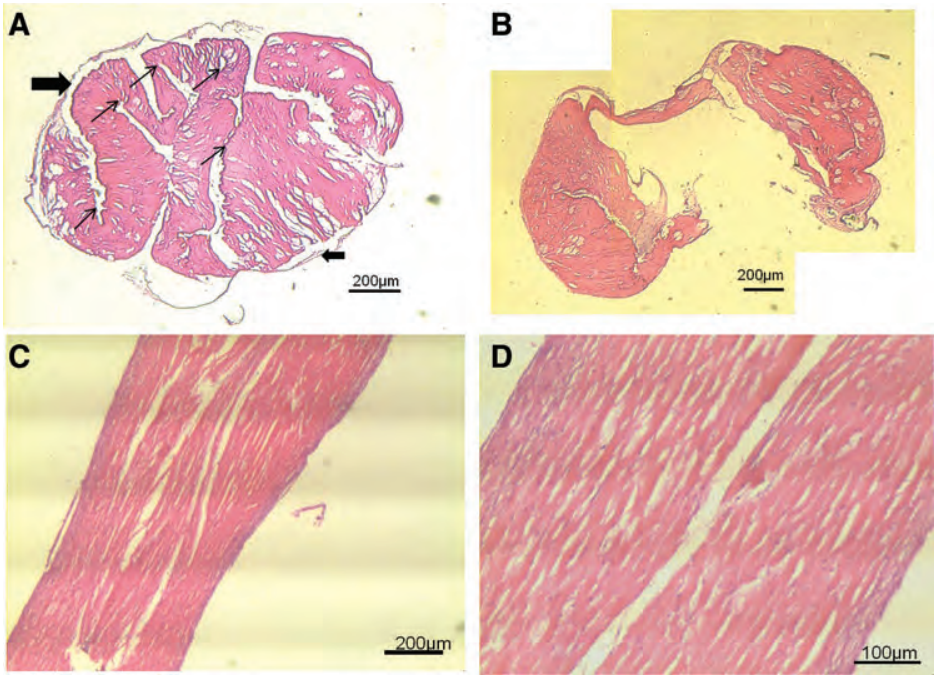

FIG. 9. Histological sections of AA+P-treated ligament-like constructs. **(A)** Transverse section from the midpoint of an AA+P-treated sample after 5 weeks in culture. The folds of the fibrin can be seen clearly (small arrows). Also, a cell layer is present on the outside of the tubular scaffold (large arrows). Stained with hematoxylin and eosin. **(B)** Transverse section of an AA+P-treated sample after 5 weeks in culture taken from the end of the construct near the cement anchor point. The midpoints of the construct have not joined together, probably due to the mechanical barrier of the cement anchor. **(C, D)** Longitudinal section of an AA+P-treated construct after 10 weeks in culture. Cell nuclei (blue) are distributed throughout the fibrous scaffold (pink), although are seen to be more prominent on the outer layers, creating a thick, dense layer on either side of the construct. Cells appear to align in the direction of tension. Color images available online at www.liebertonline.com/tea

complete scan along the length of the construct, since the morphological tapering evident in the digital images (Fig. 3) and the 3D reconstructions (Fig. 6) was not taken into account when the scans were collected. This inaccuracy in obtaining scans likely explains the variability of the cross-sectional area data and the large increase in the cross-sectional area at the 4-week time point in the unsupplemented group (Fig. 5C).

The mechanism for increased contraction in the ligament-like constructs on addition of AA+P could be multifaceted. As mentioned, exogenous addition of both AA+P lead to improved collagen accumulation; therefore, it is possible that by increasing the collagen content, collagen fibrils act to contract the fibrin matrix further as they crosslink with one another under control of the enzyme lysyl oxidase. However, contrary to this, a 1-mM dose of AA has been shown to have an inhibitory effect on lysyl oxidase activity *in vitro*,[44] although the authors performed no further experiments to establish the inhibitory ranges of AA concentrations. Furthermore, AA has been shown to have positive and negative effects on cellular proliferation depending on cell type. One reason for increased contraction could be an increase in cell number and therefore faster cell-mediated enzymatic digestion of the initial fibrin matrix. We have previously shown that 1 week of 50 μM AA+P supplementation increases the embryonic chick tendon fibroblasts cell number within the constructs.[11] Conversely, AA may act to transdifferentiate fibroblasts into a contractile myofibroblastic phenotype, with cells rich in α-smooth muscle actin as reported in smooth muscle cells[45,46] and bone mesenchymal stem cells.[47] This has been previously been reported to occur in fibroblasts on addition of transforming growth factor-β,[48] a growth factor pivotal to the collagen fibrillogenesis pathway, so it is possible that a related effect is occurring within our system. In two dimensions, addition of 250 μM AA+ 50 μM P to our fibroblast culture resulted in no significant change in the cell number (data not shown); however, since the attachment to the external environment in 2D is very different from that in 3D,[49] no conclusions can be drawn without further analysis within this tissue-engineered ligament system.

The histological analysis shows that cells populate the entire scaffold and align in the direction of tension (Fig. 9). Also, taken with the 3D scans of the ligament constructs, the formation of a dense, outer cortex can be seen (Figs. 6 and 8). Another research group has used immunohistochemical techniques to investigate the deposition of extracellular matrix (ECM) using ACL cells in this fibrin gel system.[37] Interestingly, they showed that a cortex of collagen type I was formed with mainly collagen type XII in the core of the construct.[37] Our hydroxyproline content assay does not distinguish between types of collagen, so we are currently undertaking work to give a full immunohistochemical analysis of the ECM deposited over the culture period. It may be that the mechanical environment predisposes the production of different types of collagen, and it is important to establish what these matrix proteins are within this system.

It is also likely that addition of AA+P affects matrix metalloproteinase (MMP) activity. MMPs are a family of zinc-dependent proteases that degrade components of the ECM.[50,51] Also, members of the A disintegrin and metalloproteinases with the thrombospondin motif (ADAMTS) family, known as the aggrecanases, act to degrade proteoglycans within the ECM,[52] and the enzymatic activity of both MMPs and ADAMTS is central to the control of matrix remodeling. Also, the tissue inhibitors of MMPs act to inhibit the degradative functions of MMPs in an effort to maintain homeostasis within the ECM.[27,53] Although the expression of quantification of MMP was not performed in the current study, the effect of AA+P on control of MMP activity remains an important factor to understand with regard to formation and contraction of the ligament-like constructs. Analysis of MMP will form part of our future work on this system.

Conclusions

This study has used digital imaging techniques, OCT, and histology to monitor the early-stage formation and maturation of tissue-engineered ligament-like constructs. OCT has allowed a complete cross-sectional view of the constructs during formation and the gross contraction of the fibrin-based cultures. It has also been shown that although AA+P supplementation continues to significantly improve collagen production over a 5-week period, it also causes excessive contraction of the constructs, producing a thin, round cross-sectional morphology rather than broad, flat ligament-like tissues that could prove problematic for our intended application as ACL replacement. Further analysis of effect of supplementation on the contraction method is crucial for the future development of tissue-engineered ligaments with clinically relevant morphological characteristics for implantation.

Acknowledgments

The authors would like to thank Dr. Keith Baar for his helpful comments during preparation of the article. We would also like to acknowledge the BBSRC for funding this work (Project number BB/G022356/1).

Disclosure Statement

No competing financial interests exist.

References

1. Cimino, F., Volk, B.S., and Setter, D. Anterior cruciate ligament injury: diagnosis, management, and prevention. Am Fam Physician **82,** 917, 2010.
2. Clayton, R.A., and Court-Brown, C.M. The epidemiology of musculoskeletal tendinous and ligamentous injuries. Injury **39,** 1338, 2008.
3. Benjaminse, A., Gokeler, A., and van der Schans, C.P. Clinical diagnosis of an anterior cruciate ligament rupture: a meta-analysis. J Orthop Sports Phys Ther **36,** 267, 2006.
4. Chang, S.K., Egami, D.K., Shaieb, M.D., Kan, D.M., and Richardson, A.B. Anterior cruciate ligament reconstruction: allograft versus autograft. Arthroscopy **19,** 453, 2003.
5. Louboutin, H., Debarge, R., Richou, J., Selmi, T.A., Donell, S.T., Neyret, P., *et al.* Osteoarthritis in patients with anterior cruciate ligament rupture: a review of risk factors. Knee **16,** 239, 2009.
6. Chaudhari, A.M., Briant, P.L., Bevill, S.L., Koo, S., and Andriacchi, T.P. Knee kinematics, cartilage morphology, and osteoarthritis after ACL injury. Med Sci Sports Exerc **40,** 215, 2008.
7. Kartus, J., Movin, T., and Karlsson, J. Donor-site morbidity and anterior knee problems after anterior cruciate ligament reconstruction using autografts. Arthroscopy **17,** 971, 2001.
8. Kartus, J., Stener, S., Lindahl, S., Engstrom, B., Eriksson, B.I., and Karlsson, J. Factors affecting donor-site morbidity after anterior cruciate ligament reconstruction using bone-patellar tendon-bone autografts. Knee Surg Sports Traumatol Arthrosc **5,** 222, 1997.
9. Mascarenhas, R., and MacDonald, P.B. Anterior cruciate ligament reconstruction: a look at prosthetics—past, present and possible future. Mcgill J Med **11,** 29, 2008.
10. Mastrokalos, D.S., Springer, J., Siebold, R., and Paessler, H.H. Donor site morbidity and return to the preinjury activity level after anterior cruciate ligament reconstruction using ipsilateral and contralateral patellar tendon autograft: a retrospective, nonrandomized study. Am J Sports Med **33,** 85, 2005.
11. Paxton, J.Z., Grover, L.M., and Baar, K. Engineering an *in vitro* model of a functional ligament from bone to bone. Tissue Eng Part A **16,** 3515, 2010.
12. Hsiung, P.L., Phatak, D.R., Chen, Y., Aguirre, A.D., Fujimoto, J.G., and Connolly, J.L. Benign and malignant lesions in the human breast depicted with ultrahigh resolution and three-dimensional optical coherence tomography. Radiology **244,** 865, 2007.
13. Zhou, C., Cohen, D.W., Wang, Y., Lee, H.C., Mondelblatt, A.E., Tsai, T.H., *et al.* Integrated optical coherence tomography and microscopy for *ex vivo* multiscale evaluation of human breast tissues. Cancer Res **70,** 10071, 2010.
14. Larin, K.V., Larina, I.V., Liebling, M., and Dickinson, M.E. Live Imaging of early developmental processes in mammalian embryos with optical coherence tomography. J Innov Opt Health Sci **2,** 253, 2009.
15. Larina, I.V., Furushima, K., Dickinson, M.E., Behringer, R.R., and Larin, K.V. Live imaging of rat embryos with Doppler swept-source optical coherence tomography. J Biomed Opt **14,** 050506. 2009.
16. Boppart, S.A., Tearney, G.J., Bouma, B.E., Southern, J.F., Brezinski, M.E., and Fujimoto, J.G. Noninvasive assessment of the developing Xenopus cardiovascular system using optical coherence tomography. Proc Natl Acad Sci U S A **94,** 4256, 1997.
17. Davlouros, P.A., Mavronasiou, E., Xanthopoulou, I., Karantalis, V., Tsigkas, G., Hahalis, G., *et al.* An optical coherence tomography study of two new generation stents with biodegradable polymer carrier, eluting paclitaxel vs. biolimus-A9. Int J Cardiol 2011 [Epub ahead of print]; DOI: 10.1016/j.ijcard.2010.12.072.
18. Greenberg, B.M., and Frohman, E. Optical coherence tomography as a potential readout in clinical trials. Ther Adv Neurol Disord **3,** 153, 2010.
19. Mansoori, T., Viswanath, K., and Balakrishna, N. Reproducibility of peripapillary retinal nerve fibre layer thickness measurements with spectral domain optical coherence tomography in normal and glaucomatous eyes. Br J Ophthalmol **95,** 685, 2011.
20. Drexler, W., Morgner, U., Ghanta, R.K., Kartner, F.X., Schuman, J.S., and Fujimoto, J.G. Ultrahigh-resolution ophthalmic optical coherence tomography. Nat Med **7,** 502, 2001.
21. Liang, X., Graf, B.W., and Boppart, S.A. Imaging engineered tissues using structural and functional optical coherence tomography. J Biophotonics **2,** 643, 2009.

22. Bagnaninchi, P.O., Yang, Y., Zghoul, N., Maffulli, N., Wang, R.K., and Haj, A.J. Chitosan microchannel scaffolds for tendon tissue engineering characterized using optical coherence tomography. Tissue Eng **13,** 323, 2007.
23. Chen, C.W., Betz, M.W., Fisher, J.P., Paek, A., and Chen, Y. Macroporous hydrogel scaffolds and their characterization by optical coherence tomography. Tissue Eng Part C Methods 2010 [Epub ahead of print]; DOI: 10.1089/ten.tec.2010.0072.
24. Zheng, K., Rupnick, M.A., Liu, B., and Brezinski, M.E. Three dimensional OCT in the engineering of tissue constructs: a potentially powerful tool for assessing optimal scaffold structure. Open Tissue Eng Regen Med J **2,** 8, 2009.
25. Aydin, H.M., El Haj, A.J., Piskin, E., and Yang, Y. Improving pore interconnectivity in polymeric scaffolds for tissue engineering. J Tissue Eng Regen Med **3,** 470, 2009.
26. Smith, L.E., Bonesi, M., Smallwood, R., Matcher, S.J., and MacNeil, S. Using swept-source optical coherence tomography to monitor the formation of neo-epidermis in tissue-engineered skin. J Tissue Eng Regen Med **4,** 652, 2010.
27. Levitz, D., Hinds, M.T., Ardeshiri, A., Hanson, S.R., and Jacques, S.L. Non-destructive label-free monitoring of collagen gel remodeling using optical coherence tomography. Biomaterials **31,** 8210, 2010.
28. Ahearne, M., Bagnaninchi, P.O., Yang, Y., and El Haj, A.J. Online monitoring of collagen fibre alignment in tissue-engineered tendon by PSOCT. J Tissue Eng Regen Med **2,** 521, 2008.
29. Paxton, J.Z., Donnelly, K., Keatch, R.P., Baar, K., and Grover, L.M. Factors affecting the longevity and strength in an *in vitro* model of the bone-ligament interface. Ann Biomed Eng **38,** 2155, 2010.
30. Edwards, C.A., and O'Brien, W.D., Jr. Modified assay for determination of hydroxyproline in a tissue hydrolyzate. Clin Chim Acta **104,** 161, 1980.
31. Neuman, R.E., and Logan, M.A. The determination of hydroxyproline. J Biol Chem **184,** 299, 1950.
32. Stricker, D. BrightStat.com: free statistics online. Comput Methods Programs Biomed **92,** 135, 2008.
33. Cohen, J. A power primer. Psychol Bull **112,** 155, 1992.
34. Nakagawa, S., and Cuthill, I.C. Effect size, confidence interval and statistical significance: a practical guide for biologists. Biol Rev Camb Philos Soc **82,** 591, 2007.
35. Bagnaninchi, P.O., Yang, Y., Bonesi, M., Maffulli, G., Phelan, C., Meglinski, I., *et al.* In-depth imaging and quantification of degenerative changes associated with Achilles ruptured tendons by polarization-sensitive optical coherence tomography. Phys Med Biol **55,** 3777, 2009.
36. Ugryumova, N., Jacobs, J., Bonesi, M., and Matcher, S.J. Novel optical imaging technique to determine the 3-D orientation of collagen fibers in cartilage: variable-incidence angle polarization-sensitive optical coherence tomography. Osteoarthritis Cartilage **17,** 33, 2009.
37. Bayer, M.L., Yeung, C.Y., Kadler, K.E., Qvortrup, K., Baar, K., Svensson, R.B., *et al.* The initiation of embryonic-like collagen fibrillogenesis by adult human tendon fibroblasts when cultured under tension. Biomaterials **31,** 4889, 2010.
38. Kadler, K.E., Baldock, C., Bella, J., and Boot-Handford, R.P. Collagens at a glance. J Cell Sci **120,** 1955, 2007.
39. Girgis, F.G., Marshall, J.L., and Monajem, A. The cruciate ligaments of the knee joint. Anatomical, functional and experimental analysis. Clin Orthop Relat Res 216, 1975.
40. Jagetia, G.C., Rajanikant, G.K., and Rao, S.K. Evaluation of the effect of ascorbic acid treatment on wound healing in mice exposed to different doses of fractionated gamma radiation. Radiat Res **159,** 371, 2003.
41. Jagetia, G.C., Rajanikant, G.K., Mallikarjun, and Rao, K.V. Ascorbic acid increases healing of excision wounds of mice whole body exposed to different doses of gamma-radiation. Burns **33,** 484, 2007.
42. Cabbabe, E.B., and Korock, S.W. Wound healing in vitamin C-deficient and nondeficient guinea pigs: a pilot study. Ann Plast Surg **17,** 330, 1986.
43. Silverstein, R.J., and Landsman, A.S. The effects of a moderate and high dose of vitamin C on wound healing in a controlled guinea pig model. J Foot Ankle Surg **38,** 333, 1999.
44. Kuroyanagi, M., Shimamura, E., Kim, M., Arakawa, N., Fujiwara, Y., and Otsuka, M. Effects of L-ascorbic acid on lysyl oxidase in the formation of collagen cross-links. Biosci Biotechnol Biochem **66,** 2077, 2002.
45. Kim, P.D., Peyton, S.R., VanStrien, A.J., and Putnam, A.J. The influence of ascorbic acid, TGF-beta1, and cell-mediated remodeling on the bulk mechanical properties of 3-D PEG-fibrinogen constructs. Biomaterials **30,** 3854, 2009.
46. Arakawa, E., Hasegawa, K., Irie, J., Ide, S., Ushiki, J., Yamaguchi, K., *et al.* L-ascorbic acid stimulates expression of smooth muscle-specific markers in smooth muscle cells both *in vitro* and *in vivo*. J Cardiovasc Pharmacol **42,** 745, 2003.
47. Narita, Y., Yamawaki, A., Kagami, H., Ueda, M., and Ueda, Y. Effects of transforming growth factor-beta 1 and ascorbic acid on differentiation of human bone-marrow-derived mesenchymal stem cells into smooth muscle cell lineage. Cell Tissue Res **333,** 449, 2008.
48. Desmouliere, A., Geinoz, A., Gabbiani, F., and Gabbiani, G. Transforming growth factor-beta 1 induces alpha-smooth muscle actin expression in granulation tissue myofibroblasts and in quiescent and growing cultured fibroblasts. J Cell Biol **122,** 103, 1993.
49. Cukierman, E., Pankov, R., Stevens, D.R., and Yamada, K.M. Taking cell-matrix adhesions to the third dimension. Science **294,** 1708, 2001.
50. Bedi, A., Kovacevic, D., Hettrich, C, Gulotta, L.V., Ehteshami, J.R., Warren, R.F., *et al.* The effect of matrix metalloproteinase inhibition on tendon-to-bone healing in a rotator cuff repair model. J Shoulder Elbow Surg **19,** 384, 2010.
51. Nagase, H., Visse, R., and Murphy, G. Structure and function of matrix metalloproteinases and TIMPs. Cardiovasc Res **69,** 562, 2006.
52. Riley, G. Tendinopathy—from basic science to treatment. Nat Clin Pract Rheumatol **4,** 82, 2008.
53. Karousou, E., Ronga, M., Vigetti, D., Passi, A., and Maffulli, N. Collagens, proteoglycans, MMP-2, MMP-9 and TIMPs in human achilles tendon rupture. Clin Orthop Relat Res **466,** 1577, 2008.

Address correspondence to:
Jennifer Z. Paxton, Ph.D.
School of Chemical Engineering
College of Physical Sciences and Engineering
University of Birmingham
Edgbaston
Birmingham B15 2TT
United Kingdom

E-mail: jzpaxton.research@gmail.com

Received: September 22, 2011
Accepted: March 16, 2012
Online Publication Date: May 17, 2012

References

Adirim, T. A. and Cheng, T. L. (2003). Overview of injuries in the young athlete. *Sports Medicine*, 33(1):75–81.

Ahmed, T. A., Dare, E. V., and Hincke, M. (2008). Fibrin: a versatile scaffold for tissue engineering applications. *Tissue Eng Part B Rev*, 14(2):199–215.

Ahmed, T. A., Griffith, M., and Hincke, M. (2007). Characterization and inhibition of fibrin hydrogel-degrading enzymes during development of tissue engineering scaffolds. *Tissue engineering*, 13(7):1469–1477.

Alberts, B. (2000). *Molecular biology of the cell*. Garland Science.

Albini, A., Pontz, B., Pulz, M., Allavena, G., Mensing, H., and Müller, P. K. (1988). Decline of fibroblast chemotaxis with age of donor and cell passage number. *Collagen and related research*, 8(1):23–37.

Almarza, A. J., Augustine, S. M., and Woo, S. L. (2008). Changes in gene expression of matrix constituents with respect to passage of ligament and tendon fibroblasts. *Annals of biomedical engineering*, 36(12):1927–1933.

Antonio, J. D. S. and Iozzo, R. V. (2001). *Glycosaminoglycans: Structure and Biological Functions*. John Wiley & Sons, Ltd.

Arrigoni, O. and De Tullio, M. C. (2000). The role of ascorbic acid in cell metabolism: between gene-directed functions and unpredictable chemical reactions. *Journal of Plant Physiology*, 157(5):481–488.

Arrigoni, O. and De Tullio, M. C. (2002). Ascorbic acid: much more than just an antioxidant. *Biochimica et Biophysica Acta (BBA)-General Subjects*, 1569(1):1–9.

Ashcroft, G. S., Horan, M. A., Herrick, S. E., Tarnuzzer, R. W., Schultz, G. S., and Ferguson, M. W. (1997). Age-related differences in the temporal and spatial regulation of matrix metalloproteinases (mmps) in normal skin and acute cutaneous wounds of healthy humans. *Cell and tissue research*, 290(3):581–591.

Ashcroft, G. S., Mills, S. J., and Ashworth, J. J. (2002). Ageing and wound healing. *Biogerontology*, 3(6):337–345.

Atala, A. (2007). Engineering tissues, organs and cells. *Journal of tissue engineering and regenerative medicine*, 1(2):83–96.

Aumailley, M. (2013). The laminin family. *Cell adhesion & migration*, 7(1):48–55.

Bach, J. S., Detrez, F., Cherkaoui, M., Cantournet, S., Ku, D. N., and Corté, L. (2013). Hydrogel fibers for acl prosthesis: Design and mechanical evaluation of pva and pva/uhmwpe fiber constructs. *Journal of biomechanics*.

Badylak, S. F., Freytes, D. O., and Gilbert, T. W. (2009). Extracellular matrix as a biological scaffold material: structure and function. *Acta biomaterialia*, 5(1):1–13.

Balakrishnan, B. and Banerjee, R. (2011). Biopolymer-based hydrogels for cartilage tissue engineering. *Chemical Reviews*, 111(8):4453–4474.

Ballestrem, C., Wehrle-Haller, B., Hinz, B., and Imhof, B. A. (2000). Actin-dependent lamellipodia formation and microtubule-dependent tail retraction control-directed cell migration. *Molecular biology of the cell*, 11(9):2999–3012.

Bayer, M. L., Yeung, C.-Y. C., Kadler, K. E., Qvortrup, K., Baar, K., Svensson, R. B., Peter Magnusson, S., Krogsgaard, M., Koch, M., and Kjaer, M. (2010). The initiation of embryonic-like collagen fibrillogenesis by adult human tendon fibroblasts when cultured under tension. *Biomaterials*, 31(18):4889–4897.

Benjamin, M. and McGonagle, D. (2009). Entheses: tendon and ligament attachment sites. *Scandinavian journal of medicine & science in sports*, 19(4):520–527.

Benjamin, M. and Ralphs, J. (1998). Fibrocartilage in tendons and ligaments—an adaptation to compressive load. *Journal of anatomy*, 193(4):481–494.

Benjamin, M. and Ralphs, J. R. (1997). Tendons and ligaments–an overview. *Histol Histopathol*, 12(4):1135–44. Benjamin, M Ralphs, J R Review Spain Histology and histopathology Histol Histopathol. 1997 Oct;12(4):1135-44.

Benjamin, M., Toumi, H., Ralphs, J. R., Bydder, G., Best, T. M., and Milz, S. (2006). Where tendons and ligaments meet bone: attachment sites ('entheses') in relation to exercise and/or mechanical load. *J Anat*, 208(4):471–90. Benjamin, M Toumi, H Ralphs, J R Bydder, G Best, T M Milz, S Review England Journal of anatomy J Anat. 2006 Apr;208(4):471-90.

Berrier, A. L. and Yamada, K. M. (2007). Cell-matrix adhesion. *J Cell Physiol*, 213(3):565–73. Berrier, Allison L Yamada, Kenneth M Research Support, N.I.H., Extramural Research Support, N.I.H., Intramural Review United States Journal of cellular physiology J Cell Physiol. 2007 Dec;213(3):565-73.

Bhandari, R. N., Riccalton, L. A., Lewis, A. L., Fry, J. R., Hammond, A. H., Tendler, S. J., and Shakesheff, K. M. (2001). Liver tissue engineering: a role for co-culture systems in modifying hepatocyte function and viability. *Tissue engineering*, 7(3):345–357.

Bhattacharjee, A. and Bansal, M. (2005). Collagen structure: the madras triple helix and the current scenario. *Iubmb Life*, 57(3):161–172.

Bonassar, L. J. and Vacanti, C. A. (1998). Tissue engineering: the first decade and beyond. *Journal of Cellular Biochemistry*, 72(S30–31):297–303.

Breidenbach, A. P., Gilday, S. D., Lalley, A. L., Dyment, N. A., Gooch, C., Shearn, J. T., and Butler, D. L. (2013). Functional tissue engineering of tendon: Establishing biological success criteria for improving tendon repair. *Journal of biomechanics*.

Brodsky, B. and Ramshaw, J. A. (1997). The collagen triple-helix structure. *Matrix Biology*, 15(8):545–554.

Brooks, R. (1976). Regulation of the fibroblast cell cycle by serum.

Brown, J. P., Finley, V. G., and Kuo, C. K. (2014). Embryonic mechanical and soluble cues regulate tendon progenitor cell gene expression as a function of developmental stage and anatomical origin. *Journal of biomechanics*, 47(1):214–222.

Bryant, S. J. and Anseth, K. S. (2001). The effects of scaffold thickness on tissue engineered cartilage in photocrosslinked poly (ethylene oxide) hydrogels. *Biomaterials*, 22(6):619–626.

Butler, D. L., Juncosa-Melvin, N., Boivin, G. P., Galloway, M. T., Shearn, J. T., Gooch, C., and Awad, H. (2008). Functional tissue engineering for tendon repair: A multidisciplinary

strategy using mesenchymal stem cells, bioscaffolds, and mechanical stimulation. *Journal of Orthopaedic Research*, 26(1):1–9.

Buxboim, A., Rajagopal, K., Andre'EX, B., and Discher, D. E. (2010). How deeply cells feel: methods for thin gels. *Journal of Physics: Condensed Matter*, 22(19):194116.

Caliari, S. R. and Harley, B. A. (2011). The effect of anisotropic collagen-gag scaffolds and growth factor supplementation on tendon cell recruitment, alignment, and metabolic activity. *Biomaterials*, 32(23):5330–5340.

Caliari, S. R. and Harley, B. A. (2013). Composite growth factor supplementation strategies to enhance tenocyte bioactivity in aligned collagen-gag scaffolds. *Tissue Engineering Part A*, 19(9-10):1100–1112.

Caliari, S. R., Ramirez, M. A., and Harley, B. A. (2011). The development of collagen-gag scaffold-membrane composites for tendon tissue engineering. *Biomaterials*, 32(34):8990–8998.

Calve, S., Dennis, R. G., Kosnik, P. E., Baar, K., Grosh, K., and Arruda, E. M. (2004). Engineering of functional tendon. *Tissue engineering*, 10(5-6):755–761.

Canty, E. and Kadler, K. (2002). Collagen fibril biosynthesis in tendon: a review and recent insights. *Comparative Biochemistry and Physiology Part A: Molecular & Integrative Physiology*, 133(4):979–985.

Cao, E., Chen, Y., Cui, Z., and Foster, P. R. (2003). Effect of freezing and thawing rates on denaturation of proteins in aqueous solutions. *Biotechnology and bioengineering*, 82(6):684–690.

Carlstedt, C. A. (1987). Mechanical and chemical factors in tendon healing: effects of indomethacin and surgery in the rabbit. *Acta Orthopaedica*, 58(S224):1–75.

Chambard, J.-C., Lefloch, R., Pouysségur, J., and Lenormand, P. (2007). Erk implication in cell cycle regulation. *Biochimica et Biophysica Acta (BBA) - Molecular Cell Research*, 1773(8):1299 – 1310.

Chang, H. Y., Chi, J.-T., Dudoit, S., Bondre, C., van de Rijn, M., Botstein, D., and Brown, P. O. (2002). Diversity, topographic differentiation, and positional memory in human fibroblasts. *Proceedings of the National Academy of Sciences*, 99(20):12877–12882.

Chen, F. M., Zhang, M., and Wu, Z. F. (2010). Toward delivery of multiple growth factors in tissue engineering. *Biomaterials*, 31(24):6279–308.

Chen, G., Okamura, A., Sugiyama, K., Wozniak, M. J., Kawazoe, N., Sato, S., and Tateishi, T. (2009). Surface modification of porous scaffolds with nanothick collagen layer by centrifugation and freeze-drying. *J Biomed Mater Res B Appl Biomater*, 90(2):864–72.

Chen, G., Sato, T., Ushida, T., Hirochika, R., Shirasaki, Y., Ochiai, N., and Tateishi, T. (2003). The use of a novel plga fiber/collagen composite web as a scaffold for engineering of articular cartilage tissue with adjustable thickness. *Journal of Biomedical Materials Research Part A*, 67(4):1170–1180.

Chen, G. P., Ushida, T., and Tateishi, T. (2002). Scaffold design for tissue engineering. *Macromolecular Bioscience*, 2(2):67–77. 533MD Times Cited:130 Cited References Count:107.

Chen, Q., Kinch, M. S., Lin, T. H., Burridge, K., and Juliano, R. (1994). Integrin-mediated cell adhesion activates mitogen-activated protein kinases. *Journal of Biological Chemistry*, 269(43):26602–26605.

Cheng, C. W., Solorio, L. D., and Alsberg, E. (2014). Decellularized tissue and cell-derived

extracellular matrices as scaffolds for orthopaedic tissue engineering. *Biotechnology advances*.

Chiarugi, P. and Giannoni, E. (2008). ¡ i¿ anoikis¡/i¿: A necessary death program for anchorage-dependent cells. *Biochemical pharmacology*, 76(11):1352–1364.

Chiquet, M., Sarasa-Renedo, A., and Tunç-Civelek, V. (2004). Induction of tenascin-c by cyclic tensile strain versus growth factors: distinct contributions by rho/rock and mapk signaling pathways. *Biochimica et Biophysica Acta (BBA)-Molecular Cell Research*, 1693(3):193–204.

Chiquet-Ehrismann, R., Kalla, P., Pearson, C. A., Beck, K., and Chiquet, M. (1988). Tenascin interferes with fibronectin action. *Cell*, 53(3):383–390.

Chiquet-Ehrismann, R., Mackie, E. J., Pearson, C. A., and Sakakura, T. (1986). Tenascin: an extracellular matrix protein involved in tissue interactions during fetal development and oncogenesis. *Cell*, 47(1):131–139.

Christiansen, D. L., Huang, E. K., and Silver, F. H. (2000). Assembly of type i collagen: fusion of fibril subunits and the influence of fibril diameter on mechanical properties. *Matrix Biology*, 19(5):409–420.

Clark, J. and Stechschulte, D. J. (1998). The interface between bone and tendon at an insertion site: a study of the quadriceps tendon insertion. *Journal of anatomy*, 192(4):605–616.

Clark, R., Nielsen, L. D., Welch, M. P., and McPherson, J. M. (1995). Collagen matrices attenuate the collagen-synthetic response of cultured fibroblasts to tgf-beta. *Journal of cell science*, 108(3):1251–1261.

Clark, R. A. (2001). Fibrin and wound healing. *Annals of the New York Academy of Sciences*, 936(1):355–367.

Clegg, P. D., Strassburg, S., and Smith, R. K. (2007). Cell phenotypic variation in normal and damaged tendons. *International journal of experimental pathology*, 88(4):227–235.

Cohen, S., Leshansky, L., Zussman, E., Burman, M., Srouji, S., Livne, E., Abramov, N., and Itskovitz-Eldor, J. (2010). Repair of full-thickness tendon injury using connective tissue progenitors efficiently derived from human embryonic stem cells and fetal tissues. *Tissue Engineering Part A*, 16(10):3119–3137.

Collen, A., Hanemaaijer, R., Lupu, F., Quax, P. H., van Lent, N., Grimbergen, J., Peters, E., Koolwijk, P., and van Hinsbergh, V. W. (2003). Membrane-type matrix metalloproteinase-mediated angiogenesis in a fibrin-collagen matrix. *Blood*, 101(5):1810–1817.

Conrad, G. W., Hamilton, C., and Haynes, E. (1977). Differences in glycosaminoglycans synthesized by fibroblast-like cells from chick cornea, heart, and skin. *Journal of Biological Chemistry*, 252(19):6861–6870.

Cooper, G. M. and Hausman, R. E. (2000). *The cell*. ASM press Washington.

Cowan, K. J. and Storey, K. B. (2003). Mitogen-activated protein kinases: new signaling pathways functioning in cellular responses to environmental stress. *Journal of Experimental Biology*, 206(7):1107–1115.

Cox, S., Cole, M., and Tawil, B. (2004). Behavior of human dermal fibroblasts in three-dimensional fibrin clots: dependence on fibrinogen and thrombin concentration. *Tissue engineering*, 10(5-6):942–954.

Crapo, P. M., Gilbert, T. W., and Badylak, S. F. (2011). An overview of tissue and whole organ decellularization processes. *Biomaterials*, 32(12):3233–3243.

Craven, P. A., Phillips, S. L., Melhem, M. F., Liachenko, J., and DeRubertis, F. R. (2001). Overexpression of manganese superoxide dismutase suppresses increases in collagen accumulation induced by culture of mesangial cells in high-media glucose. *Metabolism*, 50(9):1043–1048.

Crawford, S. E., Stellmach, V., Murphy-Ullrich, J. E., Ribeiro, S. M., Lawler, J., Hynes, R. O., Boivin, G. P., and Bouck, N. (1998). Thrombospondin-1 is a major activator of tgf-β1 in vivo. *Cell*, 93(7):1159–1170.

Croisier, F. and Jérôme, C. (2013). Chitosan-based biomaterials for tissue engineering. *European Polymer Journal*.

Csikász-Nagy, A., Battogtokh, D., Chen, K. C., Novák, B., and Tyson, J. J. (2006). Analysis of a generic model of eukaryotic cell-cycle regulation. *Biophysical journal*, 90(12):4361–4379.

Culav, E. M., Clark, C. H., and Merrilees, M. J. (1999). Connective tissues: matrix composition and its relevance to physical therapy. *physical therapy*, 79(3):308–319.

Cummings, S. H., Grande, D. A., Hee, C. K., Kestler, H. K., Roden, C. M., Shah, N. V., Razzano, P., Dines, D. M., Chahine, N. O., and Dines, J. S. (2012). Effect of recombinant human platelet-derived growth factor-bb-coated sutures on achilles tendon healing in a rat model: A histological and biomechanical study. *Journal of tissue engineering*, 3(1).

Daamen, W. F., Veerkamp, J., Van Hest, J., and Van Kuppevelt, T. (2007). Elastin as a biomaterial for tissue engineering. *Biomaterials*, 28(30):4378–4398.

Dado, D. and Levenberg, S. (2009). Cell–scaffold mechanical interplay within engineered tissue. In *Seminars in cell & developmental biology*, volume 20, pages 656–664. Elsevier.

Dalby, M. J., Riehle, M. O., Sutherland, D. S., Agheli, H., and Curtis, A. S. (2004). Changes in fibroblast morphology in response to nano-columns produced by colloidal lithography. *Biomaterials*, 25(23):5415–5422.

Debelle, L. and Tamburro, A. (1999). Elastin: molecular description and function. *The international journal of biochemistry & cell biology*, 31(2):261–272.

Desmouliere, A. (1995). Factors influencing myofibroblast differentiation during wound healing and fibrosis. *Cell biology international*, 19(471-A):471.

Dikovsky, D. (2008). Defining the role of matrix compliance and proteolysis in three-dimensional cell spreading and remodelingâ˜†. *Biophysical Journal*, 94(7):2914–2925.

Discher, D. E., Janmey, P., and Wang, Y. L. (2005). Tissue cells feel and respond to the stiffness of their substrate. *Science*, 310(5751):1139–43.

Douglas, T. E., Skwarczynska, A., Modrzejewska, Z., Balcaen, L., Schaubroeck, D., Lycke, S., Vanhaecke, F., Vandenabeele, P., Dubruel, P., Jansen, J. A., et al. (2013). Acceleration of gelation and promotion of mineralization of chitosan hydrogels by alkaline phosphatase. *International journal of biological macromolecules*.

Drury, J. L. and Mooney, D. J. (2003). Hydrogels for tissue engineering: scaffold design variables and applications. *Biomaterials*, 24(24):4337–51. Drury, Jeanie L Mooney, David J Review England Biomaterials Biomaterials. 2003 Nov;24(24):4337-51.

Dvir-Ginzberg, M., Gamlieli-Bonshtein, I., Agbaria, R., and Cohen, S. (2003). Liver tissue engineering within alginate scaffolds: effects of cell-seeding density on hepatocyte viability, morphology, and function. *Tissue Engineering*, 9(4):757–766.

Eagan, M. J., Zuk, P. A., Zhao, K.-W., Bluth, B. E., Brinkmann, E. J., Wu, B. M., and McAllister, D. R. (2012). The suitability of human adipose-derived stem cells for the engineering of ligament tissue. *Journal of Tissue Engineering and Regenerative Medicine*,

6(9):702–709.

Eagle, H. (1955). Nutrition needs of mammalian cells in tissue culture. *Science*, 122(3168):501–504.

Edom-Vovard, F. and Duprez, D. (2004). Signals regulating tendon formation during chick embryonic development. *Developmental dynamics*, 229(3):449–457.

Edom-Vovard, F., Schuler, B., Bonnin, M.-A., Teillet, M.-A., and Duprez, D. (2002). Fgf4 positively regulates scleraxis and tenascin expression in chick limb tendons. *Developmental biology*, 247(2):351–366.

Egeblad, M. and Werb, Z. (2002). New functions for the matrix metalloproteinases in cancer progression. *Nature Reviews Cancer*, 2(3):161–174.

Ehrbar, M., Sala, A., Lienemann, P., Ranga, A., Mosiewicz, K., Bittermann, A., Rizzi, S. C., Weber, F. E., and Lutolf, M. P. (2011). Elucidating the role of matrix stiffness in 3D cell migration and remodeling. *Biophys J*, 100(2):284–93.

Ellanti, P., Davarinos, N., Morris, S., and Rice, J. (2012). Bilateral synchronous rupture of the quadriceps tendon. *Irish journal of medical science*, 181(3):423–425.

Enoch, S. and Leaper, D. J. (2008). Basic science of wound healing. *Surgery (Oxford)*, 26(2):31–37.

Esteban, M. A., Wang, T., Qin, B., Yang, J., Qin, D., Cai, J., Li, W., Weng, Z., Chen, J., Ni, S., et al. (2010). Vitamin c enhances the generation of mouse and human induced pluripotent stem cells. *Cell Stem Cell*, 6(1):71–79.

Evan, G. I. and Vousden, K. H. (2001). Proliferation, cell cycle and apoptosis in cancer. *Nature*, 411(6835):342–348.

Even-Ram, S. and Yamada, K. M. (2005). Cell migration in 3d matrix. *Current opinion in cell biology*, 17(5):524–532.

Feland, J. B., Myrer, J. W., Schulthies, S. S., Fellingham, G. W., and Measom, G. W. (2001). The effect of duration of stretching of the hamstring muscle group for increasing range of motion in people aged 65 years or older. *Physical Therapy*, 81(5):1110–1117.

Fenwick, S. A., Hazleman, B. L., and Riley, G. P. (2002). The vasculature and its role in the damaged and healing tendon. *Arthritis research*, 4(4):252–260.

Ferry, J. D. (1952). The mechanism of polymerization of fibrinogen. *Proceedings of the National Academy of Sciences of the United States of America*, 38(7):566.

Ferry, J. D., Miller, M., and Shulman, S. (1951). The conversion of fibrinogen to fibrin. vii. rigidity and stress relaxation of fibrin clots; effect of calcium. *Archives of biochemistry and biophysics*, 34(2):424–436.

Fischbach, C., Tessmar, J., Lucke, A., Schnell, E., Schmeer, G., Blunk, T., and Göpferich, A. (2001). Does uv irradiation affect polymer properties relevant to tissue engineering? *Surface Science*, 491(3):333–345.

Ford, K. R., Myer, G. D., and Hewett, T. E. (2003). Valgus knee motion during landing in high school female and male basketball players. *Medicine and Science in Sports and Exercise*, 35(10):1745–1750.

Frame, K. K. and Hu, W.-S. (1988). A model for density-dependent growth of anchorage-dependent mammalian cells. *Biotechnology and bioengineering*, 32(8):1061–1066.

Franceschi, R. T. (1992). The role of ascorbic acid in mesenchymal differentiation. *Nutrition reviews*, 50(3):65–70.

Franchi, M., De Pasquale, V., Martini, D., Quaranta, M., Macciocca, M., Dionisi, A., and Ottani, V. (2010). Contribution of glycosaminoglycans to the microstructural integrity of

fibrillar and fiber crimps in tendons and ligaments. *ScientificWorldJournal*, 10:1932–40.

Freeman, J. W., Woods, M. D., and Laurencin, C. T. (2007). Tissue engineering of the anterior cruciate ligament using a braid–twist scaffold design. *Journal of biomechanics*, 40(9):2029–2036.

Freshney, R. I. (2005). *Defined Media and Supplements*. John Wiley & Sons, Inc.

Friedl, P. and Gilmour, D. (2009). Collective cell migration in morphogenesis, regeneration and cancer. *Nature reviews Molecular cell biology*, 10(7):445–457.

Fuchs, J. R., Nasseri, B. A., and Vacanti, J. P. (2001). Tissue engineering: a 21st century solution to surgical reconstruction. *The Annals of Thoracic Surgery*, 72(2):577–591.

Gabbiani, G. (2003). The myofibroblast in wound healing and fibrocontractive diseases. *The Journal of pathology*, 200(4):500–503.

Gagne, T., Chappell-Afonso, K., Johnson, J., McPherson, J., Oldham, C., Tubo, R., Vaccaro, C., and Vasios, G. (2000). Enhanced proliferation and differentiation of human articular chondrocytes when seeded at low cell densities in alginate in vitro. *Journal of Orthopaedic Research*, 18(6):882–890.

Gajhede-Knudsen, M., Ekstrand, J., Magnusson, H., and Maffulli, N. (2013). Recurrence of achilles tendon injuries in elite male football players is more common after early return to play: an 11-year follow-up of the uefa champions league injury study. *British journal of sports medicine*.

Gandhi, N. S. and Mancera, R. L. (2008). The structure of glycosaminoglycans and their interactions with proteins. *Chemical biology & drug design*, 72(6):455–482.

GCinzler, V. and Weidmann, K. (1997). Prolyl 4-hydroxylase! nhibitors. *Prolyl Hydroxylase, Protein Disulfide Isomerase and Other Structurally Related Proteins*, page 65.

Ge, Z., Goh, J. C., and Lee, E. H. (2005). Selection of cell source for ligament tissue engineering. *Cell Transplant*, 14(8):573–83. Ge, Zigang Goh, James Cho Hong Lee, Eng Hin Comparative Study Evaluation Studies Research Support, Non-U.S. Gov't United States Cell transplantation Cell Transplant. 2005;14(8):573-83.

Ge, Z., Yang, F., Goh, J. C., Ramakrishna, S., and Lee, E. H. (2006). Biomaterials and scaffolds for ligament tissue engineering. *J Biomed Mater Res A*, 77(3):639–52.

Gelse, K., Poschl, E., and Aigner, T. (2003). Collagens–structure, function, and biosynthesis. *Adv Drug Deliv Rev*, 55(12):1531–46.

Gilbert, T. W., Sellaro, T. L., and Badylak, S. F. (2006). Decellularization of tissues and organs. *Biomaterials*, 27(19):3675–3683.

Giron, F., Aglietti, P., Cuomo, P., Mondanelli, N., and Ciardullo, A. (2005). Anterior cruciate ligament reconstruction with double-looped semitendinosus and gracilis tendon graft directly fixed to cortical bone: 5-year results. *Knee Surgery, Sports Traumatology, Arthroscopy*, 13(2):81–91.

Gonfiotti, A., Jaus, M. O., Barale, D., Baiguera, S., Comin, C., Lavorini, F., Fontana, G., Sibila, O., Rombolà, G., Jungebluth, P., et al. (2014). The first tissue-engineered airway transplantation: 5-year follow-up results. *The Lancet*, 383(9913):238–244.

Graham, H. K., Holmes, D. F., Watson, R. B., and Kadler, K. E. (2000). Identification of collagen fibril fusion during vertebrate tendon morphogenesis. the process relies on unipolar fibrils and is regulated by collagen-proteoglycan interaction. *Journal of molecular biology*, 295(4):891–902.

Grassl, E., Oegema, T., and Tranquillo, R. (2002). Fibrin as an alternative biopolymer to type-i collagen for the fabrication of a media equivalent. *Journal of biomedical materials*

research, 60(4):607–612.

Grinnell, F. (2000). Fibroblast–collagen-matrix contraction: growth-factor signalling and mechanical loading. *Trends in cell biology*, 10(9):362–365.

Gross, G. and Hoffmann, A. (2013). Therapeutic strategies for tendon healing based on novel biomaterials, factors and cells. *Pathobiology*, 80(4):203–210.

Gross, J., Farinelli, W., Sadow, P., Anderson, R., and Bruns, R. (1995). On the mechanism of skin wound "contraction": a granulation tissue "knockout" with a normal phenotype. *Proceedings of the National Academy of Sciences*, 92(13):5982–5986.

Guilak, F., Butler, D. L., and Goldstein, S. A. (2001). Functional tissue engineering: the role of biomechanics in articular cartilage repair. *Clinical orthopaedics and related research*, 391:S295–S305.

Gunasekaran, S. and Ak, M. M. (2000). Dynamic oscillatory shear testing of foods—selected applications. *Trends in Food Science & Technology*, 11(3):115–127.

Gunn, J. S. and Ehrlich, H. P. (2012). Evidence translocation of collagen fibril segments plays a role in early intrinsic tendon repair. *Plastic and reconstructive surgery*, 129(2):300e.

Haas, T. L., Davis, S. J., and Madri, J. A. (1998). Three-dimensional type i collagen lattices induce coordinate expression of matrix metalloproteinases mt1-mmp and mmp-2 in microvascular endothelial cells. *Journal of Biological Chemistry*, 273(6):3604–3610.

Haddad-Weber, M., Prager, P., Kunz, M., Seefried, L., Jakob, F., Murray, M. M., Evans, C. H., Nöth, U., and Steinert, A. F. (2010). Bmp12 and bmp13 gene transfer induce ligamentogenic differentiation in mesenchymal progenitor and anterior cruciate ligament cells. *Cytotherapy*, 12(4):505–513.

Hadjipanayi, E., Mudera, V., and Brown, R. (2009). Close dependence of fibroblast proliferation on collagen scaffold matrix stiffness. *Journal of tissue engineering and regenerative medicine*, 3(2):77–84.

Hagerty, P., Lee, A., Calve, S., Lee, C. A., Vidal, M., and Baar, K. (2012). The effect of growth factors on both collagen synthesis and tensile strength of engineered human ligaments. *Biomaterials*, 33(27):6355–6361.

Hall, H., Baechi, T., and Hubbell, J. A. (2001). Molecular properties of fibrin-based matrices for promotion of angiogenesis in vitro. *Microvascular research*, 62(3):315–326.

Ham, R. G. (1965). Clonal growth of mammalian cells in a chemically defined, synthetic medium. *Proceedings of the National Academy of Sciences of the United States of America*, 53(2):288.

Ham, R. G. and McKeehan, W. L. (1978). Development of improved media and culture conditions for clonal growth of normal diploid cells. *In vitro*, 14(1):11–22.

Hammond, J. S., Beckingham, I. J., and Shakesheff, K. M. (2006). Scaffolds for liver tissue engineering.

Harbour, J. W. and Dean, D. C. (2000). Rb function in cell-cycle regulation and apoptosis. *Nature Cell Biology*, 2(4):E65–E67.

Hartsock, A. and Nelson, W. J. (2008). Adherens and tight junctions: structure, function and connections to the actin cytoskeleton. *Biochimica et Biophysica Acta (BBA)-Biomembranes*, 1778(3):660–669.

Hashimoto, Y., Yoshida, G., Toyoda, H., and Takaoka, K. (2007). Generation of tendon-to-bone interface "enthesis" with use of recombinant bmp-2 in a rabbit model. *Journal of Orthopaedic Research*, 25(11):1415–1424.

Hayashida, T., Poncelet, A.-C., Hubchak, S. C., and Schnaper, H. W. (1999). Tgf-&bgr; 1 activates map kinase in human mesangial cells: A possible role in collagen expression. *Kidney international*, 56(5):1710–1720.

Hayman, E. G., Pierschbacher, M. D., Ohgren, Y., and Ruoslahti, E. (1983). Serum spreading factor (vitronectin) is present at the cell surface and in tissues. *Proceedings of the National Academy of Sciences*, 80(13):4003–4007.

Hazard, S. W., Myers, R. L., and Ehrlich, H. P. (2011). Demonstrating collagen tendon fibril segments involvement in intrinsic tendon repair. *Experimental and molecular pathology*, 91(3):660–663.

He, P., Ng, K. S., Toh, S. L., and Goh, J. C. H. (2012). In vitro ligament–bone interface regeneration using a trilineage coculture system on a hybrid silk scaffold. *Biomacromolecules*, 13(9):2692–2703.

Hee, C. K., Dines, J. S., Solchaga, L. A., Shah, V. R., and Hollinger, J. O. (2012). Regenerative tendon and ligament healing: opportunities with recombinant human platelet-derived growth factor bb-homodimer. *Tissue Engineering Part B: Reviews*, 18(3):225–234.

Heino, J. (2000). The collagen receptor integrins have distinct ligand recognition and signaling functions. *Matrix Biology*, 19(4):319–323.

Heisterbach, P. E., Todorov, A., Flückiger, R., Evans, C. H., and Majewski, M. (2012). Effect of bmp-12, tgf-β1 and autologous conditioned serum on growth factor expression in achilles tendon healing. *Knee Surgery, Sports Traumatology, Arthroscopy*, 20(10):1907–1914.

Hendriks, J., Riesle, J., and van Blitterswijk, C. A. (2007). Co-culture in cartilage tissue engineering. *Journal of tissue engineering and regenerative medicine*, 1(3):170–178.

Herchenhan, A., Bayer, M. L., Svensson, R. B., Magnusson, S. P., and Kjær, M. (2013). In vitro tendon tissue development from human fibroblasts demonstrates collagen fibril diameter growth associated with a rise in mechanical strength. *Developmental Dynamics*, 242(1):2–8.

Hernandez, R. and Brown, D. T. (2010). Growth and maintenance of chick embryo fibroblasts (cef). *Current protocols in microbiology*, pages A–4I.

Hess, G. W. (2010). Achilles tendon rupture a review of etiology, population, anatomy, risk factors, and injury prevention. *Foot & Ankle Specialist*, 3(1):29–32.

Hewett, T. E., Myer, G. D., Ford, K. R., Heidt, R. S., Colosimo, A. J., McLean, S. G., van den Bogert, A. J., Paterno, M. V., and Succop, P. (2005). Biomechanical measures of neuromuscular control and valgus loading of the knee predict anterior cruciate ligament injury risk in female athletes a prospective study. *The American journal of sports medicine*, 33(4):492–501.

Hinz, B. (2007). Formation and function of the myofibroblast during tissue repair. *Journal of Investigative Dermatology*, 127(3):526–537.

Hinz, B., Celetta, G., Tomasek, J. J., Gabbiani, G., and Chaponnier, C. (2001). Alpha-smooth muscle actin expression upregulates fibroblast contractile activity. *Molecular biology of the cell*, 12(9):2730–2741.

Hinz, B. and Gabbiani, G. (2003a). Cell-matrix and cell-cell contacts of myofibroblasts: role in connective tissue remodeling. *Thrombosis and Haemostasis Stuttgart*, 90(6):993–1002.

Hinz, B. and Gabbiani, G. (2003b). Mechanisms of force generation and transmission by myofibroblasts. *Current Opinion in Biotechnology*, 14(5):538–546.

Hinz, B., Phan, S. H., Thannickal, V. J., Galli, A., Bochaton-Piallat, M.-L., and Gabbiani, G. (2007). The myofibroblast: one function, multiple origins. *The American journal of pathology*, 170(6):1807–1816.

Ho, S. P., Kurylo, M. P., Fong, T. K., Lee, S. S., Wagner, H. D., Ryder, M. I., and Marshall, G. W. (2010). The biomechanical characteristics of the bone-periodontal ligament-cementum complex. *Biomaterials*, 31(25):6635 – 6646.

Holy, C. E., Shoichet, M. S., Davies, J. E., et al. (2000). Engineering three-dimensional bone tissue in vitro using biodegradable scaffolds: investigating initial cell-seeding density and culture period. *Journal of biomedical materials research*, 51(3):376–382.

Horch, R. E. (2006). Future perspectives in tissue engineering. *J Cell Mol Med*, 10(1):4–6. Horch, Raymund E Editorial Romania Journal of cellular and molecular medicine J Cell Mol Med. 2006 Jan-Mar;10(1):4-6.

Hornemann, S., Harlin, O., Staib, C., Kisling, S., Erfle, V., Kaspers, B., Häcker, G., and Sutter, G. (2003). Replication of modified vaccinia virus ankara in primary chicken embryo fibroblasts requires expression of the interferon resistance gene e3l. *Journal of virology*, 77(15):8394–8407.

Hotary, K. B., Yana, I., Sabeh, F., Li, X.-Y., Holmbeck, K., Birkedal-Hansen, H., Allen, E. D., Hiraoka, N., and Weiss, S. J. (2002). Matrix metalloproteinases (mmps) regulate fibrin-invasive activity via mt1-mmp–dependent and–independent processes. *The Journal of experimental medicine*, 195(3):295–308.

Hsu, S. L., Liang, R., and Woo, S. L. (2010). Functional tissue engineering of ligament healing. *Sports Med Arthrosc Rehabil Ther Technol*, 2:12. Hsu, Shan-Ling Liang, Rui Woo, Savio Ly England Sports medicine, arthroscopy, rehabilitation, therapy & technology : SMARTT Sports Med Arthrosc Rehabil Ther Technol. 2010 May 21;2:12.

Hunt, N. C. and Grover, L. M. (2010). Cell encapsulation using biopolymer gels for regenerative medicine. *Biotechnology Letters*, 32(6):733–742.

Hutmacher, D. W. (2000). Scaffolds in tissue engineering bone and cartilage. *Biomaterials*, 21(24):2529–2543.

Hyland, K. (2007). Cell proliferation and its regulation. *Biochem Lecture Notes, University of California SF*.

Hynes, R. O. (1992). Integrins: versatility, modulation, and signaling in cell adhesion. *Cell*, 69(1):11–25.

Ikada, Y. (2006). Challenges in tissue engineering. *Journal of The Royal Society Interface*, 3(10):589–601.

Ireland, M. L. (1999). Anterior cruciate ligament injury in female athletes: epidemiology. *Journal of Athletic Training*, 34(2):150.

Isenberg, B. C., Williams, C., and Tranquillo, R. T. (2006). Endothelialization and flow conditioning of fibrin-based media-equivalents. *Annals of biomedical engineering*, 34(6):971–985.

Ivanova, V. and Krivchenko, A. (2012). A current viewpoint on structure and evolution of collagens. i. fibrillar collagens. *Journal of evolutionary biochemistry and physiology*, 48(2):127–139.

James, R., Kumbar, S., Laurencin, C., Balian, G., and Chhabra, A. (2011). Tendon tissue engineering: adipose-derived stem cell and gdf-5 mediated regeneration using electrospun matrix systems. *Biomedical Materials*, 6(2):025011.

Janmey, P. A., Euteneuer, U., Traub, P., and Schliwa, M. (1991). Viscoelastic properties of vimentin compared with other filamentous biopolymer networks. *The Journal of cell biology*, 113(1):155–160.

Janmey, P. A., Winer, J. P., Murray, M. E., and Wen, Q. (2009a). The hard life of soft cells. *Cell Motil Cytoskeleton*, 66(8):597–605.

Janmey, P. A., Winer, J. P., and Weisel, J. W. (2009b). Fibrin gels and their clinical and bioengineering applications. *Journal of The Royal Society Interface*, 6(30):1–10.

Jukes, J., Both, S., Post, J., van Blitterswijk, C., Karperien, M., and de Boer, J. (2008). Chapter 1 - stem cells. In van Blitterswijk, C., Thomsen, P., Lindahl, A., Hubbell, J., Williams, D. F., Cancedda, R., de Bruijn, J. D., and Sohier, J., editors, *Tissue Engineering*, pages 1–26. Academic Press, Burlington.

Juliano, R. and Haskill, S. (1993). Signal transduction from the extracellular matrix. *Journal of Cell Biology*, 120:577–577.

Kadler, K., Holmes, D., Trotter, J., and Chapman, J. (1996). Collagen fibril formation. *Biochem. J*, 316:1–11.

Kadler, K. E., Hill, A., and Canty-Laird, E. G. (2008). Collagen fibrillogenesis: fibronectin, integrins, and minor collagens as organizers and nucleators. *Current opinion in cell biology*, 20(5):495–501.

Kannus, P. (2000). Structure of the tendon connective tissue. *Scandinavian journal of medicine & science in sports*, 10(6):312–320.

Kapacee, Z., Richardson, S. H., Lu, Y., Starborg, T., Holmes, D. F., Baar, K., and Kadler, K. E. (2008). Tension is required for fibripositor formation. *Matrix Biology*, 27(4):371–375.

Kaplan, B., Gönül, B., Dinçer, S., Kaya, F. N. D., and Babül, A. (2004). Relationships between tensile strength, ascorbic acid, hydroxyproline, and zinc levels of rabbit full-thickness incision wound healing. *Surgery today*, 34(9):747–751.

Kartus, J., Movin, T., and Karlsson, J. (2001). Donor-site morbidity and anterior knee problems after anterior cruciate ligament reconstruction using autografts. *Arthroscopy: The Journal of Arthroscopic & Related Surgery*, 17(9):971–980.

Kemençe, N. and Bölgen, N. (2013). Gelatin-and hydroxyapatite-based cryogels for bone tissue engineering: synthesis, characterization, in vitro and in vivo biocompatibility. *Journal of tissue engineering and regenerative medicine*.

Kemler, R. (1993). From cadherins to catenins: cytoplasmic protein interactions and regulation of cell adhesion. *Trends in Genetics*, 9(9):317–321.

Kew, S., Gwynne, J., Enea, D., Abu-Rub, M., Pandit, A., Zeugolis, D., Brooks, R., Rushton, N., Best, S., and Cameron, R. (2011). Regeneration and repair of tendon and ligament tissue using collagen fibre biomaterials. *Acta biomaterialia*, 7(9):3237–3247.

Kim, H.-S., Shang, T., Chen, Z., Pflugfelder, S. C., and Li, D.-Q. (2004). Tgf-β1 stimulates production of gelatinase (mmp-9), collagenases (mmp-1,-13) and stromelysins (mmp-3,-10,-11) by human corneal epithelial cells. *Experimental eye research*, 79(2):263–274.

Kim, W. S., Mooney, D. J., Arany, P. R., Lee, K., Huebsch, N., and Kim, J. (2012). Adipose tissue engineering using injectable, oxidized alginate hydrogels. *Tissue Engineering Part A*, 18(7-8):737–743.

Kinoh, H., Sato, H., Tsunezuka, Y., Takino, T., Kawashima, A., Okada, Y., and Seiki, M. (1996). Mt-mmp, the cell surface activator of prommp-2 (pro-gelatinase a), is expressed with its substrate in mouse tissue during embryogenesis. *Journal of cell science*,

109(5):953–959.

Klammert, U., Reuther, T., Blank, M., Reske, I., Barralet, J. E., Grover, L. M., Kübler, A. C., and Gbureck, U. (2010). Phase composition, mechanical performance and in vitro biocompatibility of hydraulic setting calcium magnesium phosphate cement. *Acta biomaterialia*, 6(4):1529–1535.

Klein-Nulend, J., Roelofsen, J., Sterck, J. G., Semeins, C. M., and Burger, E. H. (1995). Mechanical loading stimulates the release of transforming growth factor-β activity by cultured mouse calvariae and periosteal cells. *Journal of cellular physiology*, 163(1):115–119.

Knoblich, J. A. (2008). Mechanisms of asymmetric stem cell division. *Cell*, 132(4):583–597.

Kogan, G., Šoltés, L., Stern, R., and Gemeiner, P. (2007). Hyaluronic acid: a natural biopolymer with a broad range of biomedical and industrial applications. *Biotechnology letters*, 29(1):17–25.

Kojima, S., Soga, W., Hagiwara, H., Shimonaka, M., Saito, Y., and Inada, Y. (1986). Visible fibrinolysis by endothelial cells: effect of vitamins and sterols. *Bioscience reports*, 6:1029–1033.

Kourouklis, A. P., Lerum, R. V., and Bermudez, H. (2014). Cell adhesion mechanisms on laterally mobile polymer films. *Biomaterials*, 35(17):4827–4834.

Kresse, H. and Schönherr, E. (2001). Proteoglycans of the extracellular matrix and growth control. *Journal of cellular physiology*, 189(3):266–274.

Krishnan, L. K., Vijayan Lal, A., Uma Shankar, P., and Mohanty, M. (2003). Fibrinolysis inhibitors adversely affect remodeling of tissues sealed with fibrin glue. *Biomaterials*, 24(2):321–327.

Kuo, C. K., Marturano, J. E., and Tuan, R. S. (2010). Novel strategies in tendon and ligament tissue engineering: Advanced biomaterials and regeneration motifs. *Sports Med Arthrosc Rehabil Ther Technol*, 2:20.

Kupcsik, L., Alini, M., and Stoddart, M. J. (2008). Epsilon-aminocaproic acid is a useful fibrin degradation inhibitor for cartilage tissue engineering. *Tissue Engineering Part A*, 15(8):2309–2313.

Kvist, J. (2004). Rehabilitation following anterior cruciate ligament injury. *Sports Medicine*, 34(4):269–280.

Kvist, M. (1994). Achilles tendon injuries in athletes. *Sports Medicine*, 18(3):173–201.

Lansdown, A. B., Mirastschijski, U., Stubbs, N., Scanlon, E., and Ågren, M. S. (2007). Zinc in wound healing: theoretical, experimental, and clinical aspects. *Wound repair and regeneration*, 15(1):2–16.

Lanza, R., Langer, R., and Vacanti, J. P. (2011). *Principles of tissue engineering*. Academic press.

Laurencin, C. T., Ambrosio, A. M., Borden, M. D., and Cooper, J. A., J. (1999). Tissue engineering: orthopedic applications. *Annu Rev Biomed Eng*, 1:19–46.

Laurencin, C. T. and Freeman, J. W. (2005). Ligament tissue engineering: An evolutionary materials science approach. *Biomaterials*, 26(36):7530–7536.

Leccia, M. (1996). Pharmacological uses of zinc and other trace elements in dermatology. In *Therapeutic Uses of Trace Elements*, pages 213–217. Springer.

Lecuit, T. and Lenne, P.-F. (2007). Cell surface mechanics and the control of cell shape, tissue patterns and morphogenesis. *Nature Reviews Molecular Cell Biology*, 8(8):633–644.

Lee, D. J., Rosenfeldt, H., and Grinnell, F. (2000). Activation of erk and p38 map kinases in human fibroblasts during collagen matrix contraction. *Experimental cell research*, 257(1):190–197.

Leong, N. L., Petrigliano, F. A., and McAllister, D. R. (2013). Current tissue engineering strategies in anterior cruciate ligament reconstruction. *Journal of Biomedical Materials Research Part A*.

Lin, T. W., Cardenas, L., and Soslowsky, L. J. (2004). Biomechanics of tendon injury and repair. *Journal of biomechanics*, 37(6):865–877.

Lin, Y.-C., Tambe, D. T., Park, C. Y., Wasserman, M. R., Trepat, X., Krishnan, R., Lenormand, G., Fredberg, J. J., and Butler, J. P. (2010). Mechanosensing of substrate thickness. *Physical Review E*, 82(4):041918.

Linhardt, R. J. and Toida, T. (2004). Role of glycosaminoglycans in cellular communication. *Accounts of chemical research*, 37(7):431–438.

Little, D., Guilak, F., and Ruch, D. S. (2010). Ligament-derived matrix stimulates a ligamentous phenotype in human adipose-derived stem cells. *Tissue Engineering Part A*, 16(7):2307–2319.

Lo, C.-M., Wang, H.-B., Dembo, M., and Wang, Y.-l. (2000). Cell movement is guided by the rigidity of the substrate. *Biophysical journal*, 79(1):144–152.

Lo, K. W.-H., Jiang, T., Gagnon, K. A., Nelson, C., and Laurencin, C. T. (2014). Small-molecule based musculoskeletal regenerative engineering. *Trends in biotechnology*.

Lohmander, L., Östenberg, A., Englund, M., and Roos, H. (2004). High prevalence of knee osteoarthritis, pain, and functional limitations in female soccer players twelve years after anterior cruciate ligament injury. *Arthritis & Rheumatism*, 50(10):3145–3152.

Longo, U. G., Lamberti, A., Petrillo, S., Maffulli, N., and Denaro, V. (2012). Scaffolds in tendon tissue engineering. *Stem Cells Int*, 2012:517165.

Lu, H.-F., Chua, K.-N., Zhang, P.-C., Lim, W.-S., Ramakrishna, S., Leong, K. W., and Mao, H.-Q. (2005). Three-dimensional co-culture of rat hepatocyte spheroids and nih/3t3 fibroblasts enhances hepatocyte functional maintenance. *Acta biomaterialia*, 1(4):399–410.

Lu, H. H., Subramony, S. D., Boushell, M. K., and Zhang, X. (2010). Tissue engineering strategies for the regeneration of orthopedic interfaces. *Annals of biomedical engineering*, 38(6):2142–2154.

Luck, M. R., Jeyaseelan, I., and Scholes, R. A. (1995). Ascorbic acid and fertility. *Biology of reproduction*, 52(2):262–266.

Lui, P., Lee, Y., Mok, T., Cheuk, Y., Chan, K., et al. (2013a). Alendronate reduced peri-tunnel bone loss and enhanced tendon graft to bone tunnel healing in anterior cruciate ligament reconstruction. *Eur Cell Mater*, 25:78–96.

Lui, P. P. Y., Lee, Y. W., Mok, T. Y., and Cheuk, Y. C. (2013b). Local administration of alendronate reduced peri-tunnel bone loss and promoted graft-bone tunnel healing with minimal systemic effect on bone in contralateral knee. *Journal of Orthopaedic Research*, 31(12):1897–1906.

Lutolf, M. and Hubbell, J. (2005). Synthetic biomaterials as instructive extracellular microenvironments for morphogenesis in tissue engineering. *Nature biotechnology*, 23(1):47–55.

Ma, J., Smietana, M. J., Kostrominova, T. Y., Wojtys, E. M., Larkin, L. M., and Arruda, E. M. (2011). Three-dimensional engineered bone–ligament–bone constructs for anterior

cruciate ligament replacement. *Tissue Engineering Part A*, 18(1-2):103–116.

Macara, I., Lounsbury, K., Richards, S., McKiernan, C., and Bar-Sagi, D. (1996). The ras superfamily of gtpases. *The FASEB journal*, 10(5):625–630.

Magnussen, R. A., Glisson, R. R., and Moorman, C. T. (2011). Augmentation of achilles tendon repair with extracellular matrix xenograft a biomechanical analysis. *The American Journal of Sports Medicine*, 39(7):1522–1527.

Malumbres, M. and Barbacid, M. (2001). Milestones in cell division: to cycle or not to cycle: a critical decision in cancer. *Nature Reviews Cancer*, 1(3):222–231.

Malumbres, M. and Barbacid, M. (2009). Cell cycle, cdks and cancer: a changing paradigm. *Nature Reviews Cancer*, 9(3):153–166.

Martin-Martin, B., Tovell, V., Dahlmann-Noor, A. H., Khaw, P. T., and Bailly, M. (2011). The effect of mmp inhibitor gm6001 on early fibroblast-mediated collagen matrix contraction is correlated to a decrease in cell protrusive activity. *European journal of cell biology*, 90(1):26–36.

Marturano, J. E., Arena, J. D., Schiller, Z. A., Georgakoudi, I., and Kuo, C. K. (2013). Characterization of mechanical and biochemical properties of developing embryonic tendon. *Proceedings of the National Academy of Sciences*, 110(16):6370–6375.

Marx, G. and Chevion, M. (1985). Fibrinogen coagulation without thrombin: reaction with vitamin c and copper (ii). *Thrombosis research*, 40(1):11–18.

Mason, B. N., Califano, J. P., and Reinhart-King, C. A. (2012). Matrix stiffness: A regulator of cellular behavior and tissue formation. In *Engineering Biomaterials for Regenerative Medicine*, pages 19–37. Springer.

Masur, S., Dewal, H., Dinh, T., Erenburg, I., and Petridou, S. (1996). Myofibroblasts differentiate from fibroblasts when plated at low density. *Proceedings of the National Academy of Sciences*, 93(9):4219–4223.

Matrisian, L. M. (1990). Metalloproteinases and their inhibitors in matrix remodeling. *Trends in Genetics*, 6:121–125.

Matuszewski, P. E., Chen, Y.-L., Szczesny, S. E., Lake, S. P., Elliott, D. M., Soslowsky, L. J., and Dodge, G. R. (2012). Regional variation in human supraspinatus tendon proteoglycans: decorin, biglycan, and aggrecan. *Connective tissue research*, 53(5):343–348.

Mauck, R. L., Seyhan, S. L., Ateshian, G. A., and Hung, C. T. (2002). Influence of seeding density and dynamic deformational loading on the developing structure/function relationships of chondrocyte-seeded agarose hydrogels. *Annals of biomedical engineering*, 30(8):1046–1056.

Mazia, D., Schatten, G., and Sale, W. (1975). Adhesion of cells to surfaces coated with polylysine. applications to electron microscopy. *The Journal of cell biology*, 66(1):198–200.

McCawley, L. J. and Matrisian, L. M. (2001). Matrix metalloproteinases: they're not just for matrix anymore! *Current opinion in cell biology*, 13(5):534–540.

McKeehan, W. L. and Ham, R. G. (1976). Stimulation of clonal growth of normal fibroblasts with substrata coated with basic polymers. *The Journal of cell biology*, 71(3):727–734.

McKleroy, W., Lee, T.-H., and Atabai, K. (2013). Always cleave up your mess: targeting collagen degradation to treat tissue fibrosis. *American Journal of Physiology-Lung Cellular and Molecular Physiology*, 304(11):L709–L721.

Mehr, D., Pardubsky, P., Martin, J., and Buckwalter, J. (2000). Tenascin-c in tendon regions subjected to compression. *Journal of Orthopaedic Research*, 18(4):537–545.

Midwood, K. S. and Orend, G. (2009). The role of tenascin-c in tissue injury and tumorigenesis. *Journal of cell communication and signaling*, 3(3-4):287–310.

Mimori, K., Komaki, M., Iwasaki, K., and Ishikawa, I. (2007). Extracellular signal-regulated kinase 1/2 is involved in ascorbic acid-induced osteoblastic differentiation in periodontal ligament cells. *Journal of Periodontology*, 78(2):328–334.

Mithieux, S. M. and Weiss, A. S. (2005). Elastin. *Advances in protein chemistry*, 70:437–461.

Moon, S. Y. and Zheng, Y. (2003). Rho gtpase-activating proteins in cell regulation. *Trends in cell biology*, 13(1):13–22.

Morgan, J. F. (1958). Tissue culture nutrition. *Bacteriological reviews*, 22(1):20.

Morgan, J. F., Morton, H. J., and Parker, R. C. (1950). Nutrition of animal cells in tissue culture. i. initial studies on a synthetic medium. *Experimental Biology and Medicine*, 73(1):1–8.

Morrison, S. J. and Kimble, J. (2006). Asymmetric and symmetric stem-cell divisions in development and cancer. *Nature*, 441(7097):1068–1074.

Mosesson, M. W. (2005). Fibrinogen and fibrin structure and functions. *Journal of Thrombosis and Haemostasis*, 3(8):1894–1904.

Mott, J. D. and Werb, Z. (2004). Regulation of matrix biology by matrix metalloproteinases. *Current opinion in cell biology*, 16(5):558–564.

Moulin, V. and Plamondon, M. (2002). Differential expression of collagen integrin receptor on fetal vs. adult skin fibroblasts: implication in wound contraction during healing. *British Journal of Dermatology*, 147(5):886–892.

Murad, S., Grove, D., Lindberg, K., Reynolds, G., Sivarajah, A., and Pinnell, S. (1981). Regulation of collagen synthesis by ascorbic acid. *Proceedings of the National Academy of Sciences*, 78(5):2879–2882.

Mutsuzaki, H., Sakane, M., Nakajima, H., Ito, A., Hattori, S., Miyanaga, Y., Ochiai, N., and Tanaka, J. (2004). Calcium-phosphate-hybridized tendon directly promotes regeneration of tendon-bone insertion. *Journal of Biomedical Materials Research Part A*, 70(2):319–327.

Nelson, C. M. (2009). Geometric control of tissue morphogenesis. *Biochimica et Biophysica Acta (BBA)-Molecular Cell Research*, 1793(5):903–910.

Neuman, R. E. (1950). Hydroxyproline content of the developing chick embryo. *Proc Soc Exp Biol Med*, 75(1):37–9.

NHS-Choices (2012). Introduction, ligament knee surgery, http://www.nhs.uk/conditions/repairtotendon/pages/introduction.aspx.

Nindl Waite, G. and Waite, L. (2007). *Applied Cell and Molecular Biology*. McGraw Hill Companies New York, USA.

Nussbaum, R., McInnes, R. R., and Willard, H. F. (2007). *Thompson & Thompson genetics in medicine*. Elsevier Health Sciences.

O'Brien, F. J. (2011). Biomaterials & scaffolds for tissue engineering. *Materials Today*, 14(3):88–95.

Øiestad, B. E., Engebretsen, L., Storheim, K., and Risberg, M. A. (2009). Knee osteoarthritis after anterior cruciate ligament injury a systematic review. *The American journal of sports medicine*, 37(7):1434–1443.

Osiecki, M., Ghanavi, P., Atkinson, K., Nielsen, L. K., and Doran, M. R. (2010). The ascorbic acid paradox. *Biochemical and biophysical research communications*, 400(4):466–470.

Otsuka, E., Yamaguchi, A., Hirose, S., and Hagiwara, H. (1999). Characterization of osteoblastic differentiation of stromal cell line st2 that is induced by ascorbic acid. *American Journal of Physiology-Cell Physiology*, 277(1):C132–C138.

Ottani, V., Martini, D., Franchi, M., Ruggeri, A., and Raspanti, M. (2002). Hierarchical structures in fibrillar collagens. *Micron*, 33(7):587–596.

Ottani, V., Raspanti, M., and Ruggeri, A. (2001). Collagen structure and functional implications. *Micron*, 32(3):251–260.

Padayatty, S. J., Riordan, H. D., Hewitt, S. M., Katz, A., Hoffer, L. J., and Levine, M. (2006). Intravenously administered vitamin c as cancer therapy: three cases. *Canadian Medical Association Journal*, 174(7):937–942.

Page-McCaw, A., Ewald, A. J., and Werb, Z. (2007). Matrix metalloproteinases and the regulation of tissue remodelling. *Nat Rev Mol Cell Biol*, 8(3):221–33.

Park, A., Hogan, M. V., Kesturu, G. S., James, R., Balian, G., and Chhabra, A. B. (2010). Adipose-derived mesenchymal stem cells treated with growth differentiation factor-5 express tendon-specific markers. *Tissue Engineering Part A*, 16(9):2941–2951.

Park, S., Park, C. H., Hahm, E.-R., Kim, K., Kimler, B. F., Lee, S. J., Park, H. K., Lee, S.-H., Kim, W. S., Jung, C. W., et al. (2005). Activation of raf1 and the erk pathway in response to l-ascorbic acid in acute myeloid leukemia cells. *Cellular signalling*, 17(1):111–119.

Paxton, J. Z., Donnelly, K., Keatch, R. P., and Baar, K. (2008). Engineering the bone-ligament interface using polyethylene glycol diacrylate incorporated with hydroxyapatite. *Tissue Engineering Part A*, 15(6):1201–1209.

Paxton, J. Z., Donnelly, K., Keatch, R. P., Baar, K., and Grover, L. M. (2010a). Factors affecting the longevity and strength in an in vitro model of the bone–ligament interface. *Annals of biomedical engineering*, 38(6):2155–2166.

Paxton, J. Z., Grover, L. M., and Baar, K. (2010b). Engineering an in vitro model of a functional ligament from bone to bone. *Tissue Engineering Part A*, 16(11):3515–3525.

Paxton, J. Z., Hagerty, P., Andrick, J. J., and Baar, K. (2011). Optimizing an intermittent stretch paradigm using erk1/2 phosphorylation results in increased collagen synthesis in engineered ligaments. *Tissue Engineering Part A*, 18(3-4):277–284.

Paxton, J. Z., Wudebwe, U. N., Wang, A., Woods, D., and Grover, L. M. (2012). Monitoring sinew contraction during formation of tissue-engineered fibrin-based ligament constructs. *Tissue Engineering Part A*, 18(15-16):1596–1607.

Peppas, N., Bures, P., Leobandung, W., and Ichikawa, H. (2000). Hydrogels in pharmaceutical formulations. *European journal of pharmaceutics and biopharmaceutics*, 50(1):27–46.

Peterkofsky, B. (1972). Regulation of collagen secretion by ascorbic acid in 3t3 and chick embryo fibroblasts. *Biochemical and biophysical research communications*, 49(5):1343–1350.

Phan, S. H. (2008). Biology of fibroblasts and myofibroblasts. *Proceedings of the American Thoracic Society*, 5(3):334.

Phang, J. M., Donald, S. P., Pandhare, J., and Liu, Y. (2008). The metabolism of proline, a stress substrate, modulates carcinogenic pathways. *Amino acids*, 35(4):681–690.

Phillips, J. A., Vacanti, C. A., and Bonassar, L. J. (2003). Fibroblasts regulate contractile force independent of mmp activity in 3d-collagen. *Biochemical and biophysical research communications*, 312(3):725–732.

Pikal-Cleland, K. A., Rodriguez-Hornedo, N., Amidon, G. L., and Carpenter, J. F. (2000). Protein denaturation during freezing and thawing in phosphate buffer systems: monomeric and tetrameric β-galactosidase. *Archives of biochemistry and biophysics*, 384(2):398–406.

Polak, J. M. and Bishop, A. E. (2006). Stem cells and tissue engineering: past, present, and future. *Annals of the New York Academy of Sciences*, 1068(1):352–366.

Prockop, D. J. and Juva, K. (1965). Synthesis of hydroxyproline in vitro by the hydroxylation of proline in a precursor of collagen. *Proceedings of the National Academy of Sciences of the United States of America*, 53(3):661.

Provenzano, P., Lakes, R., Keenan, T., and Vanderby Jr, R. (2001). Nonlinear ligament viscoelasticity. *Annals of biomedical engineering*, 29(10):908–914.

Radisic, M., Euloth, M., Yang, L., Langer, R., Freed, L. E., and Vunjak-Novakovic, G. (2003). High-density seeding of myocyte cells for cardiac tissue engineering. *Biotechnology and bioengineering*, 82(4):403–414.

Raftopoulou, M. and Hall, A. (2004). Cell migration: Rho gtpases lead the way. *Developmental biology*, 265(1):23–32.

Ramshaw, J. A., Shah, N. K., and Brodsky, B. (1998). Gly-xy tripeptide frequencies in collagen: a context for host–guest triple-helical peptides. *Journal of structural biology*, 122(1):86–91.

Rawson, S., Cartmell, S., and Wong, J. (2013). Suture techniques for tendon repair; a comparative review. *Muscle, Ligaments and Tendons Journal*, 3(3):220–228.

Reinhart-King, C. A., Dembo, M., and Hammer, D. A. (2008). Cell-cell mechanical communication through compliant substrates. *Biophysical Journal*, 95(12):6044–6051.

Ren, X.-D., Kiosses, W. B., Sieg, D. J., Otey, C. A., Schlaepfer, D. D., and Schwartz, M. A. (2000). Focal adhesion kinase suppresses rho activity to promote focal adhesion turnover. *Journal of cell science*, 113(20):3673–3678.

Riehl, B. D., Park, J.-H., Kwon, I. K., and Lim, J. Y. (2012). Mechanical stretching for tissue engineering: two-dimensional and three-dimensional constructs. *Tissue Engineering Part B: Reviews*, 18(4):288–300.

Rifkin, D. B., Crowe, R. M., and Pollack, R. (1979). Tumor promoters induce changes in the chick embryo fibroblast cytoskeleton. *Cell*, 18(2):361–368.

Roberts, A. B., Mccune, B. K., and Spore, B. (1992). Tgf-bold beta: Regulation of extracellular matrix. *Kidney Int*, 41(5):57–59.

Roberts, P. and Der, C. (2007). Targeting the raf-mek-erk mitogen-activated protein kinase cascade for the treatment of cancer. *Oncogene*, 26(22):3291–3310.

Robertson, A., Nutton, R., and Keating, J. (2006). Current trends in the use of tendon allografts in orthopaedic surgery. *Journal of Bone & Joint Surgery, British Volume*, 88(8):988–992.

Rodrigues, M. T., Reis, R. L., and Gomes, M. E. (2013). Engineering tendon and ligament tissues: present developments towards successful clinical products. *Journal of tissue engineering and regenerative medicine*, 7(9):673–686.

Rossi, C. A., Pozzobon, M., and De Coppi, P. (2010). Advances in musculoskeletal tissue engineering: moving towards therapy. *Organogenesis*, 6(3):167.

Rudd, T., Skidmore, M., Guerrini, M., Hricovini, M., Powell, A., Siligardi, G., and Yates, E. (2010). The conformation and structure of gags: recent progress and perspectives. *Current opinion in structural biology*, 20(5):567–574.

Rumian, A. P., Wallace, A. L., and Birch, H. L. (2007). Tendons and ligaments are anatomically distinct but overlap in molecular and morphological features–a comparative study in an ovine model. *J Orthop Res*, 25(4):458–64.

Sahoo, S. (2011). Tendon & ligament tissue engineering. *AsiaBiotech*, 15(1).

Sahoo, S., Toh, S. L., and Goh, J. C. (2010). A bfgf-releasing silk/plga-based biohybrid scaffold for ligament/tendon tissue engineering using mesenchymal progenitor cells. *Biomaterials*, 31(11):2990–2998.

Saltzman, W. M. (2004). *Tissue engineering: engineering principles for the design of replacement organs and tissues*, volume 4. Oxford university press New York, USA.

Sarasa-Renedo, A. and Chiquet, M. (2005). Mechanical signals regulating extracellular matrix gene expression in fibroblasts. *Scandinavian Journal of Medicine & Science in Sports*, 15(4):223–230.

Schneider, H., Shaw, M., Muirhead, E., and Smith, A. (1965). The¡ i¿ in vitro¡/i¿ culture of embryonic chicken heart cells. *Experimental cell research*, 39(2):631–636.

Schönbrunner, E. R. and Schmid, F. X. (1992). Peptidyl-prolyl cis-trans isomerase improves the efficiency of protein disulfide isomerase as a catalyst of protein folding. *Proceedings of the National Academy of Sciences*, 89(10):4510–4513.

Schram, K., Ganguly, R., No, E. K., Fang, X., Thong, F. S., and Sweeney, G. (2011). Regulation of mt1-mmp and mmp-2 by leptin in cardiac fibroblasts involves rho/rock-dependent actin cytoskeletal reorganization and leads to enhanced cell migration. *Endocrinology*, 152(5):2037–2047.

Schulze-Tanzil, G., Mobasheri, A., Clegg, P., Sendzik, J., John, T., and Shakibaei, M. (2004). Cultivation of human tenocytes in high-density culture. *Histochemistry and cell biology*, 122(3):219–228.

Schvartz, I., Seger, D., and Shaltiel, S. (1999). Vitronectin. *The international journal of biochemistry & cell biology*, 31(5):539–544.

Schweitzer, R., Chyung, J. H., Murtaugh, L. C., Brent, A. E., Rosen, V., Olson, E. N., Lassar, A., and Tabin, C. J. (2001). Analysis of the tendon cell fate using scleraxis, a specific marker for tendons and ligaments. *Development*, 128(19):3855–3866.

Seo, S.-J., Kim, I.-Y., Choi, Y.-J., Akaike, T., and Cho, C.-S. (2006). Enhanced liver functions of hepatocytes cocultured with nih 3t3 in the alginate/galactosylated chitosan scaffold. *Biomaterials*, 27(8):1487–1495.

Shah, J. V. and Janmey, P. A. (1997). Strain hardening of fibrin gels and plasma clots. *Rheologica Acta*, 36(3):262–268.

Shahab-Osterloh, S., Witte, F., Hoffmann, A., Winkel, A., Laggies, S., Neumann, B., Seiffart, V., Lindenmaier, W., Gruber, A. D., Ringe, J., et al. (2010). Mesenchymal stem cell-dependent formation of heterotopic tendon-bone insertions (osteotendinous junctions). *Stem Cells*, 28(9):1590–1601.

Shapira-Schweitzer, K. and Seliktar, D. (2007). Matrix stiffness affects spontaneous contraction of cardiomyocytes cultured within a pegylated fibrinogen biomaterial. *Acta biomaterialia*, 3(1):33–41.

Sharma, P. and Maffulli, N. (2006). Biology of tendon injury: healing, modeling and remodeling. *Journal of Musculoskeletal and Neuronal Interactions*, 6(2):181.

Shen, L. L., McDonagh, R. P., McDonagh, J., and Hermans Jr, J. (1974). Fibrin gel structure: influence of calcium and covalent cross-linking on the elasticity. *Biochemical and biophysical research communications*, 56(3):793–798.

Shin, H., Jo, S., and Mikos, A. G. (2003). Biomimetic materials for tissue engineering. *Biomaterials*, 24(24):4353–4364.

Shipley, G. D. and Ham, R. G. (1981). Improved medium and culture conditions for clonal growth with minimal serum protein and for enhanced serum-free survival of swiss 3t3 cells. *In vitro*, 17(8):656–670.

Silver, F. H., Freeman, J. W., and Seehra, G. P. (2003). Collagen self-assembly and the development of tendon mechanical properties. *Journal of biomechanics*, 36(10):1529–1553.

Singh, P., Carraher, C., and Schwarzbauer, J. E. (2010). Assembly of fibronectin extracellular matrix. *Annual review of cell and developmental biology*, 26:397.

Slauterbeck, J. R., Fuzie, S. F., Smith, M. P., Clark, R. J., Xu, K. T., Starch, D. W., and Hardy, D. M. (2002). The menstrual cycle, sex hormones, and anterior cruciate ligament injury. *Journal of athletic training*, 37(3):275.

Solomonow, M. (2004). Ligaments: a source of work-related musculoskeletal disorders. *Journal of Electromyography and Kinesiology*, 14(1):49–60.

Solon, J., Levental, I., Sengupta, K., Georges, P. C., and Janmey, P. A. (2007). Fibroblast adaptation and stiffness matching to soft elastic substrates. *Biophys J*, 93(12):4453–61. Solon, Jerome Levental, Ilya Sengupta, Kheya Georges, Penelope C Janmey, Paul A United States Biophysical journal Biophys J. 2007 Dec 15;93(12):4453-61.

Standeven, K. F., Ariëns, R. A., and Grant, P. J. (2005). The molecular physiology and pathology of fibrin structure/function. *Blood reviews*, 19(5):275–288.

Steinert, A. F., Kunz, M., Prager, P., Barthel, T., Jakob, F., Nöth, U., Murray, M. M., Evans, C. H., and Porter, R. M. (2011). Mesenchymal stem cell characteristics of human anterior cruciate ligament outgrowth cells. *Tissue Engineering Part A*, 17(9-10):1375–1388.

Stevens, K., Ungrin, M., Schwartz, R., Ng, S., Carvalho, B., Christine, K., Chaturvedi, R., Li, C., Zandstra, P., Chen, C., et al. (2013). Invert molding for scalable control of tissue microarchitecture. *Nature communications*, 4:1847.

Strober, W. (2001). Trypan blue exclusion test of cell viability. *Current Protocols in Immunology*, pages A–3B.

Subramony, S. D., Dargis, B. R., Castillo, M., Azeloglu, E. U., Tracey, M. S., Su, A., and Lu, H. H. (2013). The guidance of stem cell differentiation by substrate alignment and mechanical stimulation. *Biomaterials*, 34(8):1942–1953.

Sung, H. J., Meredith, C., Johnson, C., and Galis, Z. S. (2004). The effect of scaffold degradation rate on three-dimensional cell growth and angiogenesis. *Biomaterials*, 25(26):5735–5742. 829QL Times Cited:195 Cited References Count:24.

Tamayol, A., Akbari, M., Annabi, N., Paul, A., Khademhosseini, A., and Juncker, D. (2013). Fiber-based tissue engineering: Progress, challenges, and opportunities. *Biotechnology advances*, 31(5):669–687.

Tang, Z., Yang, L., Xue, R., Zhang, J., Wang, Y., Chen, P. C., and Sung, K. (2009). Differential expression of matrix metalloproteinases and tissue inhibitors of metalloproteinases in anterior cruciate ligament and medial collateral ligament fibroblasts after a mechanical injury: Involvement of the p65 subunit of nf-κb. *Wound Repair and Regeneration*,

17(5):709–716.

Taylor, K. R. and Gallo, R. L. (2006). Glycosaminoglycans and their proteoglycans: host-associated molecular patterns for initiation and modulation of inflammation. *The FASEB Journal*, 20(1):9–22.

Teh, T. K., Toh, S.-L., and Goh, J. C. (2013). Aligned fibrous scaffolds for enhanced mechanoresponse and tenogenesis of mesenchymal stem cells. *Tissue Engineering Part A*, 19(11-12):1360–1372.

Temu, T. M., Wu, K.-Y., Gruppuso, P. A., and Phornphutkul, C. (2010). The mechanism of ascorbic acid-induced differentiation of atdc5 chondrogenic cells. *American Journal of Physiology-Endocrinology and Metabolism*, 299(2):E325.

Thomopoulos, S., Genin, G. M., and Galatz, L. M. (2010). The development and morphogenesis of the tendon-to-bone insertion what development can teach us about healing. *Journal of musculoskeletal & neuronal interactions*, 10(1):35.

Thoms, B. L. and Murphy, C. L. (2010). Inhibition of hypoxia-inducible factor-targeting prolyl hydroxylase domain-containing protein 2 (phd2) enhances matrix synthesis by human chondrocytes. *Journal of Biological Chemistry*, 285(27):20472–20480.

Tibbitt, M. W. and Anseth, K. S. (2009). Hydrogels as extracellular matrix mimics for 3d cell culture. *Biotechnology and bioengineering*, 103(4):655–663.

Tischer, T., Vogt, S., Aryee, S., Steinhauser, E., Adamczyk, C., Milz, S., Martinek, V., and Imhoff, A. B. (2007). Tissue engineering of the anterior cruciate ligament: a new method using acellularized tendon allografts and autologous fibroblasts. *Archives of orthopaedic and trauma surgery*, 127(9):735–741.

Tomasek, J. J., Gabbiani, G., Hinz, B., Chaponnier, C., and Brown, R. A. (2002). Myofibroblasts and mechano-regulation of connective tissue remodelling. *Nature Reviews Molecular Cell Biology*, 3(5):349–363.

Tozer, S. and Duprez, D. (2005). Tendon and ligament: development, repair and disease. *Birth Defects Research Part C: Embryo Today: Reviews*, 75(3):226–236.

Trackman, P. C. (2005). Diverse biological functions of extracellular collagen processing enzymes. *Journal of cellular biochemistry*, 96(5):927–937.

Trobisch, P. D., Bauman, M., Weise, K., Stuby, F., and Hak, D. J. (2010). Histologic analysis of ruptured quadriceps tendons. *Knee Surgery, Sports Traumatology, Arthroscopy*, 18(1):85–88.

Tseng, H.-J., Tsou, T.-L., Wang, H.-J., and Hsu, S.-h. (2013). Characterization of chitosan–gelatin scaffolds for dermal tissue engineering. *Journal of tissue engineering and regenerative medicine*, 7(1):20–31.

Tuan, R. S. (2013). Regenerative medicine in 2012: the coming of age of musculoskeletal tissue engineering. *Nature Reviews Rheumatology*, 9(2):74–76.

Tyson, J. J. and Novak, B. (2001). Regulation of the eukaryotic cell cycle: molecular antagonism, hysteresis, and irreversible transitions. *Journal of Theoretical Biology*, 210(2):249–263.

Ulloa, F. and Briscoe, J. (2007). Morphogens and the control of cell proliferation and patterning in the spinal cord. *Cell cycle*, 6(21):2640–2649.

Uysal, C. A., Tobita, M., Hyakusoku, H., and Mizuno, H. (2012). Adipose-derived stem cells enhance primary tendon repair: Biomechanical and immunohistochemical evaluation. *Journal of Plastic, Reconstructive & Aesthetic Surgery*.

Vallet-Regi, M. and González-Calbet, J. M. (2004). Calcium phosphates as substitution of bone tissues. *Progress in Solid State Chemistry*, 32(1):1–31.

van Blitterswijk, C. (2008). *Tissue Engineering*. Academic press.

van der Flier, A. and Sonnenberg, A. (2001). Function and interactions of integrins. *Cell and tissue research*, 305(3):285–298.

Van Eijk, F., Saris, D., Riesle, J., Willems, W., Van Blitterswijk, C., Verbout, A., and Dhert, W. (2004). Tissue engineering of ligaments: a comparison of bone marrow stromal cells, anterior cruciate ligament, and skin fibroblasts as cell source. *Tissue engineering*, 10(5-6):893–903.

Van Vlierberghe, S., Dubruel, P., and Schacht, E. (2011). Biopolymer-based hydrogels as scaffolds for tissue engineering applications: A review. *Biomacromolecules*, 12(5):1387–1408.

Vaquette, C., Kahn, C., Frochot, C., Nouvel, C., Six, J.-L., De Isla, N., Luo, L.-H., Cooper-White, J., Rahouadj, R., and Wang, X. (2010). Aligned poly (l-lactic-co-e-caprolactone) electrospun microfibers and knitted structure: A novel composite scaffold for ligament tissue engineering. *Journal of Biomedical Materials Research Part A*, 94(4):1270–1282.

Ventura, A., Terzaghi, C., Legnani, C., Borgo, E., and Albisetti, W. (2010). Synthetic grafts for anterior cruciate ligament rupture: 19-year outcome study. *The Knee*, 17(2):108–113.

Vitagliano, L., Berisio, R., Mastrangelo, A., Mazzarella, L., and Zagari, A. (2001). Preferred proline puckerings in cis and trans peptide groups: Implications for collagen stability. *Protein Science*, 10(12):2627–2632. 496UZ Times Cited:89 Cited References Count:34.

Vogel, V. and Sheetz, M. (2006). Local force and geometry sensing regulate cell functions. *Nature Reviews Molecular Cell Biology*, 7(4):265–275.

Vunjak-Novakovic, G., Altman, G., Horan, R., and Kaplan, D. L. (2004). Tissue engineering of ligaments. *Annual Review of Biomedical Engineering*, 6(1):131–156.

Wang, F., Wang, H., Wang, J., Wang, H.-Y., Rummel, P. L., Garimella, S. V., and Lu, C. (2008). Microfluidic delivery of small molecules into mammalian cells based on hydrodynamic focusing. *Biotechnology and Bioengineering*, 100(1):150–158.

Wang, J. H.-C., Thampatty, B. P., Lin, J.-S., and Im, H.-J. (2007). Mechanoregulation of gene expression in fibroblasts. *Gene*, 391(1):1–15.

Wang, T., Gardiner, B. S., Lin, Z., Rubenson, J., Kirk, T. B., Wang, A., Xu, J., Smith, D. W., Lloyd, D. G., and Zheng, M. H. (2012). Bioreactor design for tendon/ligament engineering. *Tissue Engineering Part B: Reviews*, 19(2):133–146.

Watt, F. M. and Huck, W. T. (2013). Role of the extracellular matrix in regulating stem cell fate. *Nature Reviews Molecular Cell Biology*, 14(8):467–473.

Weber, G. F., Bjerke, M. A., and DeSimone, D. W. (2011). Integrins and cadherins join forces to form adhesive networks. *Journal of cell science*, 124(8):1183–1193.

Weinberg, R. A. (1995). The retinoblastoma protein and cell cycle control. *Cell*, 81(3):323–330.

Weis, W. I. and Nelson, W. J. (2006). Re-solving the cadherin-catenin-actin conundrum. *Journal of Biological Chemistry*, 281(47):35593–35597.

Weisel, J. (2007). Structure of fibrin: impact on clot stability. *Journal of Thrombosis and Haemostasis*, 5(s1):116–124.

Weisel, J. W. (2004). The mechanical properties of fibrin for basic scientists and clinicians. *Biophysical chemistry*, 112(2):267–276.

Weiss, J. A., Gardiner, J. C., and Bonifasi-Lista, C. (2002). Ligament material behavior is nonlinear, viscoelastic and rate-independent under shear loading. *Journal of biomechanics*, 35(7):943–950.

Weitz, D., Wyss, H., and Larsen, R. (2007). Oscillatory rheology: Measuring the viscoelastic behaviour of soft materials. *GIT laboratory journal Europe*, 11(3-4):68–70.

Wells, R. G. (2008). The role of matrix stiffness in regulating cell behavior. *Hepatology*, 47(4):1394–1400.

Wen, Q., Basu, A., Winer, J. P., Yodh, A., and Janmey, P. A. (2007). Local and global deformations in a strain-stiffening fibrin gel. *New Journal of Physics*, 9(11):428.

Werb, Z. (1997). Ecm and cell surface proteolysis: regulating cellular ecology. *Cell*, 91(4):439–442.

Wheeler, A. P. and Ridley, A. J. (2004). Why three rho proteins? rhoa, rhob, rhoc, and cell motility. *Experimental cell research*, 301(1):43–49.

White, D. J., Puranen, S., Johnson, M. S., and Heino, J. (2004). The collagen receptor subfamily of the integrins. *The international journal of biochemistry & cell biology*, 36(8):1405–1410.

Wolberg, A. S. and Campbell, R. A. (2008). Thrombin generation, fibrin clot formation and hemostasis. *Transfusion and Apheresis Science*, 38(1):15–23.

Woo, S. L.-Y., Orlando, C. A., Gomez, M. A., Frank, C. B., and Akeson, W. H. (1986). Tensile properties of the medial collateral ligament as a function of age. *Journal of orthopaedic research*, 4(2):133–141.

Woo, S. L.-Y., Vogrin, T. M., and Abramowitch, S. D. (2000). Healing and repair of ligament injuries in the knee. *Journal of the American Academy of Orthopaedic Surgeons*, 8(6):364–372.

Wozniak, M. A., Modzelewska, K., Kwong, L., and Keely, P. J. (2004). Focal adhesion regulation of cell behavior. *Biochim Biophys Acta*, 1692(2-3):103–19. Wozniak, Michele A Modzelewska, Katarzyna Kwong, Lina Keely, Patricia J CA076537/CA/NCI NIH HHS/United States Research Support, Non-U.S. Gov't Research Support, U.S. Gov't, Non-P.H.S. Research Support, U.S. Gov't, P.H.S. Review Netherlands Biochimica et biophysica acta Biochim Biophys Acta. 2004 Jul 5;1692(2-3):103-19.

Wu, G., Bazer, F. W., Burghardt, R. C., Johnson, G. A., Kim, S. W., Knabe, D. A., Li, P., Li, X., McKnight, J. R., Satterfield, M. C., et al. (2011). Proline and hydroxyproline metabolism: implications for animal and human nutrition. *Amino acids*, 40(4):1053–1063.

Wu, L. and Ding, J. (2004). In vitro degradation of three-dimensional porous poly (d, l-lactide-co-glycolide) scaffolds for tissue engineering. *Biomaterials*, 25(27):5821–5830.

Wufsus, A., Macera, N., and Neeves, K. (2013). The hydraulic permeability of blood clots as a function of fibrin and platelet density. *Biophysical journal*, 104(8):1812–1823.

Xu, Y., Dong, S., Zhou, Q., Mo, X., Song, L., Hou, T., Wu, J., Li, S., Li, Y., Li, P., et al. (2014). The effect of mechanical stimulation on the maturation of tdscs-poly (l-lactide-co-e-caprolactone)/collagen scaffold constructs for tendon tissue engineering. *Biomaterials*.

Yamada, Y. and Kleinman, H. K. (1992). Functional domains of cell adhesion molecules. *Current opinion in cell biology*, 4(5):819–823.

Yamaguchi, Y. (2000). Lecticans: organizers of the brain extracellular matrix. *Cellular and Molecular Life Sciences CMLS*, 57(2):276–289.

Yan, C. and Pochan, D. J. (2010). Rheological properties of peptide-based hydrogels for biomedical and other applications. *Chemical Society Reviews*, 39(9):3528–3540.

Yang, G., Rothrauff, B. B., and Tuan, R. S. (2013). Tendon and ligament regeneration and repair: Clinical relevance and developmental paradigm. *Birth Defects Research Part C: Embryo Today: Reviews*, 99(3):203–222.

Yang, M. T., Fu, J., Wang, Y.-K., Desai, R. A., and Chen, C. S. (2011). Assaying stem cell mechanobiology on microfabricated elastomeric substrates with geometrically modulated rigidity. *nature protocols*, 6(2):187–213.

Yang, T.-T. and Hawkes, S. P. (1992). Role of the 21-kda protein timp-3 in oncogenic transformation of cultured chicken embryo fibroblasts. *Proceedings of the National Academy of Sciences*, 89(22):10676–10680.

Yasuda, K., Tsujino, J., Ohkoshi, Y., Tanabe, Y., and Kaneda, K. (1995). Graft site morbidity with autogenous semitendinosus and gracilis tendons. *The American journal of sports medicine*, 23(6):706–714.

Yee Jr, H. F., Melton, A. C., and Tran, B. N. (2001). Rhoa/rho-associated kinase mediates fibroblast contractile force generation. *Biochemical and biophysical research communications*, 280(5):1340–1345.

Young, A. and McNaught, C.-E. (2011). The physiology of wound healing. *Surgery (Oxford)*, 29(10):475–479.

Zantop, T., Petersen, W., Sekiya, J. K., Musahl, V., and Fu, F. H. (2006). Anterior cruciate ligament anatomy and function relating to anatomical reconstruction. *Knee surgery, sports traumatology, arthroscopy*, 14(10):982–992.

Zhang, W. and Liu, H. T. (2002). Mapk signal pathways in the regulation of cell proliferation in mammalian cells. *Cell research*, 12(1):9–18.

Zhuge, Y. and Xu, J. (2001). Rac1 mediates type i collagen-dependent mmp-2 activation role in cell invasion across collagen barrier. *Journal of Biological Chemistry*, 276(19):16248–16256.

This thesis was prepared using a LaTeX template created by Steven Gunn and Sunil Patel. I adapted the template only moderately and the template made my crash-course in LaTeX so much easier! Thank you for making it freely available to all.

Thanks to the developers of MikTeX, the programme which I used to write, Jabref for organising my references and creators of all the packages designed to make writing such a large document easier.

The code for the front page design was obtained from the University of Birmingham's Maths Postgraduate Society web page - skeleton.tex file - and modified accordingly. Many thanks to the creators.
http://for.mat.bham.ac.uk/pgweb/latex.php

–Uchena N.G. Wudebwe–